

**DOE/PC/79850-T1
(DE92008469)**

**NITROGEN OXIDE ABATEMENT BY DISTRIBUTED FUEL ADDITION
Final Report**

**By
J. O. L. Wendt
J. B. Mereb**

September 20, 1991

Work Performed Under Contract No. AC22-87PC79850

**For
U.S. Department of Energy
Pittsburgh Energy Technology Center
Pittsburgh, Pennsylvania**

**By
University of Arizona
Tucson, Arizona**

DISCLAIMER

This report was prepared as an account of work sponsored by an agency of the United States Government. Neither the United States Government nor any agency thereof, nor any of their employees, makes any warranty, express or implied, or assumes any legal liability or responsibility for the accuracy, completeness, or usefulness of any information, apparatus, product, or process disclosed, or represents that its use would not infringe privately owned rights. Reference herein to any specific commercial product, process, or service by trade name, trademark, manufacturer, or otherwise does not necessarily constitute or imply its endorsement, recommendation, or favoring by the United States Government or any agency thereof. The views and opinions of authors expressed herein do not necessarily state or reflect those of the United States Government or any agency thereof.

This report has been reproduced directly from the best available copy.

Available to DOE and DOE contractors from the Office of Scientific and Technical Information, P.O. Box 62, Oak Ridge, TN 37831; prices available from (615)576-8401, FTS 626-8401.

Available to the public from the National Technical Information Service, U. S. Department of Commerce, 5285 Port Royal Rd., Springfield, VA 22161.

NITROGEN OXIDE ABATEMENT BY DISTRIBUTED FUEL ADDITION

Contract DE-AC22-87PC79850

DOE/PC/79850--T1

DE92 008469

Final Report

by

J. O. L. Wendt and J. B. Mereb
Department of Chemical Engineering
University of Arizona
Tucson, Arizona 85721

Prepared for

Diane Revay Madden, Project Manager
Environmental Control Division
Pittsburgh Energy Technology Center
U.S. Department of Energy
P.O. Box 10940
Pittsburgh, PA 15236

September 20, 1991

ABSTRACT

Reburning is examined as a means of NO_x destruction in a 17 kW down-fired pulverized coal combustor. In reburning, a secondary fuel is introduced downstream of the primary flame to produce a reducing zone, favorable to NO destruction, and air is introduced further downstream to complete the combustion. Emphasis is on natural gas reburning and a bituminous coal primary flame. A parametric examination of reburning employing a statistical experimental design, is conducted, complemented by detailed experiments. Mechanisms governing the inter-conversion of nitrogenous species in the fuel rich reburn zone are explored. The effect of reburning on N_2O emissions, the effect of primary flame mode (premixed and diffusion) and the effect of distributing the reburning fuel, are also investigated.

The parametric study allowed the effects of significant reburning variables to be identified and examined, but these effects could not be quantified. Detailed experiments identified optimum reburn zone stoichiometry between 0.8 and 0.9, depending on mixing in the reburn zone. Overall NO reductions, as high as 80%, were possible and depended mainly on reburn zone variables, namely, temperature, residence time and stoichiometry.

Exhaust N_2O emissions increased after air addition in the final stage of reburning, but were less than 10 ppm. Lower reductions in NO emissions were obtained when the primary flame was of the diffusion type, rather than of the premixed type, but final NO emissions below 250 ppm (dry, 0% O_2) were still possible. Reburning fuel introduction in multiple streams did not enhance NO destruction, relative to single stream injections.

Within the reburn zone, reburning mechanisms occurred in two regimes. One regime was in the vicinity of the reburning fuel flame and was distinguished by fast reactions between NO and hydrocarbons that were limited by mixing. The other regime covered the remainder of the reburn zone and was distinguished by slower reactions, without mixing complications. For the latter regime, a simplified model based on detailed gas phase chemical kinetic mechanisms and known rate coefficients was able to predict temporal profiles of NO, HCN and NH_3 . Reactions involving hydrocarbons played important roles in both regimes and N_2 fixation by hydrocarbons limited reburning effectiveness at low primary NO values. Appropriate corrections for mixing effects in early time scales of the reburn zone allowed the prediction of nitrogenous species profiles from primary NO values, as well as overall reburning effectiveness.

TABLE OF CONTENTS

LIST OF FIGURES	vii
LIST OF TABLES	xii
1.0 INTRODUCTION	1
1.1 Pulverized Coal Combustion: NO _x Formation and Destruction Mechanisms	2
1.2 NO _x Control Techniques and Mechanisms	7
1.2.1 Air Staging	7
1.2.2 Reburning or Fuel Staging	9
1.3 Reburning for NO _x Control	9
1.4 Primary Zone Parameters	10
1.4.1 Primary Zone Stoichiometry	11
1.4.2 Primary NO Concentration	11
1.5 Reburn Zone Parameters	12
1.5.1 Reburn Zone Stoichiometry	12
1.5.2 Reburn Zone Temperature	13
1.5.3 Reburn Zone Residence Time	14
1.5.4 Reburn Fuel Type and Nitrogen Content	14
1.5.5 Mixing in the Reburn Zone	15
1.6 Burnout Zone Parameters	17
1.7 Focus of This Work	17
1.7.1 Problem Statement	17
1.7.2 Approach	21

2.0	EXPERIMENTAL APPROACH	22
2.1	Experimental Facilities	22
2.1.1	Combustor Design and Construction	22
2.1.2	Burner Design	26
2.1.3	Air and Fuel Supply System	26
2.1.4	Sampling System	28
2.1.5	Reburning Fuel Injection System	30
2.2	Analytical Techniques	33
2.2.1	Continuous Analyzers	36
2.2.2	Gas Chromatographs	36
2.2.3	Gas/Ion Electrodes	37
2.3	Temperature Measurements	39
2.4	Fuel Analysis	39
3.0	N ₂ O EMISSIONS FROM COAL COMBUSTION	41
3.1	Environmental Impact of N ₂ O	41
3.2	Combustion Sources of N ₂ O	41
3.3	N ₂ O Measurements	43
3.3.1	Analytical Technique	43
3.3.2	Experimental Results	45
3.4	Summary of N ₂ O Study	48
4.0	PARAMETRIC STUDY OF REBURNING	54
4.1	Introduction	54
4.2	Statistical Design of Experiments	55
4.2.1	Central Composite Design	58
4.2.2	Application to the Study of Reburning	58

4.3	Effects of Independent Variables	61
4.4	Effects of Dependent Variables	72
4.5	Evaluation of the Statistical Design	79
4.6	Multiple Reburning Fuel Injection Schemes	81
4.7	Carbon Burnout	86
5.0	EXPERIMENTAL RESULTS:	
	EFFECT OF PRIMARY FLAME MODE	90
5.1	Premixed Primary Flame	90
5.1.1	Effect of Reburning Fuel Jet Momentum	90
5.1.2	Conversions of Nitrogenous Species	91
5.2	Diffusion Primary Flame	91
5.2.1	Nitrogenous Species Profiles in the Reburn Zone	95
5.2.2	Overall Reburning Effectiveness	97
6.0	EXPERIMENTAL RESULTS: REBURN ZONE PROFILES	100
6.1	Natural Gas Reburning	100
6.1.1	Effect of Temperature	102
6.1.2	Effect of Dilution of the Primary Flame	102
6.1.3	Effect of Stoichiometry	105
6.2	Sources of HCN Formation	105
6.3	Non Hydrocarbon Gas Reburning	107
6.4	Natural Gas Primary Flame	109
6.5	Ammonia Doped Natural Gas Primary Flame	112
6.6	Ammonia Doped Natural Gas Reburning	112
6.7	Coal Reburning	115

6.8	Effects of Reburning Fuel Type and Nitrogen Content	117
7.0	DATA ANALYSIS AND MODEL DEVELOPMENT	120
7.1	Theoretical Background	120
7.2	Calculations of Radical Concentrations	121
7.3	NO Destruction Mechanism	125
7.4	HCN Destruction Mechanism	129
7.5	HCN Formation Mechanism	132
7.6	NH ₃ Destruction and Formation Mechanism	134
7.7	OH Decay Mechanism	135
7.8	N ₂ O Destruction and Formation Mechanism	135
7.9	Kinetic Model: Nitrogenous Species Predictions	136
	7.9.1 Model Testing: Reburning	139
	7.9.2 Model Testing: Air Staging	144
	7.9.3 Model Testing: N ₂ O Predictions	150
7.10	Evaluation of the Kinetic Model	150
8.0	APPLICATIONS OF THE KINETIC MODEL	154
8.1	Predictions of Reburn Zone Nitrogenous Species	154
	8.1.1 Corrections for Mixing Effects in the Reburn Zone	154
	8.1.2 Predictions of the Extended Model	156
8.2	Prediction of Exhaust NO in the Burnout Zone	160
8.3	Prediction of Overall Reburning Effectiveness	160

8.4	Prediction of Configurations for Low NO Emissions	165
8.4.1	Effect of Temperature Quench	165
8.4.2	Effect of Residence Time	168
9.0	CONCLUSIONS AND RECOMMENDATIONS	168
10.0	REFERENCES	171
	APPENDIX A: RAW EXPERIMENTAL DATA	182
	APPENDIX B: REDUCED EXPERIMENTAL DATA	220
	APPENDIX C: PROGRAM LISTINGS	242

LIST OF FIGURES

Figure 1.1.	Paths for NO Formation and Destruction	4
Figure 2.1.	Experimental Combustor	24
Figure 2.2.	Premixed and Diffusion Burners	27
Figure 2.3.	Combustion Gas Sampling Probe	29
Figure 2.4.	Sample Analysis System	31
Figure 2.5.	Effect of Reburning Fuel Introduction on NO Radial Concentrations	32
Figure 2.6.	Effect of Reburning Fuel Injection Mode on NO Radial Concentrations	34
Figure 2.7.	Effect of Introducing N ₂ Gas with Reburning Fuel on NO Radial Concentrations	35
Figure 3.1.	Sample Chromatogram for N ₂ O Analysis by Gas Chromatography and Electron Capture Detection	44
Figure 3.2.	Typical Calibration Curve for N ₂ O Analysis by Gas Chromatography and Electron Capture Detection	46
Figure 3.3.	NO and N ₂ O Concentrations as a Function of Stoichiometric Ratio	47
Figure 3.4.	NO and N ₂ O Concentration Profiles at Various Stoichiometric Ratios - Bituminous Coal Flame	49
Figure 3.5.	NO and N ₂ O Concentration Profiles - Air Staged Combustion of Bituminous Coal	50
Figure 3.6.	NO and N ₂ O Concentration Profiles - Natural Gas Reburning and Bituminous Coal Primary Flame	51
Figure 3.7.	Effect of Air Addition on N ₂ O Emissions - Bituminous Coal Flame	52

Figure 4.1.	Effects of Reburn Zone Stoichiometry and Primary Zone Stoichiometry on NO Reduction by Reburning	70
Figure 4.2.	Effects of Controlled Variables on NO Reduction by Reburning	71
Figure 4.3.	Effects of Reburn Zone Residence Time and Reburn Zone Inlet Temperature on NO Reduction by Reburning	78
Figure 4.4.	Effects of Dependent Variables on NO Reduction by Reburning	80
Figure 4.5.	Effect of Reburn Zone Stoichiometry on Reburning Effectiveness - Comparing Two Locations for Reburning Fuel Injection	82
Figure 4.6.	Effect of Reburn Zone Stoichiometry on Reburning Effectiveness - Comparing Three Locations for Reburning Fuel Injection	83
Figure 4.7.	Comparison between Measured and Predicted NO Reduction by Reburning - Correlation in Terms of Controlled Variables	84
Figure 4.8.	Comparison between Measured and Predicted NO Reduction by Reburning - Correlation in Terms of Significant Variables	85
Figure 4.9.	Effect of Introduction of the Reburning Fuel as Multiple Stream Injections on Reburning Effectiveness - Variation with Reburn Zone Stoichiometry	87
Figure 5.1.	Variation of Reburning Effectiveness with Reburn Zone Stoichiometry - Premixed Primary Flame - N ₂ Injected with Reburning Fuel	92
Figure 5.2.	Variation of Reburning Effectiveness with Reburn Zone Stoichiometry - Premixed Primary Flame	93
Figure 5.3.	Nitrogenous Species Conversions at Various Stages of Reburning	94

Figure 5.4.	Fixed Nitrogenous Species Profiles in the Reburn Zone - Comparison between Premixed and Diffusion Primary Flame Modes	96
Figure 5.5.	Variation of Reburning Effectiveness with Reburn Zone Stoichiometry - Axial Diffusion Primary Flame with No Swirl - N ₂ Injected with Reburning Fuel	98
Figure 6.1.	Fixed Nitrogenous Species Profiles in the Reburn Zone - Fuel Rich SR = 0.7	101
Figure 6.2.	Fixed Nitrogenous Species Profiles in the Reburn Zone - Effect of Temperature	103
Figure 6.3.	Fixed Nitrogenous Species Profiles in the Reburn Zone - Effect of Dilution in the Primary Zone	104
Figure 6.4.	Fixed Nitrogenous Species Profiles in the Reburn Zone - Effect of Reburn Zone Stoichiometry	106
Figure 6.5.	Fixed Nitrogenous Species Profiles in the Reburn Zone - Non-Hydrocarbon Reburning Fuels	108
Figure 6.6.	Fixed Nitrogenous Species Profiles in the Reburn Zone - Reburning at Low Primary NO	110
Figure 6.7.	Conversions for Fixed Nitrogenous Species in the Reburn Zone - Reburning at Low Primary NO	111
Figure 6.8.	Fixed Nitrogenous Species Profiles in the Reburn Zone - Effect of Primary Fuel Type	113
Figure 6.9.	Fixed Nitrogenous Species Profiles in the Reburn Zone - Effect of Reburning Fuel Nitrogen Content	114
Figure 6.10.	Fixed Nitrogenous Species Profiles in the Reburn Zone - Effect of Reburning Fuel Type	116
Figure 6.11.	Fixed Nitrogenous Species Profiles in the Reburn Zone - Effect of Reburning Fuel Type and Nitrogen Content	118
Figure 7.1.	Typical Fuel Rich Zone Profiles in Air Staging and Reburning Configurations - Bituminous Coal Primary Flame	126

Figure 7.2.	Estimation of Initial OH Concentration in the Reburn Zone	138
Figure 7.3.	Development of a Kinetic Model to Predict Nitrogenous Species Profiles in the Reburn Zone	140
Figure 7.4.	Comparison between Measured and Predicted Nitrogenous Species Profiles in the Reburn Zone - Natural Gas + NH ₃ Primary Flame	141
Figure 7.5.	Comparison between Measured and Predicted Nitrogenous Species Profiles in the Reburn Zone - Bituminous Coal Primary Flame	142
Figure 7.6.	Comparison between Measured and Predicted Nitrogenous Species Profiles in the Reburn Zone - Effect of Temperature	143
Figure 7.7.	Comparison between Model Predictions and Measurements - Natural Gas Reburning	145
Figure 7.8.	Comparison between Measured and Predicted Nitrogenous Species Profiles in the Fuel Rich Combustion of Bituminous Coal - Effect of Stoichiometry	146
Figure 7.9.	Comparison between Measured and Predicted Nitrogenous Species Profiles in the Fuel Rich Combustion of Lignite Coal - Effect of Stoichiometry	147
Figure 7.10.	Comparison between Measured and Predicted Nitrogenous Species Profiles in the Fuel Rich Combustion of Bituminous Coal at SR of 0.6 - Effect of Dilution of the Primary Flame	148
Figure 7.11.	Comparison between Model Predictions and Measurements - Fuel Rich Combustion of Coal	149
Figure 7.12.	Comparison between Measured and Predicted N ₂ O Concentrations - Bituminous Coal Flame	151
Figure 7.13.	Comparison between Model Predictions and Measurements - Natural Gas Reburning - NH + NO Gives N ₂ O	153

Figure 8.1.	Comparison between Model Predictions and Measurements for Reburn Zone Residence Times Less than 0.2 Seconds - Bituminous Coal Primary Flame - Natural Gas Reburning	157
Figure 8.2.	Effect of CH ₄ Concentration at the Reburning Fuel Injection Point on NO Predictions in the Reburn Zone	158
Figure 8.3.	Comparison between Measured and Predicted Nitrogenous Species Profiles in the Reburn Zone - Predictions from Primary NO Concentrations	159
Figure 8.4.	Comparison between Measured and Predicted NO Exhaust Emissions (Dry, 0% O ₂) in the Final Stage of Reburning . . .	161
Figure 8.5.	Comparison between Measured and Predicted Reburning Effectiveness - Predictions of the Extended Kinetic Model	163
Figure 8.6.	Predictions of the Extended Kinetic Model	164
Figure 8.7.	Effect of Temperature Quench Rate on Predicted Nitrogenous Species Concentrations in the Reburn Zone . . .	166
Figure 8.8.	Effect of Temperature Quench Rate on Predicted Nitrogenous Species Concentrations in the Fuel Rich Combustion of Coal	167
Figure 8.9.	Predicted Nitrogenous Species Profiles in the Reburn Zone at Optimum Temperature Quench Rate	169
Figure 8.10.	Predicted Nitrogenous Species Profiles in the Fuel Rich Combustion of Coal at Optimum Temperature Quench Rate	170

LIST OF TABLES

Table 1.1.	Description of the Tasks	18
Table 2.1.	Fuel Composition	40
Table 4.1.	Example of 2^3 Factorial Design	57
Table 4.2.	Coordinates of a Central Composite Design	59
Table 4.3.	Controlled Variables in the Statistical Design	62
Table 4.4.	The Proposed Experimental Design	63
Table 4.5.	Experimental Data for the Statistical Design	64
Table 4.6.	Description of the Reburning Variables	65
Table 4.7.	Replicate Tests	66
Table 4.8.	Components of the Statistical Design	67
Table 4.9.	Regression Results in Terms of Controlled Variables	68
Table 4.10.	Variables in the Modified Statistical Design	74
Table 4.11.	Components of the Modified Statistical Design	75
Table 4.12.	Regression Results - Identifying Significant Variables	76
Table 4.13.	Regression Results in Terms of Significant Variables	77
Table 4.14.	Carbon Burnout	88
Table 7.1.	Equilibrium Constants for Species	122
Table 7.2.	Reaction Mechanism Forward Rate Coefficients	128
Table 7.3.	Expressions for Functions f_i	130

1.0 INTRODUCTION

Coal is the most abundant fuel in the world, accounting for about 75% of the world's resources of fossil fuels (Elliot, 1981). Pulverized coal combustion is an important source of energy and remains the preferred method of combustion in utility boilers. In the last two decades, energy from coal has lost some ground to oil and nuclear energy as a result of strict regulations on stack flue gas emissions and increasing demand to burn coal in an environmentally acceptable manner. Coal is a dirty fuel, compared to oil and natural gas and contains varying amounts of sulfur and nitrogen. The nitrogen content of coal can be as high as 2% and the sulfur as high as 7% (Elliot, 1981). When coal is burned, these elements are released into the atmosphere in the form of nitrogen oxides and sulfur oxides in combustion flue gases. These pollutants have damaging effects on the environment, the most visible of which is their contribution to acid rain. In addition, coal combustion results in the emission of particulate pollutants and trace metal compounds into the atmosphere. Nevertheless, coal remains the dominant fuel in the utility industry, due to the large number of existing coal fired power plants. The impact of these pollutants on the environment presents a serious limitation to the increased utilization of coal combustion as an economical and abundant energy source. Therefore, there is an urgent need for a better understanding of the processes that control the formation of combustion generated pollutants.

In the last two decades, SO_x emissions have been decreasing whereas NO_x emissions have been increasing. In 1988, NO_x emissions in the U.S. were about 20 million tons, 55% of which were due to stationary fuel combustion (McInnes et al., 1990). The Clean Air Act Amendments of 1990 are expected to be a major driving force toward increased emission control. This act is expected initially to target electric utilities for the greatest reductions in NO_x emissions. Thus, there is immediate need for more effective NO_x abatement technology. NO_x is implicated as a major contributor to acid precipitation and atmospheric visibility. Nitrogen oxides (NO_x) include both nitric oxide (NO) and nitrogen dioxide (NO_2), with NO as the dominant species in combustion flue gases. In the atmosphere, NO is oxidized to form NO_2 which may initiate the formation of ozone or undergo oxidation to form nitric acid, a precursor to acid rain. NO_x control is of major concern in the utility industry with most of the activity directed towards existing coal fired power plants, since these plants emit about 5 million tons of NO_x a year, corresponding to about 15% of NO_x from man made sources in the U.S. (Gerber, 1986).

The pressing demand for more stringent regulations to control the emissions of nitrogen oxides from coal combustion requires a better understanding of existing and emerging pollution abatement technologies. A promising technique for the control of NO_x emissions is referred to as "reburning." Reburning is a combustion modification technique used for NO_x control, where portions of both fuel and air are diverted to locations downstream of the primary flame. In a reburning configuration, three combustion zones are established which can be manipulated to reduce NO_x emissions. The primary combustion zone is operated fuel lean, in which NO and other combustion products are formed. A secondary combustion zone is created by introducing a secondary fuel downstream of the

primary firing zone. This stage is usually operated under reducing conditions, which favor the destruction of NO to form N_2 and other nitrogenous species, namely, HCN and NH_3 . In a third stage, additional air is introduced to complete the combustion process. Reburning has the potential to reduce NO_x emissions in combustion flue gases by as much as 70% (Overmoe et al., 1986; Yang et al., 1986). The examination of the physical and chemical processes that define the application of reburning for NO_x abatement in coal combustion flue gases is the motivation for this work.

1.1 Pulverized Coal Combustion: NO_x Formation and Destruction Mechanisms

In coal combustion, pulverized coal particles are carried with air into a hot combustion chamber, where the particles are heated at rates on the order of 10^4 to 10^6 K/s. The classic model of coal combustion describes three processes that are not entirely independent and may overlap, namely, devolatilization, volatile combustion and char combustion. Devolatilization involves the release of volatile matter from the coal particles upon heating. The remaining coal residue, following the release of volatile gases, constitutes the char. The oxidation reactions that follow may involve both the volatile gases and the char, and result in the formation of nitrogen oxides and sulfur oxides in combustion flue gas. The processes that occur in the early stages of coal combustion are reviewed by Wendt (1980) and Morrison (1986). Only the chemical processes that lead to the formation and destruction of nitrogen oxides and other nitrogenous species in post flame flue gases of pulverized coal combustion are discussed here. It is the fate of nitrogenous species and their emissions from coal combustion configurations that is of interest in this investigation.

In coal combustion, NO can be formed by three distinct mechanisms, denoted as Thermal NO, Prompt NO and Fuel NO. The relative significance of these paths of NO_x formation depend on temperature, stoichiometry and coal type, and influence the choice of a suitable NO_x reduction technique. Here, "stoichiometry" is defined as the molar air to fuel ratio divided by the theoretical ratio for complete combustion, and is a measure of the availability of the oxidant.

Thermal NO is formed as a result of the thermal fixation of molecular nitrogen in combustion air at the high temperatures that are associated with combustion, as originally proposed by Zeldovich (1946). The Zeldovich mechanism accounts for NO formation due to $N_2 + O$ and $N + O_2$ reactions. The extended Zeldovich mechanism includes NO formation due to $N + OH$ reaction. Thermal NO formation is a strong function of temperature and residence time and is of minor significance at temperatures below 1800 K (Morrison, 1986).

Fuel NO formation is the dominant source of NO in coal combustion, accounting for more than 80% of NO emissions (Pershing and Wendt, 1977). Conversion of fuel nitrogen to NO depends on the local combustion environment and fuel characteristics, with a weak dependence on temperature. During coal combustion, the chemically bound nitrogen in the coal is split between that in the volatile fraction and that in the char. Reactions involving

the volatile fraction, as well as those involving the char, result in the formation of NO. The contribution of char nitrogen to NO formation depends on temperature, with lower conversions at higher temperatures and lower stoichiometries (Song et al., 1982a, 1982b).

Pershing and Wendt (1977) showed that under practical coal combustion conditions, the oxidation of char nitrogen was of minor significance in the formation of NO. In another study, Wendt et al. (1979) used artificial oxidants to demonstrate that under most conditions, Fuel NO formation dominates under fuel rich conditions. Similar results were obtained by Pohl and Sarofim (1977) under fuel lean conditions, with 80% of NO_x formation due to the oxidation of volatile nitrogen. The conversion of volatile nitrogen to NO_x decreased with decreasing stoichiometry and with increasing temperatures. The effect of stoichiometry is due to delayed contact between the volatile nitrogen and oxygen which reduces the formation of NO_x. The weak dependence on temperature of Fuel NO formation was discussed by Song et al. (1982b). At higher temperatures, more nitrogen evolves in the volatile fraction. However, the conversion of volatile nitrogen to NO decreases with temperature and both effects seem to cancel out. The effect of fuel characteristics on NO formation was investigated by Chen et al. (1982), who conducted a parametric study of 50 different coals. An empirical correlation was developed that showed an increase in NO emissions with the nitrogen content in the coal. A similar observation was reported by England et al. (1981) in a study of the effect of fuel type in the combustion of nitrogen containing liquid fuels. Overall NO emissions and Fuel NO formation correlated linearly with the nitrogen content in the fuel. An oxidant that excluded N₂ was used in the primary flame to examine the formation of Fuel NO.

In short, most of the Fuel NO from coal combustion is formed as a result of the oxidation of fuel nitrogen that evolves during devolatilization. Fuel NO formation decreases with stoichiometry because of delayed contact between fuel nitrogen and oxygen, and has a weak dependence on temperature. The dependence of Fuel NO on fuel characteristics is mainly due to volatility properties and nitrogen content in the fuel.

Coal nitrogen evolves from coal in the form of high molecular weight nitrogenous compounds, which are then converted to simple nitrogenous species, namely, hydrogen cyanide (HCN), ammonia (NH₃), nitric oxide (NO) and molecular nitrogen (N₂). These species are fixed during combustion and can be measured in combustion flue gases. The generally accepted sequence of nitrogenous species in combustion is that HCN and NH₃ are formed as products of coal devolatilization, with HCN as the dominant nitrogenous species. This sequence is shown in Figure 1.1. The conversion of fuel nitrogen to HCN is very rapid and is not rate limiting (Miller et al., 1984). NH₃ is formed homogeneously from HCN, with two competing routes of NH₃ reactions to form NO or N₂ (Haynes, 1977a, 1977b; Fenimore 1971, 1976). The reactions between NO and NH₃ species, resulting in their mutual destruction to form N₂, are inhibited if NO levels are too low, which can occur under extreme fuel rich combustion conditions. Under fuel lean conditions, HCN and NH₃ are converted to NO or N₂. Under fuel rich conditions, N₂ formation path is favored over NO formation and all fixed nitrogenous species are present (HCN, NH₃, NO and N₂).

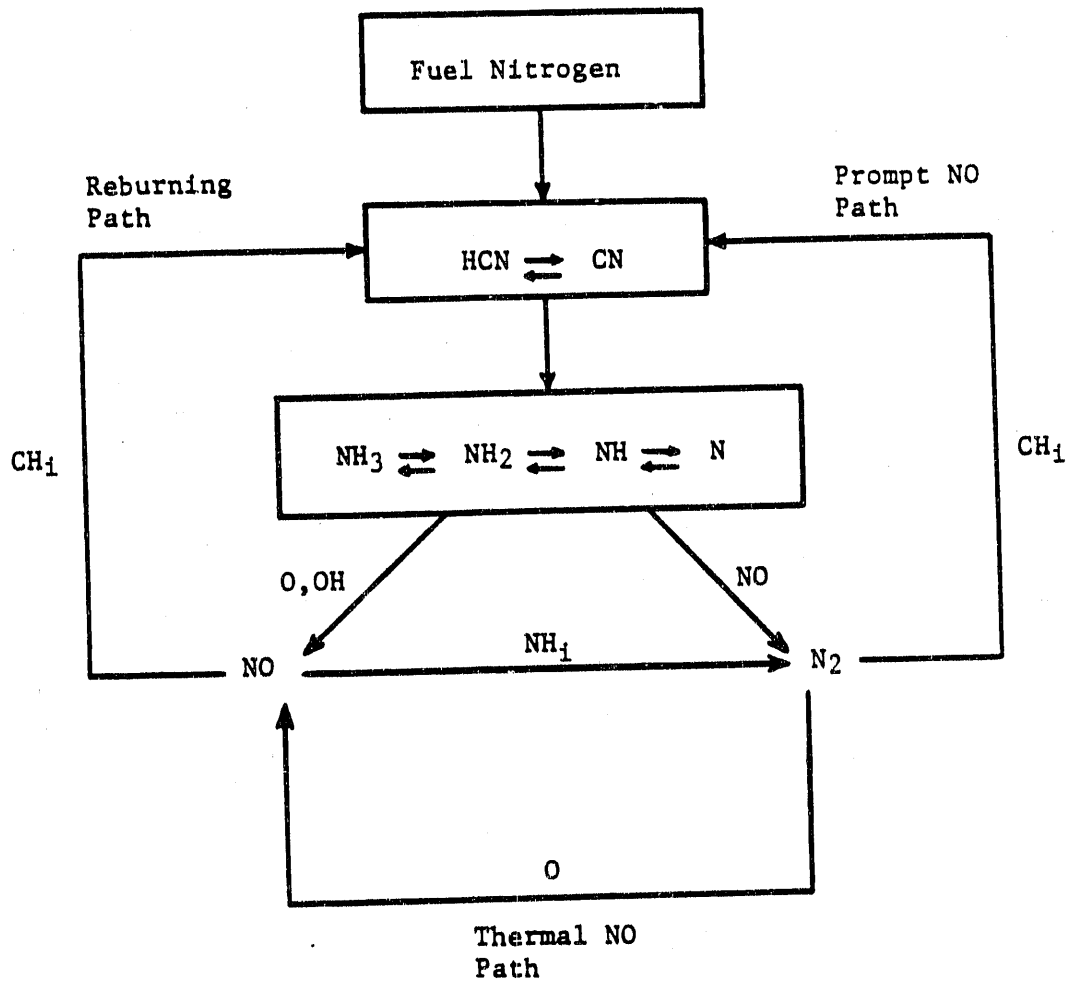


Figure 1.1. Paths for NO Formation and Destruction.

Prompt NO formation (Figure 1.1) was first identified by Fenimore (1971) who showed that under fuel rich conditions, additional NO can be formed in the presence of N_2 in hydrocarbon, but not H_2 or CO flames. The additional NO could not be described by the Zeldovich mechanism in fuel rich flames. This path for NO formation increases in significance as the hydrocarbon concentration increases. It is initiated by the reaction of hydrocarbon radicals with N_2 to form HCN, mainly due to $CH + N_2$ reaction. NH_3 is formed homogeneously from HCN, followed by oxidation reactions of NH_3 to form NO, as seen in the path described in Figure 1.1. A similar path in which a methyl radical reacts with N radicals ($CH_3 + N$) to form NO through HCN intermediate, was proposed by Haynes (1977a).

The inter-conversion of nitrogenous species in post flame flue gases is complex and results from a sequence of elementary reactions. Great progress has been made in the study of the homogeneous gas phase reactions involving the formation and destruction of nitrogenous species. A review of the works of various researchers is provided by Bose (1989). Most notable are the pioneering works of Fenimore (1971, 1976) and Haynes (1977a, 1977b). Comprehensive kinetic sets of elementary gas phase reactions and the corresponding kinetic parameters were compiled by Glarborg et al. (1986) and Miller and Bowman (1989). These works provide much needed understanding of the nitrogen chemistry that govern the inter-conversion of nitrogenous species in combustion processes. The mechanism of Glarborg, Miller and Kee (1986) consisted of 213 reactions and included those accounting for the interaction between hydrocarbons and nitrogen. These reactions demonstrated that large quantities of nitrogen are continuously cycled between NO and cyanide species, mostly HCN. The mechanism of Miller and Bowman (1989) is similar to the one that was proposed by Glarborg et al., but included more reactions involving N_2O and NO_2 . Miller and Bowman compared detailed kinetics calculations to the experimental data of previous works, covering a wide range of temperatures, stoichiometries and fuel types. The model successfully predicted nitrogenous species concentrations and accounted for Thermal NO, Prompt NO, NO_2 and N_2O formation, as well as fuel nitrogen conversions.

Heterogeneous processes involving NO formation and destruction were investigated by various researchers (Song et al., 1982a, 1982b; Glass and Wendt, 1982; Wendt et al., 1979). These studies focused on the combustion of coal char and thus, excluded the complications associated with the early stages of devolatilization. Song et al. (1982a) showed that coal char nitrogen could undergo devolatilization in parallel with oxidation. In another study (Song et al., 1982b), the conversion of char nitrogen to NO was shown to decrease with stoichiometry, and conversions as high as 35% were calculated under excess air conditions. Wendt et al. (1979) and Glass and Wendt (1982) studied the fuel rich combustion of coal char in a down-flow combustor. Their results showed that NO was formed and then destroyed, suggesting that NO could be reduced on char surfaces. Kinetic expressions were derived to describe the heterogeneous formation and destruction of NO under fuel rich conditions. However, processes involving char should not be judged separately from the early stages of devolatilization. Glass and Wendt (1982) showed that heterogeneous reduction of NO on char surfaces was too slow to account for the observed

NO decay and concluded that homogeneous gas phase kinetics dominate the destruction of NO in the fuel rich coal post flame. The significance of heterogeneous processes in NO formation and destruction mechanism has been demonstrated in the combustion of coal char, but their contribution in coal combustion remains to be quantified. In the literature, there is strong evidence to suggest that homogeneous gas phase kinetics dominate the inter-conversion of nitrogenous species in fuel rich coal post flames (Glass and Wendt, 1982; Bose et al., 1988; Bose and Wendt, 1988).

In recent years, interest has been evoked with respect to an additional oxide of nitrogen, namely, nitrous oxide (N_2O). N_2O has been implicated as a contributor to the depletion of the ozone in the stratosphere and as a greenhouse gas. Furthermore, N_2O concentrations in the atmosphere have been increasing at a rate of 0.18-0.26% per year (Weiss, 1981). The contribution of coal combustion to this increase is not yet clear. A study by Hao et al. (1987) suggests that N_2O concentrations in fossil fuel combustion flue gases can exceed 100 ppm. However, more recent studies (Linak et al., 1990; Kramlich et al., 1989), dispute this claim and suggest that the high N_2O concentration may be the result of a sampling artifact involving the use of sample containers. This sampling artifact was first discovered by Muzio and Kramlich (1988), who demonstrated that N_2O could be produced from NO when stored in sample containers in the presence of SO_2 and water vapor. The use of sampling containers was common in field testing which required the collection of a sample for subsequent analysis for N_2O at a later time. This brings into question the validity of coal combustion N_2O data in studies that involved container sampling. Thus, reliable N_2O data from coal combustion flue gases are mostly limited to few studies conducted after 1988. Furthermore, the effect of NO_x control techniques on N_2O emissions has not yet been fully examined.

The mechanisms that govern the formation and destruction of N_2O in combustion flue gases were examined by Kramlich et al. (1988) in a plug flow simulator. N_2O concentrations as high as 250 ppm were measured in post flame flue gases when cyano species were introduced in the fuel lean post flame, but not in the flame zone. The net formation of N_2O was found to be a strong function of temperature and occurred only under fuel lean conditions at temperatures between 1150 and 1500 K. On the other hand, N_2O concentrations were less than 10 ppm when NH_3 was introduced instead of cyano species. The researchers proposed HCN as a precursor to N_2O formation in a narrow temperature range, in which net formation would occur only within fuel lean environments, corresponding to low H radical concentrations. N_2O formation was due to $NH + NO$ and $NCO + NO$ reactions. Imperfect mixing and carry over of char nitrogen beyond the flame zone into the cooler regions of the combustor were proposed as possible routes for N_2O formation through reaction paths starting from HCN. The formation of N_2O within the flame was judged to be unlikely due to its rapid destruction by $N_2O + H$ reactions.

1.2 NO_x Control Techniques and Mechanisms

Two options are traditionally utilized for controlling NO_x emissions: flue gas treatment and combustion control. An example of a post combustion flue gas treatment method is the Thermal DeNO_x, developed by Exxon (Lyon, 1975). It involves the injection of ammonia into the post combustion exhaust gas to reduce NO emissions by enhancing reactions with NH₃ to form N₂ in a fuel lean environment. In general, flue gas treatment methods for NO_x control are associated with high cost and potential reliability problems. On the other hand, combustion control techniques are more attractive for NO_x control. These techniques include low NO_x burners and combustion modification. NO_x reduction by combustion modification is the focus of this work.

Combustion modification refers to the modification of the combustion configuration to create conditions that would enhance the destruction of the nitrogenous species in the post flame combustion flue gas. Air staging and reburning are two examples of combustion modification techniques that have been shown to be effective tools in reducing the emissions of nitrogen oxides from coal combustion. Air staging is a two stage combustion process in which the primary combustion zone is operated fuel rich and the air required to complete the combustion process is introduced downstream of the main firing zone. On the other hand, reburning is a three stage combustion process. It involves the injection of a secondary fuel downstream of a fuel lean primary combustion zone to create a fuel rich environment and additional air is added further downstream to obtain an overall fuel lean environment. Both forms of combustion modification have attractive features and are capable of reducing NO emissions by more than 50%, depending on various parameters. Air staging and reburning are two different configurations in terms of temperature profiles and local hydrocarbon concentrations, but also have similar features. In both configurations, most of the destruction of nitrogenous species takes place in an oxygen deficient environment that favors the formation of N₂, followed by air addition in a final combustion stage. Although the emphasis in this investigation is on the study of reburning, an examination of air staging is useful in understanding the physical and chemical processes that control the destruction of NO in the reburning process.

1.2.1 Air Staging

The first zone in an air staged combustion configuration is operated fuel rich which inhibits the formation of NO and all fixed nitrogenous species are present (NO, HCN and NH₃). The dominant variables that affect the destruction of nitrogenous species in staged combustion are stoichiometry, residence time and primary fuel type. Various studies of staged combustion (Chen et al., 1982; Rees et al., 1981; England et al., 1981; Kremer and Schulz, 1986) have shown that a decrease in first stage stoichiometry corresponded to lower NO concentrations and higher HCN and NH₃ concentrations. Therefore, there is an optimum first stage stoichiometry that would correspond to a minimum concentration of the sum of concentrations of NO, HCN and NH₃ (total fixed nitrogen). Furthermore, since HCN and NH₃ are partially converted to NO after the addition of staged air, a minimum

concentration of NO in the exhaust would also exist for an optimum first stage stoichiometry. Optimum reductions in NO by air staging were obtained in various studies (Song et al., 1981; Rees et al., 1981; England et al., 1981; Kremer and Schulz, 1986; Chen et al., 1982) at first stage stoichiometries ranging from 0.6 to 0.8.

In the study of air staged combustion of various coals, Chen et al. (1982) showed that the distribution of nitrogenous species in the first stage depended on coal rank. HCN concentrations in the first stage were higher than NH_3 concentrations for bituminous coals and lower than NH_3 concentrations for lignite coals. The nitrogenous species concentrations showed little sensitivity to changes in temperature and mostly depended on stoichiometry. Similar effects of temperature and coal type were reported by Kremer and Schulz (1986) in their study of air staged combustion under nearly isothermal conditions. Higher temperatures enhanced the conversion of nitrogenous species to NO in the second stage of bituminous coal combustion. An opposite trend was observed in the staged combustion of lignite coal. Chen et al. (1982) attributed these trends to selective NO reduction by NH_3 species which would be more significant for low rank coals, where high levels of NH_3 and low levels of NO might exit the first stage.

The effect of fuel characteristics and temperature on NO_x emissions in the staged combustion of liquid fuels, containing varying amounts of nitrogen, were investigated by England et al. (1981). This study showed that the conversion of fuel nitrogen to nitrogenous species was mostly dependent on first stage stoichiometry and relatively insensitive to fuel type. Lower concentrations of nitrogenous species were measured at higher temperatures which is consistent with the observations of Bose et al. (1988), but in contrast with the results of Chen et al. (1982) and Kremer and Schulz (1986).

In the second zone of air staging, air is added and a fraction of the oxidizable nitrogenous species (HCN and NH_3) is converted to NO. As discussed earlier, this conversion depends on first stage stoichiometry, temperature and coal type, since these variables affect the distribution of the nitrogenous species leaving the first stage. NO levels in the second stage may increase or decrease, relative to those in the first stage, depending on a number of variables. Thermal DeNO_x reduction of NO by NH_3 radicals can be important if the temperature range is 1100 K to 1400 K in the second stage, and if NH_3 levels are relatively high (Lyon, 1975). A complication in the air staged combustion of coal is the retention of nitrogen in the char, which is partly oxidized in the second stage to form NO. Chen et al. (1982) showed that the conversion of char nitrogen to NO in the second stage depended on first stage stoichiometry, and was less than 20% in most cases. An empirical correlation was developed to relate exhaust NO emissions with gas phase total fixed nitrogen and char nitrogen entering the second stage.

The effect of residence time on nitrogenous species speciation in the fuel rich stage was studied by Wendt et al. (1979). NO was formed rapidly and then slowly destroyed. Residence time in the first stage affected final NO emissions, with more dramatic effects at lower stoichiometries in the first stage.

To summarize, exhaust NO emissions in an air staged combustion configuration depend on stoichiometry in the fuel rich stage, temperature, residence time and fuel characteristics. There is an optimum first stage stoichiometry that corresponds to minimum exhaust NO emissions. This optimum and the final NO level depend on process parameters and may vary from a first stage stoichiometry of 0.6 to 0.8. Higher temperatures and longer residence times in the fuel rich stage enhance the destruction of nitrogenous species. The application of air staging for NO_x control in a practical combustor requires long residence times (greater than 1 second) and high temperatures which can create problems due to corrosion and insufficient space availability. These problems are greatly reduced in a reburning configuration which allows the destruction of nitrogenous species in a fuel rich environment and shorter residence times are required.

1.2.2 Reburning or Fuel Staging

In reburning, nitrogen oxides are formed in a fuel lean primary combustion zone and then destroyed in a fuel rich secondary zone, created by introducing a secondary fuel. The introduction of a secondary fuel generates high concentrations of hydrocarbon radicals, which enter into reactions with NO to produce HCN intermediate, which initiates a path that favors N₂ formation in a fuel rich environment. This form of NO_x reduction is referred to as reburning, fuel staging, distributed fuel addition, staged fuel injection, or in furnace NO_x reduction. These terms are used alternately by different researchers to refer to the process, in which a source of hydrocarbon radicals is introduced in a secondary combustion stage to react with NO generated in a primary combustion stage.

One of the early observations of NO reactions with hydrocarbon radicals was reported by Myerson et al. (1957) in a study of burning mixtures of propane and nitrogen dioxide. The first process that applied reburning as a technique to destroy NO_x from nitric acid tail gases was developed by John Zinc Company (Reed, 1969). In this process, NO₂ and NO were introduced into an incinerator where they were destroyed by hydrocarbons to form N₂ in a reducing environment. The first application of secondary fuel injection to reduce NO_x emissions inside furnaces was presented by Wendt et al. (1973), who introduced the term "reburning" to refer to this NO_x control technique. In this study, 50% reductions in NO_x were achieved by injecting methane as a secondary fuel. The application of reburning to large furnaces was first tested in Japan (Takahashi et al., 1981). These tests suggested no negative impact on boiler efficiency and 50% reductions in NO_x emission levels were reported. These encouraging results renewed interest in reburning in the U.S. as a technically and economically feasible technique for NO_x control in coal fired utility boilers.

1.3 **Reburning for NO_x Control**

In a practical combustor, reburning would have two applicable advantages. First, diverting a portion of the fuel from the primary firing zone and introducing it as a reburning fuel would reduce the heat release in the first stage. Consequently, less NO would be produced in the primary zone, because of reduced temperatures and thus, reduced formation

of NO through the Zeldovich mechanism (Thermal NO). Second, diverting a fraction of the excess air from the primary flame and introducing it in the final stage would result in further reduction in the primary NO. Nevertheless, commercial application of reburning in the U.S. has been limited and many questions remain answered. What are the effects of the different process variables on the overall reduction in NO? What role do hydrocarbons play and what are the mechanisms that govern NO destruction in reburning? What are the limitations to the reburning process and can these limits be extended to achieve further reductions in NO emissions?

The introduction of secondary fuel and secondary air streams, downstream of the primary flame, creates three sequential combustion zones. Each of the three zones of the reburning process involve a number of variables that affect the outcome of reburning, namely, the overall reduction in NO_x emissions or reburning effectiveness. The first stage of reburning is referred to as the primary zone, the second stage as the reburning (or reburn) zone and the final stage as the burnout zone. The following is a review of the effects of the various parameters that affect reburning effectiveness. It serves to demonstrate the complexity of the reburning process and the need for further examination of reburning parameters and their effects. The parameters that are associated with each of the stages of reburning are discussed separately.

1.4 Primary Zone Parameters

In the first stage of reburning, the primary fuel is burned under fuel lean conditions and combustion products, including NO, are formed. The dominant variables in this stage are: stoichiometry, the primary NO level, temperature and residence time. The effect of primary zone temperature is examined through its effect on other variables, such as the primary NO level, residence time and temperatures in the other two stages of reburning.

The effect of residence time in the primary zone was discussed by Chen et al. (1986) and Overmoe et al. (1986). The researchers suggested that for reburning to be effective, a high degree of primary fuel burnout would be necessary and thus, sufficient residence time should be allowed in the primary zone. Otherwise, oxygen carryover into the reburn zone might result in leaner reburn zone stoichiometric ratios which would effect reburning effectiveness, depending on the desired stoichiometry in the reburn zone. This effect is greater at higher primary zone stoichiometries which are accompanied by shorter residence times. Chen et al. (1986) suggested a residence time requirement of at least 0.3 seconds in the primary zone. The majority of the reburning tests in this study satisfy this requirement.

The primary fuel type has an indirect effect on reburning effectiveness since it affects the temperature profile and the primary NO level. Chen et al. (1986) examined different primary fuels and showed that reburning was insensitive to the fuel type, except for its effect on the primary NO level. Similar results were reported in a study by Greene et al. (1985), in which minor differences in reburning effectiveness were observed using coal or propane doped with NO primary fuels.

1.4.1 Primary Zone Stoichiometry

In the application of reburning, lower primary zone stoichiometries are desirable in order to reduce the amount of reburning fuel that is required to produce the desired reburn zone stoichiometry. However, a certain amount of oxidant is required in the reburn zone to initiate the generation of hydrocarbon radicals from the reburning fuel (Myerson, 1975). Furthermore, oxygen containing radicals promote the conversion of HCN to NH_3 . A primary zone stoichiometry of 1.1 was recommended by LaFond et al. (1987).

A number of researchers have shown that variation in primary zone stoichiometry has a minor effect on reburning effectiveness (Kelly et al., 1983; Mulholland et al., 1986; Overmoe et al., 1986; Greene et al., 1985). Kelly et al. (1983) obtained better reductions in NO at lower stoichiometries, whereas, Yang et al. (1986) showed that higher stoichiometries might improve reburning effectiveness. However, the effect of primary zone stoichiometry cannot be examined separately, since it affects both temperature and residence time. Additionally, as the primary stoichiometry is increased, a greater amount of reburning fuel must be introduced to produce the desired reburn zone stoichiometry. This affects mixing at the entrance to the reburn zone, which may produce more fuel pockets around the reburn fuel jet and variations in the local stoichiometry. Greene et al. (1985) studied the effect of varying the primary stoichiometry at constant residence time and constant primary NO levels. No significant changes in reburning effectiveness were reported at two primary NO levels of 170 and 570 ppm. Thus, different studies suggest a minor effect of varying the primary zone stoichiometry on reburning effectiveness, provided the primary zone is operated fuel lean. However, changes in primary zone stoichiometry introduce changes in other reburning parameters, such as temperature and residence time, which need to be further examined.

1.4.2 Primary NO Concentration

Nitrogen oxides that are formed in the primary zone are the dominant nitrogenous species under the oxidizing conditions of this stage. The primary NO leaving the first stage is an important parameter that affects the overall effectiveness of the reburning process.

The large scale reburning results of Takahashi et al. (1983) suggested that the destruction of NO was independent of primary NO levels in the range of 10 to 250 ppm, relative to uncontrolled baseline emissions. These conclusions have been shown to be misleading, since other nitrogenous species were not measured after the introduction of the reburning fuel and thus, the reburning effectiveness was not properly reflected (Lanier, 1984). Other studies have shown a definite effect of the primary NO level on reburning effectiveness, especially at lower values of primary NO (Mulholland et al., 1986; Miyamae et al., 1986; Greene et al., 1985; Chen et al., 1986; Lanier et al., 1986).

Brown et al. (1986) and Greene et al. (1985) showed that the reburning effectiveness decreased with primary NO concentrations below 600 ppm and a minor dependence was

observed at higher concentrations. Greene et al. (1985) attributed this effect to lower conversions of the primary NO to other nitrogenous species in the reburn zone at higher levels of primary NO. The conversion of nitrogenous species to NO in the final stage was relatively insensitive to the primary NO level. Similar results were reported by Miyamae et al. (1986), who examined a wide range of primary NO concentrations. At concentrations above 500 ppm, the conversion of primary NO to other nitrogenous species (HCN + NH₃) showed little dependence on the primary NO level.

The dependence of reburning effectiveness on the primary NO level is expected, since the destruction of NO by hydrocarbon radicals to form HCN depends on the initial NO concentration. Furthermore, HCN and NH₃ are partially oxidized to form NO in the final stage of reburning. At primary NO levels below 200 ppm, an added complication might be the formation of additional HCN as a result of N₂ fixation by hydrocarbon radicals (Fenimore, 1971), mainly due to CH + N₂ reaction. Thus, NO and N₂ may compete for the consumption of hydrocarbon radicals as the primary NO concentration decreases. The significance of this mechanism under practical coal combustion conditions has not yet been fully investigated. In the study of natural gas reburning in a package boiler simulator, Lanier et al. (1986) showed that at primary NO level below 100 ppm, the total fixed nitrogen concentration can increase in the reburn zone due to the formation of HCN and the destruction of N₂. However, this conclusion has not been substantiated by other works, and the significance of N₂ fixation by hydrocarbons under reburning conditions need to be further examined. This path for HCN formation may present a serious limitation to the effectiveness of reburning and is further discussed in the study of mechanisms.

1.5 Reburn Zone Parameters

The reburning zone is the second stage of the reburning process, created by introducing a secondary fuel downstream of the primary combustion stage. This zone is usually operated fuel rich which allows the destruction of a fraction of NO that is formed in the primary zone to form N₂ and other nitrogenous species (HCN and NH₃). As in the case of air staging, the parameters that are associated with the fuel rich stage are critical parameters that affect final NO emissions.

1.5.1 Reburn Zone Stoichiometry

In air staging, a decrease in the stoichiometry of the fuel rich stage is accompanied by a decrease in NO levels and increases in HCN and NH₃ levels. Consequently, there is an optimum fuel rich stoichiometry that corresponds to a minimum concentration of the total fixed nitrogen (NO + HCN + NH₃). Similarly, there is an optimum fuel rich stage stoichiometry in a reburning configuration that corresponds to maximum reduction in NO emissions. Literature data on optimum reburn zone stoichiometries are conflicting and sometimes misleading because other factors, such as mixing and temperature effects should also be considered. Typical values of optimum reburn zone stoichiometries range from 0.8 to 0.9 (Chen et al., 1986; Greene et al., 1985; Kolb et al., 1988). Other studies (Kelly et al.,

1986; Lanier et al., 1986; Miyamae et al., 1986) showed no clear optimum as the reburn zone stoichiometry decreased. The results of Lanier et al. (1986), Mulholland and Lanier (1985) and Mulholland and Hall (1986) in a package boiler simulator suggest that an optimum reburning effectiveness might be obtained at reburn zone stoichiometries below 0.7. Furthermore, the small scale reburning tests of Miyamae et al. (1986) and Myerson (1975) identify optimum reburn zone stoichiometries above 0.94. In a review by LaFond and Chen (1987), it was suggested that reburning effectiveness would be strongly dependent on the size of the combustor. In addition, the researchers hypothesized that reburning effectiveness would be a sharper function of stoichiometry and higher reductions would be possible, as the size of the system decreased. The location of this optimum is clearly dependent on the combustor scale, mostly due to the effects of mixing. Large scale experiments are affected by poor mixing which can create large variations in local stoichiometries.

Greene et al. (1985) showed that up to 20% NO reduction could be obtained under overall fuel lean conditions in the reburn zone. This was attributed to the diffusion nature of the reburning fuel flame, which would allow the development of local fuel rich regions around the fuel jet. Consequently, pockets of fuel rich stoichiometries might exist in an overall fuel lean environment in the reburn zone. Similar observations were obtained by Overmoe et al. (1986). Other factors, such as residence time and temperature, would also affect the location of an optimum reburn zone stoichiometry (Brown et al., 1986; Greene et al., 1985; Miyamae et al., 1986).

The results of various researchers clearly suggest that the effect of reburn zone stoichiometry on reburning effectiveness is dependent on mixing, temperature and residence time. However, the interdependence of these variables is not yet clear and is further investigated in this study.

1.5.2 Reburn Zone Temperature

The effect of temperature in the reburn zone cannot be easily examined, since other factors must also be considered. There is somewhat a general agreement (Myerson, 1975; Lanier, 1984; Greene et al., 1985), indicating that higher temperatures in the reburn zone can enhance reburning effectiveness under most conditions. Greene et al. (1985) showed that an increase in the reburn zone inlet temperature increased the destruction of NO in reburning tests in which gaseous reburning fuels were used. When coal was used as the reburning fuel, the effect of temperature in the reburn zone might be reversed, since the temperature in the final stage would also be affected. At higher temperatures, reburning effectiveness became a sharper function of reburn zone stoichiometry. In addition, the effect of temperature was reversed as the reburn zone stoichiometry approached the fuel lean side (greater than 0.95) and lower temperatures produced higher reburning

effectiveness. This observation was deduced from the work of Greene et al. (1985) and no similar effects were addressed in other studies. Therefore, the effect of temperature on the reburning process, when the reburn zone is operated fuel lean or close to the fuel lean side, is lacking and is examined in this study.

NO destruction in the reburn zone is mostly due to $\text{NO} + \text{CH}_i$ reactions and $\text{NO} + \text{NH}_i$ reactions (see Figure 1.1). The temperature dependence of the kinetic rate coefficients of these reactions (Glarborg et al., 1986) show that NO destruction by CH_i species is favored at higher temperatures, whereas, NO destruction by NH_i species is favored at lower temperatures. Furthermore, higher temperatures promote the decay of HCN due to reactions with O and OH radicals. The effect of temperature on HCN is possibly the dominant factor in the reburn zone, since HCN is an intermediate in the path that favors N_2 formation under fuel rich conditions. An added complication is the enhanced decay of hydrocarbons at higher temperatures. This can partially explain the reversed effect of temperature on reburning effectiveness when the reburn zone stoichiometry is close to the fuel lean side where low concentrations of HCN and hydrocarbons are present.

1.5.3 Reburn Zone Residence Time

It is expected that longer residence times in the reburn zone would improve NO reduction by reburning, by allowing the nitrogenous species in the fuel rich zone to decay to lower values. The effect of residence time is strongly dependent on temperature in the reburn zone and the primary NO level. Various studies suggest that rapid reduction in NO may be possible within short time scales of less than 0.1 seconds (Miyamae et al., 1986; Myerson, 1975; Lanier et al., 1986). If the temperature in the reburn zone is increased, HCN and NH_3 decay is enhanced and additional residence time may be required to allow these nitrogenous species to decay to low levels (Miyamae et al., 1986). The results of Greene et al. (1986) and Chen et al. (1986) indicate that the residence time requirement is greater at higher levels of primary NO concentrations.

In short, the residence time requirement in the reburn zone is a crucial factor that effects the overall reduction in NO. This requirement depends on the conditions of the reburn zone, and on the primary NO entering the reburn zone, and thus, should be examined in view of the effects of these factors.

1.5.4 Reburn Fuel Type and Nitrogen Content

The introduction of the reburn fuel in the second stage of reburning serves two purposes. First, it creates a fuel rich environment which promotes the destruction of NO through a path that favors N_2 formation, and second, it supplies a source of hydrocarbon radicals which initiates the destruction of NO. Thus, it is expected that the properties of the secondary fuel would have a crucial effect of the outcome of the reburning process.

Greene et al. (1985) compared the use of non hydrocarbon gases (CO and H₂) as reburning fuels, to propane reburning fuel. As expected, the reburning effectiveness was greater with hydrocarbon reburning fuels than with H₂ or CO, except when the reburn zone was operated at stoichiometries below 0.8. That was attributed to higher levels of HCN and NH₃ in the reburn zone at lower stoichiometries, when hydrocarbon reburning fuels were used. Non hydrocarbon fuels produced very low levels of HCN and NH₃ in the reburn zone. Similar observations were reported by Chen et al. (1986). The advantage of using hydrocarbon reburning fuels became more apparent as the primary NO level increased. Greene et al. (1985) showed that with H₂ reburning, most of the reduction in NO occurred in the final stage after final air addition and a minor effect of temperature was detected. The results of Myerson (1975) and Miyamae et al. (1986) suggested that more complex hydrocarbons would be more effective reburning fuels, possibly due to greater generation of CH_i radicals.

The effect of nitrogen content in the reburning fuel is of great interest in the application of reburning on a large scale in coal fired utility boilers, since it would be desirable to divert a portion of the primary coal stream and to inject it as reburning fuel. Various studies have shown that an increase in the nitrogen content in the reburning fuel would reduce the effectiveness of the reburning process (Kelly et al., 1986; Mulholland and Hall, 1986; Chen et al., 1986; Miyamae et al., 1986; Greene et al., 1985). This is expected, since part of the nitrogen in the reburning fuel would be converted to nitrogenous species, which increases the total fixed nitrogen pool in the reburn zone. The volatility of the nitrogen in the reburning fuel was also shown to have an effect on reburning effectiveness. Greene et al. (1985) compared reburning with coal to reburning with propane doped with ammonia to the same nitrogen content as in the coal. Better results were obtained with gaseous reburning fuels. Mulholland and Hall (1986) also showed a dependence on the nature of the nitrogen content in the reburning fuel by comparing NH₃ and pyridine as additives to natural gas. However, Chen et al. (1986) reported that the conversion of the total nitrogen, from the primary zone and that introduced with the reburning fuel, was insensitive to the fuel type. The researchers proposed that introducing fuel nitrogen into the system with the reburning fuel would effectively be similar to proportional increases in primary NO levels. A similar observation was made by Greene et al. (1985). The focus of the studies described above, was on the overall outcome of reburning. Consequently, the effect of reburning fuel type and nitrogen content on nitrogenous species formation and destruction in long time scales in the reburn zone was not fully examined.

1.5.5 Mixing in the Reburn Zone

Reburn fuel mixing with the primary effluent is an important factor in the reburning process. Mixing can limit NO destruction by hydrocarbon radicals that are generated from the secondary fuel, since mixing affects the contact of the primary NO with the reburning fuel. Also, mixing affects the contact of the reburning fuel with the oxygen from the primary zone and consequently, the decomposition of the reburning fuel to reducing radicals. Therefore, it is expected that improved mixing would produce greater destruction of NO in

reburning. This has been suggested in the works of several researchers (Chen et al., 1986; Kolb et al., 1988; LaFond and Chen, 1987; Miyamae et al., 1986; Overmoe et al., 1986).

Overmoe et al. (1986) tested different fuel jet velocities and suggested that reburning effectiveness would increase with jet penetration and mixing. In addition, mixing effects were found to increase the effect of primary NO concentrations. Similar observations were reported by Chen et al. (1986), in examining the effects of mixing on natural gas reburning in a 3 MW down-fired pilot scale combustor. These results clearly demonstrated an improvement in reburning effectiveness with improved mixing conditions in the reburn zone. However, for nitrogen containing reburning fuels, Chen et al. (1986) argued that a well mixed reburn zone would create a tradeoff between reduced NO emissions and increased conversion of the nitrogen in the reburning fuel. The use of inert carrier, such as N_2 , was recommended to reduce the oxidation of the reburning fuel in large excess of oxygen (air transport) and thus, to reduce the conversion of fuel nitrogen to NO. In another study, Kolb et al. (1988) suggested that insufficient mixing would create non optimal local fuel rich and fuel lean pockets. The fuel lean pockets would not be favorable for reducing NO and the fuel rich pockets would produce more HCN in the reburn zone and more NO in the final stage. Greene et al. (1985) hypothesized that improved mixing would be beneficial to the reburning process because it would allow more hydrocarbons to interact with the primary NO before the consumption of the reburn fuel. Consequently, less fuel rich pockets would be formed in the reburn zone, less nitrogenous species and less NO in the exhaust. Furthermore, improved fuel and oxygen contact produced higher temperatures in the reburn zone. When the reburn zone was operated close to the fuel lean side, poor mixing enhanced NO reduction.

The impact of mixing is more severe as the scale of the system increases, because of the larger distances across which mixing must occur and it is harder to achieve adequate mixing. The results of Myerson (1975) and Miyamae et al. (1986) suggest that reburning in small, well mixed bench scale systems can create sharp dependencies on stoichiometry in the reburn zone. Also, NO reductions, higher than 80%, would be possible. Results on larger scale systems typically result in lower reburning effectiveness and a broader dependence on reburn zone stoichiometry (Lanier et al., 1986; Lanier and Mulholland, 1988). The results of Chen et al. (1986) demonstrate that successful scale up of reburning is possible, if adequate mixing conditions can be maintained in the reburn zone.

In short, poor mixing in the reburn zone can create local variations in stoichiometry which would prevent complete optimization of the reburning process. That can produce lower reductions in overall NO emissions and a broader dependence on reburn zone stoichiometry in a practical combustor, as compared to a bench scale system, where better mixing conditions can be achieved. However, poor mixing may enhance reburning effectiveness if the reburn zone is operated fuel lean or close to the fuel lean side, where the presence of fuel rich pockets can be beneficial in destroying NO (Greene et al., 1985).

1.6 Burnout Zone Parameters

In the burnout zone, air is added to complete the combustion, the remaining fuel is oxidized, and the oxidizable nitrogenous species (HCN and NH_3) are converted to NO and N_2 . The parameters that are associated with this stage are of minor significance since the overall reduction in NO is dependent on the levels and distribution of the nitrogenous species exiting the reburn zone. An important exception is the effect of temperature if it falls within the range characteristic of the Thermal DeNO_x process, and if relatively high levels of NH_3 exit the reburn zone. Under these conditions, additional destruction in NO is possible by selective reduction of NO by NH_i species (Chen et al., 1986; Greene et al., 1985). However, the low temperatures associated with this process (1100 - 1400 K) are too low for any practical application in reburning.

The results of Lanier et al. (1986) and Greene et al. (1985) indicated that not all HCN and NH_3 are oxidized to NO in the burnout zone. The conversion of these nitrogenous species to NO decreased with stoichiometry in the reburn zone and with the primary NO level. Greene et al. (1985) investigated the effects of stoichiometry and mixing in the burnout zone and showed minor effects due to variations in these two variables. Thus, there is a general agreement in the literature with respect to the minor significance of burnout zone parameters, with the exception of temperature under certain conditions.

1.7 Focus of This Work

The focus of this investigation is on the reburning process as a combustion modification technique to reduce the emissions of nitrogen oxides from combustion flue gases. Three main objectives are defined in this study. First, to investigate various aspects of the reburning process, including the effects of key reburning parameters and their interactions, the effectiveness of multiple reburning fuel injections, the effect of the primary flame mode (premixed and diffusion), and the impact of reburning on N_2O emissions. Second, to explore mechanisms that govern the inter-conversion of nitrogenous species in the fuel rich stage of reburning and to develop a predictive model that is based on fundamental kinetics, yet simple enough to allow its applications in a practical combustor. Finally, the third objective is to promote the application of the kinetic model to predict the overall reburning effectiveness, and to identify kinetic limits in achieving low levels of final NO emissions under practical combustion conditions.

1.7.1 Problem Statement

The proposed research plan (Wendt, 1986) consisted of three tasks, namely, Screening Experiments, Technology Definition, and Turbulent Diffusion Flames. The division of the tasks in this report differs from that in the proposed plan. The differences are summarized in Table 1.1.

Five tasks are undertaken in this report:

Table 1.1
Description of the Tasks.

<u>Proposed Plan</u>	<u>This Report</u>	<u>Section</u>
Task 1: Screening Experiments (premixed Configuration)	Task 1: N ₂ O Study	3.0
	Task 2: Parametric Study effect of mixing	4.0 5.1
	Task 3 (part 1): No. of Injection Points	4.6
	Reburn Zone Profiles	6.1
Task 2: Technology Definition (Premixed Configuration)	Task 4: Mechanisms Various Primary and Reburning Fuel Types Model Development	6.0 7.0
	Task 5: Model Applications	8.0
	Task 3 (part 2): Type A Flame	5.2
Task 3: Turbulent Diffusion Flame		

Task 1

This task focuses on nitrous oxide (N_2O) concentrations in combustion flue gases under various coal combustion configurations, including reburning. The primary purpose of this examination is to demonstrate the effectiveness of reburning in reducing NO emissions with no significant increases in N_2O emissions. Thus, a technique is developed for N_2O analysis and is used to measure N_2O concentrations in combustion flue gases under various conditions.

Task 2

This task involves a parametric investigation of reburning. The preceding literature review demonstrates the complexity of the reburning process, as a result of the large number of variables that are associated with it. These variables have been examined by a large number of researchers, using reburning configurations that varied in size and method of operation. Many of these variables are dependent on one another, making it difficult to examine the effect of each variable separately. Thus, many questions remain unanswered, such as the effect of stoichiometry and how it interacts with other reburning parameters. Furthermore, temperature has been identified as a significant variable in the reburn zone, but its effects have not been fully characterized, especially, in view of the effects of other parameters. The interdependence of the effects of different process parameters can explain some of the conflicting results in the literature. In order to compare the results of previous studies, it is necessary to examine the effect of each process parameter separately, in addition to interaction effects between pairs of variables.

A statistical approach is undertaken to conduct a parametric study of reburning. The objective is to identify the significant variables in reburning, to examine the effects of these variables, and to identify optimum or near optimum conditions that can be applied in a practical combustor. Statistically designed experiments are used to derive empirical correlations relating reburning effectiveness to operating parameters. This approach is complemented by detailed tests in which one variable is varied at a time. This combination can yield greater insight and understanding of reburning.

Task 3

This task is concerned with the examination of reburning under conditions that can provide a broader understanding of the process. Specifically:

1. The feasibility of a reburning configuration in which the reburning fuel is split into multiple streams is examined in an effort to improve the effectiveness of reburning. It is possible that the distribution of the secondary fuel down the combustor can provide a continuous supply of super equilibrium concentrations of free radicals to enhance the overall destruction of NO.

2. The performance of reburning in a premixed primary flame mode is compared to that in a diffusion primary flame mode. This provides insight into the application of reburning under practical conditions that exist in utility boilers.

Task 4

This task focuses on the examination of mechanisms that govern the inter-conversion of nitrogenous species in the fuel rich reburn zone and the development of a kinetic model. A screening study is essential in understanding the physical processes that are associated with reburning, but does not provide fundamental understanding, which is the motivation for this part of the study.

The inter-conversion of nitrogenous species in the gas phase has been extensively investigated by various researchers and the mechanisms are well understood. Detailed kinetic models, consisting of homogeneous gas phase reactions and the corresponding kinetic parameters, are available in the literature (Glarborg et al., 1986; Miller and Bowman, 1989). The mechanism of Miller and Bowman was successfully applied to describe gas phase nitrogen data that were derived from bench scale studies of other researchers over a wide range of conditions. However, these studies were limited to data acquisition and testing in the vicinity of the flame front and involved short time scales. None of these models has been successfully applied to describe coal nitrogen kinetics in post flame flue gases at the high temperatures and residence times characteristic of practical coal combustors.

Glass (1981) used a single homogeneous reaction ($\text{NH}_2 + \text{NO}$) to account for the observed decay in NO under fuel rich coal combustion conditions. This simple mechanism could correlate data for individual coals but was unsuccessful when applied to data from various coals (Bose et al., 1988). A more successful model was developed by Bose and Wendt (1988) in a study of the fuel rich combustion of pulverized coal. The model successfully predicted NO decay in coal post flame flue gases and HCN profiles in gaseous post flame flue gases. In another study, Knill and Morgan (1989) used a model that did not account for hydrocarbon reactions and were able to predict the destruction of both NO and HCN in the fuel rich zone for selected coal reburning experiments in an isothermal plug flow reactor.

None of the previous works yielded a mechanism that could successfully predict profiles of all nitrogenous species (NO, HCN and NH_3) in the fuel rich zone of a coal combustion configuration, such as reburning and air staging. Thus, there is still a need for a simple mechanism that can describe coal nitrogen kinetics under fuel rich conditions, which is the objective of this task. The emphasis is on understanding the mechanisms that govern the inter-conversion of nitrogenous species in the reburn zone and the development of a predictive kinetic model. Thus, the study does not involve a detailed study of kinetics or the calculation of kinetic parameters, which is beyond the scope of this work. Instead, the kinetic parameters and equilibrium data that are used in this study, are extracted from the literature without any adjustments. The applicability of the model in describing the fate

of coal nitrogen in the fuel rich zone is tested under reburning and air staging configurations.

Task 5

This task is concerned with applications of the predictive kinetic model. The ultimate goal is to develop a model that can predict final NO emissions from known process variables. Specific points of interest are:

1. To examine the effect of mixing on model predictions in the reburn zone.
2. To combine the kinetic model with correlations, both derived and taken from the literature, to allow the prediction of reburning effectiveness from known process parameters.
3. To apply the kinetic model to predict configurations for low total fixed nitrogen and to determine kinetic limits that would prevent complete destruction of nitrogenous species under fuel rich conditions.

1.7.2 Approach

The experiments are conducted on a down-fired, laboratory size combustor which allows self sustaining combustion of 1-2 kg/h coal with no external heating. The configuration is representative of practical units in terms of characteristic times and temperatures, and is well defined to allow the extraction of mechanisms. The unit is designed to bridge the gap between the more fundamental flat flame and drop tube experiments, and pilot and full scale coal combustion experiments.

The emphasis in this study is on a reburning configuration in which the primary flame is that of Utah bituminous coal in a premixed mode and the reburning fuel is natural gas. Some experiments involve other reburning configurations and are described in various parts of this study. Time resolved measurements of temperature and concentrations of O₂, CO₂, CO and NO are made for all tests. Other concentrations of HCN, NH₃, H₂ and hydrocarbons are made only in experiments that examine the kinetics of coal nitrogen in the reburn zone. N₂O concentrations are measured in selected experiments only.

2.0 EXPERIMENTAL APPROACH

This section describes the experimental facilities that are employed in this investigation. A description of the sampling and analysis techniques is also presented.

2.1 Experimental Facilities

The experimental facilities consist of an experimental combustor, a premixed burner and a diffusion burner, two volumetric coal feeders, air and natural gas supply system, and a sampling system. A description of these facilities and their applications in the various experiments is presented in the following sections.

2.1.1 Combustor Design and Construction

The experimental combustor, shown in Figure 2.1, was used in Tasks 3, 4, and 5. The combustor that was used in Tasks 1 and 2 had a similar construction, but without the inner layer of silicon carbide and with differences in the construction of the utility ports. After the completion of Task 2, it became necessary to reconstruct the furnace due to the deterioration of the inner wall. Minor modifications were implemented in the construction of the new furnace to reduce the cost and to prolong the expected service time. However, no changes in the experimental properties of the combustor, in terms of temperature and concentration profiles, were detected after reconstruction. The construction of the original furnace and the modifications that were incorporated in the new design are discussed, following a description of the salient features of the experimental combustor.

The combustor has a thermal rating of 17 kW, corresponding to a coal feed of about 2 kg/h. It is a down-fired, laboratory size combustor that allows self sustaining combustion of 1-2 kg/h of coal with no external heating. It has the time and temperature attributes of practical units, but well defined aerodynamically to allow the examination of mechanisms and the extraction of kinetic rates. The scale is an intermediate between the more fundamental flat flame and drop tube experimental units, and pilot and full scale combustion units.

The flows inside the furnace are characterized by fast diffusion in the radial direction (Taylor-Aris diffusion), resulting in flat radial concentrations (Wen and Fan, 1975). Radial measurements of temperature and concentrations, under coal combustion conditions, support this conclusion. Furthermore, the effects of axial dispersion have been shown to be negligible under the operating conditions of the combustor (Bose, 1989). Consequently, a reacting flow system inside the combustor can be modeled assuming one-dimensional plug flow behavior. Earlier works on similar combustors (Pershing and Wendt, 1977; Glass and Wendt, 1982; Wendt et al., 1979; Bose and Wendt, 1988) have shown that experimentation on a combustor of this type can relate to phenomena in practical units, especially those involving the fate of coal nitrogen. Thus, the experimental combustor is appropriate for the experimental work designed to complete the tasks that were described in Section 1.7.

The combustor that was used in Tasks 1 and 2 consisted of a fire tube, 15.2 cm in diameter, constructed from three concentric, vacuum formed, Zircar alumina cylinders. The cylinders consisted of 30.5 cm long sections, and extended over a length of 180 cm, with an outside diameter of 28 cm. A steel shell, 80 cm in outside diameter and 0.64 cm thick, surrounded the fire tube as seen in Figure 2.1. The space between the alumina cylinders and the steel shell was packed with Kaowool 2300 insulation fiber (Babcock and Wilcox) to a density of $0.14 \pm 0.02 \text{ g/cm}^3$.

Seven utility ports allowed access to the inside of the furnace for sampling, temperature measurements, or the introduction of a desired feed stream. These ports consisted of 5 cm mullite tubes connected to steel pipes, 10 cm long, and welded to the exterior of the steel shell. Gate valves and unions allowed the insertion of water cooled probes, equipped with appropriate fittings, through the desired port.

A cone, made of castable refractory, provided smooth expansion for the burning fuel at the entrance to the combustor. The cone extended from a diameter of 5 cm to 15.2 cm over a length of 22.9 cm. A 15 cm cylindrical tunnel, at the base of the furnace, connected the fire tube to a convection section, where the exhaust gases would be cooled before discharge into an exhaust hood.

Experiments for Tasks 1 and 2 resulted in the destruction of large sections of the inner lining of the experimental furnace. This was caused by the high temperatures and the erosive slagging conditions of the reburning experiments, especially in the fuel rich reburn zone, corresponding to the furnace midsection. As the coal was burned, metal rich slag diffused into the inner surface of the fire tube and eventually became a part of it. Additional usage of the combustor caused further deposition of slag on the surface. Consequently, the slag buildup became heavy, causing it to slump and collapse, taking with it parts of the furnace lining (Zircar material). As the destruction of the furnace wall became more pronounced, the support for the utility ports, consisting of 5 cm mullite tubes, became weak. Cracking of the mullite tubes and shifting of the port locations followed. This slow process eventually resulted in the reduction of the insulating quality of the fire tube wall, in addition to changes in the geometry of the furnace and the flow patterns inside it. Consequently, the rebuilding of the furnace became necessary after the completion of Task 2.

The design of the new combustor (Figure 2.1) was similar to that of the previous one. However, new features were incorporated in the new design to construct a longer lasting furnace, at a lower cost. Two modifications were included in the construction of the new combustor:

1. An inner layer of silicon carbide refractory replaced the inner layer of alumina cylinders.

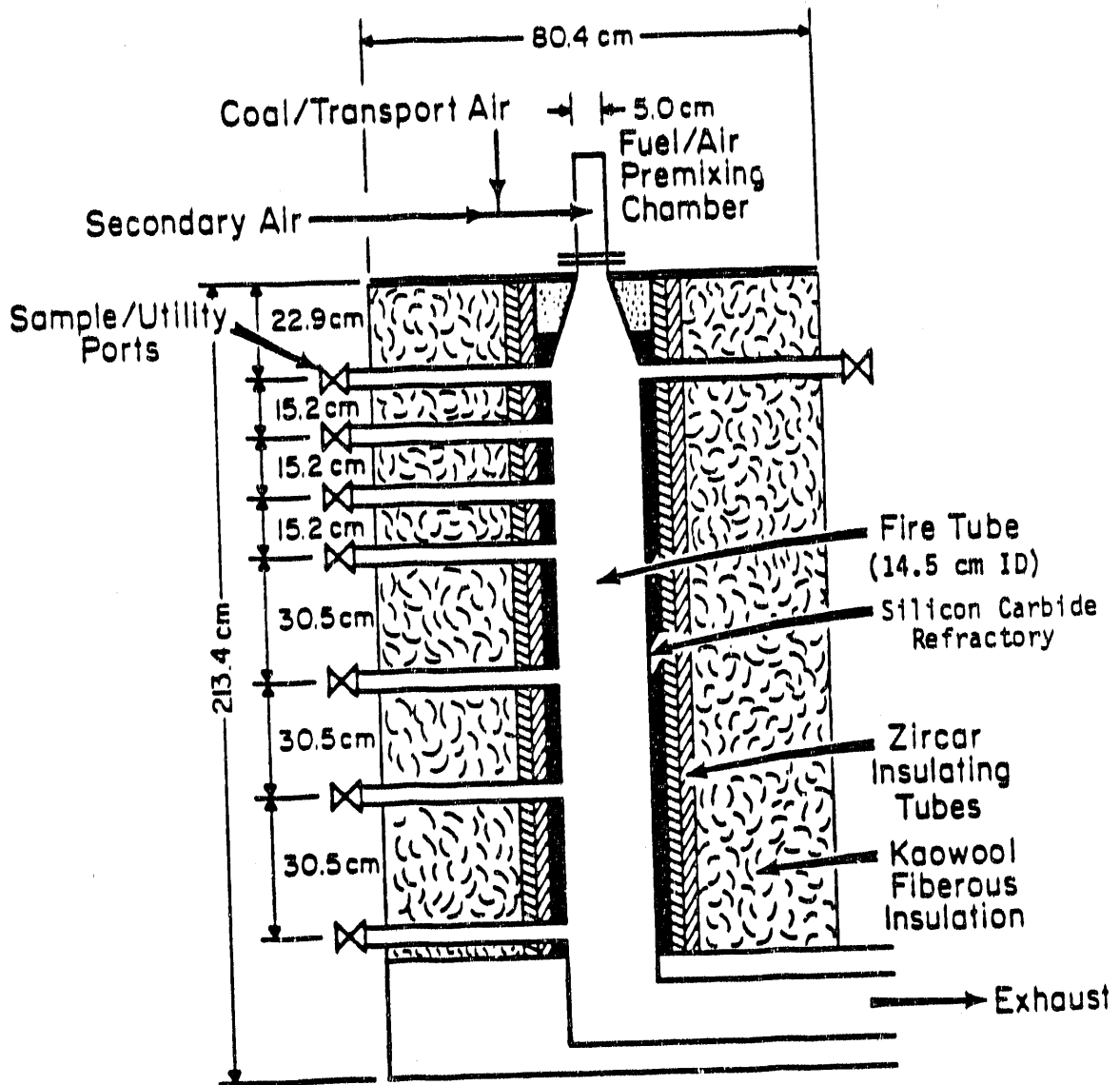


Figure 2.1. Experimental Combustor.

2. A slab was constructed to support cylindrical tunnels that would serve as utility ports instead of the mullite tubes.

The inner layer of alumina cylinders was replaced by a layer of silicon carbide castable refractory. This material provided excellent resistance to abrasion and slag, as well as protection of the two layers of the expensive Zircar, surrounding the refractory layer. Silicon carbide (Carborundum 11-LIG) was casted in place using hard cardboard forms. Information provided by the manufacturer (Sohio, Refractories Division) suggested that its low iron content of about 0.5% would assure good resistance to corrosive slag, in addition to strength that was more than 10 times that of Zircar. Thus, the silicon carbide layer provided a solid structure that prevented the bending and shifting of the fire tube. Furthermore, its non porous structure would prevent the slag from penetrating the refractory. The high thermal conductivity of silicon carbide (approaching that of alloy steel at high temperatures), would distribute slag formation uniformly over the refractory, which would act as an additional wear resistant shield.

Two layers of high purity Zircar cylinders (grade ASH, recommended to 1430 C) constituted the remainder of the fire tube wall. The space between the tube wall and the surrounding steel shell was packed with Kaowool 2300 insulation fiber (Babcock and Wilcox) to a density of $0.20 \pm 0.02 \text{ g/cm}^3$.

A slab, 11.5 cm thick, was constructed of Kaolite 2200 (Babcock and Wilcox) insulating refractory extending from the outer surface of the fire tube to the cylindrical steel shell. The purpose of this slab was to provide an alternative to the use of the expensive mullite tubes as utility ports. Cylindrical tunnels, 5.1 cm in diameter, supported by the structure of the slab and providing access into the furnace, served the same purpose, in addition to a longer expected service time.

At the top of the furnace, an expansion cone, 22.9 cm high, was made from Kaocrete 28-Li castable refractory (Babcock and Wilcox) expanding from a diameter of 5 cm at the entrance to the full 14.5 cm of the combustor internal diameter.

The new combustor had two advantages over the previous one:

1. Silicon carbide provided excellent erosive service. Consequently, the new combustor would be expected to have longer service time and reduced maintenance downtime.
2. The cost of rebuilding the combustor, estimated in April of 1989 at \$2100, was reduced by 35%.

Subsequent coal combustion experiments demonstrated that the performance of the new combustor was similar to that of the previous one, at steady state operating conditions.

No changes in temperature or concentration profiles were detected, relative to those of the previous combustor, although the measured temperatures were higher because of an improvement in the insulation quality after reconstruction.

2.1.2 Burner Design

The function of the burner is to deliver the fuel and the combustion air into the combustor and to act as a radiation shield to prevent pre-ignition of the fuel before entering the combustor. Figure 2.2 shows a description of the two types of burners that were used in this study. The majority of the experimental work in this investigation involved the use of the premixed burner. The diffusion burner was used in some tests to examine reburning phenomena downstream of an axial diffusion primary flame. The results of these experiments are presented in Section 5.2.

The premixed burner allowed thorough mixing of the air stream transporting the pulverized coal and the preheated combustion air stream, before entering the combustor. The burner consisted of a 5 cm steel pipe with two sets of perpendicular cooling water tubes near the base. Each set consisted of two perpendicular rows of tubes in which seven 0.32 cm tubes were placed 0.7 cm apart in each row. This arrangement of cooling tubes produced thorough mixing of the fuel and air mixture, and provided adequate cooling to prevent pre-ignition inside the burner.

The diffusion burner was designed to introduce the primary air stream transporting the pulverized coal into the combustor as a separate stream from the preheated combustion air. The two streams were introduced axially into the combustor as open jets. The burner consisted of a 2.5 cm steel pipe, water cooled at the base, and a water cooled fuel injector. The fuel injector consisted of three concentric stainless steel tubes, with the outermost two serving as a cooling water jacket. The injector had an inside diameter of 0.81 cm and an outside diameter of 1.59 cm. The diffusion burner was designed to produce a type A long axial diffusion flame with no swirl (Beer and Chigier, 1972). The construction of the burner allowed an axial air velocity of about 17 m/s, based on an air flow rate of 140 slm and an inlet air temperature of 590 K. The primary air feed was adjusted to produce a jet velocity close to that of the axial air, corresponding to an air flow of about 22 slm.

The two burners (Figure 2.2) represent two extremes of near field fuel/air contacting. One extreme is to have coal and all the combustion air completely "premixed," which comprises a well defined inlet mixture. The other extreme is to have coal (plus transport air) and secondary air, slowly mixed, as in long axial flames or tangentially fired boilers. The latter configuration does not lend itself to simple characterization mathematically.

2.1.3 Air and Fuel Supply System

The pulverized coal was supplied from a twin screw Acrison Model 105 volumetric feeder. A variable speed motor allowed the control of the feed rate. Feed problems were

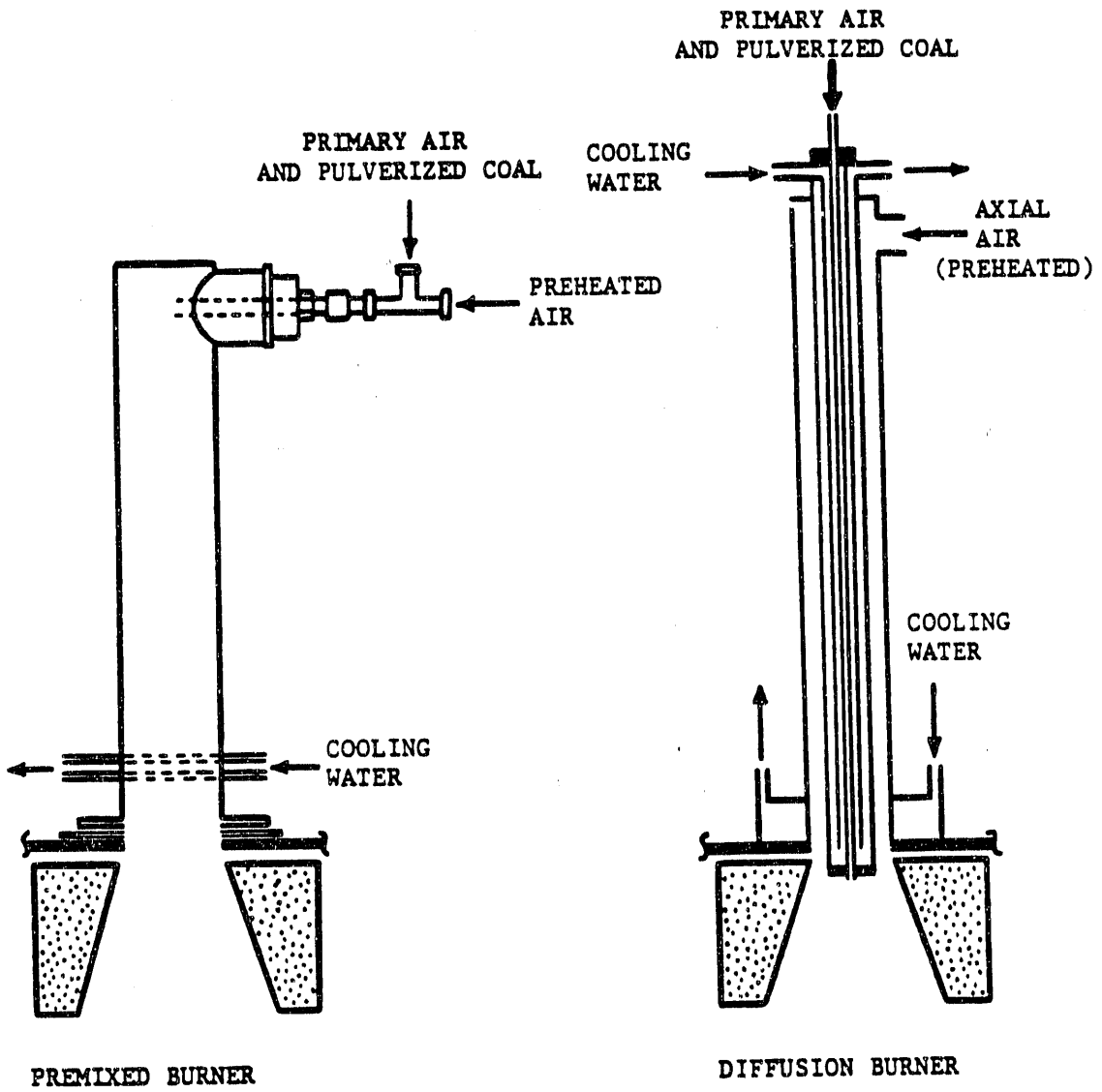


Figure 2.2. Premixed and Diffusion Burners.

minimized by placing the feeder directly above the burner, attaching one pneumatic vibrator to the side of the hopper to prevent channeling, and another at the outlet of the feeder to dampen coal pulsing. The coal feed was calibrated with coal before each experiment and periodically at the end of the experiment to verify the accuracy of the feed rate. Differences of less than 1% were detected in most cases. This feeder was used in all coal burning tests to supply the primary fuel into the combustor. Air flow at a rate of about 28 slm was used to transport the pulverized coal from the outlet of the feeder to the burner.

A secondary coal feeder was constructed following the design of the primary feeder. The secondary feeder was used only in reburning experiments in which coal was introduced as a reburning fuel. Calibration of the secondary feeder showed a reproducibility of about 8%. Thus, the use of this feeder was restricted to the delivery of coal reburning fuel, with N₂ transport gas at a rate of about 18 slm.

The air supply was provided from a 25 hp air compressor. The various air flows were individually regulated and measured with Meriam laminar flow elements. The main combustion air was preheated to a temperature of 590 K using a 9 kW Chromalox electrical heater. All other air flows were supplied at room temperature.

Natural gas was available from the local gas company (Southwest Gas) at a pressure of 18 cm of water above atmospheric. Natural gas was used to heat the combustor prior to burning coal, and as reburning fuel in natural gas reburning experiments. Calibrated rotameters were used to monitor the flows of natural gas.

The combustion control system was equipped with control circuits to shut off all fuel supplies to the combustor under conditions of potential safety hazards. The system was designed to shut down in cases of loss of supply air pressure or loss of the combustion flame, detected by an ultraviolet OH radical sensor. Furthermore, an emergency button allowed immediate shut down of all fuel supplies by the operator when deemed necessary.

2.1.4 Sampling System

A water cooled and water quenched sampling probe was used for in situ sampling of combustion gases. The probe consisted of three concentric stainless steel tubes, with an outside diameter of 1.27 cm and an inside diameter of 0.63 cm. The outermost two tubes constituted a water cooling jacket that allowed the introduction of the probe into the furnace. A fourth tube, 0.16 cm in diameter, extended through the inner tube, as seen in Figure 2.3. This tube was closed at one end and allowed the introduction of quench water inside the inner tube in fine jets through four 0.03 cm holes, drilled near the tip. The quench water rate was maintained between 45 and 60 cm³/min to minimize the plugging of the probe, by keeping it washed free of solid particles.

The combustion sample and the quench water mixture flow under vacuum generated by a sampling pump, to a separator where the quench water and solid particles are

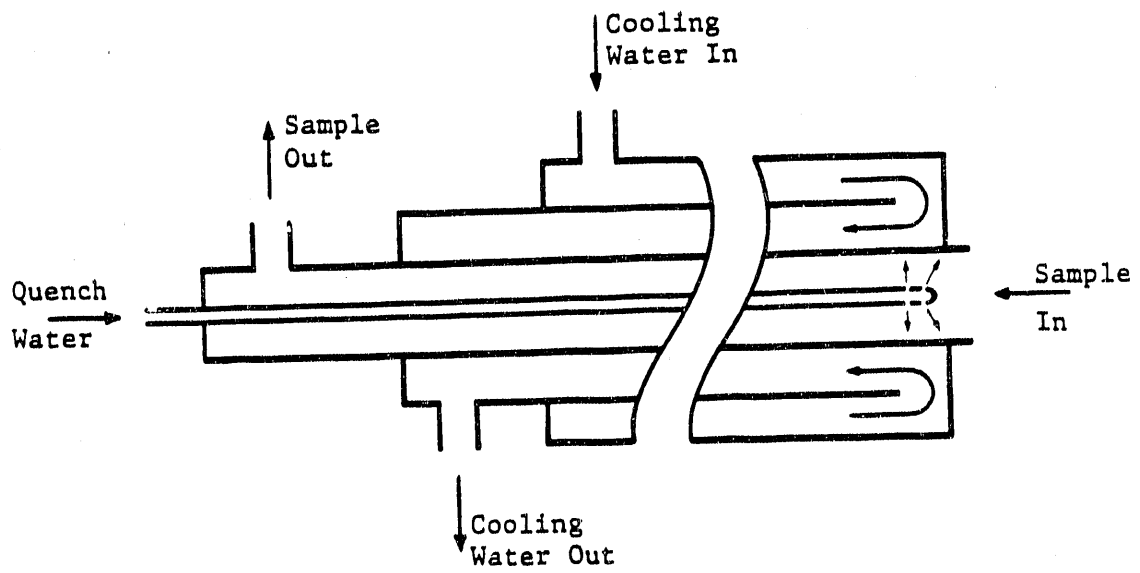


Figure 2.3. Combustion Gas Sampling Probe.

separated from the combustion gases. The quench water and solids mixture, flows through a barometric leg to a drain or to a collection container, where a sample can be collected and analyzed for NH_3 and HCN content. The combustion gases flow under vacuum through filters to remove any remaining particulates and then into a refrigerated condenser. The gases are cooled down to a temperature of 277 K and water vapor is removed. The dry and clean gases are then introduced through continuous analyzers for various measurements. The sample flow system is described in Figure 2.4. The system allows the diversion of the sample leaving the CO analyzer to the desired chromatograph, or to a bubbler where the remaining HCN in the gaseous sample can be captured and analyzed.

2.1.5 Reburning Fuel Injection System

The design of the reburning fuel injector is important, since mixing is a key variable in determining reburning effectiveness, as demonstrated in the reburning studies of Chen et al. (1986), Overmoe et al. (1986) and Kolb et al. (1988). The reburning fuel injector consisted of a water cooled, stainless steel probe and an injector tip that was sealed at the end, with several holes drilled at the sides. The injector tip consisted of a piece of stainless steel tubing, 1.3 cm long, that allowed radial flow of the reburning fuel with respect to the probe axis, through eight 0.14 cm holes.

The reburning experiments of Tasks 1 and 2 involved the introduction of the reburning fuel through the injector without a transport medium. Figure 2.5 shows the results of an experiment in which radial NO concentrations were measured before and after the injection of natural gas reburning fuel, and bituminous coal was used as the primary fuel. Radial NO measurements, prior to the introduction of the reburning fuel, produced flat radial profiles, which suggested a uniform distribution of the coal inside the fire tube. However, measured radial profiles after the introduction of the secondary fuel produced parabolic concentration profiles. That was an indication of uneven distribution of the fuel inside the reburn zone, as a result of poor mixing conditions. The extent of mixing in the reburn zone was not of interest in Tasks 1 and 2, since the focus was on the overall effect of reburning on NO destruction. Furthermore, the introduction of relatively high flows of burnout air produced adequate mixing in the final stage of reburning.

The extent of mixing in the reburn zone is of great significance in the examination of the kinetics of nitrogenous species conversions. A well mixed reburn zone is essential to validate the assumption of one dimensional plug flow behavior in the combustor. Therefore, it became necessary to modify the injection mode of the reburning fuel to generate better mixing conditions in the reburn zone. The design of the injection scheme that was used in Tasks 3, 4 and 5, evolved as a result of many tests, as described below. The objective was to produce concentration profiles that were independent of radius at the first port downstream of the reburning fuel injection point. Consequently, a study was conducted to investigate the conditions under which a well mixed reburn zone could be obtained, using

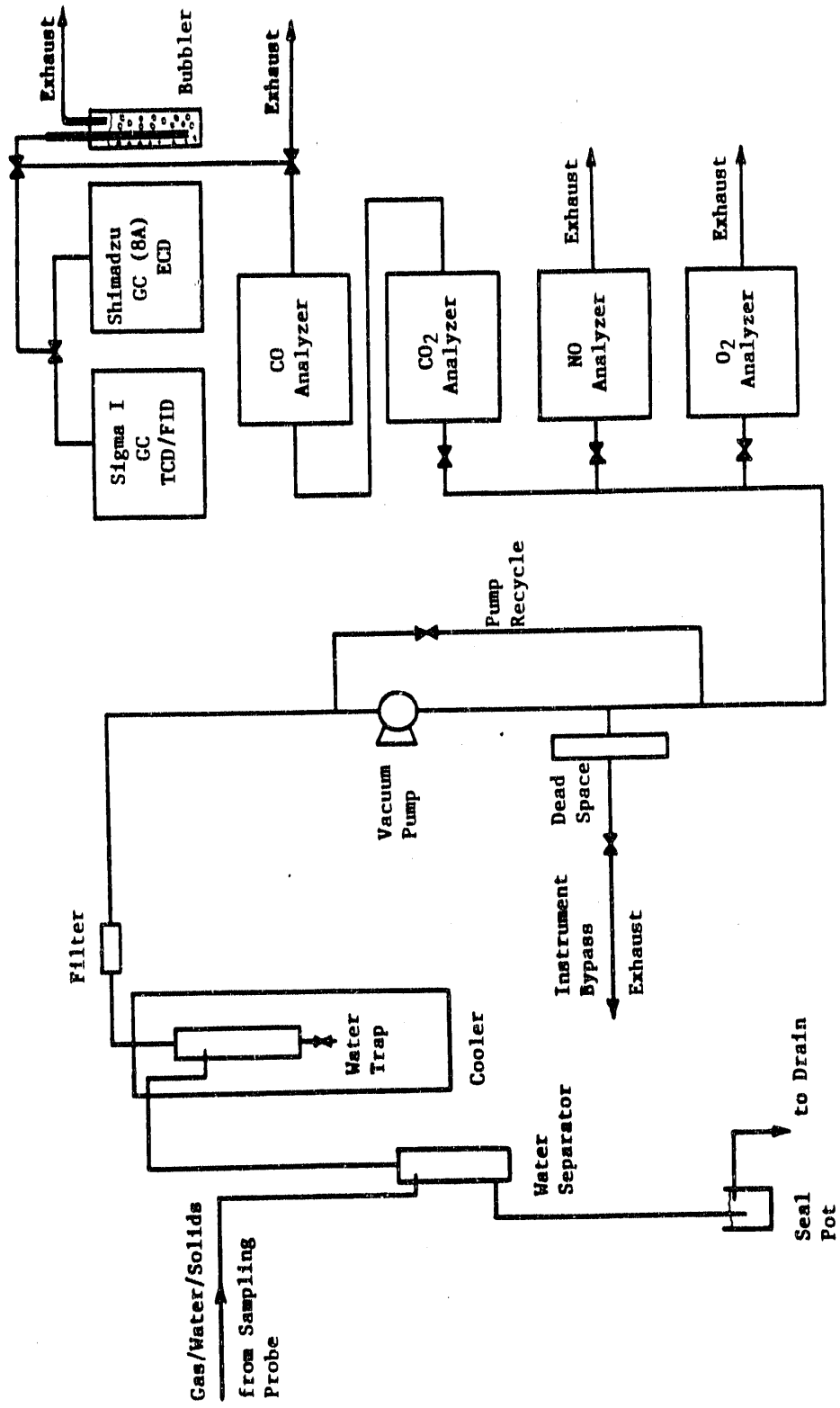


Figure 2.4. Sample Analysis System.

BITUMINOUS COAL PRIMARY FLAME, NATURAL GAS REBURNING
Reburning Fuel at Port 5
Primary SR = 1.2, Reburn Zone SR = 0.8

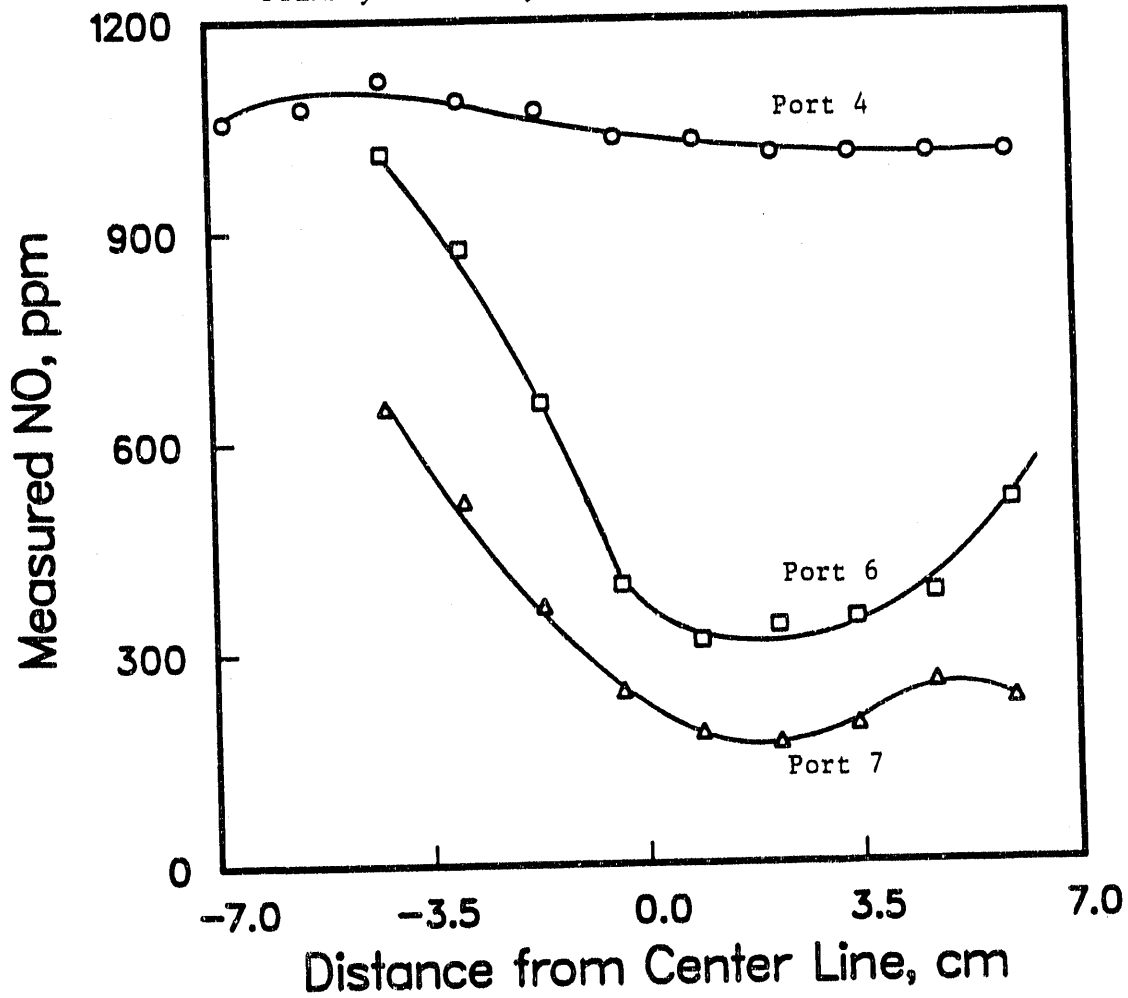


Figure 2.5. Effect of Reburning Fuel Introduction on NO Radial Concentrations.

radial measurements of NO as a guide. A variation in the radial concentration of less than 10%, with respect to an average NO concentration, was assumed to be an indication of an adequate level of mixing in the reburn zone.

Various natural gas reburning fuel injection schemes were tested, in which the length of the injector tip, the orientation (axial or radial injections), the size and the number of holes were varied. No single configuration produced the desired level of mixing in the reburn zone (Figure 2.6). Other configurations, in which two injectors were used, each introducing half the amount of the reburning fuel into each side of the furnace, were also unsuccessful (Figure 2.6). In other words, all configurations that involved the introduction of the reburning fuel without a transport medium produced parabolic radial concentration profiles downstream of the injection point. Consequently, it became necessary to introduce an inert gas (N_2) with the reburning fuel to produce higher jet velocities. Figure 2.7 shows the progress of these tests.

The final configuration for natural gas reburning fuel injections involved the use of the same injector as in the previous reburning experiments, but variable amounts of N_2 gas were added to the reburning fuel to produce hole exit velocities that were at least 70 times the bulk primary flue gas velocity (1 m/s). This configuration produced adequate mixing within 0.18 seconds, beyond which radial profiles demonstrated that the furnace did exhibit plug flow behavior, as far as concentration profiles were concerned. Thus, mixing effects were limited to the region in the reburn zone between the point of reburning fuel introduction and the first port downstream of the injection point. Mixing complications were of minor significance in the remainder of the reburn zone.

The effects of improved mixing conditions in the reburn zone on reburning effectiveness are discussed in Section 5.1.1. The examination of mechanisms that govern the inter-conversion of nitrogenous species in the reburn zone and the development of a kinetic model, are restricted to the well mixed region of the reburn zone, as discussed in Sections 6.0 and 7.0. The modification of the kinetic model to account for mixing effects in early time scales of the reburn zone is discussed in Section 8.1.

2.2 Analytical Techniques

The analytical systems employed in this study consist of continuous analyzers, two gas chromatographs, and an ionalyzer. The continuous analyzers allowed continuous on-line monitoring of O_2 , CO, CO_2 , and NO concentrations. The gas chromatographs were used for H_2 , CH_4 , C_2H_2 , C_2H_6 , and N_2O analyses. The ionalyzer was used for wet chemistry analysis, in which HCN and NH_3 concentrations were measured using ion and gas specific electrodes, respectively.

BITUMINOUS COAL PRIMARY FLAME, NATURAL GAS REBURNING

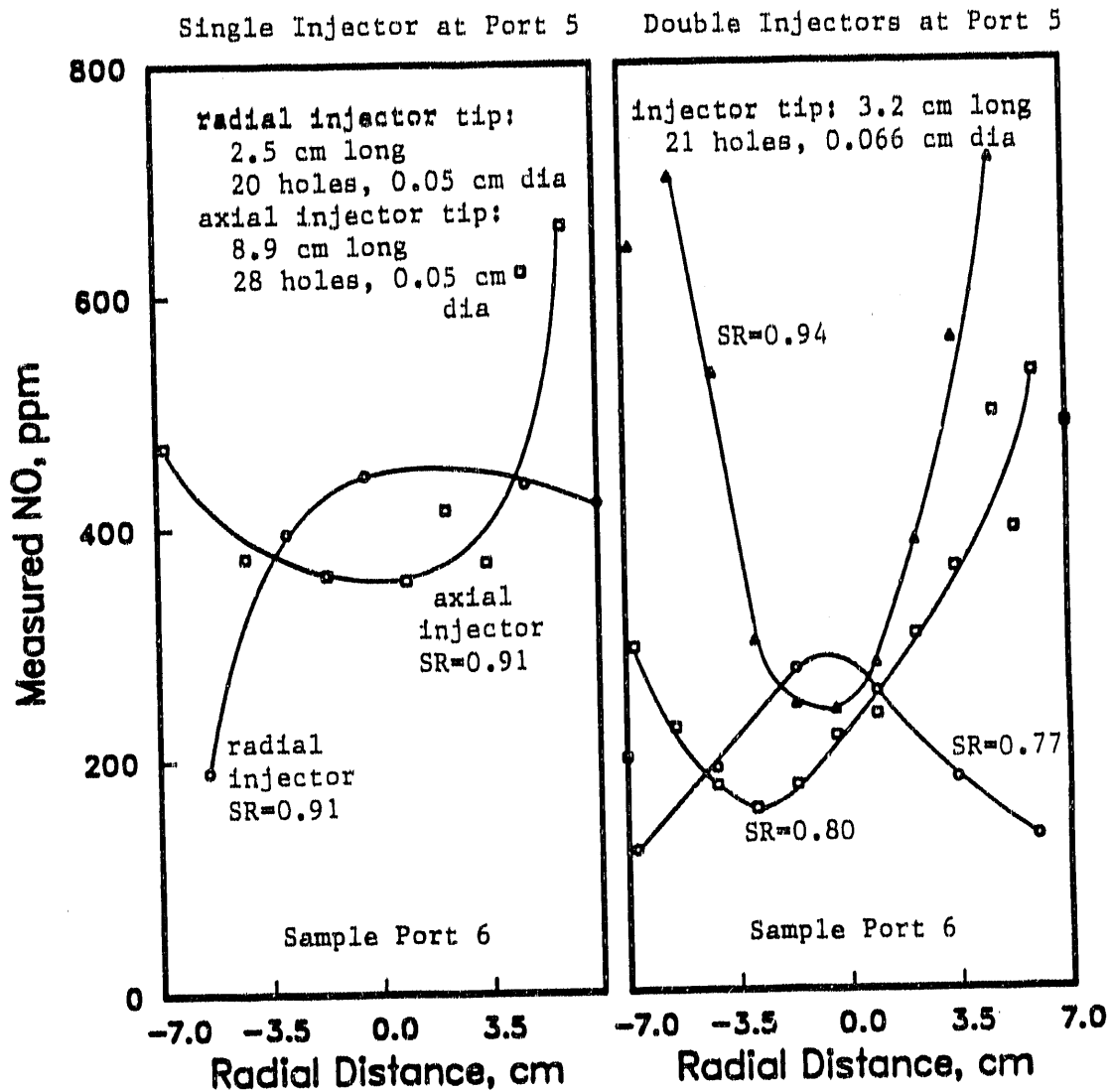


Figure 2.6. Effect of Reburning Fuel Injection Mode on NO Radial Concentrations.

BITUMINOUS COAL PRIMARY FLAME, NATURAL GAS REBURNING
 Reburning Fuel at Port 5, Sample Port 6
 Axial Injections, Tip: 3.2 cm long, 21 holes, 0.1 cm dia

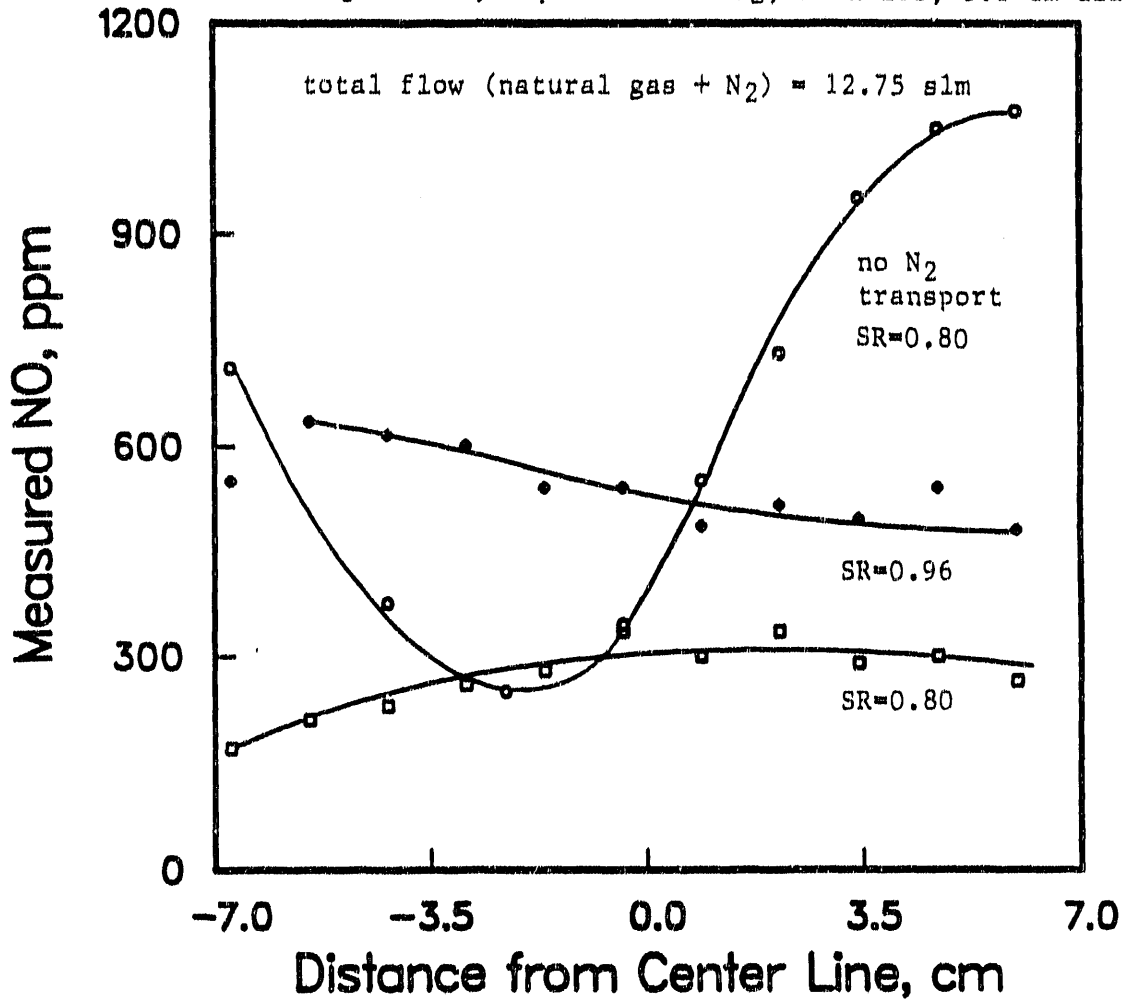


Figure 2.7. Effect of Introducing N₂ Gas with Reburning Fuel on NO Radial Concentrations.

2.2.1 Continuous Analyzers

Four continuous analyzers were available for on-line measurements of O₂, CO, CO₂, and NO concentrations during an experiment. The combustion gases were introduced as separate streams to each instrument. A bypass line and rotameters equipped with needle valves allowed the regulation of the sampling flow rate to each instrument, as seen in Figure 2.4.

Oxygen concentration was measured using a Beckman Paramagnetic Model F3 O₂ analyzer. The instrument measures the magnetic susceptibility of a gas sample, determined mainly due to the presence of O₂ which has strong paramagnetic properties. The NO_x gases in the sample also have magnetic properties, but their concentrations in combustion flue gases are in the ppm range, and would have a negligible effect on O₂ measurements.

Two Beckman Infrared Model 864 analyzers were used to measure CO and CO₂ concentrations. In these instruments, one infrared beam is directed through a sample cell and another beam of equal intensity is directed through a reference cell. The difference in the absorbed infrared energy between the two cells is a measure of the concentration of the component gas (CO or CO₂) in the sample.

A Thermal Electron Model 10 AR analyzer was used to measure NO concentrations via chemiluminescence. The instrument consists of an ozone generator, in which ozone is produced from dry air, and a reaction chamber where the ozone can react with NO to produce NO₂ in an excited state. The excited NO₂ molecules decay to the ground state, emitting light of a certain frequency (chemiluminescence). The intensity of the light is measured on a photomultiplier tube and is directly proportional to NO concentration in the sample.

The continuous analyzers were calibrated before each experiment, using N₂ gas to establish a zero setting, and certified Matheson calibration gases. Three separate calibration gases were used for O₂, CO/CO₂, and NO measurements.

2.2.2 Gas Chromatographs

A Perkin-Elmer Model Sigma I gas chromatograph was used to measure H₂ and hydrocarbon concentrations. The chromatograph was equipped with a Thermal Conductivity Detector (TCD) and a Flame Ionization Detector (FID), and had two columns. H₂ was separated on a 5A molecular sieve column (45/60 mesh) at 413 K and TCD temperature of 473 K. Hydrocarbons were separated on a Porapak T column (60/80 mesh) at 413 K and FID temperature of 523 K. Only three hydrocarbon species were detected and measured, namely, CH₄, C₂H₂ and C₂H₆. The concentrations of C₂H₆ were always less than 0.01% and were often ignored. Argon was used as a carrier gas at a flow rate of 60 cm³/min through each column. Each column was 180 cm long with an outside diameter of 0.32 cm.

A Valco 10-port pressure actuated switching valve with two 1-cm³ sample loops would first inject a sample into the molecular sieve column. Forty five seconds later, a second sample would be introduced into the Porapak column. The sample intake pressure was maintained at 15.5 cm Hg above atmospheric. The retention times for H₂, CH₄ and C₂H₂ were 18, 67 and 97 seconds, respectively, after the start of the analysis. A calibration curve was prepared for each measured species before data acquisition on an experimental day. Certified Matheson calibration gases were used, diluted to the desired concentration with N₂ gas. In all cases, linear responses were obtained with respect to all concentrations.

The analysis for N₂O was by gas chromatography and electron capture detection. Techniques for N₂O measurements, unlike those of most other combustion gases, require certain precautions to protect the detector and to ensure reproducibility of the analysis. An Electron Capture Detector (ECD) is one of the most sensitive detectors used in gas chromatography and is highly selective to electron capturing compounds, such as O₂ and N₂O. The ECD cell contains a radioactive source which is oxidized in the presence of O₂ in the cell. Consequently, the sensitivity of the detector can be severely reduced if samples containing significant amounts of O₂ are analyzed. Furthermore, the presence of CO₂ in combustion flue gases may interfere with N₂O analysis due to co-elution. Thus, it was necessary to develop a reliable and reproducible technique for N₂O sampling and analysis, and to investigate possible interferences of other combustion gases with N₂O measurements. The development of an analytical technique to measure N₂O concentrations is described in detail in Section 3.3.1 and only a brief description is presented here.

The instrumental setup consisted of a Shimadzu GC-8A gas chromatograph equipped with ECD, a Valco 6-port sampling valve with 1-cm³ loop, a Supelco High Capacity Heated Gas Purifier for O₂ and H₂O removal from the carrier gas, and a Supelco OMI-1 indicating tube for O₂ and H₂O detection. N₂O was separated on a Porapak Q column (80/100 mesh) at 308 K and ECD temperature of 523 K. The column, 365 cm long and 0.32 cm in diameter, was periodically conditioned at 493 K. A gas mixture of argon and 5% CH₄ was used as the carrier gas at a flow rate of 20 cm³/min through the column. The analysis was calibrated using a certified Matheson calibration gas containing 95 ppm N₂O, diluted to the desired concentration with N₂ gas.

2.2.3 Gas/Ion Electrodes

The analyses for HCN and NH₃ in the combustion gas sample were based on aqueous phase measurements of CN⁻ and NH₃, using an Orion Model 901 Ionalyzer, an Orion cyanide ion specific electrode and an Orion ammonia gas specific electrode. The ionalyzer allowed direct reading of concentrations in the aqueous phase after proper calibration. The procedure for calibration and analysis was as recommended by the manufacturer. Standard solutions of 100 ppmw CN⁻ and 1000 ppmw N, diluted to the desired concentration with distilled water, were used for calibration.

A quench water sample of about 250 ml was collected at the end of the barometric leg. The sample was vacuum filtered and divided into two parts, 100 ml each. Then, 1 ml of 10 M NaOH solution was added to each part to stabilize CN^- and NH_3 in solution, by adjusting the pH to about 13. One portion was immediately analyzed for NH_3 using the ammonia electrode. About 0.1 g of CdSO_4 was added to the other portion to precipitate any sulfides in solution, which would interfere with the silver in the cyanide electrode and affect CN^- measurements. The sample was then stored in a sealed container for CN^- analysis at the end of the experiment. The storage time (less than 10 hours), created errors that corresponded to less than 1 ppmv of HCN in the gas phase, due to the stability of CN^- ions in basic solutions. However, it was necessary to analyze the sample for NH_3 as soon as possible, after the collection of the quench water sample, to prevent loss of NH_3 . In all the tests, the analysis for NH_3 was done within five minutes after the collection of the sample.

Quench water sampling would be expected to capture over 95% of the NH_3 in the gaseous sample (Bose, 1989). In order to verify this high recovery of NH_3 , the gas sample from the exhaust of the CO analyzer (Figure 2.4) was directed to a bubbler containing 100 ml of distilled water. Analysis of the water for NH_3 accounted for less than 2 ppmv of NH_3 in the gas phase which, would be of minor significance, considering that the detection limit of the instrument was about 1 ppmv of NH_3 . Nevertheless, the quench water captured only 50-70% of the HCN in the gas phase. Thus, it was necessary to direct the dry gas sample through a bubbler containing 100 ml of 0.1 M solution of NaOH to capture the remaining HCN. The metered gas sample from the exhaust of the CO analyzer was used for this purpose. A second bubbler proved unnecessary and recovered less than 1 ppmv HCN, which was below the instrumental detection limit. Thus, HCN that was not absorbed in the quench water was captured in the basic solution in the bubbler.

The concentrations of the HCN and NH_3 in the combustion gas phase can be calculated from measured concentrations of CN^- and NH_3 in the aqueous phase, and a molar balance. The calculation for NH_3 is as follows:

$$\begin{aligned} \text{molar rate } \text{NH}_3, \text{ gas phase} &= \text{molar rate } \text{NH}_3, \text{ aqueous phase} \\ (\text{mole fraction } \text{NH}_3, \text{ gas}) * (\text{gas molar rate}) &= \\ (\text{mass fraction } \text{NH}_3, \text{ solution}) * (\text{aqueous volumetric rate}) / 17 \end{aligned}$$

The mole fraction in the gas phase gives the desired concentration of NH_3 . The gas molar rate can be calculated from known temperature, pressure and metered sample flow rate, using ideal gas law. The mass fraction of NH_3 in the solution is the measured concentration in the aqueous phase. The aqueous volumetric rate is calculated from metered quench water rate and assuming a density of 1 g/ml.

A similar calculation can be made for HCN. If the measurement is based on a sample taken from the bubbler, the aqueous volumetric rate is calculated by dividing the volume of the solution in the bubbler (100 ml) by the time allowed for the gas sample to flow through the bubbler.

2.3 Temperature Measurements

Gas temperature measurements were made using a bare, type R (Pt / Pt-13% Rd) thermocouple, supported in a water cooled holder. The thermocouple probe could be introduced into the furnace at the desired location through one of the utility ports. The wire connection to the thermocouple could be moved inside the probe to allow radial measurements of temperature. However, temperature changes in the radial direction were less than 20 K over a radial distance of 10 cm. Thus, in this study, it was assumed that temperature changes were in the axial direction only.

The measured thermocouple temperature would not be the true gas temperature due to radiation heat losses to the cooler walls of the furnace. In a combustor of a similar construction to the one used in this study, Bose (1989) measured a difference of less than 20 K between gas and wall temperatures and showed that corrected gas temperatures were always less than 35 K higher than measured values. The correction was based on a local heat balance around the thermocouple, combined with a heat balance down the combustor. The measured and corrected temperatures of Bose were correlated and the corrections were extrapolated to the temperatures that were measured in this study. Temperature differences of less than 10 K were calculated. This crude analysis led to the assumption that the measured gas temperatures could be used as the actual gas temperatures in this study and only minor errors would be introduced.

2.4 Fuel Analysis

Utah Bituminous coal was used in all experiments involving coal flames except for one experiment in which a Beulah Lignite coal was burned to compare N_2O emissions with those of bituminous coal. Utah Bituminous #2 coal was used in Tasks 1 and 2, and Utah Bituminous #3 coal was used in Tasks 3, 4 and 5. Table 2.1 shows the proximate and ultimate analysis for all three coals that were used in this study. The analyses were carried out by Desert Analytics in Tucson, Arizona.

The natural gas composition, shown in Table 2.1, was based on information provided by the local gas company, Southwest Gas, in January of 1987.

Table 2.1.
Fuel Composition.

Pulverized Coal Composition:

Proximate Analysis	% Moisture	% Ash	% Volatile Matter	% Fixed Carbon
Beulah Lignite Low Na	18.64	10.22	38.14	33.00
Utah Bituminous #2	1.71	6.81	48.11	43.37
Utah Bituminous #3	2.07	10.18	45.65	42.10

Ultimate Analysis	%C	%H	%N	%S	%O	%Ash
Beulah Lignite Low Na	54.93	3.86	0.72	2.09	24.47	11.07
Utah Bituminous #2	70.42	5.04	1.47	0.62	16.25	6.91
Utah Bituminous #3	70.58	5.09	1.30	0.27	11.84	10.46

Natural Gas Composition:

Gas	%Volume
CH ₄	92.66
C ₂ H ₆	3.71
N ₂	2.19
C ₃ H ₈	0.61
CO ₂	0.55
C ₄ H ₁₀	0.20
C ₅ H ₁₂	0.05

3.0 N₂O EMISSIONS FROM COAL COMBUSTION

The objective of the work reported in this section is to examine the significance of N₂O emissions in coal combustion and to determine the effect of combustion modification techniques for NO_x control (air staging and reburning) on N₂O emissions. This section also describes the development of a technique for N₂O measurement by gas chromatography and electron capture detection. This analysis technique is used to measure N₂O concentrations in combustion flue gases, under various coal combustion configurations.

3.1 Environmental Impact of N₂O

In the last decade, there has been increasing concern over N₂O emissions into the environment. The atmospheric concentration of N₂O is increasing at a rate of 0.18-0.26% per year, with a present concentration of about 0.3 ppm (Weiss, 1981). There are no known atmospheric sinks for N₂O, which has a lifetime greater than 100 years (Lanier et al., 1986b).

Nitrous oxide is a trace gas that contributes to the destruction of the ozone in the stratosphere. The depletion of the ozone layer is a major environmental concern, since it would allow increasing amounts of ultraviolet radiation to reach the Earth's surface. This presents potential health problems, in addition to potentially serious effects on agricultural production. The role of N₂O in the depletion of ozone in the stratosphere is through its reaction with O radicals to produce NO, which initiates an ozone destruction cycle (Lanier et al., 1986b). Nitrogen oxide gases released by processes such as coal combustion, are reactive in the atmosphere and do not reach the stratosphere where ozone is present. However, the relatively stable nature of N₂O allows its transport into the stratosphere, where it can initiate ozone destruction reactions.

The implication of N₂O as a contributor to the greenhouse effect is another environmental concern. The greenhouse effect is often associated with the phenomenon of global warming, usually attributed to increasing CO₂ concentrations in the atmosphere. The contribution of N₂O to this effect is due to its ability to absorb infrared radiations, which are normally transparent in the atmosphere (Lanier et al., 1986b). This acts as a heat trap which reduces the cooling of the Earth's surface in what is commonly known as the greenhouse effect.

3.2 Combustion Sources of N₂O

There is some dispute whether combustion is a major source for the increase of N₂O concentrations in the atmosphere. The rise in ambient N₂O concentration correlates with the rise of fossil fuel combustion activities, as well as with measured increases in ambient CO₂ concentration (Lanier et al., 1986b). Hao et al. (1987) presented evidence implicating fossil fuel combustion as a significant source of N₂O. The data suggested that direct N₂O emissions from fossil fuel combustion could exceed 100 ppm. In another study, Kramlich

et al. (1989) proposed that significant formation of N_2O would be possible in combustion flue gases, due to the release of fuel nitrogen from fossil fuel in the cooler regions of a combustor. A narrow temperature range (1150-1500 K) was identified, in which N_2O formation would be favorable. However, the researchers reported direct N_2O emissions that were lower than 10 ppm in the combustion of bituminous coal at various stoichiometries.

The role of coal combustion as a source of N_2O emissions was further complicated by the recent discovery of a sampling artifact (Muzio and Kramlich, 1988), which raised questions regarding the validity of the data base on N_2O emissions from coal combustion prior to 1988. The use of containers to store combustion flue gas samples for subsequent analysis was shown to introduce errors in N_2O measurements. The researchers demonstrated that N_2O could be produced from NO inside the container, in the presence of O_2 , SO_2 and water vapor, during storage periods as short as two hours. Container sampling was commonly used in field testing, which required the collection of a sample for subsequent analysis for N_2O at a different location. This might explain the high N_2O emissions that were measured in coal and oil combustion flue gases, but not in gas flame flue gases (Kramlich et al., 1989).

The data gathering phase, as described in section 3.3, was initiated before the discovery of the sampling artifact. Regardless, the sampling technique that was employed in this study was not affected by any known artifact. However, it became necessary to reconcile previous data with the results presented here. Furthermore, the discovery of the sampling artifact required a re-evaluation of combustion sources of N_2O and of the various studies of N_2O in the literature that involved container sampling. Linak et al. (1990) examined on-line emission measurements of N_2O from coal fired utility boilers, laboratory and pilot scale combustors, based on the work of different research groups. Direct N_2O emission levels were less than 5 ppm, when no combustion modification for low NO emissions was applied. In addition, no direct relationship was observed between NO and N_2O emissions, which is in contrast with the conclusions of Hao et al. (1987) who proposed a constant molar ratio relating NO and N_2O emissions. However, the researchers did not rule out an indirect relationship between NO emissions and the global increase in N_2O concentrations.

In summary, recent studies have shown that direct N_2O emissions from coal combustion are of minor significance, and N_2O levels less than 10 ppm would be expected in combustion flue gases. Also, N_2O can be produced in storage containers in the presence of NO, O_2 , SO_2 and water vapor at concentrations typical of those in coal combustion flue gases. Thus, on line sampling of N_2O is essential to eliminate the possibility of N_2O formation in the combustion gas sample outside the combustor.

3.3 N₂O Measurements

The recent discovery of a sampling artifact (Muzio and Kramlich, 1988) suggested a dependence of N₂O measurements from combustion flue gases on the sampling technique. Subsequent studies of direct N₂O emissions from coal combustion (Kramlich et al., 1989; Linak et al., 1990) showed that these emissions were of minor significance under practical conditions. However, Kramlich et al. (1989) proposed the possibility of significant formation of N₂O in coal post flame flue gases under conditions that would allow the transport of HCN into the cooler regions of the combustor, where N₂O could be produced under fuel lean conditions. The researchers hypothesized that imperfect mixing and coal char would be two possible suppliers of HCN, a precursor to N₂O formation. Thus, although N₂O emissions from coal combustion were judged to be of minor significance in recent studies, these observations were based on limited data. Consequently, it became necessary to verify the findings of other researchers under the experimental conditions of this study. Furthermore, the influence of NO_x control technologies on N₂O emissions has not been fully examined.

An examination of the issues described above requires the development of a reliable and reproducible technique for N₂O measurements. The development of this technique is described and is followed by a presentation of experimental results, in which N₂O concentrations are examined under various coal combustion conditions, including air staging and reburning configurations.

3.3.1 Analytical Technique

In this study, all N₂O measurements involved on-line sampling as described in section 2.1.4, and the analysis was performed using gas chromatographic separation and electron capture detection. The sample was withdrawn through a water quenched and water cooled stainless steel sampling probe. Then, the gas sample was passed through a water separator and a refrigerated condenser, through filters and CO and CO₂ non dispersive infrared analyzers, and through the gas chromatograph sample loop. The chromatograph was equipped with a 6 port sampling valve in which the sample could be injected manually from a 1 cm³ sample loop. Figure 3.1 shows a typical chromatogram and a list of the instrumental parameters. The response of the detector to trace amounts of O₂ and N₂O in the sample demonstrates the extreme sensitivity of the ECD to these compounds. However, the presence of O₂ in the sample would oxidize the ⁶³Ni foil in the detector, which would reduce the sensitivity of the ECD with time. The choice of Ar/CH₄ mixture as the carrier gas was based on the conclusions of previous works (Lanier et al., 1986b; Kramlich et al., 1987). Nitrogen gas would not be a suitable choice for carrier gas because the sensitivity of the detector would then depend on other trace impurities in the carrier gas. Furthermore, the separation of CO₂ and N₂O peaks might be more difficult to achieve using N₂ as a carrier

Instrumental Parameters:

Sampling: On-line
Instrument: Shimadzu GC-8A gas chromatograph
Column: Porapak Q, 365 cm x 0.32 cm, stainless steel conditioned at 493 K
Oven Temperature: 308 K
Detector: Electron Capture, ^{63}Ni at 623 K
Carrier Gas: Argon - 5.22% CH_4 at 20 cm^3/min
Carrier gas passes through a carrier gas purifier for $\text{O}_2/\text{H}_2\text{O}$ removal and an indicating tube for $\text{O}_2/\text{H}_2\text{O}$ detection before entering the column
Sample: 1 cm^3 loop at 15.5 cm Hg above atm intake pressure
Calibration Gas: 15.14% CO_2 , 1% O_2 , 95 ppmv N_2O , balance N_2
Recorder Input Voltage: 1 mV

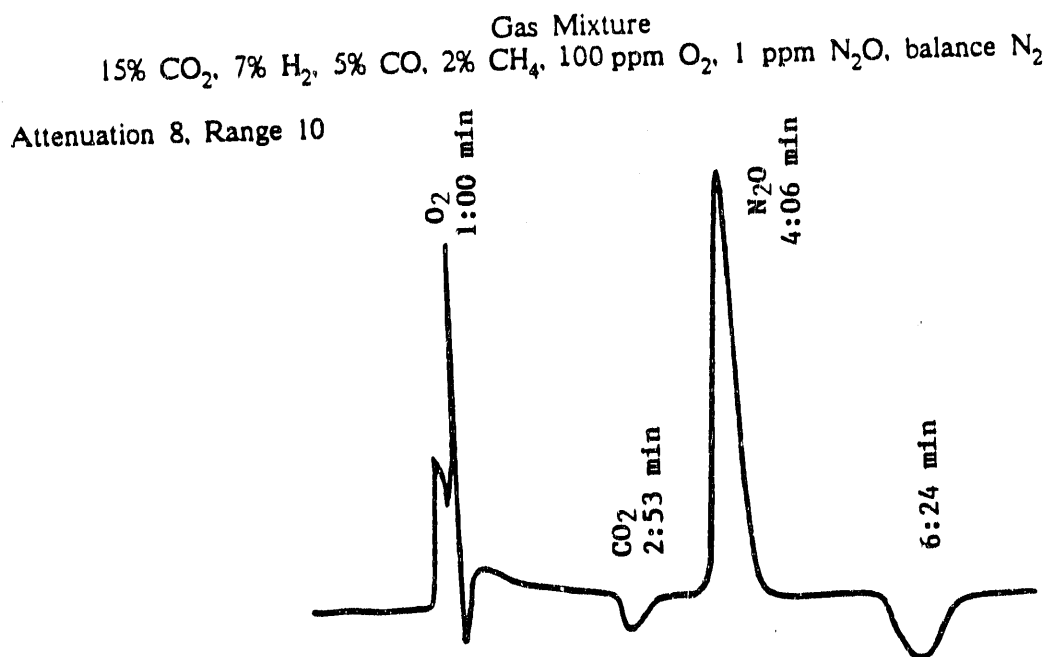


Figure 3.1. Sample Chromatogram for N_2O Analysis by Gas Chromatography and Electron Capture Detection.

gas, which might interfere with N_2O measurements. Such an interference was not observed when an Ar/CH_4 mixture was used as a carrier gas (Kramlich et al., 1987). The carrier gas was passed through a purifier to remove traces of O_2 and water vapor and through an indicating tube for O_2 and H_2O detection before entering the gas chromatograph.

A calibration gas containing 95 ppmv N_2O (Figure 3.1) was used after dilution with N_2 gas to the desired concentration. A typical calibration curve is shown in Figure 3.2. N_2O response was linear in the 30-95 ppm range and non linear at concentrations lower than 30 ppm. The detection limit for N_2O was about 0.1 ppm and consecutive tests were reproducible with a maximum difference of 3%. The calibration held to within 3% over five days of testing and column memory effects were not observed. However, after about three weeks of usage, reduced sensitivity of the detector was observed, since the presence of O_2 in the gas samples caused partial oxidation of the ^{63}Ni foil in the detector cell. A lower detection temperature of 523 K was later employed to reduce the damaging effects of O_2 in the sample. The sensitivity of the detector at 523 K was reduced by a factor of about six, compared to that at 623 K, but was necessary to extend the life time of the ECD.

A set of measurements was performed to examine the effect of the presence of CO_2 , H_2 , CO , CH_4 , O_2 and NO gases on N_2O response. This was accomplished by dilution of the calibration gas with other gases containing known quantities of various combustion gases. The effect of water vapor on N_2O response was also examined by passing the calibration gas through a bubbler and/or a drying tube. The calibration curves that were obtained were not different from those in which N_2 gas was used for dilution. No measurable interference by CO_2 or any other combustion product was observed.

Calibration was conducted before and after an experiment and the column was periodically reconditioned (after 40 tests), by raising the oven temperature to 493 K for at least 15 hours. Carrier gas flow through the detector was maintained at all times to minimize the contamination of the ECD by air diffusion from the atmosphere.

To summarize, a reliable and reproducible analytical procedure was developed for on-line N_2O analysis. This procedure was used to measure N_2O concentrations in coal combustion flue gases under various conditions.

3.3.2 Experimental Results

Various experiments were conducted in which N_2O (and NO) concentrations were measured in coal combustion flue gases under various configurations. The objective was to evaluate the role of coal combustion as a source of N_2O and to determine the effect of NO_x control techniques, such as air staging and reburning, on N_2O emissions. The effect of stoichiometry on NO and N_2O emissions was also examined in the combustion of a bituminous coal and a lignite coal.

Figure 3.3 shows exhaust NO and N_2O values as a function of stoichiometry in the

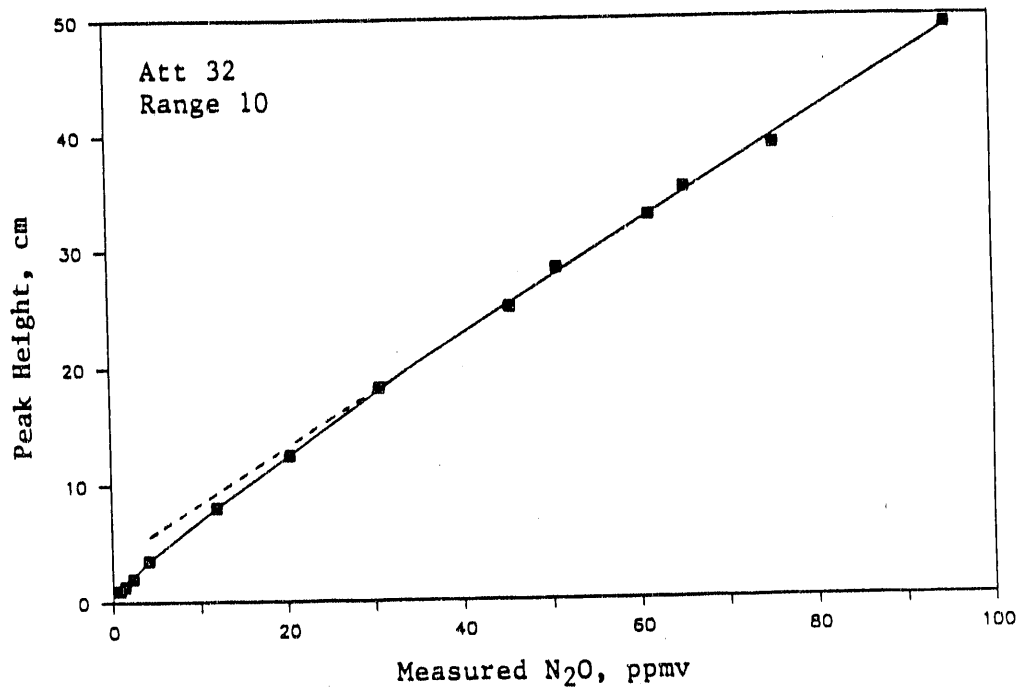


Figure 3.2. Typical Calibration Curve for N₂O Analysis by Gas Chromatography and Electron Capture Detection.

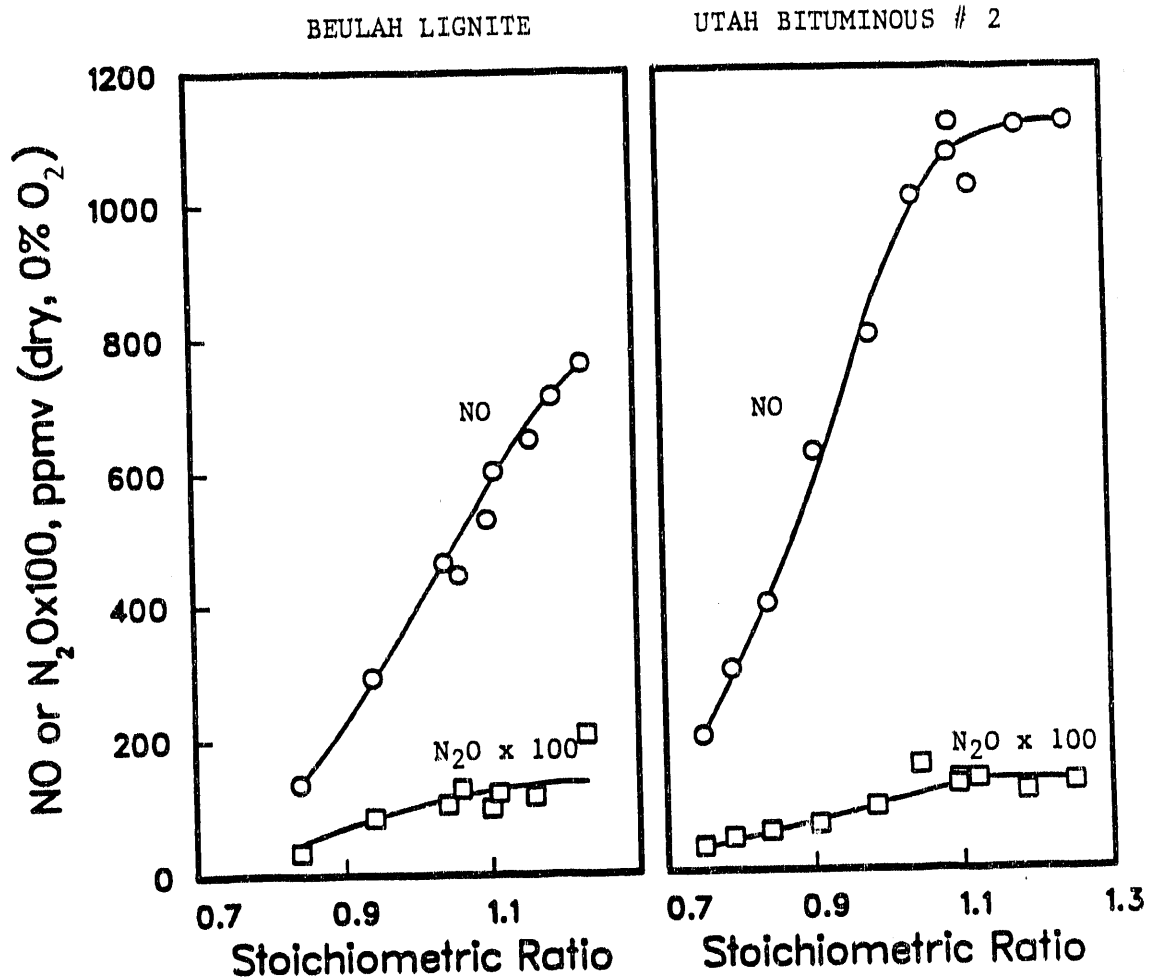


Figure 3.3. NO and N₂O Concentrations as a Function of Stoichiometric Ratio.

combustion of two coals, a bituminous coal and a lignite coal. In both cases, N_2O levels increased with increasing stoichiometry, but were always less than 2 ppm and significantly lower than those reported by Hao et al. (1987). Similar trends were observed by Kramlich et al. (1989), although N_2O levels as high as 9 ppm were obtained at a stoichiometry of 1.25. The researchers suggested that N_2O emissions would be lower at richer stoichiometries, since higher concentrations of H radicals would be present and would enhance N_2O destruction due to $N_2O + H$ reaction.

Residence time resolved profiles of NO and N_2O are shown in Figure 3.4 at three different stoichiometries. Again, lower N_2O levels were detected at lower stoichiometries. The variation of N_2O values with residence time would be difficult to examine since these values were less than 2 ppm.

Figure 3.5 shows residence time resolved profiles of NO and N_2O during air staging for two experiments at different stoichiometries in the fuel rich zone and a final stoichiometry of 1.1. In both cases, an increase in N_2O level was detected after the staging point, followed by slow decay of N_2O to a lower level. The increase in N_2O levels after air addition was higher at richer stoichiometries in the fuel rich zone. Similar observations were reported by Kramlich et al. (1989) after air addition in coal reburning experiments. This was attributed to the release of char nitrogen into cooler regions of the combustor, where N_2O formation would be favored, through reaction paths initiated by HCN. However, final N_2O levels were still exceedingly low (less than 4 ppm) and the increase in N_2O after air addition would not be of practical significance.

Figure 3.6 shows residence time resolved profiles of NO and N_2O during a typical natural gas reburning experiment. The addition of natural gas reburning fuel reduced both NO and N_2O levels. However, final air addition was followed by an increase in N_2O levels, similar to that observed under air staged conditions. This is in contrast with the natural gas reburning results of Kramlich et al. (1989), who measured lower levels of N_2O after the application of reburning, relative to uncontrolled emissions. The researchers proposed that complete char burnout before the point of gas addition might account for the reduction in N_2O exhaust concentration, since less N_2O precursors would be present at the air staging point. Nevertheless, in all cases, N_2O levels were less than 8 ppm and the effect of natural gas reburning on N_2O emissions would not be of practical significance. An increase in N_2O levels might be possible under coal reburning conditions, depending on process conditions and temperature profiles.

3.4 Summary of N_2O Study

On-line measurements of N_2O concentrations in coal combustion flue gases showed that N_2O levels increased with stoichiometry, but uncontrolled emissions were always less than 2 ppm. These levels increased after air addition in air staging and reburning configurations, but measured values of N_2O did not exceed 10 ppm. Figure 3.7 presents a summary of the effect of air addition, downstream of a fuel rich zone, as in air staging and

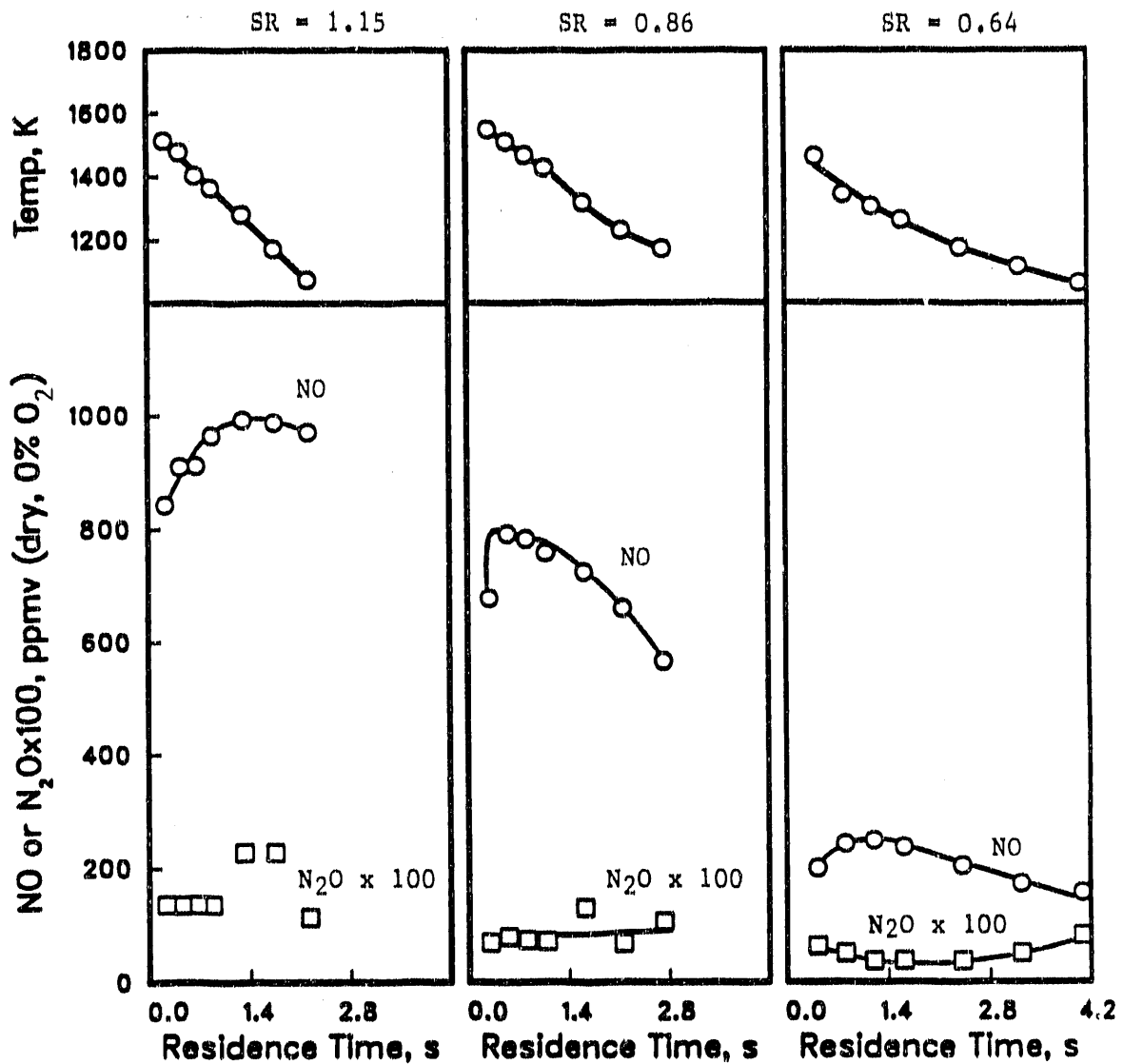


Figure 3.4. NO and N₂O Concentration Profiles at Various Stoichiometric Ratios - Bituminous Coal Flame.

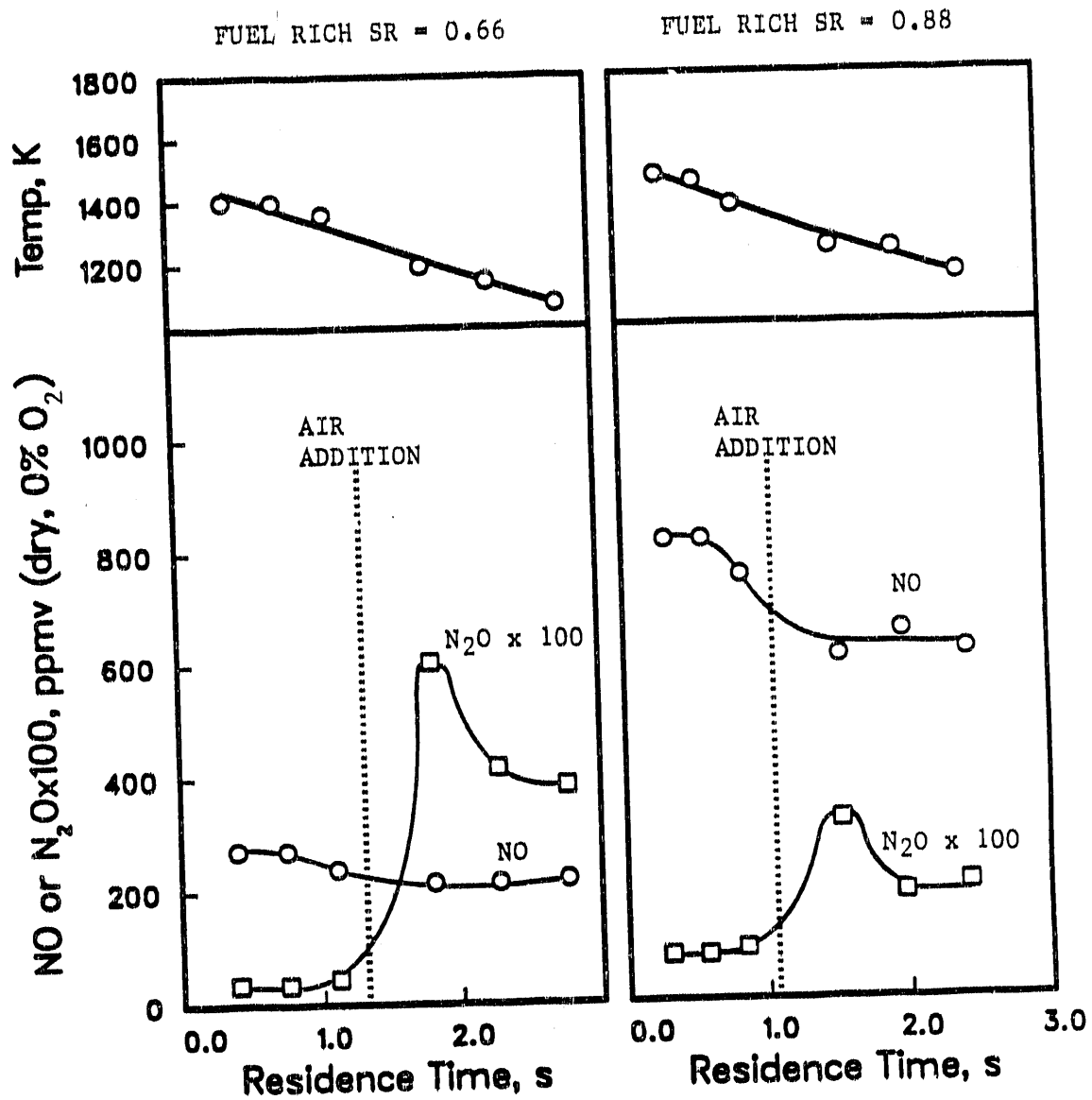


Figure 3.5. NO and N₂O Concentration Profiles - Air Staged Combustion of Bituminous Coal.

FUEL RICH SR = 0.90 FINAL SR = 1.10

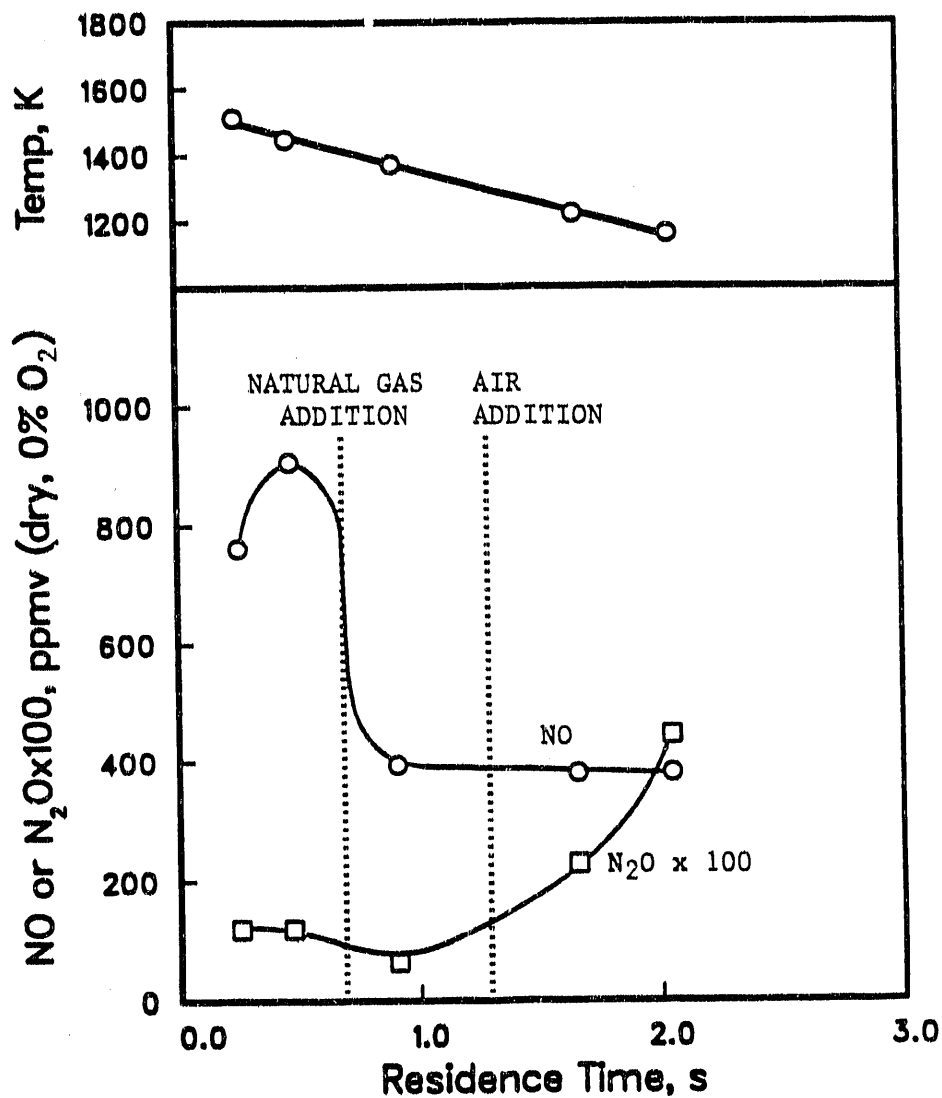


Figure 3.6. NO and N₂O Concentration Profiles - Natural Gas Reburning and Bituminous Coal Primary Flame.

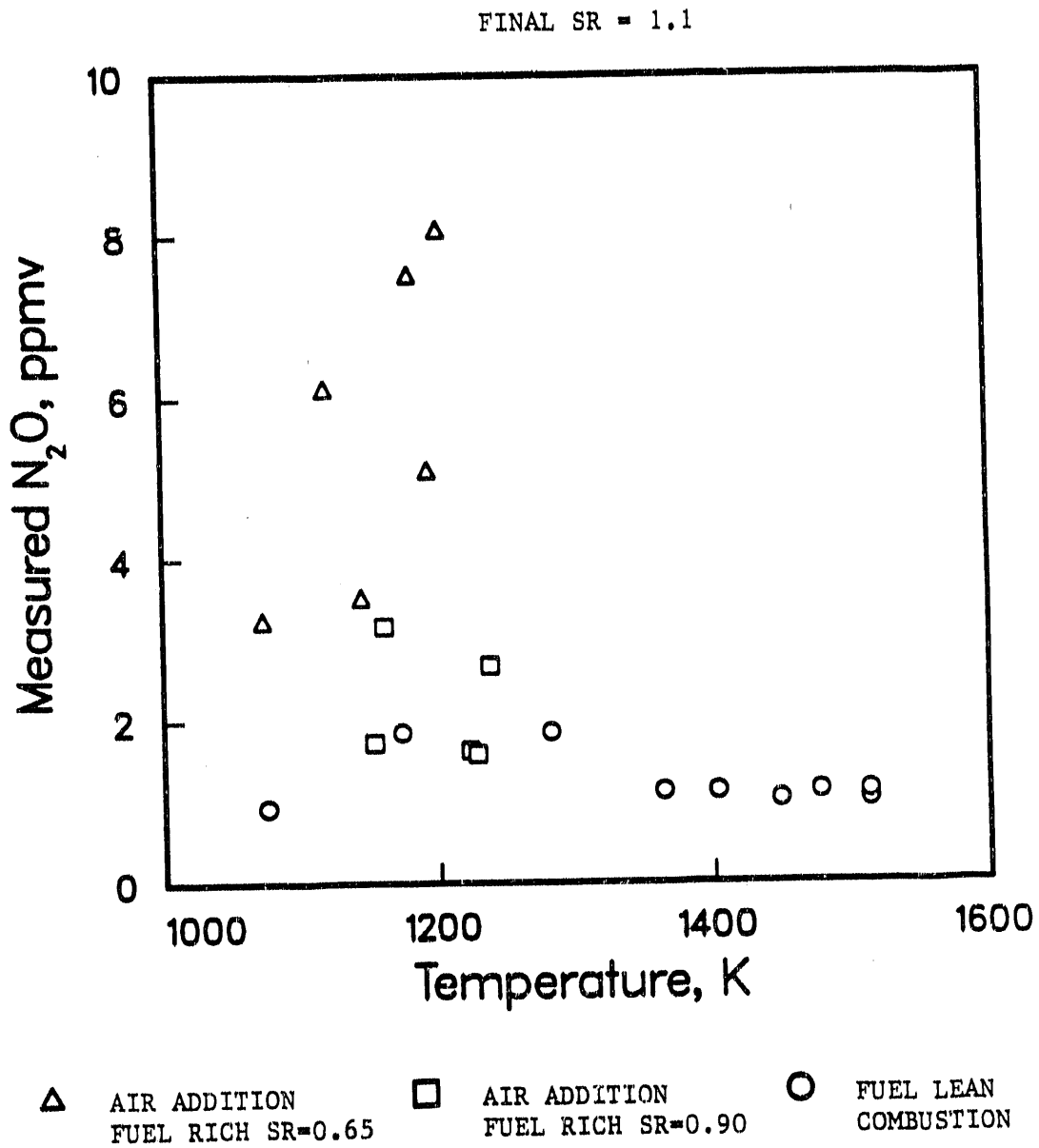


Figure 3.7. Effect of Air Addition on N₂O Emissions - Bituminous Coal Flame.

reburning configurations. Measured N_2O values are shown at various temperatures. The effect of air addition on final N_2O emissions depends on the stoichiometry of the fuel rich zone. These results support the hypothesis that HCN is a precursor to N_2O formation under fuel lean conditions, as proposed by Kramlich et al. (1989). Nevertheless, under practical combustion conditions, N_2O emissions are of minor significance, even under combustion modification conditions for low NO_x emissions (air staging and reburning) and N_2O levels less than 10 ppm would be expected. The effects of temperature and residence time on N_2O profiles could not be fully examined in this study, since the N_2O concentrations were too low to suggest any measurable trends. The results reported here, combined with those of others, have been incorporated into the paper by Linak et al. (1990), which dealt with the role of fossil fuel combustion on global N_2O emissions.

4.0 PARAMETRIC STUDY OF REBURNING

In this section, a parametric study of reburning is conducted to examine the effect of process variables on the effectiveness of reburning in reducing NO concentrations. The objectives are to identify the significant variables that affect the outcome of reburning, and to examine the effect of each variable separately. Furthermore, it is desired to define optimum or near optimum conditions under which reburning can be most effective. The bulk of the screening study consists of a statistically designed parametric investigation, in which empirical correlations are derived to relate reburning effectiveness to process parameters. This approach is coupled with detailed tests to allow a better understanding of the reburning process.

4.1 Introduction

Reburning is a complex process involving a large number of variables, that are associated with each of the three stages of the process. Many of the experimental variables are interdependent and thus, the effect of one variable cannot be easily isolated from other effects. In order to compare the reburning results of this investigation to those of others, it is necessary to examine the effect of each variable separately. Furthermore, an understanding of the individual effects of the reburning parameters might explain some of the conflicting results in the literature, such as the effects of temperature and stoichiometry in the reburn zone. Temperature effects have not yet been fully established. The results of Myerson (1975), Lanier (1984) and Greene et al. (1985) suggest that higher reburn zone temperatures might enhance reburning effectiveness. However, a close examination of the data indicate that these conclusions may not be generally valid. The effect of temperature seems to vary with stoichiometry and lower temperatures might enhance reburning effectiveness if the reburn zone is close to the fuel lean side. In general, observations of lower NO emissions at lower fuel rich zone temperatures, have been attributed to selective NO reduction by NH_i species (Thermal DeNO_x). Consequently, the interaction between temperature and stoichiometry in the reburn zone needs to be further examined.

An efficient method to examine the effects of different reburning parameters is to employ a statistically correct design of experiments. A parametric study, based on a statistical design, involves a small number of tests, compared to a parametric study in which only one variable is varied at a time. In addition, empirical correlations derived from a statistical design allow further flexibility in examining the different variables and their interactions.

The variables that are of interest in this investigation are: stoichiometries, temperatures, residence times, and primary NO concentration. Some variables were clearly shown in previous works to have minor or no effect on reburning effectiveness under

practical conditions, and were not included in the analyses. Examples are residence times in the primary zone and in the burnout zone, and the stoichiometry after final air addition. The results of tests RA#9, 10, 13, 14 and 15 (Appendix B) verify the minor effect of final stoichiometry on reburning effectiveness.

4.2 Statistical Design of Experiments

Statistical methods can be used to design experiments, in which various factors are varied over an experimental range of interest, and the effects of these factors and their interactions can be predicted. A response is the desired outcome of the experiment and is determined by the values of the controlled variables of the process. A controlled variable is a parameter that can be changed from one level to another, without a change in any other parameter. In a statistical design, the desired response can be expressed as a continuous function in terms of the controlled variables that determine the value of the response.

One of the methods employed in the statistical design of experiments is referred to as response surface experimentation (Bradley, 1958; Davies, 1956; Hicks, 1982; Hunter, 1958; Linak et al., 1987). The concept of a response surface involves a response and several measurable variables, which can be related by an empirical correlation based on an experiment involving a minimal number of tests. This is an efficient method, since it can provide information about the optimum or near optimum of the response surface. This method incorporates some features of factorial design and uses multiple regression to derive a relationship between the response and the controlled parameters in the experimental region of interest. The following functional relationship is proposed between a response y and factors x_1, x_2, \dots, x_k , affecting that response:

$$y = \sum_{i=0}^k b_i x_i + \sum_{i=1}^k \sum_{j=1}^k b_{ij} x_i x_j$$

where x_0 is always unity and k is the number of the controlled variables. The coefficients, b_i and b_{ij} , can be estimated using a multiple regression procedure, based on the principle of least squares. In least squares curve fitting, the sum of the squares of the difference between the measured response and the response predicted by the correlation, is minimized. In the above relationship, it is assumed that effects of order higher than the second can be ignored.

A factorial experimental design is an arrangement of tests, such that all the levels of a given factor are combined with all the levels of every other factor in the experiment (Davies, 1956; Hicks, 1982). The result is a combination of all possible treatment levels, corresponding to n^k number of tests, where n is the number of levels for each factor and k is the number of factors. It is obvious that the complexity of the design and the number of tests increase rapidly as the number of levels increase. The simplest form of a factorial

design is one that corresponds to 2^k tests, in which each factor has two possible levels throughout the experiment. In this form, the two levels of each factor correspond to predetermined low and high values and determine the experimental range of the design. The advantages of a factorial arrangement of experiments are:

1. It is more efficient than methods in which the factors are varied individually, one at a time, and requires fewer experiments.
2. All observations can be used in evaluating all effects.
3. The experiment can be designed to cover the experimental range of interest.

An example of a 2^3 factorial is shown in Table 4.1, with the low and high settings of each variable coded as -1 and +1, respectively. The scaling of all variables, to vary from -1 to +1, is designed to give equal weight to each variable by eliminating numerical bias due to possible differences in numerical magnitudes among the different variables. However, the main purpose of the scaling is to generate orthogonal vectors from the first order variables, x_i , and their interactions, $x_i x_j$, as seen in Table 4.1:

$$\sum_{m=1}^N x_i = 0 ; \quad \sum_{m=1}^N x_i x_j = 0 ; \quad \text{for } i, j = 1, 2, \dots, k ; \quad i \neq j$$

where k is the number of variables (3 in this example) and $N = 2^k$ is the number of tests. A factorial design can produce an empirical correlation based on variables, x_i , and their interactions, $x_i x_j$. However, the design cannot account for second order variables, x_i^2 , since these variables are indistinguishable, with a value of +1.

In general, orthogonality of variables can be obtained for equally spaced increments of the controlled variables. This is always true in a 2^k factorial, where each variable has only two levels. The property of orthogonality has some advantages in the derivation of empirical correlations:

1. The predicted coefficients of first order effects and their interactions would be independent of each other and thus, individual effects can be estimated independently. Furthermore, the magnitude of each coefficient is an indication of the significance of the corresponding effect.
2. Second order effects can be added to the derived correlation if a quadratic trend is desired, independently of the effects already included in the model.

The tests in a factorial arrangement can be used to generate empirical correlations, using a multiple regression procedure and the principle of least squares. However,

Table 4.1.
Example of 2^3 Factorial Design.

Test	<u>First Order Terms</u>				<u>Interaction Terms</u>			<u>Second Order Terms</u>		
	x_0	x_1	x_2	x_3	x_1x_2	x_1x_3	x_2x_3	x_1^2	x_2^2	x_3^2
1	1	-1	-1	-1	1	1	1	1	1	1
2	1	1	-1	-1	-1	-1	1	1	1	1
3	1	-1	1	-1	-1	1	-1	1	1	1
4	1	1	1	-1	1	-1	-1	1	1	1
5	1	-1	-1	1	1	-1	-1	1	1	1
6	1	1	-1	1	-1	1	-1	1	1	1
7	1	-1	1	1	-1	-1	1	1	1	1
8	1	1	1	1	1	1	1	1	1	1

correlations based on a factorial design would include only first order effects and their interactions. Additional tests would be required if second order effects are desired in the correlation.

In summary, a statistical design based on a factorial arrangement of tests, can be used to generate empirical correlations that would include first order effects of the desired parameters and their interactions. These effects are independent of one another and thus, the derived correlation would be a convenient tool in the examination of the individual effects of each of the variables that are included in the design. However, second order effects cannot be derived from a 2^k factorial design and additional tests would be required.

4.2.1 Central Composite Design

A central composite design allows the evaluation of second order effects, in addition to first order effects and their interactions (Hunter, 1959). Thus, the design includes the components of a factorial design, in addition to tests that are selected to preserve the orthogonality features of the experimental design. Table 4.2 shows an example of central composite design for three factors. The tests of the factorial design are used to estimate the coefficients of first order effects and their interactions, and the tests of the star design are used to estimate the coefficients of second order effects. A simple choice for a value of α in Table 4.2 is 1. The advantage of a composite design is that it allows the work to proceed in stages. A correlation including first order effects and their interactions can be derived. If the coefficients of first order effects are relatively small and the coefficients of interaction effects are large, it may be necessary to expand the design to include second order effects and additional tests can be simply added.

4.2.2 Application to the Study of Reburning

A composite design is used in this study to conduct a parametric examination of reburning, in which the effects of different reburning parameters are investigated. The objectives are: to identify the significant variables, to examine their individual contributions, and to determine optimum or near optimum conditions under which reburning would be most effective. This is accomplished by generating empirical correlations, based on the statistical design, and using these correlations to generate response curves. The independent variables that are selected in this study are: stoichiometry in the primary zone (SR_1), stoichiometry in the reburn zone (SR_2), the length of reburn zone (x_1), and the coal feed rate (x_4). These are the controlled parameters of the system that can be manipulated in such a way, that a variation in one parameter can be accomplished without a change in any other parameter. It should be noted that the length of the reburn zone and the coal feed rate are specific to the experimental configuration in the study. However, these two parameters affect residence time and temperature in the reburn zone, which are dependent variables. The extension of the analysis to study the effect of dependent variables on the outcome of reburning is also discussed. At this point, it is emphasized that the formulation

Table 4.2.
Coordinates of a Central Composite Design.

	x_1	x_2	x_3
	---	---	---
2^3	-1	-1	-1
Factorial	1	-1	-1
	-1	1	-1
	1	1	-1
	-1	-1	1
	1	-1	1
	-1	1	1
	1	1	1
Star	-a	0	0
Design	a	0	0
	0	-a	0
	0	a	0
	0	0	-a
	0	0	a

of a statistical design is based on controlled variables, which can be varied independently and some of which may be experiment specific.

The low and high levels of each controlled variable were partly determined by the existing experimental configuration, and partly based on previous work. Table 4.3 shows the experimental limits of these variables and the coding equations that were applied to produce orthogonal vectors. An intermediate setting of zero was not possible for variable x_1 , since some of the existing utility ports of the experimental combustor were not equally spaced. Thus, the proposed test matrix, shown in Table 4.4 is a slight modification of the type of composite design presented in Table 4.2. Nevertheless, the orthogonality property of the matrix is preserved. The first 16 tests of the matrix correspond to 2^4 factorial arrangement and would be sufficient to compute linear relationships relating the response to the parameters. The additional 14 tests constitute a hybrid form of a star design in a central composite design and would allow a quadratic model to be formulated, as well as providing additional tests for computing the main effects and two factor interactions.

The response describes reburning effectiveness and is defined as:

$$y = 100 - 100 * (\text{NO}_{\text{exhaust}} / \text{NO}_{\text{primary}})$$

where exhaust values are after final air addition and primary values are those leaving the primary coal flame zone. NO concentrations in the exhaust and in the primary zone are on a dry basis and are corrected for dilution effects to 0% excess O_2 . The correction factor is calculated by dividing the molar rate of the flue gas at the measured location, by the molar rate corresponding to theoretical combustion at a stoichiometry of one. The calculations are as follows:

$$\text{theoretical O}_2 \text{ molar rate} = 0.01 * (\%C/12 + \%H/12 + \%S/32 - \%)/32 \\ * \text{dry coal feed rate}$$

$$\text{dry coal feed rate} = \text{coal feed rate} * (1 - \% \text{moisture}/100)$$

where the percentages are those listed in Table 2.1.

$$\text{theoretical air molar rate} = \text{theoretical O}_2 \text{ molar rate} / 0.209$$

$$\text{air feed molar rate} = \text{theoretical air molar rate} * \text{stoichiometry}$$

$$\text{theoretical flue gas molar rate at} \\ \text{stoichiometry of one} = \text{theoretical air molar rate} * 0.791 + 0.01 * \\ (\%C/12 + \%N/28 + \%S/32)$$

$$\text{actual dry flue gas molar rate} = \text{N}_2 \text{ molar rate} / \text{mole fraction N}_2$$

$$\text{N}_2 \text{ molar rate} = \text{air feed molar rate} * 0.791$$

$$\text{mole fraction N}_2 = 1 - (\text{mole fraction O}_2 + \text{mole fraction CO}_2)$$

It should be noted that under fuel lean conditions, O₂ and CO₂ are the only two major species that are measured in the dry combustion flue gas.

$$\begin{aligned} \text{correction for dilution} &= \text{flue gas molar rate} / \text{theoretical flue gas} \\ &\text{molar rate at stoichiometry of one NO}_{\text{corrected}} \\ &= \text{NO}_{\text{measured}} * \text{correction for dilution} \end{aligned}$$

Coal was burned at the desired feed rate and the inlet air was adjusted to obtain the desired stoichiometry in the primary zone. After all the instruments indicated steady state baseline conditions of stable temperatures and exhaust concentrations, natural gas reburning fuel was introduced at the desired location (port 3 or port 5). The natural gas feed rate was adjusted to produce the desired stoichiometry in the reburn zone. For all the tests, final air addition was introduced at the same location (port 6) and the final stoichiometry was maintained at 1.10. The results of the tests, corresponding to those of the statistical design are shown in Table 4.5. A description of the controlled and the derived variables, including the response, is shown in Table 4.6.

Other tests were conducted to examine the replicability of the experiments and the results are shown in Table 4.7. The average value of the experimental error, based on 10 replicated tests, was estimated at 7% with respect to the response (Y). The level of the error is used as a guide in the inclusion of the various contributions in the regression, as is discussed in the following section.

4.3 Effects of Independent Variables

The independent or controlled variables of the experimental test matrix (Table 4.5), were coded using the equations listed in Table 4.3, to generate a matrix of orthogonal vectors. A list of the coded variables is shown in Table 4.8. The derived vector for x₄ created a minor shift from orthogonality, which could not be avoided, since the coal feed rate (corresponding to x₄) could not be accurately controlled. However, the minor differences between the derived and the goal values of x₄ would not effect the general conclusions of this study.

A quadratic correlation was fitted to the data using SPSS-X (1986) multiple regression procedure. The regression program, FAC.SPS, is listed in Appendix C. The analysis accounted for linear and quadratic effects of each variable, as well as for interaction terms between pairs of variables. A quadratic term was not included for x₁, since an intermediate setting of zero was not possible.

Table 4.9 shows the final step of the regression analysis using the Stepwise method. This method evaluates the contribution of each term, in each step of the regression. The exclusion of a certain contribution by the regression is based on an evaluation of the F ratio,

Table 4.3.
Controlled Variables in the Statistical Design.

<u>Variable</u>	<u>Low Limit</u>	<u>High Limit</u>	<u>Coding Equation</u>
x_1	0.305 port 5	0.762 port 3	$(x_1 - 0.5335)/0.2285$
SR_1	1.10	1.35	$(SR_1 - 1.225)/0.125$
SR_2	0.73	0.98	$(SR_2 - 0.855)/0.125$
x_4	1.15	2.00	$(x_4 - 1.575)/0.425$

Table 4.4
The Proposed Experimental Design.

Test	x_1	SR_2	SR_1	x_4
1	-1	-1	-1	-1
2	1	1	-1	-1
3	1	-1	1	-1
4	-1	1	1	-1
5	1	-1	-1	-1
6	-1	1	-1	-1
7	-1	-1	1	-1
8	1	1	1	-1
9	1	-1	-1	1
10	-1	1	-1	1
11	-1	-1	1	1
12	1	1	1	1
13	-1	-1	-1	1
14	1	1	-1	1
15	1	-1	1	1
16	-1	1	1	1
17	-1	1	0	0
18	-1	-1	0	0
19	-1	0	1	0
20	-1	0	-1	0
21	-1	0	0	1
22	-1	0	0	-1
23	1	0	0	0
24	-1	0	0	0
25	1	1	0	0
26	1	-1	0	0
27	1	0	1	0
28	1	0	-1	0
29	1	0	0	1
30	1	0	0	-1

Table 4.5.
Experimental Data for the Statistical Design.

RUN	X ₁	SR ₁	SR ₂	X ₄	RT	NO _p	T ₁	T ₂	T ₃	Y
RS#21B	0.305	1.100	0.729	1.170	0.242	999	1496	1319	1278	58.4
RS#22A	0.762	1.100	0.980	1.170	0.904	994	1526	1438	1209	45.3
RS#18A	0.762	1.350	0.730	1.164	0.604	1064	1432	1431	1327	69.7
RS#17B	0.305	1.350	0.980	1.074	0.287	1003	1447	1314	1291	42.2
RS#21A	0.762	1.100	0.729	1.170	0.755	999	1503	1438	1277	69.6
RS#22B	0.305	1.100	0.980	1.170	0.337	994	1527	1317	1230	40.5
RS#16B	0.305	1.350	0.730	1.074	0.214	964	1419	1310	1289	49.4
RS#19A	0.762	1.350	0.980	1.164	0.705	1100	1432	1436	1320	55.4
RS# 7A	0.762	1.100	0.730	1.980	0.392	1129	1672	1617	1469	77.8
RS# 8B	0.305	1.100	0.980	1.980	0.165	1018	1672	1562	1501	22.4
RS# 1B	0.305	1.350	0.730	2.100	0.091	1138	1660	1584	1547	57.1
RS# 4A	0.762	1.350	0.980	2.100	0.337	1085	1610	1641	1555	43.3
RS# 7B	0.305	1.100	0.730	1.980	0.121	1129	1688	1589	1519	56.4
RS# 8A	0.762	1.100	0.980	1.980	0.452	1018	1664	1640	1497	30.7
RS# 1A	0.762	1.350	0.730	2.100	0.287	1138	1668	1658	1565	79.4
RS# 4B	0.305	1.350	0.980	2.100	0.126	1085	1553	1548	1530	30.3
RS#10B	0.305	1.225	0.980	1.590	0.189	982	1587	1492	1472	31.9
RS# 9B	0.305	1.225	0.730	1.590	0.142	975	1577	1496	1455	57.0
RS#14B	0.305	1.350	0.855	1.554	0.159	1040	1473	1427	1413	43.7
RS#15B	0.305	1.100	0.855	1.554	0.196	949	1562	1459	1400	36.0
RS# 6B	0.305	1.225	0.855	1.980	0.129	1093	1602	1523	1506	38.4
RS#20B	0.305	1.225	0.855	1.164	0.253	1091	1452	1320	1304	48.5
RS#13A	0.762	1.225	0.855	1.554	0.521	1032	1514	1504	1372	67.5
RS#13B	0.305	1.225	0.855	1.554	0.181	1032	1513	1407	1362	44.7
RS#10A	0.762	1.225	0.980	1.590	0.516	982	1572	1569	1485	47.7
RS# 9A	0.762	1.225	0.730	1.590	0.452	975	1551	1547	1441	76.2
RS#14A	0.762	1.350	0.855	1.554	0.459	1040	1463	1515	1444	62.1
RS#15A	0.762	1.100	0.855	1.554	0.585	949	1546	1503	1366	73.1
RS# 6A	0.762	1.225	0.855	1.980	0.377	1093	1629	1625	1489	65.7
RS#20A	0.762	1.225	0.855	1.164	0.726	1091	1485	1446	1311	73.5

Table 4.6.
Description of the Reburning Variables.

x_1 = Length of Reburn Zone in Meters

SR_1 = Primary Zone Stoichiometry

SR_2 = Reburn Zone Stoichiometry

x_4 = Primary Fuel Load in kg/h (Utah Bituminous #2 Coal)

RT = Residence Time in the Reburn Zone

NO_p = Primary NO Concentration in ppmv (dry, 0% O_2)

T_1 = Peak Temperature in the Primary Zone in K

T_2 = Temperature in Inlet to Reburn Zone in K

T_3 = Temperature at Inlet to Burnout Zone in K

Y = Response as Percent in NO Destruction by Reburning

Table 4.7.
Replicate Tests.

RUN	X ₁	SR ₁	SR ₂	X ₄	RT	NO _p	T ₁	T ₂	T ₃	Y
RS# 1A	0.762	1.350	0.730	2.100	0.287	1138	1668	1658	1565	79.4
RS# 3A	0.762	1.350	0.725	2.070	0.293	1090	1602	1631	1557	80.2
RS# 1B	0.305	1.350	0.730	2.100	0.091	1138	1660	1584	1547	57.1
RS# 3B	0.305	1.350	0.725	2.070	0.093	1090	1554	1561	1551	60.4
RS#10A	0.762	1.225	0.980	1.590	0.516	982	1572	1569	1485	47.7
RS#12A	0.762	1.225	0.980	1.554	0.574	1014	1464	1462	1347	43.3
RS#10B	0.305	1.225	0.980	1.590	0.189	982	1587	1492	1472	31.9
RS#12B	0.305	1.225	0.980	1.554	0.214	1014	1475	1354	1327	33.3
RS#11A	0.762	1.225	0.855	1.590	0.474	1032	1563	1582	1519	66.1
RS#13A	0.762	1.225	0.855	1.554	0.521	1032	1514	1504	1372	67.5
RS#11B	0.305	1.225	0.855	1.590	0.164	1032	1575	1507	1478	43.8
RS#13B	0.305	1.225	0.855	1.554	0.181	1032	1513	1407	1362	44.7
RS#16A	0.762	1.350	0.730	1.074	0.665	964	1422	1406	1308	65.7
RS#18A	0.762	1.350	0.730	1.164	0.604	1064	1432	1431	1327	69.7
RS#16B	0.305	1.350	0.730	1.074	0.214	964	1419	1310	1289	49.4
RS#18B	0.305	1.350	0.730	1.164	0.195	1064	1432	1346	1309	55.0
RS#17A	0.762	1.350	0.980	1.074	0.771	1003	1440	1424	1302	62.8
RS#19A	0.762	1.350	0.980	1.164	0.705	1100	1432	1436	1320	55.4
RS#17B	0.305	1.350	0.980	1.074	0.287	1003	1447	1314	1291	42.2
RS#19B	0.305	1.350	0.980	1.164	0.262	1100	1435	1335	1311	49.4

Table 4.8.
Components of the Statistical Design.

RUN	X_1	SR_1	SR_2	X_4	Y
-----	----	-----	-----	-----	-----
RS#21B	-1	-1	-1	-0.95	58.4
RS#22A	1	-1	1	-0.95	45.3
RS#18A	1	1	-1	-0.97	69.7
RS#17B	-1	1	1	-1.18	42.2
RS#21A	1	-1	-1	-0.95	69.6
RS#22B	-1	-1	1	-0.95	40.5
RS#16B	-1	1	-1	-1.18	49.4
RS#19A	1	1	1	-0.97	55.4
RS# 7A	1	-1	-1	0.95	77.8
RS# 8B	-1	-1	1	0.95	22.4
RS# 1B	-1	1	-1	1.24	57.1
RS# 4A	1	1	1	1.24	43.3
RS# 7B	-1	-1	-1	0.95	56.4
RS# 8A	1	-1	1	0.95	30.7
RS# 1A	1	1	-1	1.24	79.4
RS# 4B	-1	1	1	1.24	30.3
RS#10B	-1	0	1	0.04	31.9
RS# 9B	-1	0	-1	0.04	57.0
RS#14B	-1	1	0	-0.05	43.7
RS#15B	-1	-1	0	-0.05	36.0
RS# 6B	-1	0	0	0.95	38.4
RS#20B	-1	0	0	-0.97	48.5
RS#13A	1	0	0	-0.05	67.5
RS#13B	-1	0	0	-0.05	44.7
RS#10A	1	0	1	0.04	47.7
RS# 9A	1	0	-1	0.04	76.2
RS#14A	1	1	0	-0.05	62.1
RS#15A	1	-1	0	-0.05	73.1
RS# 6A	1	0	0	0.95	65.7
RS#20A	1	0	0	-0.97	73.5

Table 4.9.
Regression Results in Terms of Controlled Variables.

* * * * Multiple Regression * * * * *

Dependent Variable: Y

Variable(s) Entered on Step Number 5: $SR_1 * SR_2$

Multiple R	.95432
R Square	.91073
Adjusted R Square	.89213
Standard Error	5.21127

Variables in the Equation:

Variable	B	F	Significance of F
SR_2	-12.865562	121.898	.0000
X_1	9.369599	96.952	.0000
$X_4 * SR_2$	-4.775651	15.112	.0007
X_4	-2.332722	4.350	.0478
$SR_1 * SR_2$	2.611762	4.020	.0564
(Constant)	53.160398	3120.789	.0000

Variables not in the Equation:

Variable	F	Significance of F
SR_1	1.073	.3111
$SR_1 * SR_1$	2.213	.1504
$SR_2 * SR_2$	2.569	.1226
$X_4 * X_4$.018	.8930
$X_1 * SR_1$.051	.8227
$X_1 * SR_2$	2.731	.1120
$X_1 * X_4$.317	.5786
$X_4 * SR_1$	1.391	.2502

which is a measure of the variation in the predicted response due to the contribution of certain term, relative to the variation of the residual. The variation of the residual is a measure of the sum of the squares of the difference between the measured response and the predicted response, which is the value that is minimized by the regression, based on the principle of least squares. The significance of the F ratio, is a measure of the probability of a certain contribution being different from zero. This probability can be compared to the level of the experimental error and thus, the significance of a certain contribution can be evaluated. In this analysis, a significance of 7% (experimental error) is used as a guide in the rejection or the inclusion of a certain term. Therefore, terms that do not contribute significantly to the variation of the correlation are excluded, as indicated by a significance level, much larger than 7%. In all cases, contributions with border line significance levels are included in the correlation.

The coefficients of the controlled variables of the system (x_1 , SR_1 , SR_2 , and x_4) are calculated by the regression, as seen in Table 4.9. All the controlled variables are represented in the correlation and 91% of the variation among the 30 data points is accounted for by the variation of the controlled variables. However, all quadratic effects are excluded by the regression and thus, a linear correlation is obtained, with respect to all variables. This is a cause for concern, since the derived correlation is also linear with respect to reburn zone stoichiometry. Consequently, no optimum reburn zone stoichiometry would be predicted by the correlation.

An examination of the coefficients of the various effects (Table 4.9), shows that the effect of SR_1 is significant only through its interaction with SR_2 . The results can be best interpreted through response surface plots as seen in Figure 4.1. The coal feed rate is fixed at 1.5 kg/h and the distance in the reburn zone corresponds to the introduction of the reburning fuel (natural gas) through port 3. The curves show that reburn zone stoichiometry dominates the reduction of NO by reburning and determines the level of contribution of the stoichiometry in the primary zone. The experimental data points are included in Figure 4.1 and serve only as an indication of the experimental range of the controlled variables, SR_1 and SR_2 . The effect of the controlled variables is further examined, using the derived correlation, as seen in Figure 4.2. Greater reductions in NO are obtained at reburning fuel injections through port 3, relative to those through port 5. This is expected, since the introduction of the reburning fuel at a location that is closer to the primary flame corresponds to longer residence times in the reburn zone, in addition to higher reburn zone inlet temperatures. Again, it is obvious that reburn zone stoichiometry (SR_2) dominates the reduction in NO and the effect of stoichiometry in the primary zone (SR_1). If the reburn zone is operated in a stoichiometric range between 0.8 and 0.9, the effect of SR_1 is of minor significance. As the reburn zone approaches the fuel lean side ($SR_2 > 0.9$), higher values of SR_1 enhance reburning effectiveness. This is possibly due to the introduction of greater amounts of the reburning fuel (natural gas) to produce the desired SR_2 , as SR_1 increases, which can create more fuel rich pockets around the secondary fuel jet. The effect of SR_1 on reburning effectiveness is reversed if the reburn zone is sufficiently fuel rich ($SR_2 < 0.8$). In this case, two possible effects may create the observed increase in NO reduction at lower

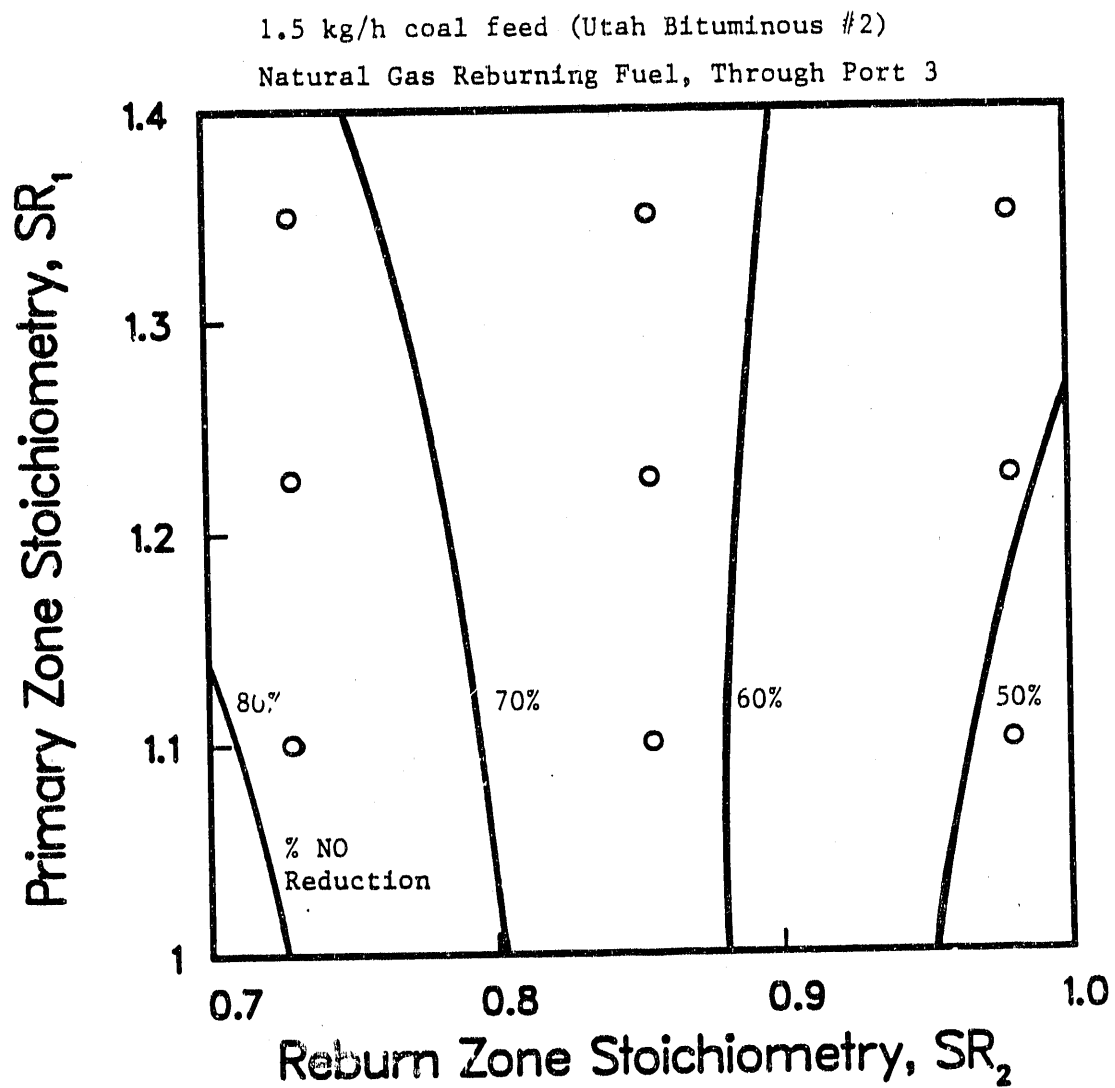


Figure 4.1. Effects of Reburn Zone Stoichiometry and Primary Zone Stoichiometry on NO Reduction by Reburning.

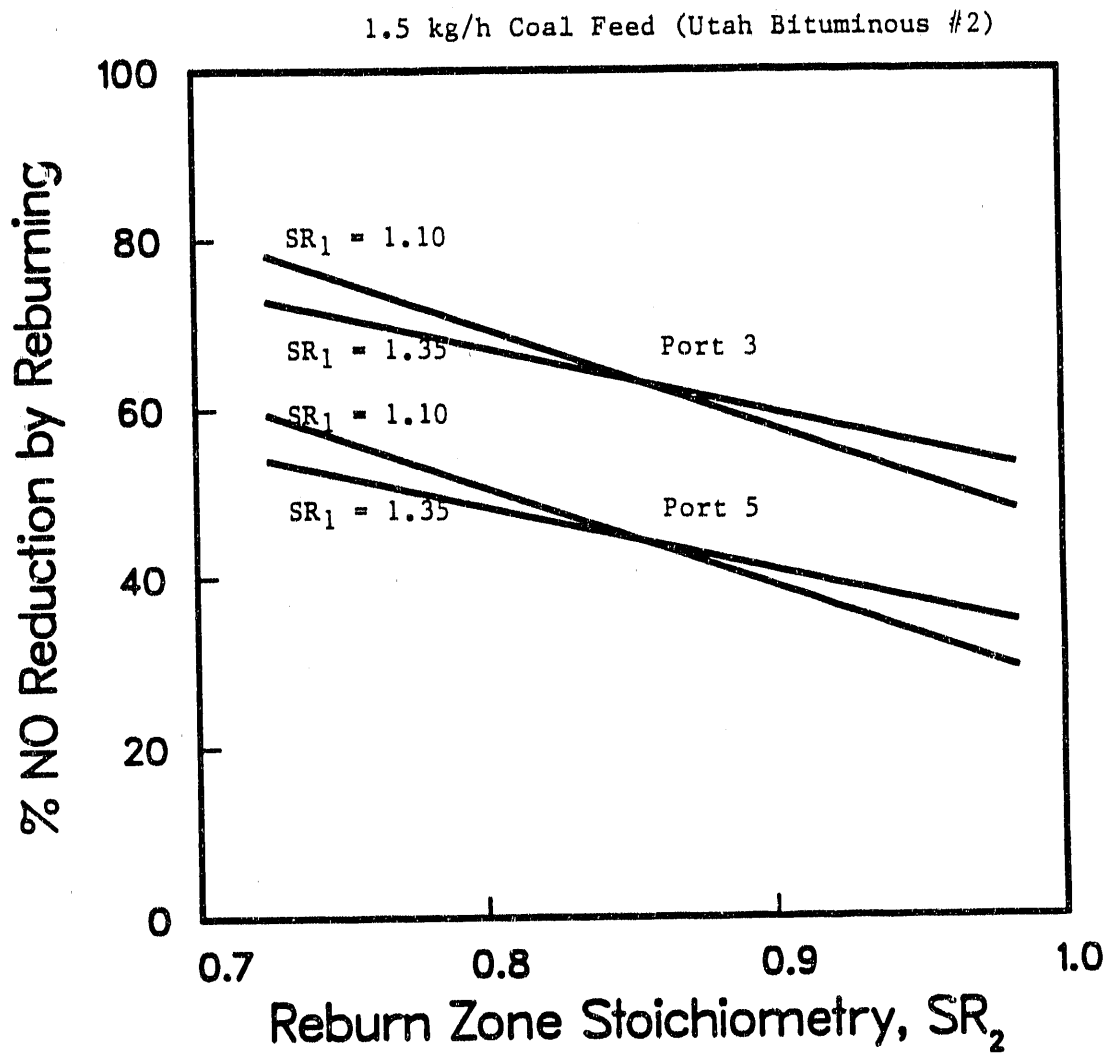


Figure 4.2. Effects of Controlled Variables on NO Reduction by Reburning.

stoichiometries in the primary zone. First, a decrease in SR_1 corresponds to longer residence times in the reburn zone, which enhances the destruction of nitrogenous species. Second, higher values of SR_1 may result in increasing amounts of oxygen to enter the reburn zone, which can reduce reburning effectiveness, if the reburn zone is sufficiently fuel rich ($SR_2 < 0.8$). Thus, in this study, it is suggested that the effect of SR_1 is of minor significance in the typical operation range of SR_2 (0.8-0.9). Furthermore, the effect of SR_1 is attributed mostly to mixing inhomogeneities, which would create variations in the local stoichiometry in the reburn zone. These observations are consistent with those of Greene et al. (1985) and Chen et al. (1986).

An examination of the effects of the other controlled variables, namely, x_1 and x_4 , does not provide useful information. These variables, corresponding to the length of the reburn zone and the coal feed, respectively, are specific to the experimental configuration in this study. However, these two variables have significant effects on reburning effectiveness, since they determine the primary NO level, residence times and the temperature profile. These are derived or dependent variables of the system, that are measured with the response. The previous analysis provides valuable information regarding the effects of stoichiometries in the primary zone and in the reburn zone on reburning effectiveness, but does not allow the examination of the derived variables. Furthermore, no optimum configuration could be identified, since a linear correlation is derived with respect to all controlled variables, including SR_2 (Table 4.9). Thus, it is necessary to expand the analysis to allow the examination of the dependent variables and to explore for an optimum configuration.

4.4 Effects of Dependent Variables

A statistically correct experimental design is usually based on controlled variables that can be varied independently of each other. However, an examination of controlled variables only is restrictive and provides only limited information, as seen in the previous section. In this section, the restriction of the statistical design, with respect to the use of controlled variables only, is relaxed. Both dependent and independent variables are combined to generate a test matrix, that would allow the examination of dependent, as well as independent variables. The results of the statistically designed test matrix (Table 4.5) are used for this purpose. It should be noted that the inclusion of dependent variables in the test matrix results in the loss of some of the orthogonality properties of the matrix. However, that is necessary to allow the examination of variables, that are known to have significant effects on reburning effectiveness, such as residence time and temperature, based on the findings of previous works (Greene et al., 1985; Chen et al, 1986; Lanier et al., 1986). Furthermore, the results of the analysis would be limited to a qualitative examination of the effects of the different variables.

The variables that are of interest in this investigation are: stoichiometries in the primary zone and in the reburn zone, the primary NO level, residence time in the reburn zone, and the three inlet temperatures, corresponding to the three stages of reburning.

Table 4.10 shows the experimental limits of these variables and the corresponding coding equations. The coding equations produced orthogonal vectors in SR_1 and SR_2 only. Nevertheless, the scaling of all the variables was useful in eliminating numerical bias in the regression analysis, that would exist due to differences in the numerical magnitudes among the different variables. The derived test matrix is shown in Table 4.11.

The derivation of a correlation, relating the response to the significant variables, was accomplished in two stages. In the first stage, a regression analysis was performed, in which only the main effects of the variables were examined. The purpose of this analysis was to isolate the important variables, and to exclude the variables whose contributions were of minor statistical significance. Table 4.12 shows the final step of the regression analysis, using the Backward method. In this method, all the variables are initially included in the regression, then the contribution of each variable to the variation of the response is evaluated, and the corresponding variable is either included or excluded. The significance levels of the different variables (based on the F ratio), show a clear split between the variables that significantly contributed to the variation of the response and those whose contributions were not statistically significant (Table 4.12). The important variables are identified in the following order of significance: stoichiometry in the reburn zone (SR_2), residence time in the reburn zone (RT), reburn zone inlet temperature (T_2), and stoichiometry in the primary zone (SR_1). The other variables, namely, the primary NO concentration (NO_p), the peak temperature in the primary zone (T_1) and the inlet temperature to the burnout zone (T_3), were of minor significance in the experimental range that was covered. It is emphasized that these conclusions might not hold outside the experimental range of this study. An example is the primary NO level, a variable with significant effects on the overall reburning effectiveness, as demonstrated in previous works (Greene et al., 1985; Brown et al., 1986; Chen et al., 1986; Lanier et al., 1986; Miyamae et al., 1986). A minor dependence of reburning effectiveness on NO_p levels above 600 ppm was reported by Greene et al. (1985) and Miyamae et al. (1986). In this study, NO_p values varied from 945 ppm to 1135 ppm (dry, 0% O_2). Thus, the conclusion of this analysis with respect to the significance of NO_p , is consistent with the observations of other researchers. The exclusion of the other two variables, T_1 and T_3 , is also consistent with the results of previous works (Greene et al., 1985; Chen et al., 1986).

In the second stage of analysis, only the variables that were identified in the first stage as significant, were included. Then, a quadratic correlation was fitted to the relevant data of Table 4.11, using multiple regression procedure. The derivation of a predictive correlation was performed in a similar manner, as in the treatment of the controlled variables. Table 4.13 shows the final step of the regression analysis, using the Stepwise method. The correlation included the quadratic effects of SR_2 and RT, and accounted for 95% of the variation among the 30 data points.

The derived correlation can be used to examine the effects of residence time and temperature in the reburn zone. Figure 4.3 shows response contour plots, as a function of reburn zone residence times and temperatures. The experimental data points are included

Table 4.10.
Variables in the Modified Statistical Design.

<u>Variable</u>	<u>Low Limit</u>	<u>High Limit</u>	<u>Coding Equation</u>
SR ₁	1.10	1.35	$(SR_1 - 1.225)/0.125$
SR ₂	0.73	0.98	$(SR_2 - 0.855)/0.125$
RT	0.10	0.60	$(RT - 0.35)/0.25$
NO _p	945	1135	$(NO_p - 1040)/95$
T ₁	1400	1700	$(T_1 - 1550)/150$
T ₂	1310	1670	$(T_2 - 1490)/180$
T ₃	1235	1575	$(T_3 - 1405)/170$

Table 4.11.
Components of the Modified Statistical Design.

RUN	SR ₁	SR ₂	RT	NO _p	T ₁	T ₂	T ₃	Y
RS#21B	-1	-1	-0.43	-0.43	-0.36	-0.95	-0.75	58.4
RS#22A	-1	1	2.22	-0.48	-0.16	-0.29	-1.15	45.3
RS#18A	1	-1	1.02	0.25	-0.79	-0.33	-0.46	69.7
RS#17B	1	1	-0.25	-0.39	-0.69	-0.98	-0.67	42.2
RS#21A	-1	-1	1.62	-0.43	-0.31	-0.29	-0.75	69.6
RS#22B	-1	1	-0.05	-0.48	-0.15	-0.96	-1.03	40.5
RS#16B	1	-1	-0.54	-0.80	-0.87	-1.00	-0.68	49.4
RS#19A	1	1	1.42	0.63	-0.79	-0.30	-0.50	55.4
RS# 7A	-1	-1	0.17	0.94	0.81	0.71	0.38	77.8
RS# 8B	-1	1	-0.74	-0.23	0.81	0.40	0.56	22.4
RS# 1B	1	-1	-1.04	1.03	0.73	0.52	0.84	57.1
RS# 4A	1	1	-0.05	0.47	0.40	0.84	0.88	43.3
RS# 7B	-1	-1	-0.92	0.94	0.92	0.55	0.67	56.4
RS# 8A	-1	1	0.41	-0.23	0.76	0.83	0.54	30.7
RS# 1A	1	-1	-0.25	1.03	0.79	0.93	0.94	79.4
RS# 4B	1	1	-0.90	0.47	0.02	0.32	0.74	30.3
RS#10B	0	1	-0.64	-0.61	0.25	0.01	0.39	31.9
RS# 9B	0	-1	-0.83	-0.68	0.18	0.03	0.29	57.0
RS#14B	1	0	-0.76	0.00	-0.51	-0.35	0.05	43.7
RS#15B	-1	0	-0.62	-0.96	0.08	-0.17	-0.03	36.0
RS# 6B	0	0	-0.88	0.56	0.35	0.18	0.59	38.4
RS#20B	0	0	-0.39	0.54	-0.65	-0.94	-0.59	48.5
RS#13A	0	0	0.68	-0.08	-0.24	0.08	-0.19	67.5
RS#13B	0	0	-0.68	-0.08	-0.25	-0.46	-0.25	44.7
RS#10A	0	1	0.66	-0.61	0.15	0.44	0.47	47.7
RS# 9A	0	-1	0.41	-0.68	0.01	0.32	0.21	76.2
RS#14A	1	0	0.44	0.00	-0.58	0.14	0.23	62.1
RS#15A	-1	0	0.94	-0.96	-0.03	0.07	-0.23	73.1
RS# 6A	0	0	0.11	0.56	0.53	0.75	0.49	65.7
RS#20A	0	0	1.50	0.54	-0.43	-0.24	-0.55	73.5

Table 4.12.
Regression Results - Identifying Significant Variables.

* * * * Multiple Regression * * * *

Dependent Variable: Y

Variable Removed on Step Number 10: NO_p

Multiple R .89506
R Square .80113
Adjusted R Square .76931
Standard Error 7.62116

Variables in the Equation:

Variable	B	F	Significance of F
SR ₂	-14.498204	71.133	.0000
SR ₁	2.976114	2.963	.0975
RT	10.354805	39.401	.0000
T ₂	4.413992	3.338	.0797
(Constant)	52.584924	1422.418	.0000

Variables not in the Equation:

Variable	F	Significance of F
NO _p	.794	.3818
T ₁	.046	.8328
T ₃	.216	.6464

Table 4.13.
Regression Results in Terms of Significant Variables.

* * * * Multiple Regression * * * * *

Dependent Variable: Y

Variable(s) Entered on Step Number 9: $SR_1 * T_2$

Multiple R .97309
R Square .94691
Adjusted R Square .92301
Standard Error 4.40257

Variables in the Equation:

Variable	B	F	Significance of F
SR_2	-14.135477	201.736	.0000
RT	14.066672	128.695	.0000
$RT * RT$	-4.961942	20.932	.0002
$SR_2 * T_2$	-7.244480	21.533	.0002
SR_1	2.483460	6.114	.0225
T_2	3.525260	6.113	.0225
$SR_1 * SR_2$	2.366654	4.598	.0445
$SR_2 * SR_2$	-3.283802	3.613	.0718
$SR_1 * T_2$	2.994562	3.612	.0719
(Constant)	58.269670	1449.960	.0000

Variables not in the Equation:

Variable	F	Significance of F
$SR_1 * SR_1$	1.247	.2781
$T_2 * T_2$.352	.5600
$SR_1 * RT$.280	.6026
$SR_2 * RT$	1.302	.2680
$RT * T_2$.357	.5573

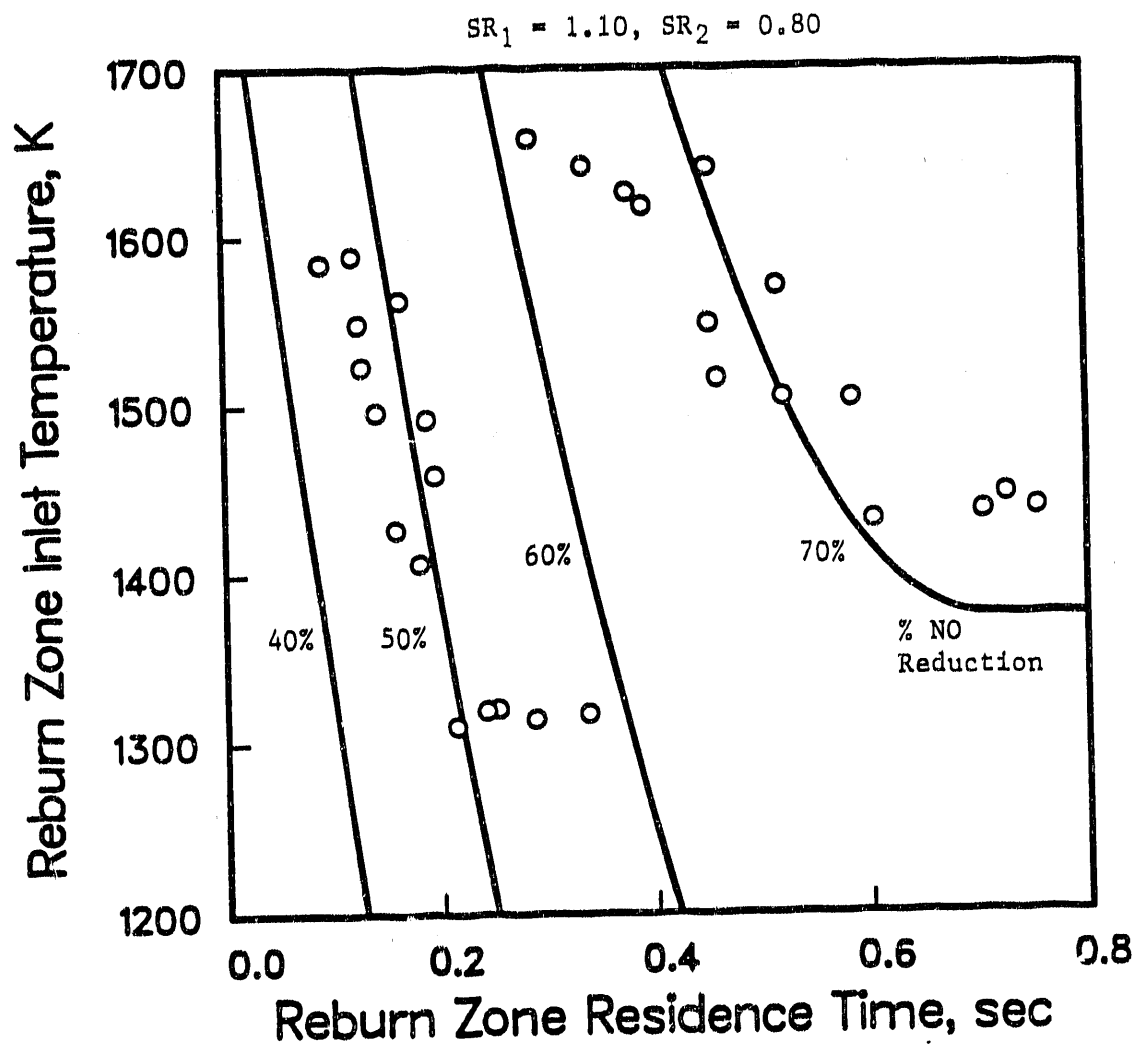


Figure 4.3. Effects of Reburn Zone Residence Time and Reburn Zone Inlet Temperature on NO Reduction by Reburning.

only to identify the experimental domain, in which the predicted curves are based. This serves as a reminder that the predictive curves can be used for interpolation only, and not for extrapolation. The curves indicate that residence time effects dominate at residence times less than 0.5 seconds, whereas, temperature effects dominate at longer residence times. However, in all cases, the residence time requirement to achieve a certain level of NO reduction is dependent on temperature. Figure 4.4 shows the effects of reburn zone stoichiometry, temperature and residence time on the predicted response, based on the derived correlation. In all cases, the curves do not predict an optimum reburn zone stoichiometry. The effect of residence time is as expected and greater reductions in NO are predicted at longer residence times. The effect of temperature is greatly dependent on SR_2 , where an increase in temperature corresponds to an improvement in reburning effectiveness, only at stoichiometries richer than 0.87. Under less fuel rich conditions ($SR_2 > 0.87$), the effect of temperature is reversed. Higher temperatures enhance the decay of HCN in the reburn zone, mostly due to reactions with O and OH radicals. This explains the improvement in reburning effectiveness at higher temperatures, under the more fuel rich reburn zone conditions. However, if the reburn zone is close to the fuel lean side, low concentrations of HCN would be present and higher temperatures promote the destruction of hydrocarbon species to form neutral products, mainly due to reactions with O radicals (Glarborg et al., 1986). Consequently, less hydrocarbon species are available at higher temperatures and less NO is destroyed by $NO + CH_1$ reactions. The reversed effect of temperature, when the reburn zone is close to the fuel lean side, has not been addressed in the literature, but can be deduced from the results of Myerson (1975) and Greene et al. (1985). The predicted value of 0.87 for SR_2 , at which the effect of temperature is reversed, should not be accepted as the true value, since the derived correlations are not appropriate for quantitative predictions.

To summarize, the variables that are associated with the reburn zone, namely, stoichiometry, temperature, and residence time, dominate the overall destruction of NO in reburning. Empirical correlations, derived from a statistical experimental design, show that the effect of each of these variables is greatly dependent on the effects of the other two. The correlations also show that the effect of stoichiometry in the primary zone is of minor significance under practical reburning conditions. The correlations failed to predict an optimum configuration and thus, their use should be restricted to a qualitative examination of reburning.

4.5 Evaluation of the Statistical Design

The empirical correlations, that were derived in the previous sections, were used to examine the effects of different reburning parameters and their interactions. However, the correlations failed to predict an optimum reburn zone stoichiometry. Such an optimum would be expected for SR_2 value between 0.8 and 0.9, based on the reburning results of previous works (Greene et al., 1985; Chen et al., 1986; Kolb et al., 1988). Consequently, additional natural gas reburning experiments were performed to further examine the effect of reburn zone stoichiometry (SR_2) on reburning effectiveness. The results are shown in

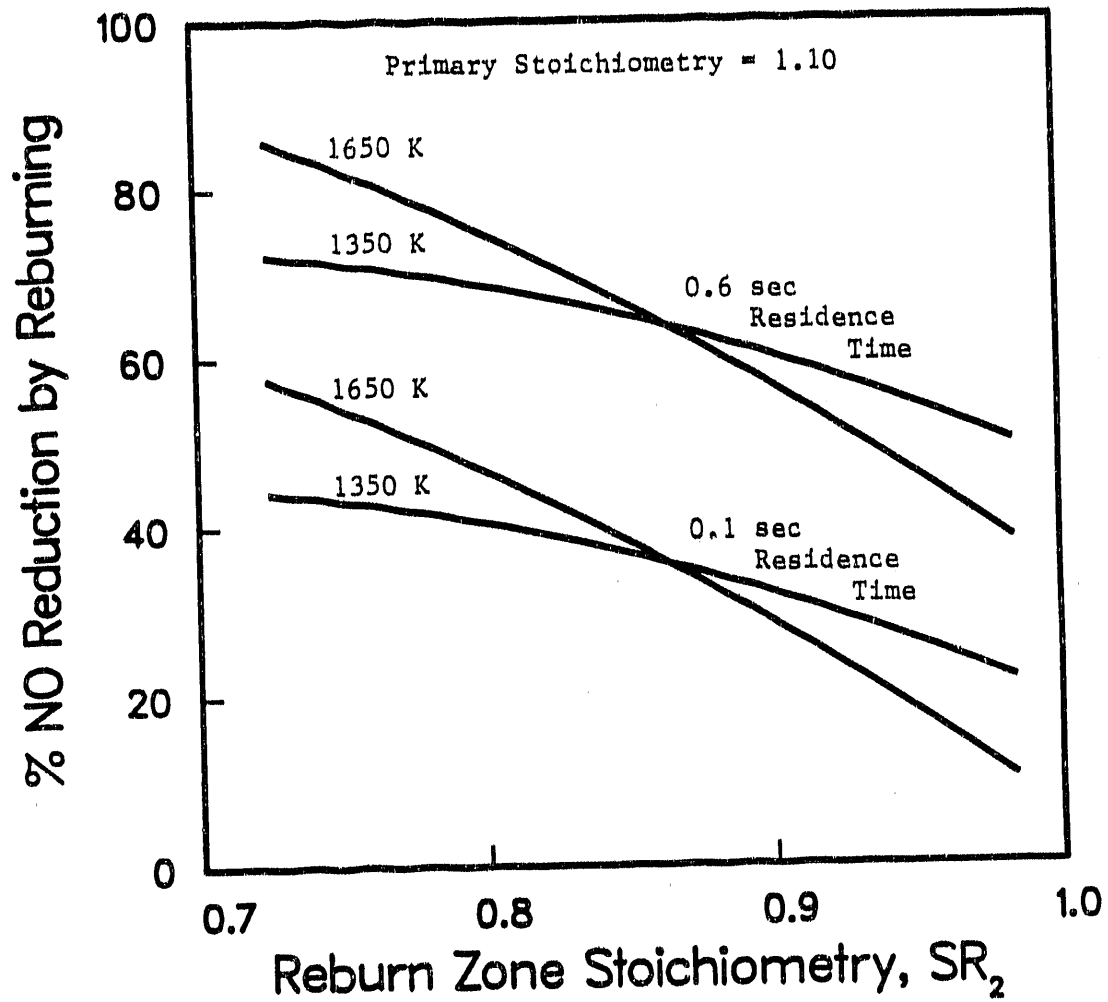


Figure 4.4. Effects of Dependent Variables on NO Reduction by Reburning.

Figures 4.5 and 4.6. The experimental data suggest an optimum SR_2 at about 0.8, below which little or no further improvement in reburning effectiveness is detected. Figure 4.7 shows a comparison between the measured response and that predicted from controlled variables only, using a derived correlation (see Table 4.9). Figure 4.8 shows a similar comparison, in which the correlation is based on all the significant variables (see Table 4.13). In both cases, the correlations do not predict an optimum SR_2 and relatively poor fits are obtained. The discrepancy between the experimental data and the predicted values is due to the existence of a weak optimum. Consequently, a least squared fit, based on the small number of tests in the statistical design (30 tests), could not account for the optimum. Furthermore, the statistical design allowed for only three different values of SR_2 , which apparently were not sufficient to detect the presence of an optimum. This demonstrates a weakness in the statistical experimentation, and suggests that such an approach should be complemented by detailed tests, in which one variable is varied at a time. The limitations to the statistical approach are summarized as follows:

1. The use of the derived correlations for quantitative predictions can be misleading, as seen in Figures 4.7 and 4.8. Furthermore, the correlations do not predict an optimum configuration.
2. The correlations can be used for interpolation only in the experimental range, within which the correlations are derived.
3. The choice of the variables of the statistical design is restricted by the experimental configuration, which may not allow independent variation of all the variables that are of interest in the investigation. In addition, some independent variables may be specific to the experimental configuration.

In short, a parametric study based on a statistical experimental design was an efficient method to yield a qualitative, rather than a quantitative understanding of the reburning process. Furthermore, the study would not provide fundamental understanding of the reburning process.

4.6 Multiple Reburning Fuel Injection Schemes

Mixing of the reburning fuel with the primary effluent is an important factor that affects the overall destruction of NO in reburning. Poor mixing conditions can limit reburning effectiveness by delaying the contact of the primary NO with CH_1 radicals that are generated from the reburning fuel. Thus, improved mixing conditions may enhance reburning effectiveness, as is suggested in previous works (Chen et al., 1986; Miyamae et al., 1986; Overmoe et al., 1986; La Fond and Chen, 1987; Kolb et al., 1988). At the point of reburning fuel introduction, oxygen and NO compete for CH_1 radicals, and enhanced reburning effectiveness would be expected if NO contact with CH_1 radicals can be improved. This may be accomplished by distributing the reburning fuel over a longer time span. Experiments were conducted to test this hypothesis. In these experiments, the effect of

BITUMINOUS COAL PRIMARY FLAME, NATURAL GAS REBURNING

$\text{NO}_p \sim 1100 \text{ ppm (dry, 0\% O}_2\text{)}$

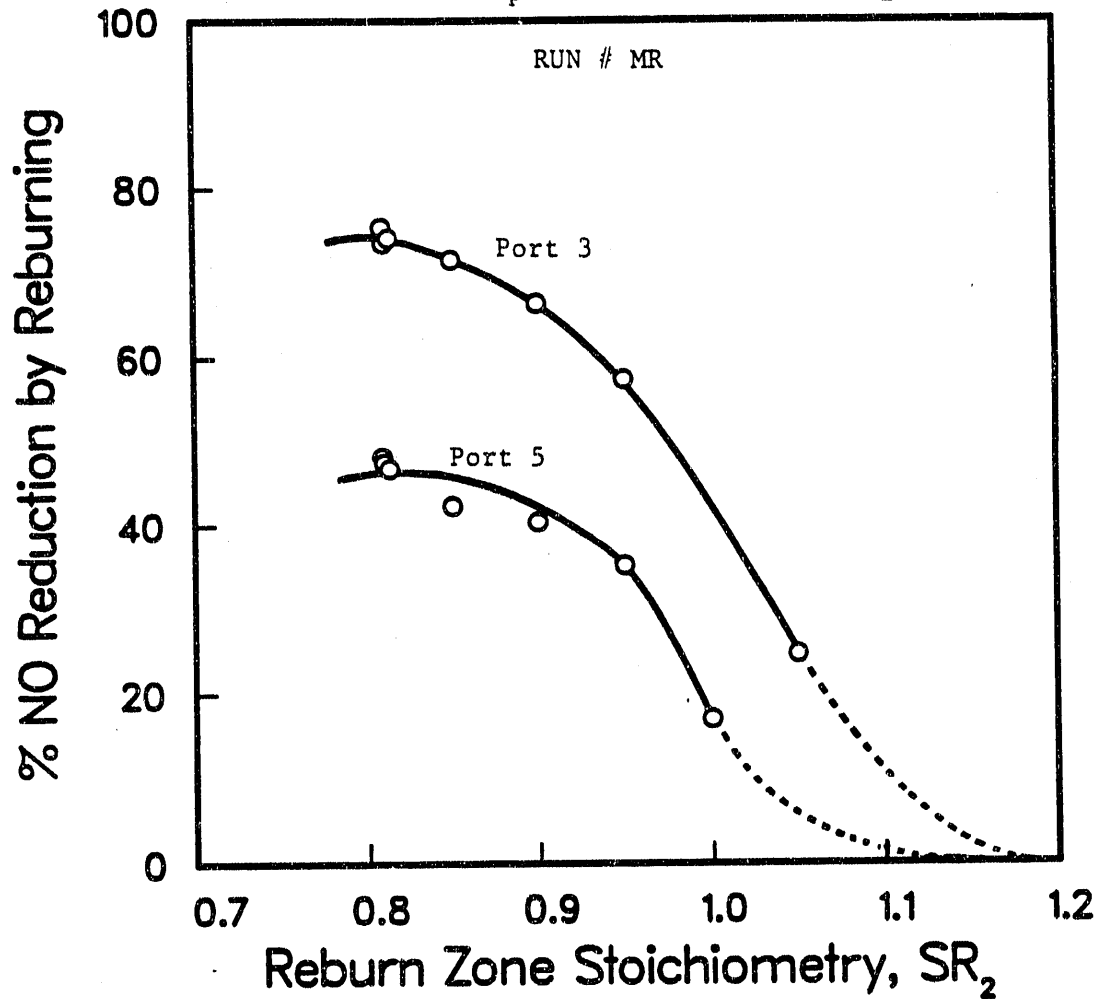


Figure 4.5. Effect of Reburn Zone Stoichiometry on Reburning Effectiveness - Comparing Two Locations for Reburning Fuel Injection.

BITUMINOUS COAL PRIMARY FLAME, NATURAL GAS REBURNING
 $\text{NO}_p \sim 950 \text{ ppm (dry, 0\% O}_2\text{)}$

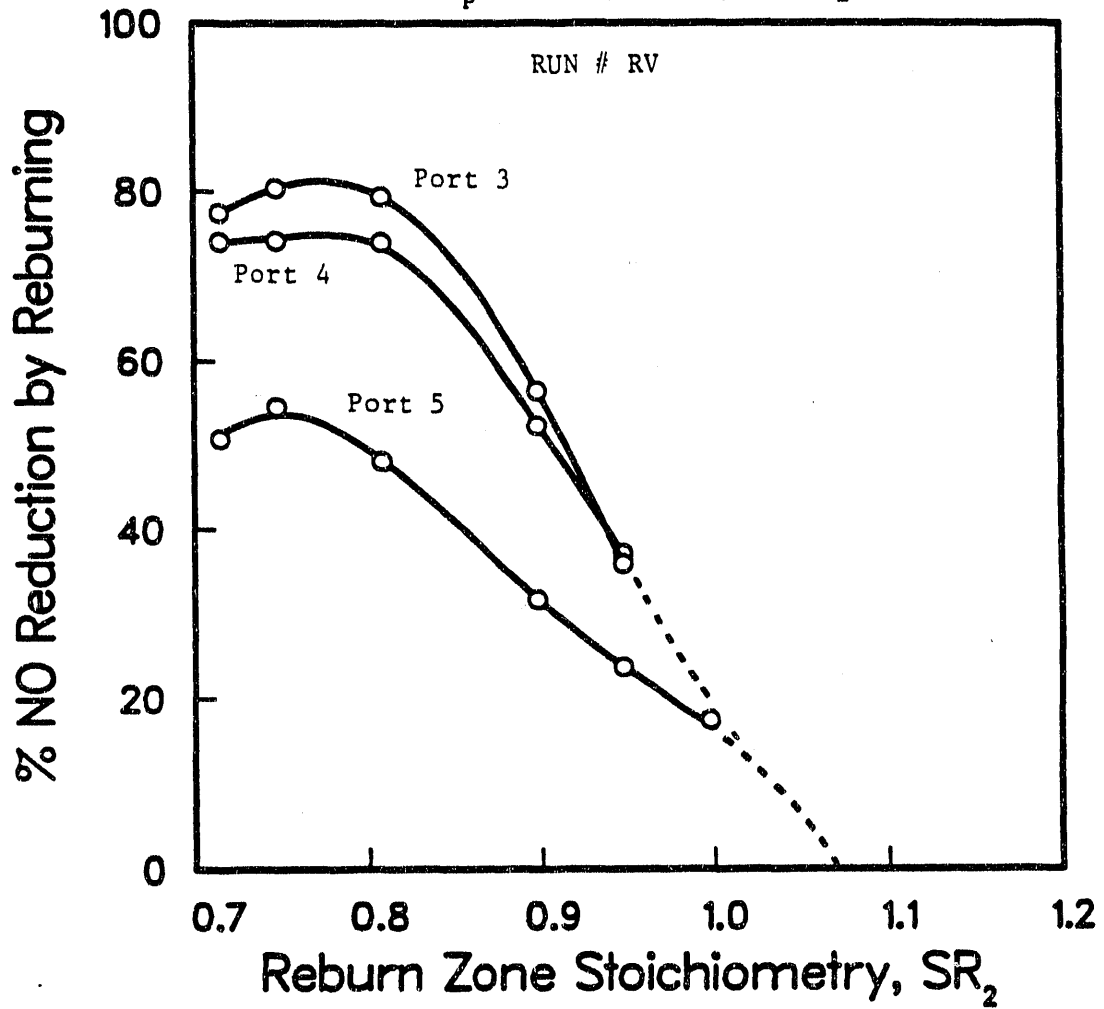


Figure 4.6. Effect of Reburn Zone Stoichiometry on Reburning Effectiveness - Comparing Three Locations for Reburning Fuel Injection.

BITUMINOUS COAL PRIMARY FLAME, NATURAL GAS REBURNING
Reburn Zone: Time = 0.33-0.43 s, Temp = 1550-1600 K
 $NO_p \sim 900$ ppm (dry, 0% O_2)

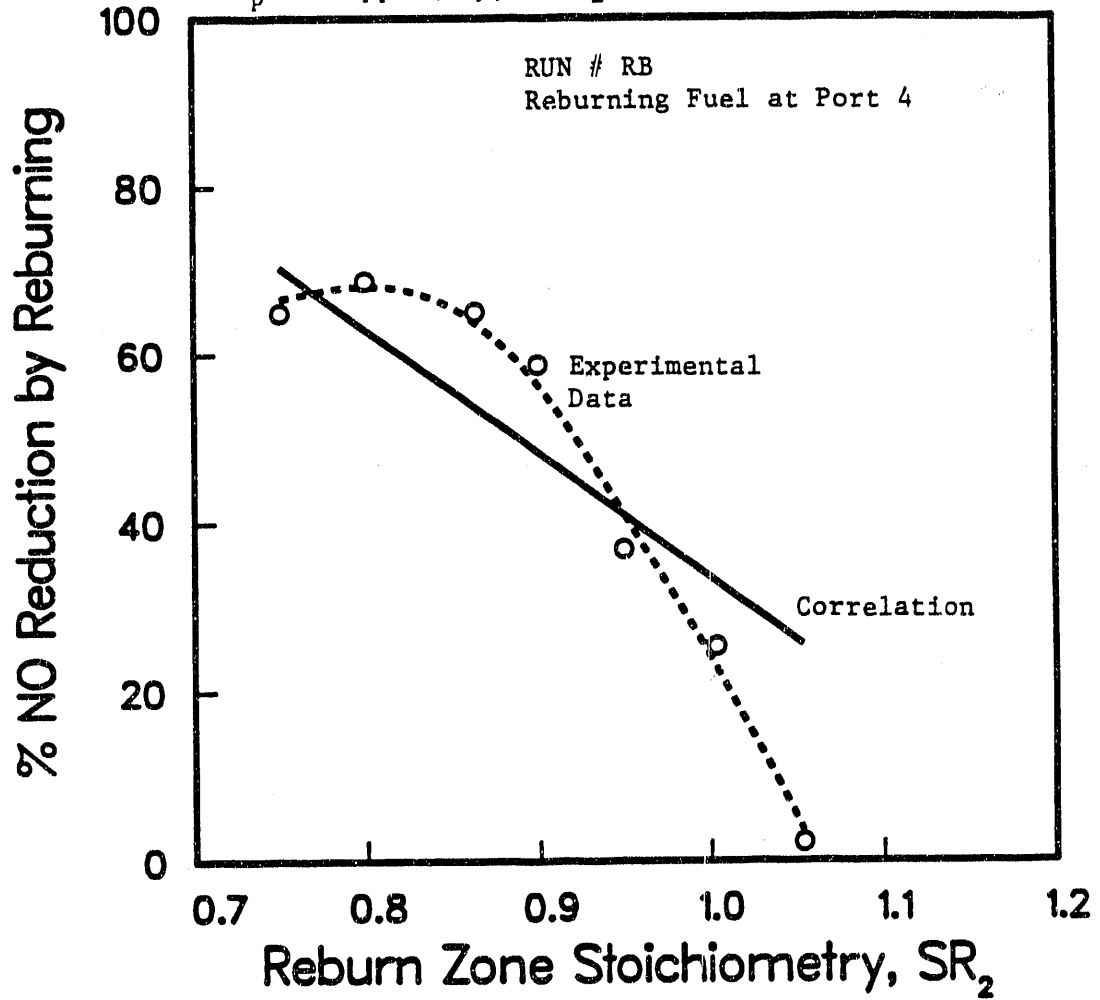


Figure 4.7. Comparison between Measured and Predicted NO Reduction by Reburning - Correlation in Terms of Controlled Variables.

BITUMINOUS COAL PRIMARY FLAME, NATURAL GAS REBURNING
Reburn Zone: Time = 0.33-0.43 s, Temp = 1550-1600 K
NO_p ~ 900 ppm (dry, 0% O₂)

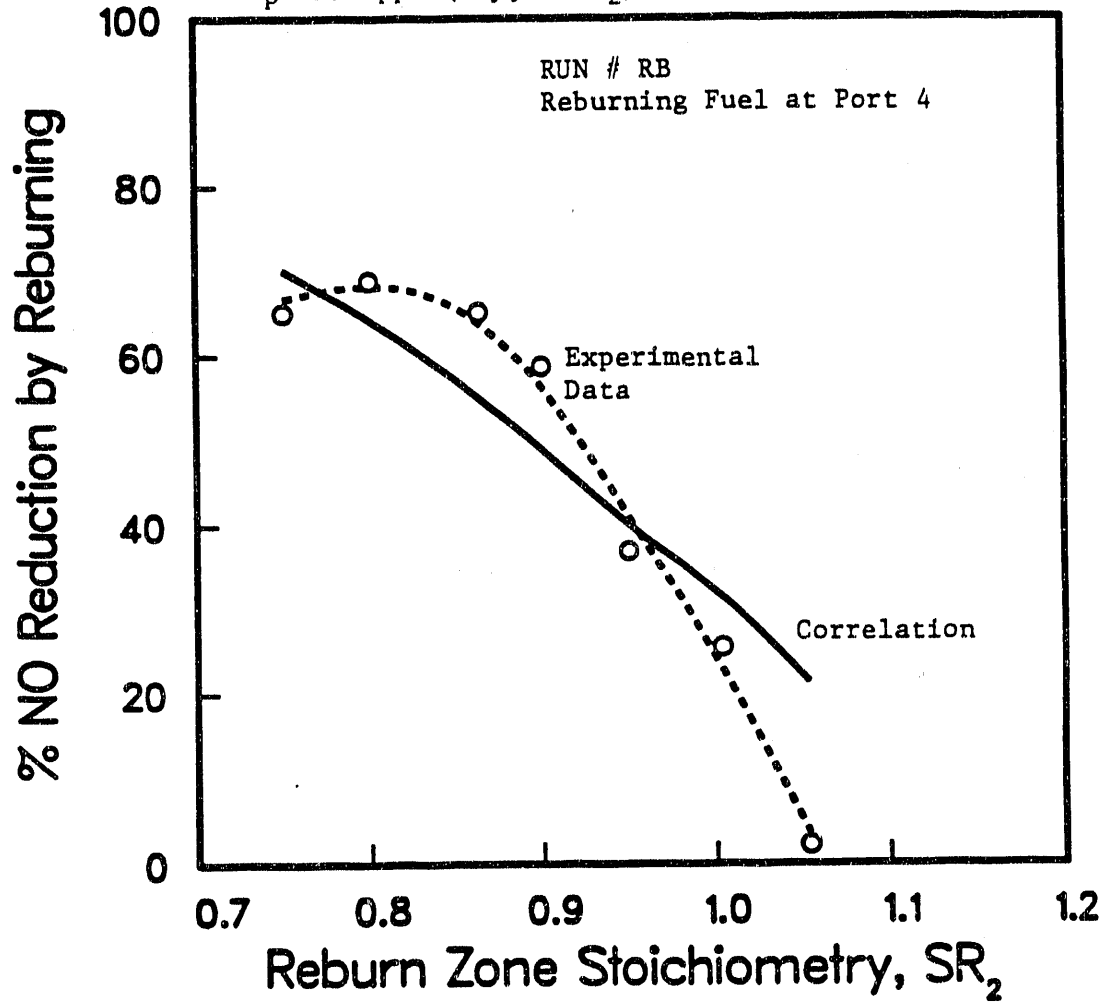


Figure 4.8. Comparison between Measured and Predicted NO Reduction by Reburning - Correlation in Terms of Significant Variables.

splitting the reburning fuel into more than one stream is examined, as seen in Figure 4.9. The total amount of reburning fuel at a certain reburn zone stoichiometry was kept constant. In tests involving double reburning fuel injections, an equal amount of natural gas was introduced in each stream. No improvement in reburning effectiveness could be achieved, relative to single stream injections of the reburning fuel. That is possibly due to a trade off between improved NO and CH₄ contact, and reduced effective residence times and temperature in the reburn zone. The introduction of the reburning fuel in multiple streams involved the injection of a fraction of the reburning fuel further downstream of the primary flame, which corresponded to lower temperatures and shorter residence times.

In short, multiple reburning fuel injections, in which the total amount of reburning fuel was kept constant, did not improve reburning effectiveness, relative to single stream injections through port 3. An optimum reburning fuel injection mode involved a single stream injection, through port 3. That produced a reburn zone that was as close to the primary flame as possible, while allowing a residence time of at least 0.25 seconds for primary fuel burnout, before the injection of the reburning fuel.

4.7 Carbon Burnout

In reburning, the failure to complete oxidation of the fuel in the final combustion stage is a major concern, since it can produce higher CO emissions in the exhaust, relative to uncontrolled emissions, as well as reduction in carbon burnout. In this study, the carbon content in the ash was not analyzed, and the CO analyzer was designed to measure only high levels of CO (reducing conditions), with a detection limit of about 0.04%. Consequently, the effect of reburning on carbon burnout could not be quantified, but a qualitative estimate was possible, based on gas phase measurements and a carbon balance. The mass balance program, MASS.FOR, is listed in Appendix C. The fraction of carbon that was unaccounted for in the mass balance was evaluated, but it would not be an exact measure of carbon burnout, since it would also include experimental errors. Furthermore, most natural gas reburning tests did not involve gas phase measurements of hydrocarbons, which would introduce additional errors in the carbon balance.

The effect of reburning on carbon burnout is estimated by examining the fraction of carbon that is unaccounted for, based on gas phase measurements of uncontrolled exhaust emissions, emissions in the primary zone, and exhaust emissions after air addition in the final stage of reburning. The experimental data of the statistical design are used for this purpose and the results are listed in Table 4.14. A comparison between the calculations corresponding to uncontrolled exhaust emissions (no reburning) and those corresponding to the primary zone of reburning, shows minor differences in the calculated errors in the carbon balance. This suggests that allowing a residence time of at least 0.25 seconds in the primary zone would be sufficient for char burnout at the reburning fuel injection point. Consequently, greater errors in the carbon balance after the application of reburning would be due to the presence of unburned gaseous hydrocarbons in the exhaust, which is an indication of insufficient carbon burnout.

BITUMINOUS COAL PRIMARY FLAME, NATURAL GAS REBURNING
 Primary SR = 1.10, $\text{NO}_p \sim 1000$ ppm (dry, 0% O_2)
 RUN # RH

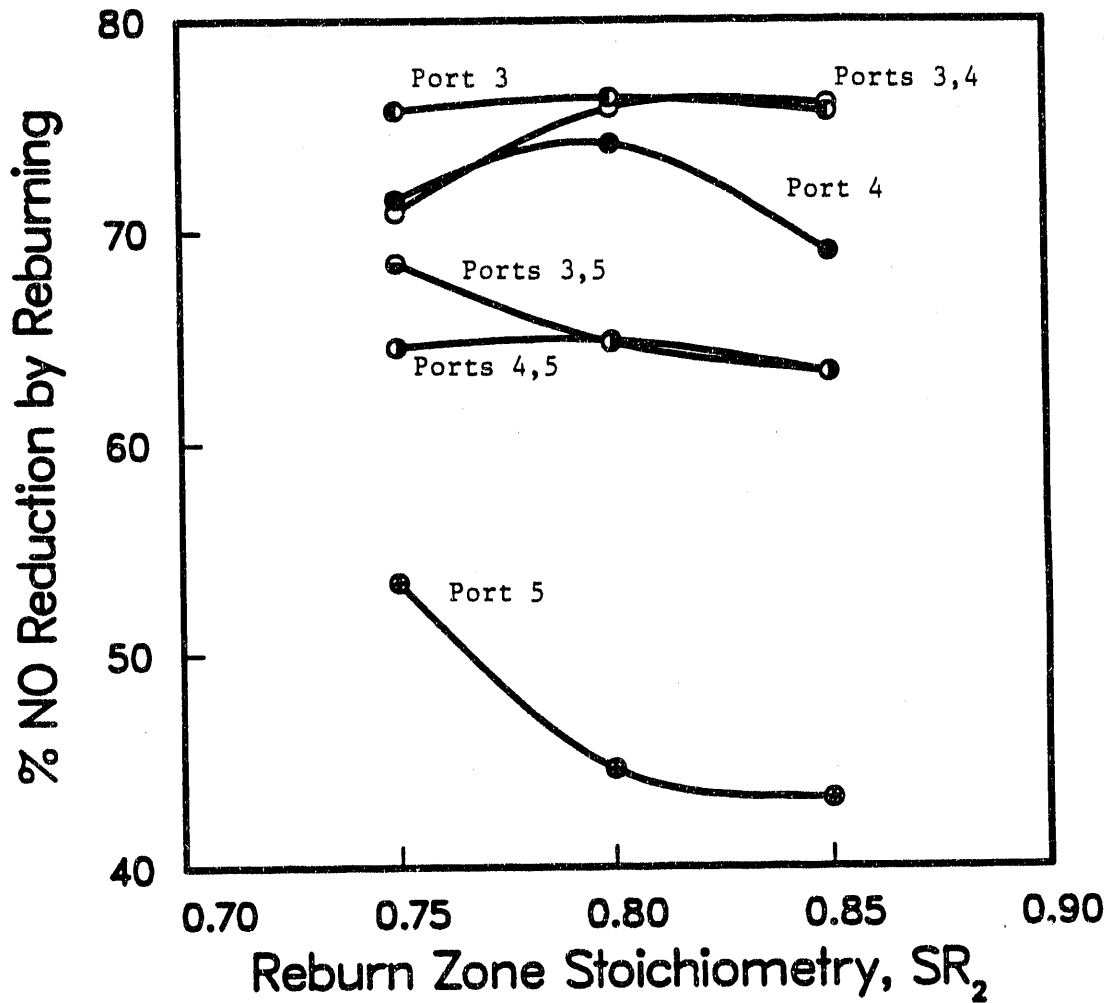


Figure 4.9. Effect of Introduction of the Reburning Fuel as Multiple Stream Injections on Reburning Effectiveness - Variation with Reburn Zone Stoichiometry.

Table 4.14.
Carbon Burnout.

Percentage of Carbon Unaccounted for

Run	Direct Emissions	Primary Zone	<u>R E B U R N I N G</u>		SR ₂	T ₁
			Port 3	Port 5		
RS# 1	10.1	4.6	20.5	19.0	0.73	1664
RS# 4	8.5	8.5	4.4	4.4	0.98	1582
RS# 6	8.0	8.7	12.5	11.5	0.855	1616
RS# 7	7.8	8.7	20.0	20.9	0.73	1680
RS# 8	7.8	6.9	3.9	0.9	0.98	1668
RS# 9	8.7	7.9	25.9	24.2	0.73	1564
RS#10	8.7	10.7	5.3	6.3	0.98	1580
RS#13	7.8	11.2	9.1	4.3	0.855	1514
RS#14	9.9	10.4	11.0	9.3	0.855	1468
RS#15	4.9	8.7	2.9	4.8	0.855	1554
RS#16	9.7	9.2	13.3	15.6	0.73	1421
RS#17	9.7	5.4	0.3	2.6	0.98	1444
RS#18	9.4	9.2	16.8	16.9	0.73	1432
RS#19	9.4	7.7	2.9	1.2	0.98	1434
RS#20	7.0	6.5	2.7	6.9	0.855	1469
RS#21	7.8	9.5	14.5	13.9	0.73	1500
RS#22	7.8	8.9	7.1	7.7	0.98	1527

A comparison of the calculated errors in the carbon balance (Table 4.14), corresponding to two locations of reburning fuel injection (ports 3 and 5), three reburn zone stoichiometries (0.73, 0.855 and 0.98), and different peak temperatures in the primary zone (1420-1680 K), suggest that problems with carbon burnout might occur under very fuel rich conditions in the reburn zone ($SR_2 = 0.73$). The location of the reburn zone and the temperature in the primary zone show minor effects on char burnout in the primary zone, or on carbon burnout after the application of reburning. The stoichiometry in the reburn zone appears to be the dominant factor that determines the degree of carbon burnout. The introduction of the reburning fuel might create problems with gaseous hydrocarbon burnout, under very rich conditions in the reburn zone ($SR_2 = 0.73$). Minor effects are detected at higher reburn zone stoichiometries of 0.855 and 0.98.

5.0 EXPERIMENTAL RESULTS: EFFECT OF PRIMARY FLAME MODE

The experimental studies described earlier were conducted on a laboratory pulverized coal combustor that was operated in a premixed plug flow mode. The premixed burner allowed thorough mixing of the air stream transporting the coal particles with the preheated combustion air stream. In order to investigate reburning under practical diffusion flame conditions, other experiments were performed in which another burner was used to produce a long axial flame with no swirl. The construction of both types of burners was described in Section 2.1.2. In this section, the results of reburning experiments in a turbulent diffusion primary flame mode are presented and the effects of primary flame mode are discussed. The interpretation of the results is qualitative and serves only to demonstrate the outcome of reburning and its limitations when applied under more practical conditions.

5.1 Premixed Primary Flame

Premixed flames are not common in practical pulverized coal combustors, since they produce more NO_x in post flame flue gases. Premixing enhances the contact of fuel nitrogen with oxygen in the early stage of combustion, which increases the oxidation of fuel nitrogen to NO. Nevertheless, a premixed plug flow mode can provide valuable information on residence times, temperature profiles and the local environment, since these properties would then depend only on the axial position and can be well defined. Furthermore, a premixed environment is useful in the study of kinetics and the determination of kinetic limits that govern the fate of nitrogenous species in post flame flues gases. In pulverized coal combustion, results from premixed flames are applicable in practical units, since fuel nitrogen oxidation kinetics occur in a diffusion flame environment, even when the coal particles are premixed with air (Wendt, 1980).

5.1.1 Effect of Reburning Fuel Jet Momentum

The effect of reburn zone stoichiometry on reburning effectiveness was discussed in Section 4.0. The distribution of the reburning fuel inside the reburn zone was not of interest, since the overall effect of reburning was examined. Nevertheless, mixing is a key variable in reburning and is expected to affect the overall reduction in NO and the location of the optimum reburn zone stoichiometry. Poor mixing in the reburn zone creates local variations in reburn zone stoichiometry which would prevent complete optimization of the reburning process. In addition, a well mixed reburn zone is necessary to validate the assumption of one dimensional plug flow behavior throughout the combustor. Consequently, the reburning fuel injection mode was modified to produce adequate mixing within 0.18 seconds in the reburn zone, by injecting nitrogen gas with the reburning fuel. The effect of reburning fuel injection mode on radial concentrations was discussed in Section 2.1.5.

An experiment was conducted to examine the effect of improved mixing in the reburn zone on reburning effectiveness. In these tests, the total flow of reburning fuel and transport N_2 was held constant at 15.6 slm (0.55 scfm), and was introduced through port 4.

The results are presented in Figure 5.1 as the variation of reburning effectiveness with reburn zone stoichiometry. The trend is similar to that observed in previous experiments in which no transport gas was injected with the reburning fuel. However, the optimum reburn zone stoichiometry is closer to 0.9, corresponding to NO reduction of 75%, compared to an optimum stoichiometry of 0.8 that was identified in previous experiments. Comparing the results of this experiment at optimum conditions to those of Figure 5.2, in which no N_2 was injected with the reburning fuel, shows an improvement of about 5% in reburning effectiveness, although both experiments are not entirely comparable, due to minor differences in primary NO levels, residence times and temperatures.

In short, poor mixing reduces the overall reburning effectiveness, results in a broader dependence on reburn zone stoichiometry and creates a shift in the optimum reburn zone stoichiometry to the richer side. This is consistent with the results of previous studies (Chen et al., 1986; Kolb et al., 1988).

5.1.2 Conversions of Nitrogenous Species

Figure 5.3 shows the results of a reburning experiment in which detailed measurements of nitrogenous species were made at the exit of the fuel rich reburn zone at various stoichiometries, in addition to exhaust NO measurements after final air addition. This allows the examination of nitrogenous species inter-conversion in the reburn zone, the burnout zone and the overall effect of reburning on NO concentrations. The results of this experiment are typical and clearly demonstrate the tradeoff which determines an optimum reburn zone stoichiometry. As the stoichiometry decreases, HCN and NH_3 concentrations increase, whereas, NO concentration decreases in the reburn zone. Thus, stoichiometry determines the distribution of nitrogenous species leaving the reburn zone and subsequently, the conversion of the total fixed nitrogen to NO in the final stage of reburning. This conversion is sensitive to variations in reburn zone stoichiometry, and approaches 100% as the stoichiometry approaches the fuel lean side, corresponding to HCN and NH_3 levels approaching zero (Figure 5.3). Similar trends, under various experimental conditions were discussed by Greene et al. (1985).

In this experiment, an optimum reburn zone stoichiometry was identified at 0.84, corresponding to an overall destruction of about 80% of the primary NO.

5.2 Diffusion Primary Flame

In a turbulent diffusion flame mode, pulverized coal particles are transported by primary air, and are injected into the furnace where they are contacted by a secondary air stream. At the injection point, fuel nitrogen evolves in an oxygen deficient environment, which favors its conversion to N_2 . Delayed contact between nitrogenous species and oxygen reduces the conversion of fuel nitrogen to NO. Thus, in a diffusion flame mode, there is less oxidation of fuel nitrogen to NO, relative to that in a premixed flame mode.

BITUMINOUS COAL PRIMARY FLAME, NATURAL GAS REBURNING

Primary SR = 1.23, $\text{NO}_p \sim 1070$ ppm (dry, 0% O_2)

Reburn Zone: Time = 0.4-0.5 s, Temp = 1500-1600 K

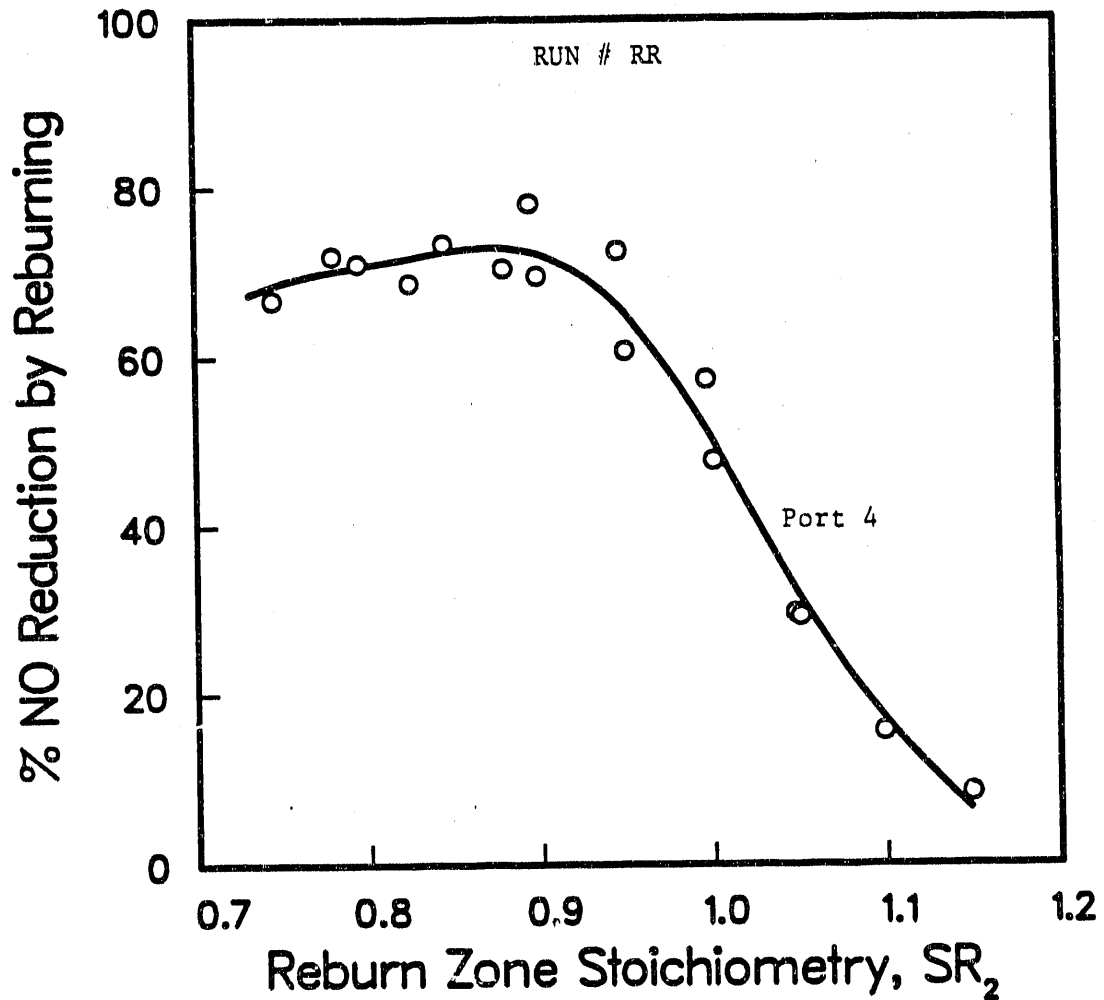


Figure 5.1. Variation of Reburning Effectiveness with Reburn Zone Stoichiometry - Premixed Primary Flame - N_2 Injected with Reburning Fuel.

BITUMINOUS COAL PRIMARY FLAME, NATURAL GAS REBURNING
Reburn Zone: Time = 0.33-0.43 s, Temp = 1550-1600 K
 $\text{NO}_p \sim 900$ ppm (dry, 0% O_2)

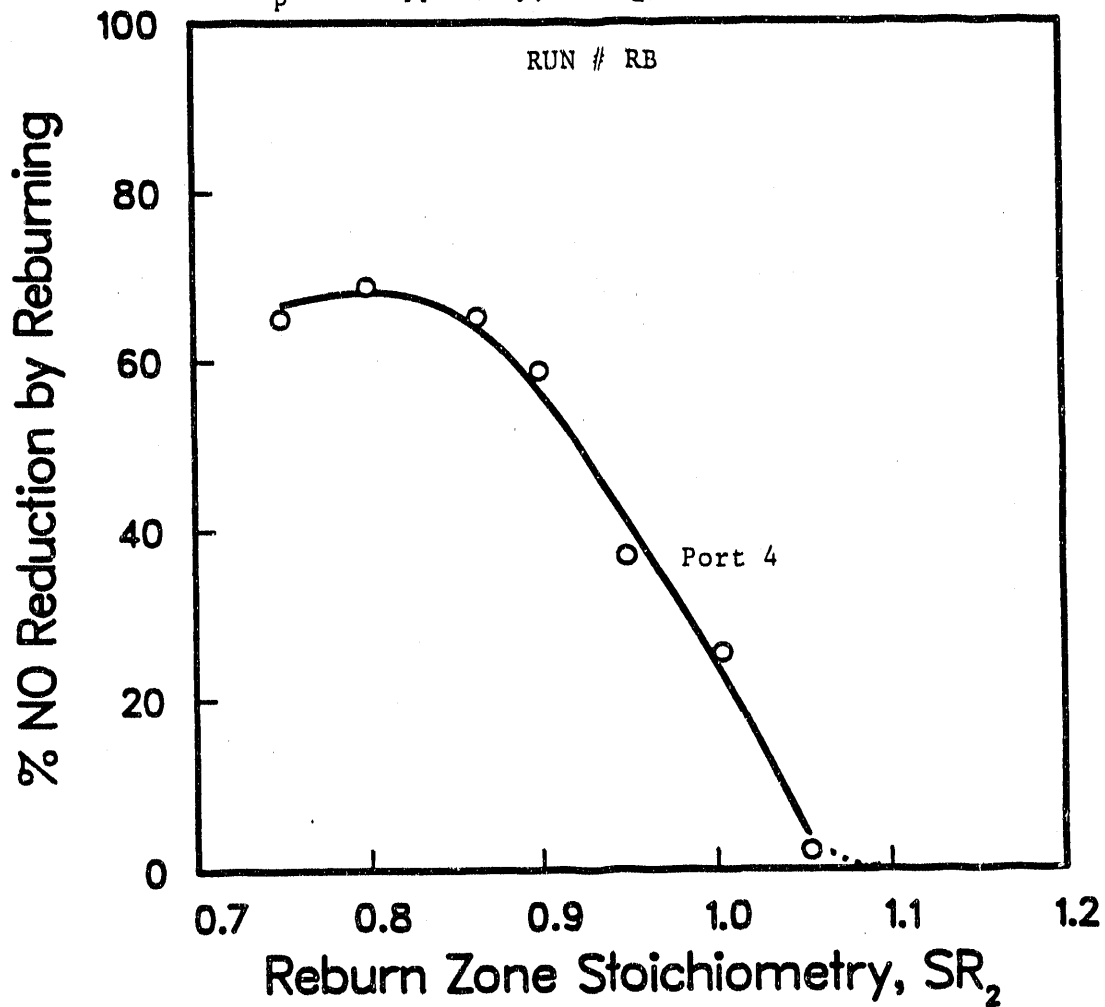


Figure 5.2. Variation of Reburning Effectiveness with Reburn Zone Stoichiometry - Premixed Primary Flame.

BITUMINOUS COAL PRIMARY FLAME, NATURAL GAS REBURNING
 Primary Zone: SR = 1.18, NO_p = 1030 ppm (dry, 0% O₂)
 Reburn Zone: Time ~ 0.7 s, Temp ~ 1570 K

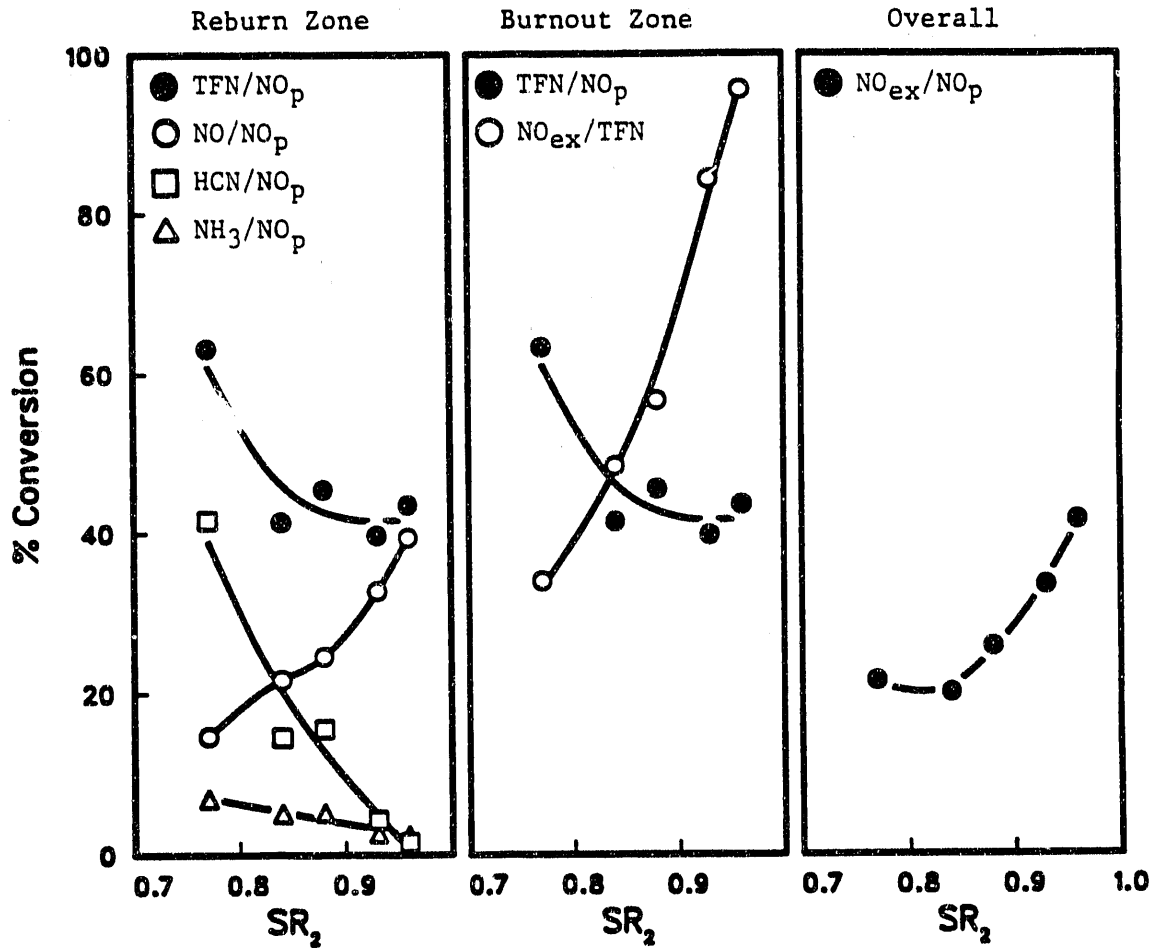


Figure 5.3. Nitrogenous Species Conversions at Various Stages of Reburning.

Experiments were conducted in which the premixed burner was replaced by a burner that produced a long axial flame with no swirl (type A.) The results in this case are more complex to interpret than in a premixed mode, but relate more closely to flames in industrial applications. Typically, axial pulverized coal flames without swirl are difficult to stabilize if the combined heat of wall radiation and convection of hot combustion gases is not sufficient to ignite the fuel. No problem with flame stability was experienced in these experiments, possibly due to the properties of the silicon carbide refractory that constituted the inside wall of the combustor.

Two reburning experiments were performed in which the primary flame was a bituminous coal axial diffusion flame and natural gas transported by N_2 gas was the reburning fuel. In one experiment, time resolved nitrogenous species profiles in the reburn zone were compared to those in which the primary flame was premixed. The results of the second experiment show the variation of reburning effectiveness with reburn zone stoichiometry.

5.2.1 Nitrogenous Species Profiles in the Reburn Zone

Figure 5.4 shows residence time resolved nitrogenous species profiles along the center line axis in the reburn zone for two types of primary flames, a premixed flame and a type A axial diffusion flame (Beer and Chigier, 1972). The overall stoichiometries in the primary zone (1.10) and in the reburn zone (0.86), and temperature profiles were similar in both cases. Visual inspection of the primary flames showed a displacement of the diffusion flame of about 25 cm from the burner, compared to a displacement of less than 10 cm of the premixed flame. Furthermore, no penetration of the primary flame into the reburn zone was observed in either case. In these experiments, the reburning fuel was transported by N_2 and introduced through port 3. Residence times in the primary zone were calculated as 0.29 seconds in the premixed flame mode and 0.37 seconds in the diffusion flame mode. However, a calculated time would not be an exact measure of the actual residence time, due to the displacement of the primary flame from the burner.

In the primary zone, gas phase measurements and a carbon balance resulted in 10.4% carbon that was unaccounted for when the primary flame was in the diffusion mode, and 6.6% in the premixed flame mode. This might suggest a minor difference in char burnout at the reburning fuel injection point between the two flame modes. However, in the diffusion mode, the high CO concentrations of 0.3% (wet basis) suggested insufficient char burnout at the exit of the primary zone. The difference in the fraction of the carbon that was unaccounted for, would be more likely the result of experimental error and would not be a good measure of the degree of char burnout. In the premixed primary flame mode, CO measurements were below the detection limit of the CO analyzer (0.04%).

In the reburn zone, the concentrations of hydrocarbons, CO_2 , CO, H_2 , N_2 and H_2O were similar in both experiments. However O_2 concentrations were higher when the

BITUMINOUS COAL PRIMARY FLAME, NATURAL GAS REBURNING

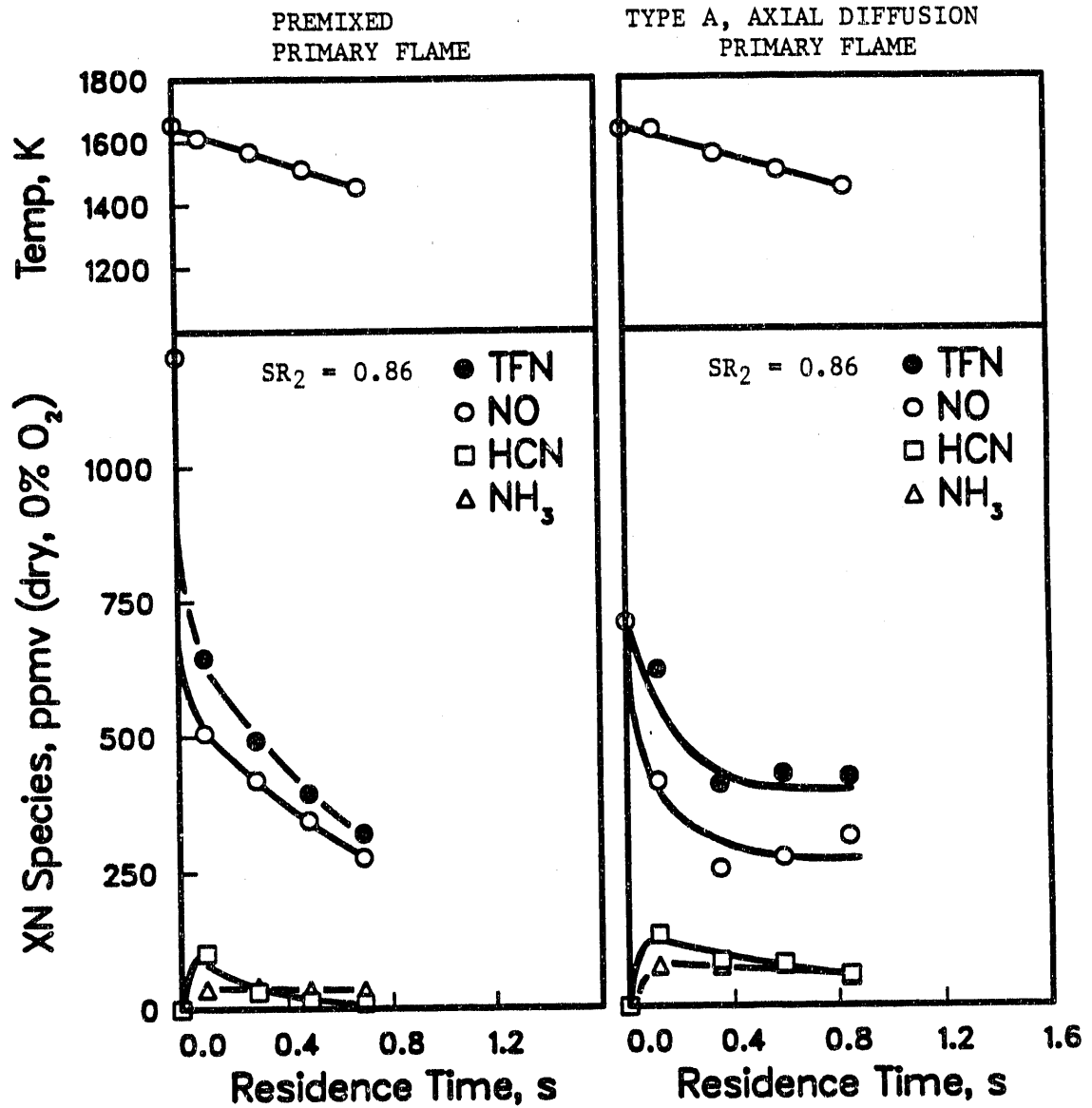


Figure 5.4. Fixed Nitrogenous Species Profiles in the Reburn Zone - Comparison between Premixed and Diffusion Primary Flame Modes.

primary flame was the diffusion type, which is an indication of poor mixing conditions in the reburn zone. The concentrations of the various species are listed in Appendix B (Coal #7 and Coal #21).

The primary NO level was 1200 ppm (dry, 0% O₂) in the premixed flame mode and 700 in the diffusion mode (Figure 5.4). The difference in the primary NO level was due to the difference in the level of contact between the fuel nitrogen in the volatile fraction and oxygen in the primary zone, which affects the conversion of coal nitrogen to NO. The concentrations of HCN and NH₃ in the reburn zone were higher in the diffusion flame mode and the decay of all nitrogenous species proceeded at a slower rate. That was partly due to the lower concentration of the primary NO and partly due to the nature of the diffusion flame, which could create variations in the local stoichiometries in the primary zone and in the reburn zone. The presence of extremely fuel rich pockets in the reburn zone would account for the relatively high levels of HCN and NH₃ in the diffusion flame mode.

Significant destruction of NO was observed in the reburn zone in both reburning experiments (Figure 5.4), and NO decayed to about the same low level of 270 ppm (dry, 0% O₂). However, the total fixed nitrogen concentration (NO + HCN + NH₃) was higher in the diffusion flame mode, relative to that in the premixed flame mode. Therefore, the application of reburning downstream of a low NO_x burner (diffusion flame) produced greater levels of nitrogenous species, in comparison with reburning downstream of a high NO_x burner (premixed flame). This conclusion might not always be valid and would be partly dependent on the stoichiometry in the reburn zone, as discussed in the following section.

5.2.2 Overall Reburning Effectiveness

A reburning experiment was performed in which the primary flame was that of bituminous coal in the diffusion mode and the reburning fuel was natural gas. The reburning fuel was transported by N₂ gas and introduced through port 4. Figure 5.5 shows the results of this experiment, presented as the variation of reburning effectiveness with reburn zone stoichiometry. NO reductions as high as 65% were obtained and no optimum reburn zone stoichiometry was identified in the experimental range that was covered. Similar results were obtained by Lanier et al. (1986) in a study of natural gas reburning in a pilot scale package boiler simulator. An optimum reburn zone stoichiometry might exist at stoichiometries richer than 0.8, due to poor mixing conditions that are associated with diffusion flames.

The concentrations of CO (wet basis) in the primary zone ranged from 0.5% to 1.2%, which indicated insufficient char burnout at the reburning fuel injection point. However, CO concentrations after final air addition ranged from 0.1% to 0.3%, and were similar to those corresponding to uncontrolled emissions (no reburning). Therefore, the degree of char burnout would be more likely due to the diffusion nature of the primary flame and less likely due to reburning action.

BITUMINOUS COAL PRIMARY FLAME, NATURAL GAS REBURNING

Primary SR = 1.18, $\text{NO}_p \sim 700$ ppm (dry, 0% O_2)

Reburn Zone: Time = 0.43-0.52 s, Temp = 1550-1600 K

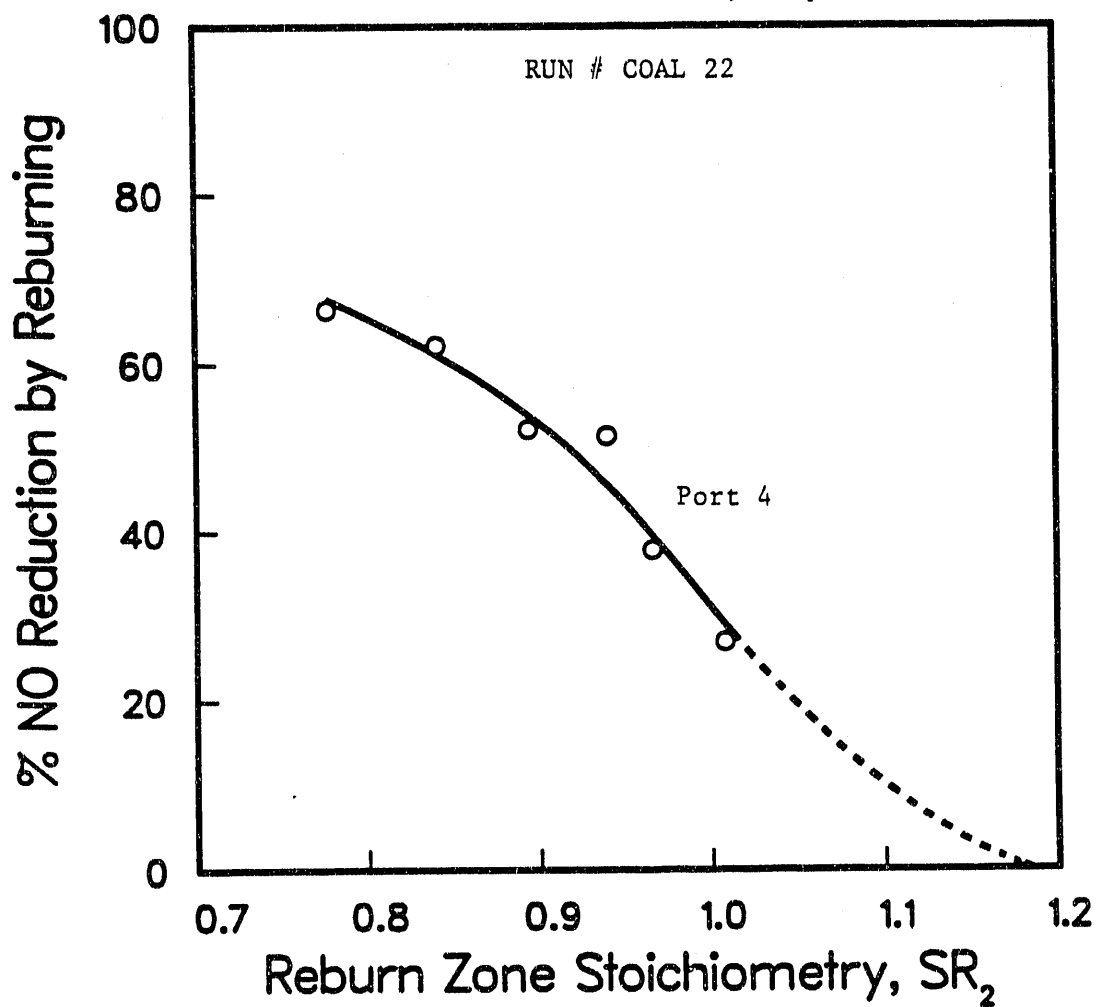


Figure 5.5. Variation of Reburning Effectiveness with Reburn Zone Stoichiometry - Axial Diffusion Primary Flame with No Swirl - N_2 Injected with Reburning Fuel.

Comparison of Figures 5.5 and 5.1 shows that the reburning effectiveness in a premixed flame mode is higher than that in a diffusion primary flame mode. However exhaust NO emission levels are comparable in both cases, reaching levels below 325 ppm (dry, 0% O₂) at reburn zone stoichiometries below 0.9. Thus, the application of reburning downstream of a coal diffusion primary flame is effective in reducing NO emissions. Higher reburning effectiveness would be expected if the primary flame is in a premixed mode, rather than the diffusion type, but low NO emissions would be possible in both cases.

6.0 EXPERIMENTAL RESULTS: REBURN ZONE PROFILES

The screening study, reported in Section 4.0, provides a general understanding of the reburning process. However, a fundamental understanding of reburning is required in order to develop confidence in theoretical models that predict the overall destruction of NO. In the literature, there is no agreement on a simple mechanism that can adequately describe the inter-conversion of nitrogenous species under practical coal combustion conditions. The specific issues that are addressed in this study are: what is the contribution of hydrocarbons, compared to other combustible species in governing NO destruction? which are the various sources of HCN formation? and what is the relative significance of homogeneous and heterogeneous mechanisms in the overall reburning process? The examination of mechanisms that govern the inter-conversion of nitrogenous species and the development of predictive NO_x abatement models comprise the remainder of this investigation.

In this section, the attention is focused on the fuel rich reburn zone, since the actions in that zone determine the levels and the distribution of the various nitrogenous species, and ultimately, final NO emissions after air addition in the burnout zone. The objective is to identify dominant reaction paths that govern the formation and destruction of nitrogenous species in the fuel rich reburn zone. For this purpose, the reburn zone is examined under various conditions, involving different reburning fuels, and gaseous as well as coal primary flames in the premixed mode. All the tests involve the introduction of the reburning fuel at port 3, corresponding to residence times in the primary zone of 0.4-0.6 seconds. The results are presented as time resolved nitrogenous species profiles in the reburn zone on a dry basis and corrected to 0% oxygen, with time zero starting at the inlet to the reburn zone. The concentrations of nitrogenous species and other combustion products are listed in Appendix B, on a wet basis. A dilution correction factor (DCF) can be used to convert wet concentrations to dry values and 0% excess O₂. The calculation of the correction factor was described in Section 4.2.2.

6.1 Natural Gas Reburning

Experiments were conducted to examine the effects of temperature and stoichiometry on nitrogenous species profiles in the reburn zone for a configuration in which the primary flame was that of bituminous coal, and natural gas was the reburning fuel. Natural gas is especially attractive as a reburning fuel since it contains no fuel nitrogen and can be easily delivered into the reburn zone.

Figure 6.1 shows nitrogenous species profiles in the reburn zone for two natural gas reburning experiments, at a fuel rich stoichiometry of 0.7. These profiles are typical and show that the change in nitrogenous species occurs over fairly long time scales that may exceed one second, during which NO decays to a lower level, whereas, HCN and NH₃ concentrations increase with time. Methane concentrations range from 0.9% to 1.35% (wet basis). These concentrations and those of other combustion products are listed in Appendix B (Coal #2 and 9). Nitrogenous species profiles suggest that there are two regimes for NO

BITUMINOUS COAL PRIMARY FLAME, NATURAL GAS REBURNING

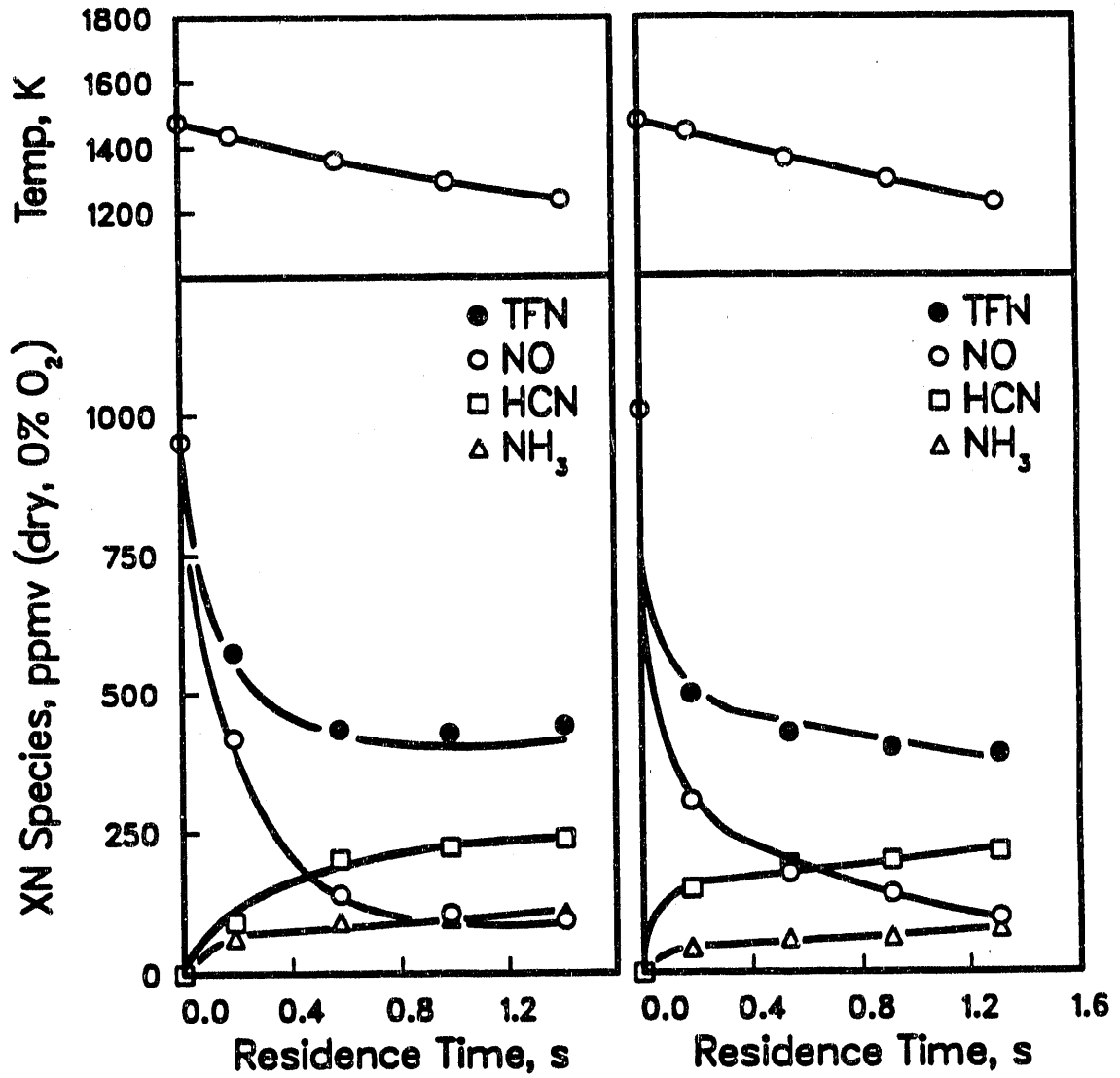


Figure 6.1. Fixed Nitrogenous Species Profiles in the Reburn Zone - Fuel Rich SR = 0.7.

destruction in the reburn zone. First, between the inlet to the reburn zone and the first measured point downstream, there is rapid destruction of NO that corresponds to rapid formation of HCN and NH₃. In this regime, mixing effects are important and can limit NO destruction by hydrocarbon radicals. Second, for the remainder of the reburn zone, there are no mixing complications and nitrogen chemistry controls the inter-conversion of nitrogenous species. In the examination of mechanisms, the focus is on the second region in the reburn zone where mixing effects are not important.

The increase in HCN concentrations with time (Figure 6.1) suggests a source of HCN formation in the reburn zone. Otherwise, HCN would be expected to decay to correspond to increasing NH₃ concentrations, since NH₃ is formed homogeneously from HCN. Similar observations were reported by Bose et al. (1988) in the study of the fuel rich combustion of various coals. Thus, this behavior of HCN is not limited to a reburning configuration. The different sources of HCN formation in the reburn zone are addressed in a later section.

6.1.1 Effect of Temperature

The change in temperature profiles was accomplished by varying the coal feed rate (primary fuel). Greater coal feeds produced higher temperatures, but also resulted in shorter residence times and higher primary NO concentrations due to the increased formation of Thermal NO. Figure 6.2 shows the results of three natural gas reburning experiments at different temperature profiles in the reburn zone. The effect of temperature is difficult to isolate, since the change in temperature is accompanied by other changes as well. Nevertheless, a comparison of the profiles in Figure 6.2 suggests a minor effect of temperature at residence times shorter than 0.1 seconds. At longer residence times, higher temperatures accelerated the destruction of all three nitrogenous species (NO, HCN and NH₃). The high temperature test (Coal #7) corresponded to a reburn zone inlet temperature of 1655 K and the decay in HCN values was accompanied by a decay in CH₄ concentrations to levels below 0.05% within 0.3 seconds. The concentrations of CH₄ in the reburn zone of the other two tests (Coal #10 and 12) ranged from 0.3% to 0.45% (wet basis). The observed effect of temperature on HCN profiles is in contrast with the results of Bose (1989) under fuel rich coal combustion conditions and at comparable temperatures. However, the results of Bose also suggest a correspondence between the profiles of HCN and those of CH₄. Thus, the presence of hydrocarbons in the fuel rich zone is expected to play a key role in HCN formation and destruction mechanism.

6.1.2 Effect of Dilution of the Primary Flame

A natural gas reburning experiment (Coal #3) was conducted in which the primary combustion flame was enriched with oxygen. The results of this experiment were compared to those of a reburning experiment (Coal #6) in which only air was used in the primary flame, as seen in Figure 6.3. The purpose of these experiments was to examine the effect of dilution of the primary flame on nitrogenous species profiles in the reburn zone. Enriching the primary flame with O₂ produced higher values of all measured species, since

BITUMINOUS COAL PRIMARY FLAME, NATURAL GAS REBURNING
 FUEL RICH SR = 0.86

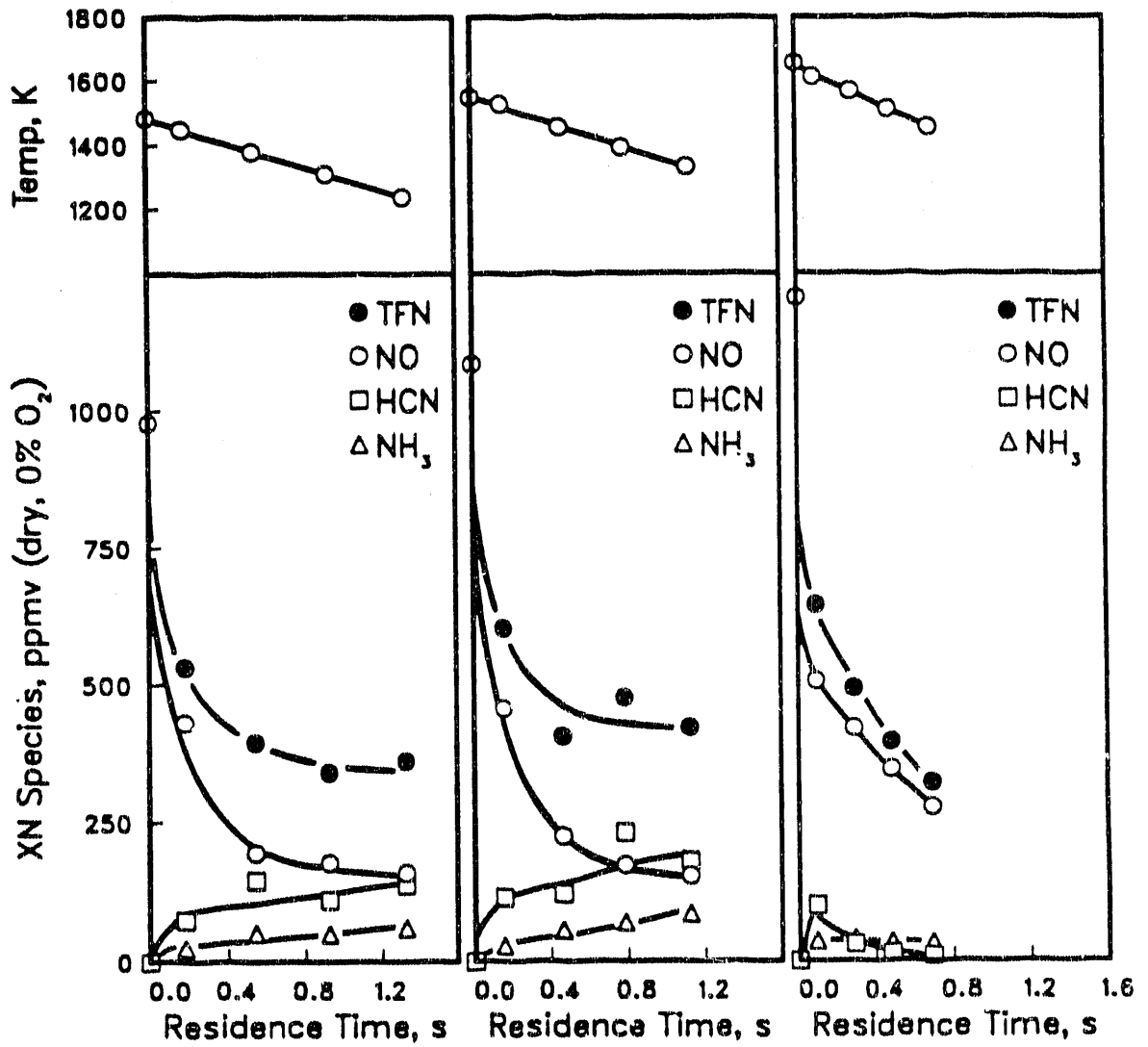


Figure 6.2. Fixed Nitrogenous Species Profiles in the Reburn Zone - Effect of Temperature.

BITUMINOUS COAL PRIMARY FLAME, NATURAL GAS REBURNING
 FUEL RICH SR = 0.80

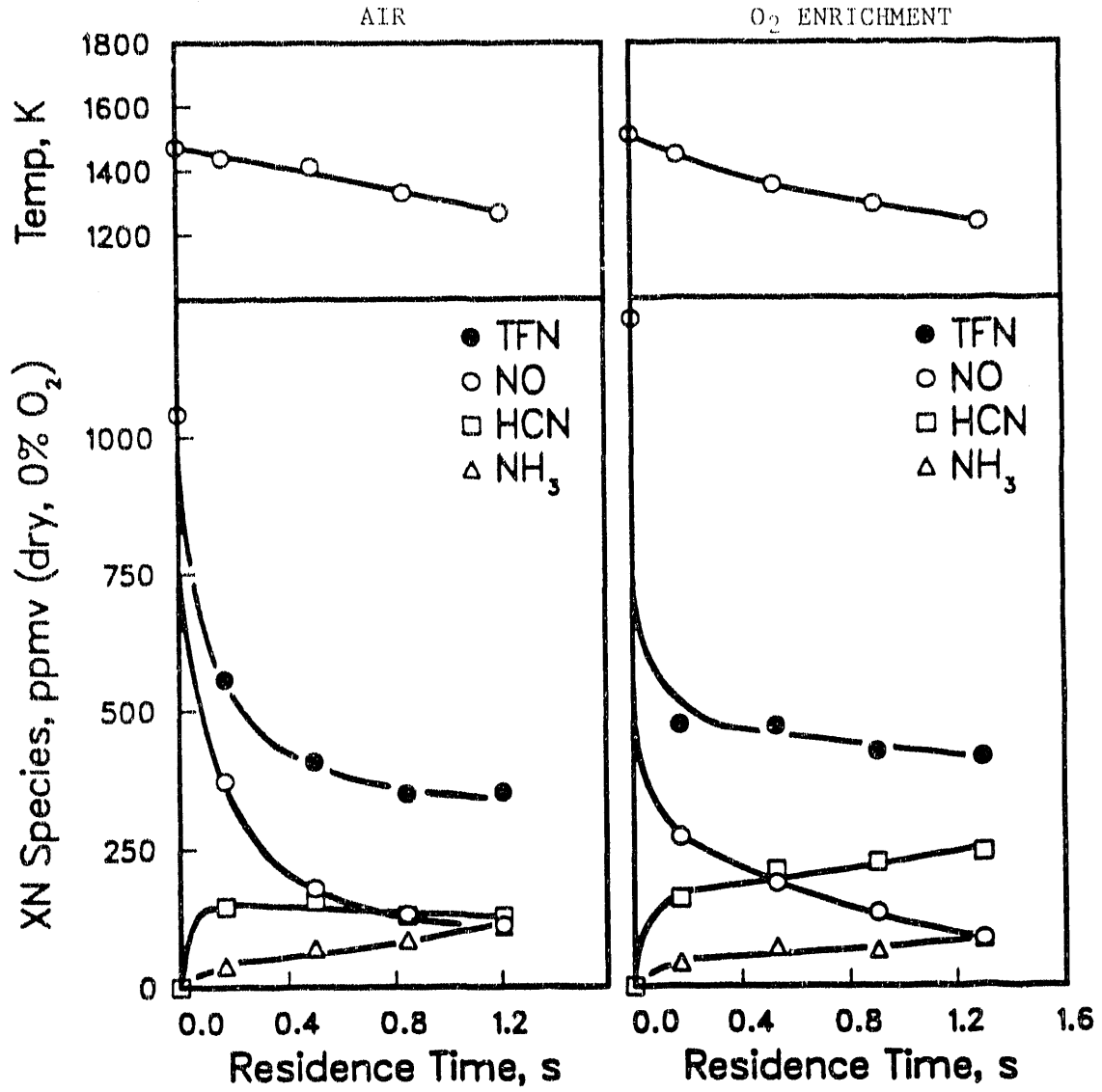


Figure 6.3. Fixed Nitrogenous Species Profiles in the Reburn Zone - Effect of Dilution in the Primary Zone.

the dilution of the combustion products with N_2 was reduced. Improved contact between CH_1 radicals and NO accelerated the destruction of NO. This effect was limited to the vicinity of the reburning fuel flame (Figure 6.3) and was offset by enhanced formation of HCN further downstream. However, the observed differences in nitrogenous species profiles between the two experiments were relatively minor and no general conclusions could be derived.

6.1.3 Effect of Stoichiometry

Figure 6.4 shows nitrogenous species profiles in the reburn zone at three different stoichiometries. The effect of stoichiometry in the reburn zone on nitrogenous species profiles is as expected. Lower levels of NO and higher levels of HCN and NH_3 are observed at lower stoichiometries. The results of these experiments (Coal #2, 4 and 10) are listed in Appendix B.

Under fuel lean conditions in the reburn zone ($SR_2 = 1.03$), 45% of the primary NO was destroyed and the measured concentrations of HCN and NH_3 were less than 4 ppm throughout the reburn zone. The destruction of NO (Figure 6.4) was mainly due to $NO + CH_1$ reactions and occurred within residence times less than 0.15 seconds. Thus, NO reduction was mainly limited to the poorly mixed region of the reburn zone, where methane concentrations were greater than 0.09% (wet basis). In the remainder of the reburn zone, CH_4 concentrations were about 0.01%. These results demonstrate that significant reductions in NO can be achieved using secondary fuel injections, without the formation of an overall fuel rich environment in the reburn zone. Under these conditions, mixing inhomogeneities can enhance NO destruction by hydrocarbon radicals if the reburn zone is operated under fuel lean conditions. Greene et al. (1985) observed a similar phenomenon, which was attributed to the formation of local fuel rich and fuel lean pockets in the vicinity of the reburning fuel jet.

The low concentrations of HCN in the fuel lean reburn zone (Figure 6.4) suggest that mixing inhomogeneities also affect HCN formation and destruction. The results show the destruction of NO by hydrocarbon radicals is not necessarily accompanied by the formation of significant amounts of HCN. The formation of HCN due to NO reactions with CH_1 radicals is offset by the destruction of HCN by oxygen containing radicals (O and OH), which is also affected by mixing. The effects of mixing on NO destruction and HCN formation in the poorly mixed region of the reburn zone are addressed in Section 8.1.

6.2 Sources of HCN Formation

The results of the natural gas reburning experiments suggested a source of HCN formation in the fuel rich reburn zone, since in most cases, HCN did not decay to correspond to increasing NH_3 concentrations. These observations are consistent with the fuel rich coal combustion data of Bose et al. (1988) and Bose and Wendt (1988). The researchers hypothesized a heterogeneous source of HCN formation, in which the slow

BITUMINOUS COAL PRIMARY FLAME, NATURAL GAS REBURNING

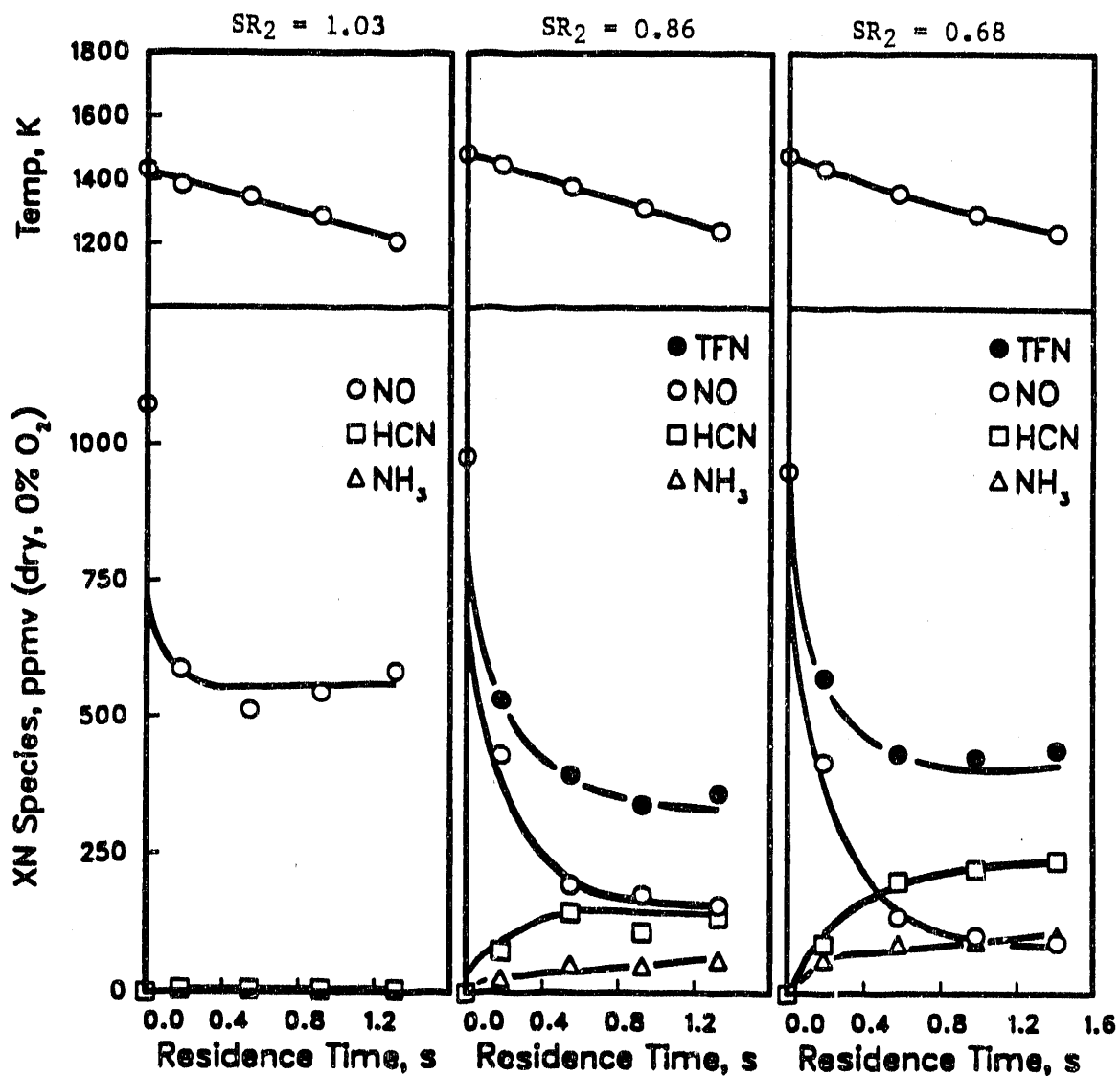


Figure 6.4. Fixed Nitrogenous Species Profiles in the Reburn Zone - Effect of Reburn Zone Stoichiometry.

release of nitrogen from the coal residue would form additional HCN in the fuel rich post flame. However, no direct evidence was presented to support this claim. Furthermore, homogeneous sources of HCN formation could not be excluded.

An examination of HCN and CH₄ measured profiles in this study (Appendix B), as well as of those in the fuel rich combustion study of Bose (1989), showed that a decay in HCN values occurred when CH₄ concentrations were below 0.1%. This observation strongly suggests that HCN is mainly formed due to reactions involving hydrocarbon radicals. The contribution of a reburning path, in which NO is destroyed by hydrocarbons to form HCN, is not disputed in the literature, although the time scale of this path is not yet clear. However, there is no general agreement, with respect to the significance of other reactions that can form HCN from hydrocarbons. Fenimore (1971) proposed a path in which HCN would be formed due to the fixation of N₂ by hydrocarbons, as an intermediate in Prompt NO formation. This path was identified by Lanier et al. (1986) as a major limitation to the effectiveness of the reburning process at low primary NO values. Another path for HCN formation, in which hydrocarbons react with radicals, was proposed by Haynes (1977a).

To summarize, various sources of HCN formation are possible and can create the observed rise in HCN concentrations with residence time in the fuel rich reburn zone. Under fuel rich conditions, HCN can be produced through a heterogeneous path, in which the release of nitrogen from the coal residue provides a continuous source of HCN. Furthermore, HCN can be formed through a homogeneous path, which involves reactions of nitrogen species (NO, N₂, or N) with hydrocarbons. The relative significance of the various sources of HCN formation is addressed in the following sections.

6.3 Non Hydrocarbon Gas Reburning

Two reburning experiments (Coal #5 and 8) were conducted, in which non hydrocarbon gases, namely, CO and H₂, were used as reburning fuels and bituminous coal was used as the primary fuel. The results are presented in Appendix B. Non hydrocarbon reburning fuels were used to examine the formation and destruction of nitrogenous species in the absence of hydrocarbons in the fuel rich reburn zone, as shown in Figure 6.5. Both experiments were conducted under a reburn zone stoichiometry of 0.9 and similar temperature environments. Hydrocarbon concentrations in the reburn zone were below the detection limit of the FID throughout the reburn zone, and were estimated to be lower than 100 ppm.

The primary NO level was reduced by less than 30% in CO reburning and by less than 10% in H₂ reburning, after a residence time of about one second in the reburn zone. In addition, HCN concentrations were less than 13 ppm (dry, 0% O₂) and NH₃ concentrations were less than 20 ppm (dry, 0% O₂). Similar observations were reported by Greene et al. (1985) who showed that the reburning effectiveness of CO and H₂ reburning

BITUMINOUS COAL PRIMARY FLAME, FUEL RICH SR = 0.90

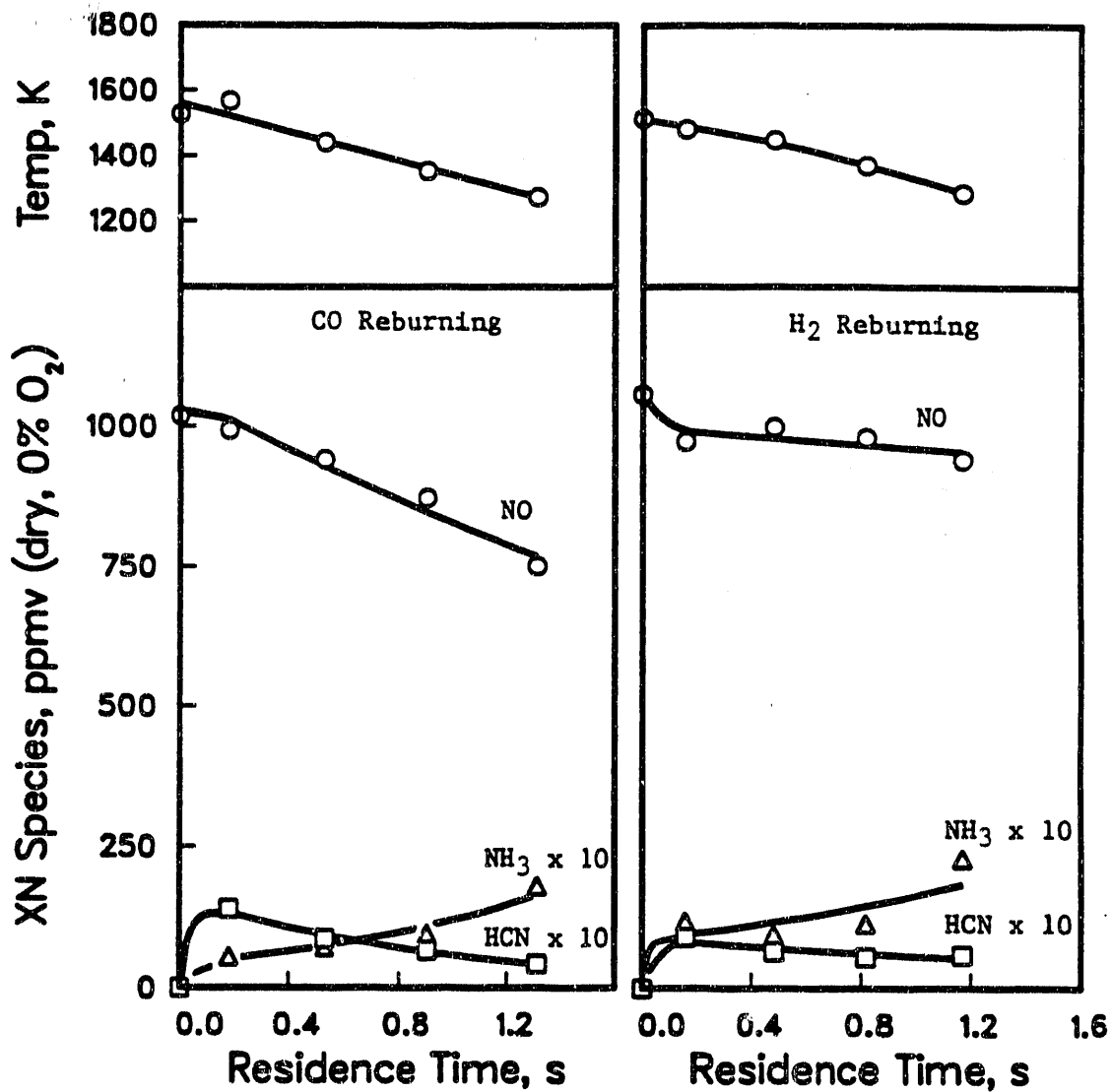


Figure 6.5. Fixed Nitrogenous Species Profiles in the Reburn Zone - Non-Hydrocarbon Reburning Fuels.

fuels was far below that of hydrocarbon reburning fuels, under practical reburning conditions. These results demonstrate the significance of hydrocarbons in destroying NO, under the fuel rich conditions of the reburn zone.

The formation of HCN in short residence times in the reburn zone (less than 0.18 seconds), was followed by slow decay of HCN to values that were lower than those of NH₃ (Figure 6.5). That was possibly due to higher secondary flame temperatures when CO and H₂ were the reburning fuels, relative to those of natural gas reburning fuels. Higher temperatures would favor HCN destruction reactions. The low values of HCN and NH₃ in the reburn zone demonstrate that the carry over of char nitrogen from the primary flame is a minor contributor to HCN formation. Consequently, homogenous gas phase kinetics can be used to describe the inter-conversion of nitrogenous species in the fuel rich reburn zone. Furthermore, a heterogenous source of HCN formation cannot describe the observed trends of HCN in natural gas reburning experiments, and homogeneous sources of HCN formation need to be further investigated.

6.4 Natural Gas Primary Flame

The destruction of NO by hydrocarbon radicals has been established as a significant contributor to HCN formation. In order to explore the significance of other homogeneous gas phase hydrocarbon reactions in forming HCN, the contribution of NO + CH_i reactions in the reburn zone was minimized. This was accomplished by using natural gas as the primary fuel to produce low primary NO levels. That would limit the formation of NO in the primary zone, mainly to that of Thermal NO. The primary natural gas feed was introduced at low flow rates to produce relatively low temperatures in the primary zone (less than 1500 K), and thus, low primary NO concentrations were obtained. Natural gas was also used as the reburning fuel and was introduced in a similar manner as described earlier.

Figure 6.6 shows the results of two reburning experiments (Gas #7 and 4), in which primary NO levels of 35 and 45 ppm (dry, 0% O₂) are obtained, respectively. Measured CH₄ values (wet basis) are between 0.4% and 0.7% (Appendix B). The focus of these experiments is on HCN concentrations in the reburn zone. These levels are relatively high (greater than 60 ppm) and exceed the primary NO level in both cases. In addition, the profiles show an increase in the total fixed nitrogen (TFN = NO + HCN + NH₃), relative to the primary NO level. Figure 6.7 shows the same results as in Figure 6.6, but the results are presented in terms of conversions. The conversion is the molar rate of the nitrogenous species, divided by molar rate of the primary NO. The conversions for HCN and the total fixed nitrogen (TFN) exceed 100% in both cases. Therefore, nitrogenous species inter-conversion reactions cannot account for all the formation of HCN. Clearly, significant amounts of HCN can be produced from hydrocarbons due to N₂ + CH_i and N + CH_i reactions.

Under the conditions of these experiments (Figure 6.6), NH₃ concentration in the reburn zone were less than 6 ppm (dry, 0% O₂) and thus, low concentrations of N radicals

NATURAL GAS PRIMARY FLAME, NATURAL GAS REBURNING
 FUEL RICH SR = 0.86

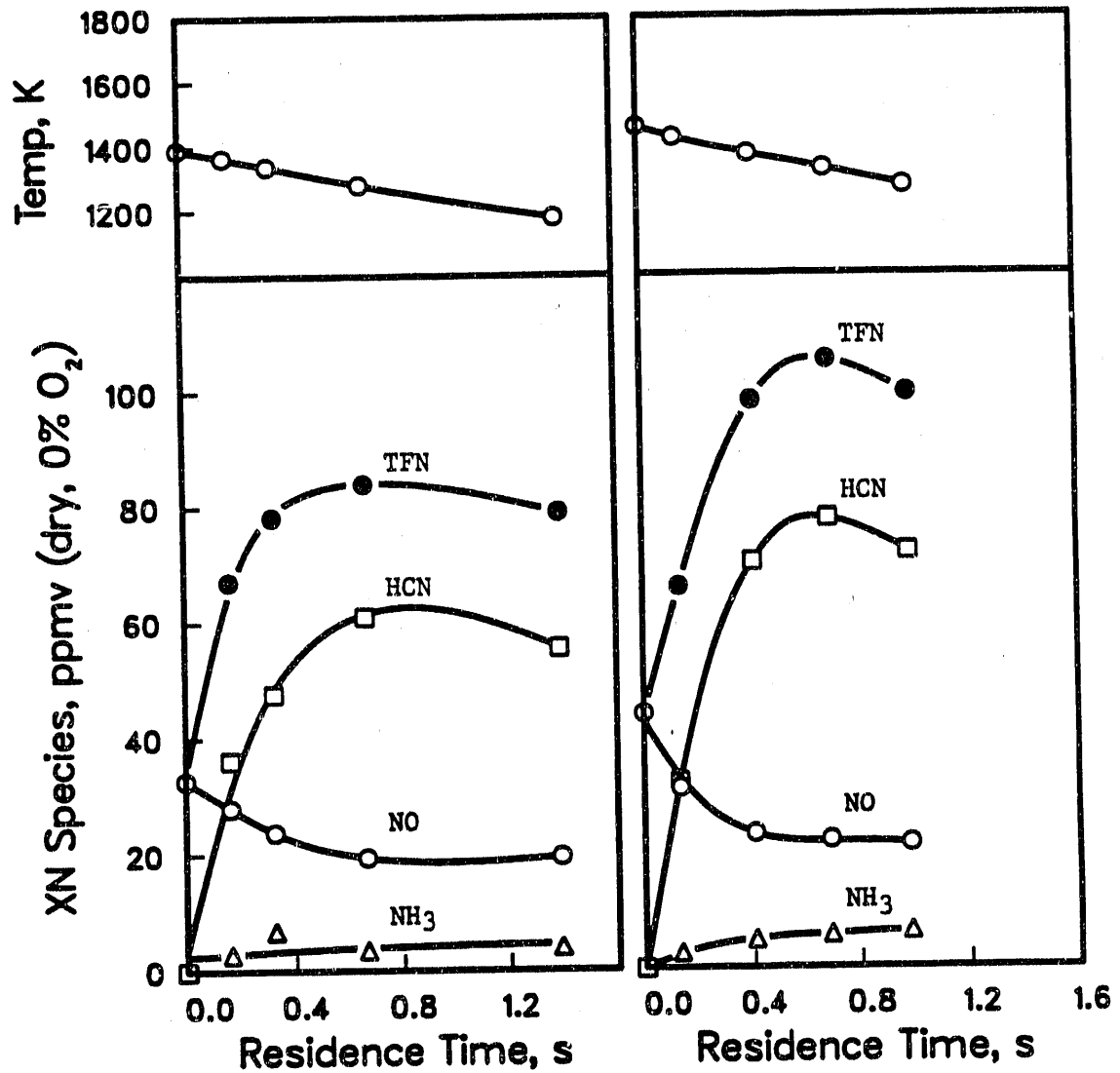


Figure 6.6. Fixed Nitrogenous Species Profiles in the Reburn Zone - Reburning at Low Primary NO.

NATURAL GAS PRIMARY FLAME, NATURAL GAS REBURNING
 FUEL RICH SR = 0.86

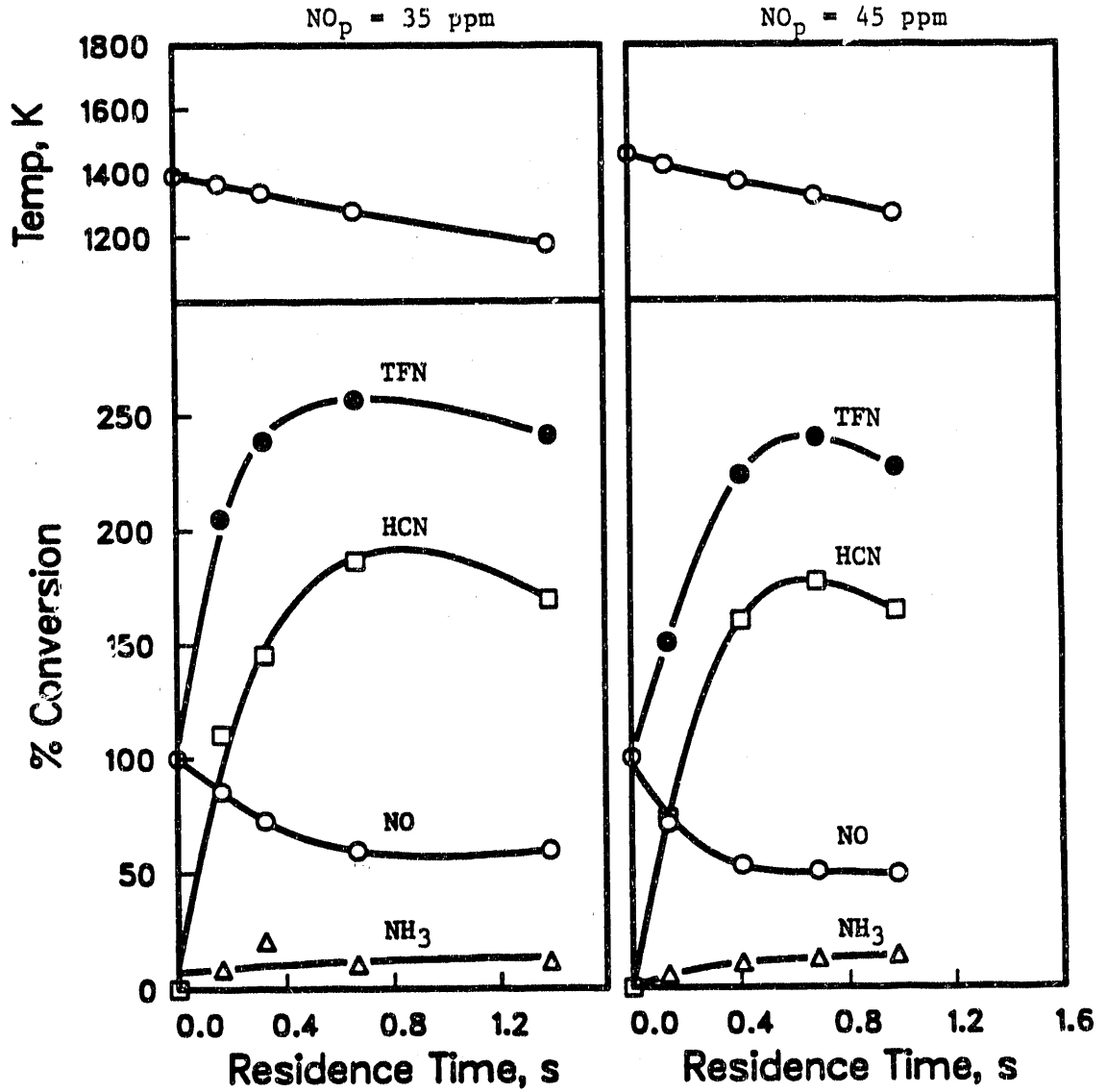


Figure 6.7. Conversions for Fixed Nitrogenous Species in the Reburn Zone - Reburning at Low Primary NO.

would be expected. Consequently, HCN formation was mainly due to the fixation of N_2 by hydrocarbon radicals, as originally proposed by Fenimore (1971). The significance of this path for HCN formation increases as the primary NO concentration decreases, since both N_2 and NO compete for CH_i radicals. This result is of major significance in the application of reburning, since it presents a serious limitation to the effectiveness of the process, especially at low primary NO levels. The fixation of N_2 by hydrocarbon radicals increases in significance as NO reactions with CH_i radicals reduce NO concentrations in the reburn zone to lower values. This can limit further destruction of NO, since less hydrocarbon radicals are available to react with NO, in addition to the destruction of N_2 to form HCN. Similar observations were reported by Lanier et al. (1986), in an examination of natural gas reburning in a package boiler simulator.

6.5 Ammonia Doped Natural Gas Primary Flame

Natural gas reburning experiments were conducted to examine the effect of primary fuel type on nitrogenous species profiles in the reburn zone. Figure 6.8 compares the results of an experiment in which the primary fuel was bituminous coal (Coal #10), to those of an experiment in which the primary fuel was natural gas doped with NH_3 (Gas #2). The gaseous primary flame involved the addition of NH_3 to the primary natural gas feed to produce a primary NO level comparable to that of a bituminous coal flame. Figure 6.8 shows that the profiles for all nitrogenous species are similar in both cases, which is further indication that homogenous processes dominate the inter-conversion of nitrogenous species in the reburn zone. The values of HCN in the reburn zone, downstream of the coal primary flame are lower than those corresponding to the gaseous primary flame, which suggests a minor contribution of heterogeneous sources to HCN formation. The differences in the values of the nitrogenous species between the two experiments are possibly due to differences in the measured concentrations of the major species (O_2 , H_2O , CO, CO_2 , CH_4 , H_2 and N_2) in the reburn zone. These concentrations are listed in Appendix B.

6.6 Ammonia Doped Natural Gas Reburning

Experiments were conducted to examine the effect of nitrogen content in the reburning fuel on the distribution of nitrogenous species in the reburn zone. An increase in the nitrogen content of the reburning fuel is expected to produce higher levels of nitrogenous species, due to the introduction of additional fuel nitrogen into the reburn zone. Figure 6.9 shows fixed nitrogenous species profiles in the reburn zone for two natural gas reburning tests at similar temperature profiles and a stoichiometry of 0.85 in the reburn zone. For one test (Coal #12), the reburning fuel was natural gas and for the other (Gas #13), the reburning fuel was natural gas doped with NH_3 to a nitrogen content of about 1.1% nitrogen (% mass). The results of these two tests are presented in Appendix B.

The profiles in Figure 6.9 show that at residence times greater than 0.4 seconds, the levels of nitrogenous species are about the same in both cases. However, at the first measurement downstream of the reburning fuel injection point, the presence of nitrogen in

NATURAL GAS REBURNING, FUEL RICH SR = 0.86

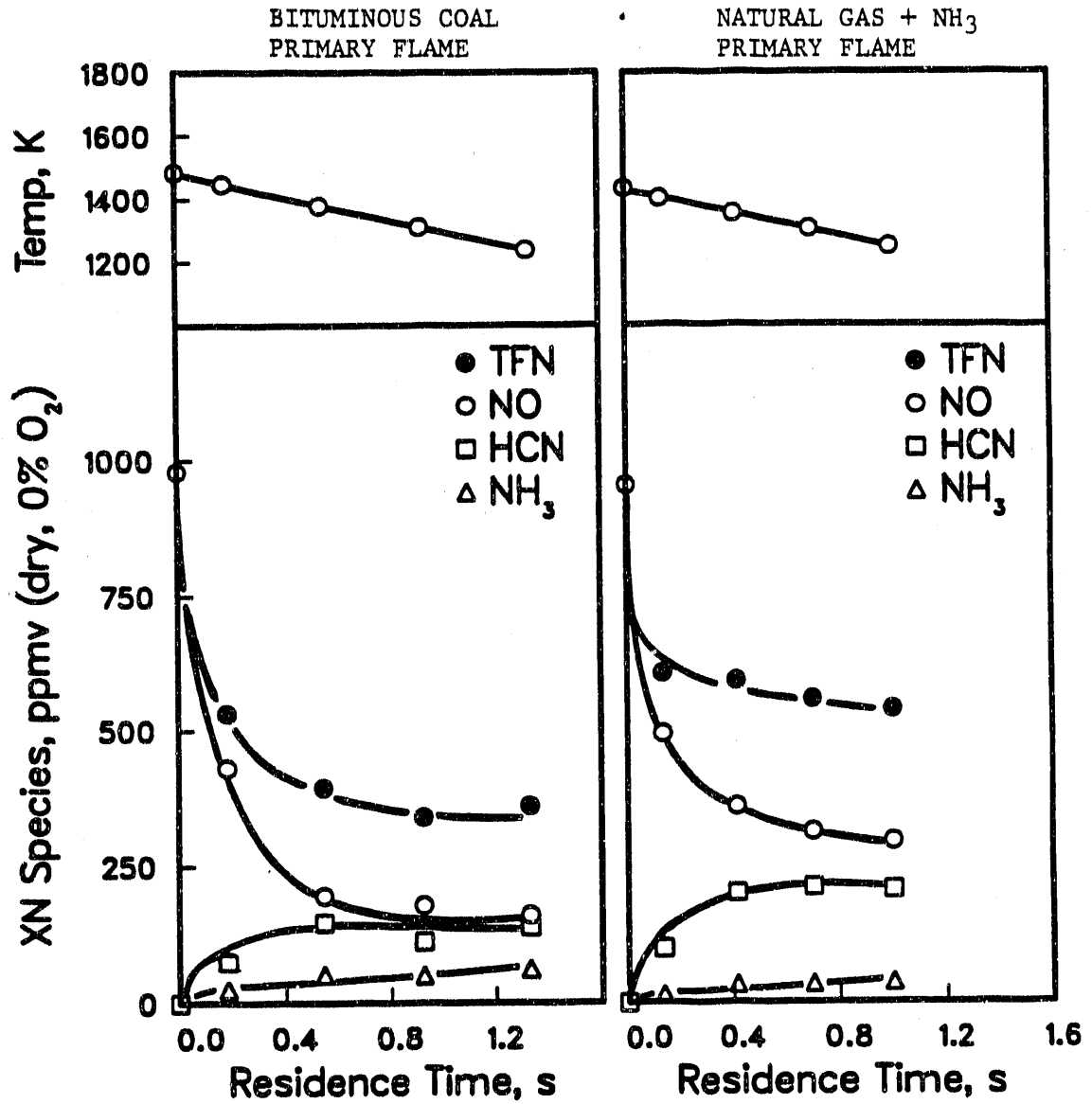


Figure 6.8. Fixed Nitrogenous Species Profiles in the Reburn Zone - Effect of Primary Fuel Type.

BITUMINOUS COAL PRIMARY FLAME, FUEL RICH SR = 0.85

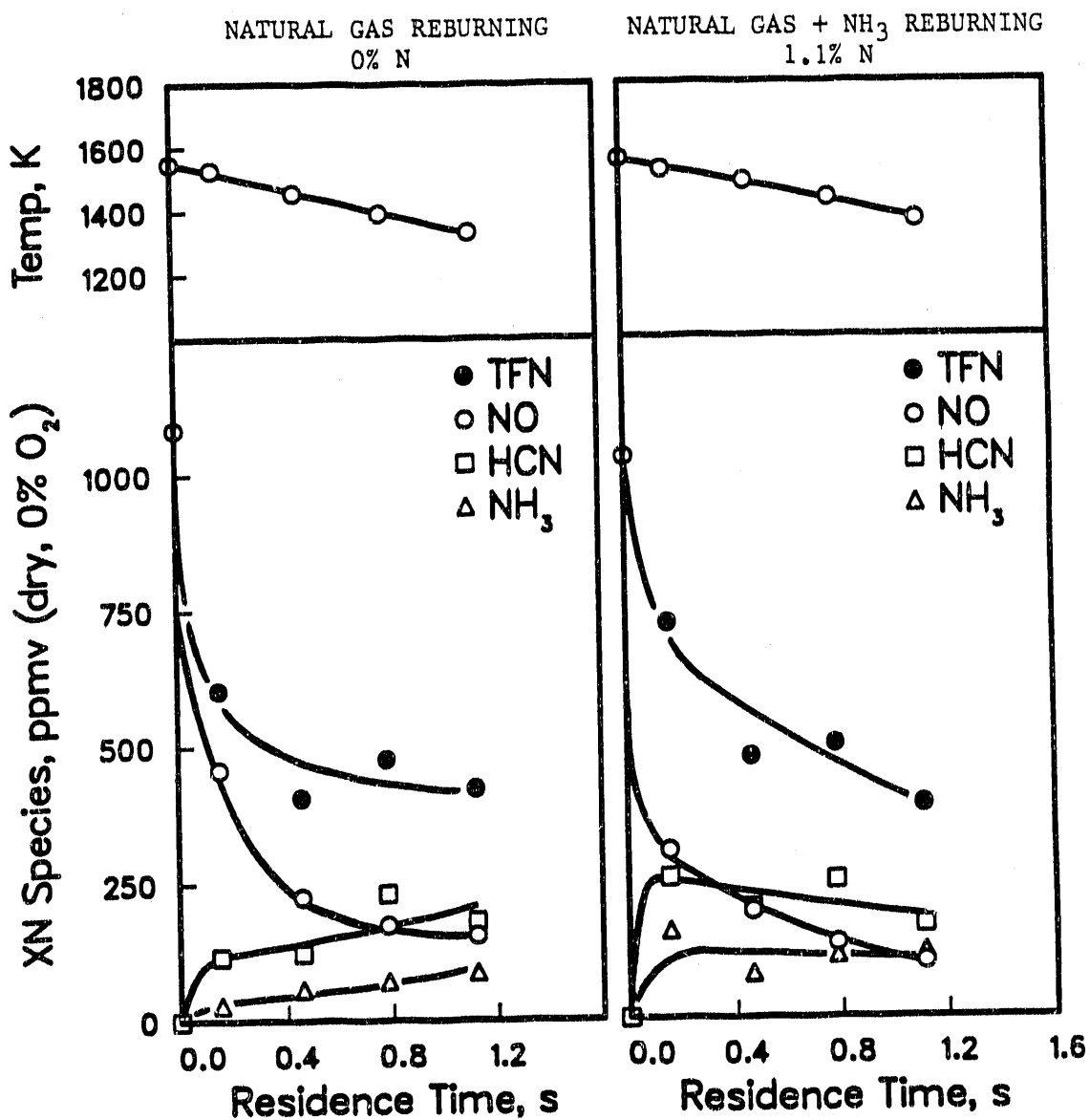


Figure 6.9. Fixed Nitrogenous Species Profiles in the Reburn Zone - Effect of Reburning Fuel Nitrogen Content.

the reburning fuel produced significantly higher levels of HCN and NH_3 , due to the enhanced formation of HCN from $\text{CH}_3 + \text{N}$ reaction. Furthermore, NO decay rate was more rapid when NH_3 was injected with the reburning fuel, possibly due to enhanced NO destruction by NH_1 radicals.

The results demonstrate that the effect of fuel nitrogen in the volatile form in the reburning fuel, is strongly dependent on the residence time that is allowed in the reburn zone. The introduction of fuel nitrogen with the reburning fuel into the reburn zone can significantly increase HCN and NH_3 concentrations for residence times less than 0.4 seconds. This results in higher concentrations of the total fixed nitrogen, although NO decay may be enhanced in the presence of higher levels of NH_3 . For residence times greater than 0.4 seconds in the reburn zone, the overall effect of the fuel nitrogen that is introduced into the reburn zone is of minor significance. All the nitrogenous species decay to lower levels that are comparable to those observed in natural gas reburning experiments.

6.7 Coal Reburning

The use of coal as a reburning fuel is attractive in the application of reburning in a commercial coal fired boiler. Literature data on the use of coal as a reburning fuel downstream of a coal primary flame are scarce. Most studies of coal reburning involved configurations in which gaseous primary flames, doped with nitrogenous species, were used to simulate coal combustion flue gases in the primary zone. In this study, coal reburning experiments involved the use of a bituminous coal as the primary fuel and as the reburning fuel. As in natural gas reburning experiments, N_2 gas was used to transport the coal reburning fuel, but a different injector tip was used that consisted of four holes, each 0.64 cm in diameter. A secondary coal feeder was used to introduce the coal reburning fuel at the desired feed rate.

Figure 6.10 shows nitrogenous species profiles in the reburn zone for a natural gas reburning test (Coal #3) and a coal reburning test (Coal #15), at a reburn zone stoichiometry of 0.80. The introduction of coal into the reburn zone produced high levels of HCN and NH_3 within 0.14 seconds, where HCN values exceeded 600 ppm (dry, 0% O_2) and NH_3 values exceeded 90 ppm. At longer residence times, HCN and NH_3 decayed to lower levels, that were comparable to those typical of natural gas reburning. However, in coal reburning, higher NO levels and lower NO decay rates were observed throughout the reburn zone, relative to those in natural gas reburning. The lower NO decay rates were due to the reduced production of hydrocarbons from the coal reburning fuel, where measured CH_4 values were less than 0.07% in the reburn zone. In natural gas reburning and under similar conditions, CH_4 values in the reburn zone were 0.3-0.4%. The concentrations of the various species are listed in Appendix B. In the presence of low hydrocarbon concentrations in the reburn zone (less than 0.1%), NO destruction by hydrocarbon radicals would be of minor significance and $\text{NO} + \text{NH}_1$ reactions would dominate NO decay. These results are consistent with the coal reburning results of Knill and Morgan (1989), who used a model based only on $\text{NO} + \text{NH}_1$ reactions to describe NO decay in the reburn zone.

BITUMINOUS COAL PRIMARY FLAME, FUEL RICH SR = 0.80

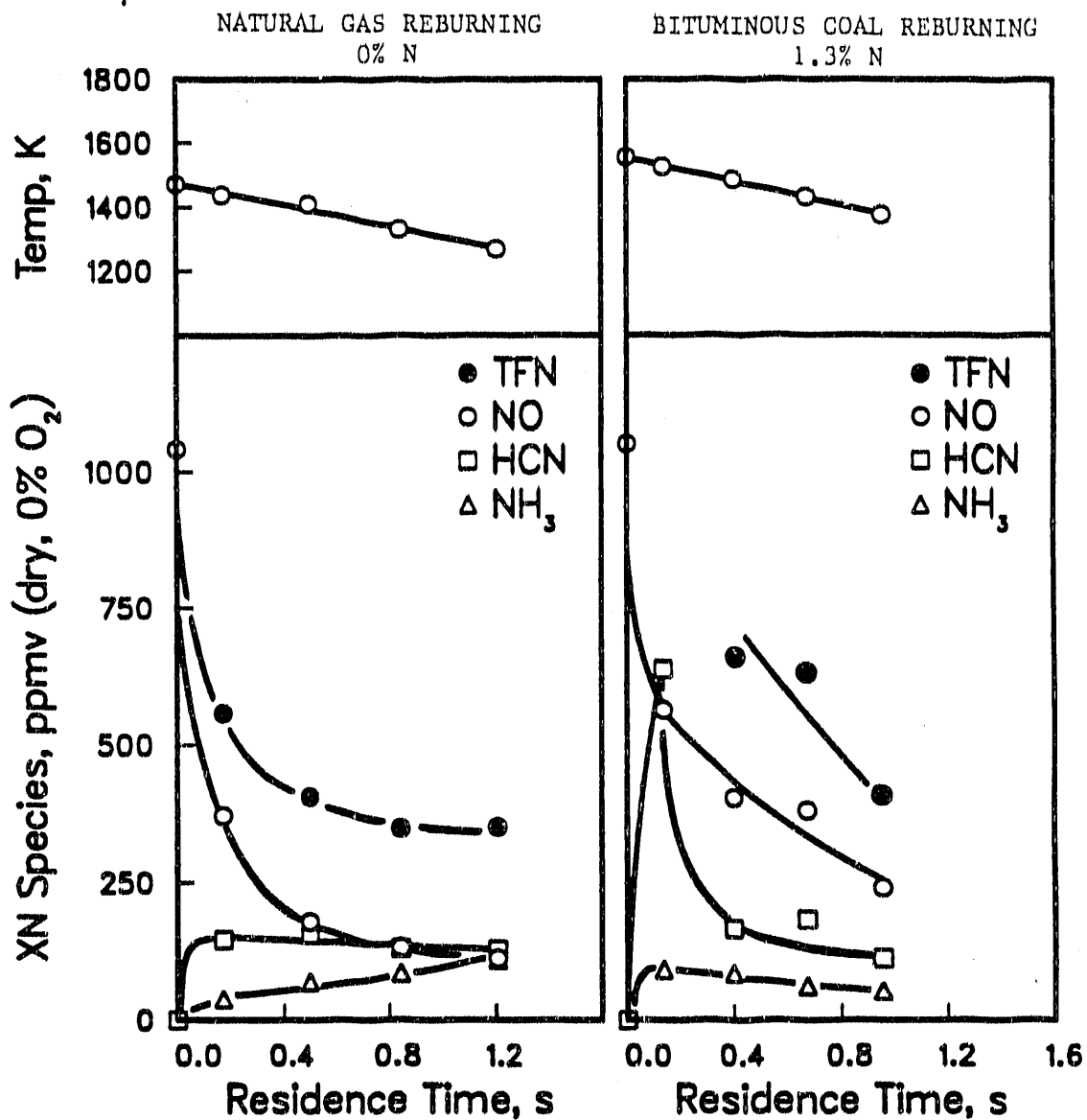


Figure 6.10. Fixed Nitrogenous Species Profiles in the Reburn Zone - Effect of Reburning Fuel Type.

The results of the coal reburning test suggest that the effect of introducing coal nitrogen into the reburn zone on the distribution of nitrogenous species, is limited to short residence times in the vicinity of the reburning fuel flame. This effect is of minor significance at residence times greater than 0.4 seconds in the reburn zone, since the nitrogenous species decay to lower levels. Similar conclusions are derived from NH_3 doped natural gas reburning experiments.

6.8 Effect of Reburning Fuel Type and Nitrogen Content

Figure 6.11 shows nitrogenous species profiles in the reburn zone for three tests, in which different reburning fuels were used, namely, natural gas (Coal #19), natural gas doped with NH_3 to a nitrogen content of 1.4% (Coal #20), and bituminous coal containing 1.3% nitrogen (Coal #17). Primary NO levels and temperature profiles in the reburn zone were similar in all cases, and the reburn zone stoichiometry was at 0.9. HCN and NH_3 concentrations were less than 100 ppm throughout the reburn zone. Minor difference in NO profiles were observed, when gaseous reburning fuel were used, regardless of the nitrogen content. However, NO decayed at a slower rate in coal reburning and corresponded to low methane levels of less than 0.02%. Methane concentrations in the reburn zone were 0.1-0.15%, when gaseous reburning fuels were used (Appendix B). Similar results were reported by Greene et al. (1985) in a comparison of coal, and gaseous reburning fuels doped with NH_3 to the same nitrogen content. Lower NO decay rates were obtained with coal reburning, but HCN and NH_3 yields were the same as with gaseous reburning, over a wide range of stoichiometries and a reburn zone residence time of 0.4 seconds.

The effect of nitrogen content in the reburning fuel is less obvious at leaner stoichiometries in the reburn zone, possibly due to mixing inhomogeneities and oxygen availability in the vicinity of the reburning fuel flame, corresponding to short residence time. The presence of oxygen in the early stage of the reburn zone enhances the decay of HCN and NH_3 , and the effect of introducing fuel nitrogen with the reburning fuel is diminished. In coal reburning (Figure 6.11), HCN values decayed to levels below 20 ppm within 0.6 seconds. These low levels are due to the dominance of HCN destruction reactions in the reburn zone, since HCN formation from hydrocarbons is of minor significance when the hydrocarbon concentrations are low. These results further support the hypothesis that HCN formation in long time scales is mostly due to hydrocarbon reactions, and the slow release of nitrogen from the coal residue is of minor significance.

To summarize, the effect of nitrogen content in the reburning fuel is strongly dependent on reburn zone residence time and stoichiometry. This effect is limited to short residence times (less than 0.4 seconds), during which HCN and NH_3 are formed from the nitrogen in the reburning fuel. At longer residence times, HCN and NH_3 decay to lower levels that depend on stoichiometry, temperatures, and local hydrocarbon concentrations in the reburn zone. Coals are less effective reburning fuels in destroying NO than gaseous hydrocarbon fuels, since coal produces lower levels of hydrocarbons. Consequently, in coal reburning, $\text{NO} + \text{NH}_3$ reactions may dominate the destruction of NO in the reburn zone.

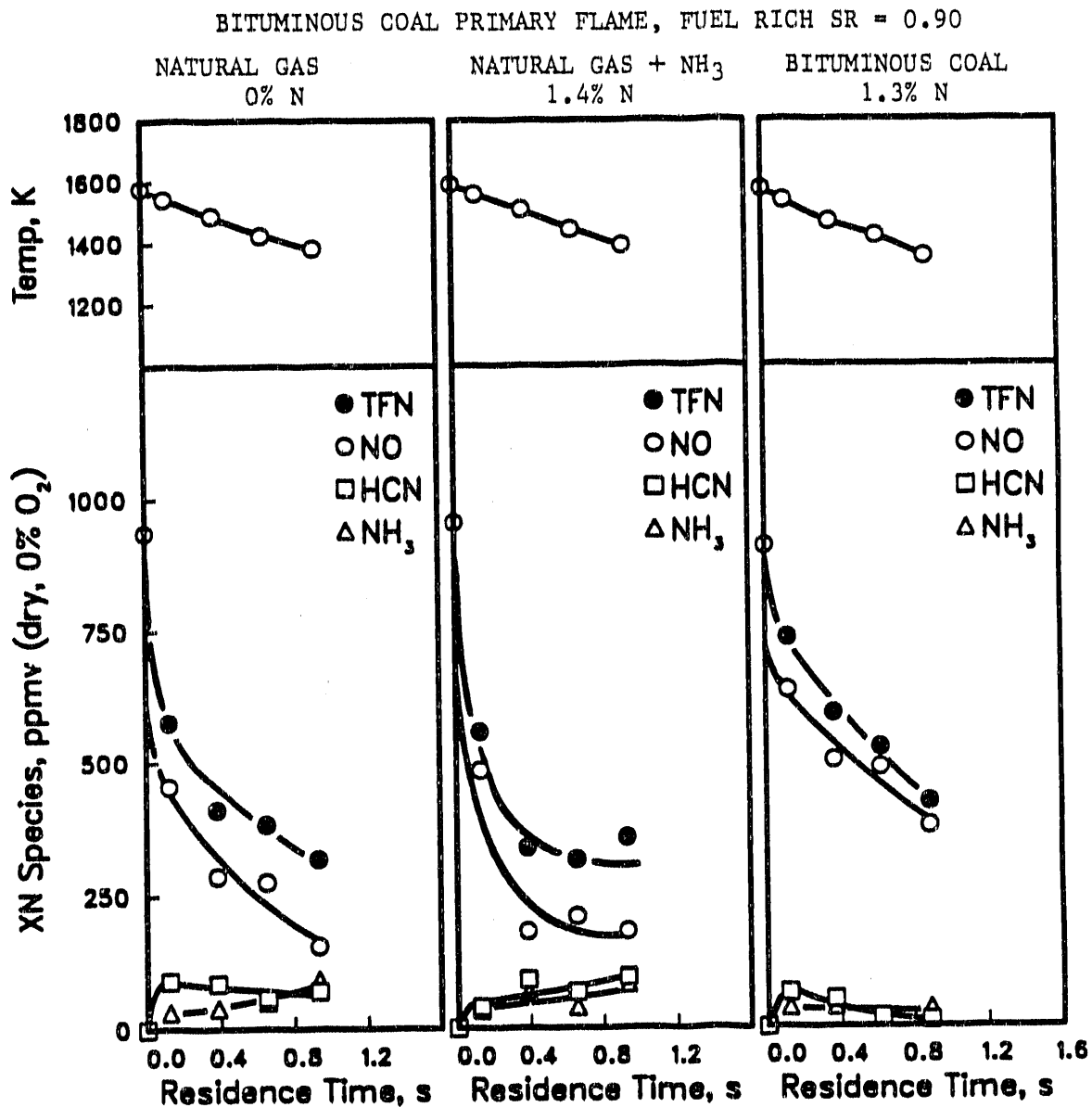


Figure 6.11. Fixed Nitrogenous Species Profiles in the Reburn Zone - Effect of Reburning Fuel Type and Nitrogen Content.

There is no evidence to indicate that the reduced effectiveness of coal as a reburning fuel, relative to natural gas, is due to enhanced formation of HCN and NH₃, provided a residence time of at least 0.4 seconds is allowed in the reburn zone. The lower NO decay rates in coal reburning are most likely due to the production of low levels of hydrocarbons by coal reburning fuels, which reduces the significance of NO + CH₄ reactions.

7.0 DATA ANALYSIS AND MODEL DEVELOPMENT

This section focuses on the development of a theoretical model to describe the inter-conversion of nitrogenous species in the fuel rich stage of reburning. The objective is to create an engineering model that is based on fundamental kinetics, and simple enough, so that it can be used in more complex models of practical combustors. The analysis is based on detailed mechanisms that are available in the literature, and the reburning results of Section 6.0. The validity of the kinetic model is tested using the natural gas reburning data generated in this study, as well as the fuel rich coal combustion data of others.

7.1 Theoretical Background

The processes that govern the inter-conversion of nitrogenous species in the fuel rich reburn zone were examined under various conditions in Section 6.0. There is strong evidence in the literature to suggest that homogenous reactions dominate the fate of coal nitrogen in post flame flue gases under fuel rich conditions. The results of Section 6.0 support this conclusion, and give no indication that heterogenous processes are significant, under fuel rich reburning conditions. Consequently, the development of a predictive model in this work is based on homogenous gas phase kinetics and known reaction paths. The scope of the analysis does not involve the calculation of kinetic parameters or a detailed study of nitrogen chemistry. Instead, the analysis is based on known kinetic parameters taken from the literature, coupled with simplifying partial equilibrium assumptions. Again, it is emphasized that the objective is the development of a simple kinetic model to describe the fate of coal nitrogen in the fuel rich reburn zone. The successful model can provide valuable information regarding rates, needed for the design of combustion configurations, in addition to desired flexibility to permit its application in practical combustors. Simplicity is an essential feature in practical applications, where a kinetic model can be incorporated with other models that simulate flow patterns inside the combustor.

Currently, there is no simple kinetic model that can be successfully applied to describe coal nitrogen kinetics in post flame flue gases under practical combustor conditions. Glass and Wendt (1982) proposed a simple model for NO destruction, that was based on a single homogenous reaction ($\text{NH}_2 + \text{NO}$). This model was successful in predicting NO decay in the fuel rich combustion of bituminous coal, but failed when applied to combustion data from other coals (Bose et al., 1988).

Bose and Wendt (1988) examined the fuel rich zone of air staging in the combustion of lignite and bituminous coals. A coal independent model was developed and was successfully applied to describe NO decay in the fuel rich coal post flame, under various conditions. However, HCN and NH_3 could not be quantitatively predicted, and the model used measured values of NH_3 and an empirical correlation to calculate OH concentrations in the fuel rich zone. The analysis of Bose and Wendt was based on the work of Glarborg et al. (1986), to identify the important reactions and for the values of the kinetic rate coefficients that were used. No adjustments of the rate constants were made and the

analysis was based on known detailed kinetic mechanisms taken from the literature, coupled with partial equilibrium assumptions.

The mechanism of Glarborg et al. (1986) consisted of a kinetic set of 213 elementary gas phase reactions, including the dominant reaction paths that were identified in the pioneering works of Fenimore (1971, 1976), Haynes (1977a, 1977b) and Myerson (1975), among others. Thus, this detailed mechanism included reactions that accounted for the inter-conversion of nitrogenous species in combustion flue gases, as well as for the interaction between hydrocarbons and nitrogen. The corresponding kinetic parameters were based on best estimates of these coefficients, taken from the literature. A similar kinetic set was compiled by Miller and Bowman (1989), but included more reactions to allow the prediction of N_2O and NO_2 , as well as NO , and a more recent update of the corresponding kinetic parameters. However, reactions involving NO destruction and the corresponding rate coefficients were the same as those reported by Glarborg et al.. The kinetic parameters that are used throughout this work are those of Glarborg et al. (1986). The use of the more recent estimates for these parameters would be a logical choice in any future work.

In summary, none of the previous works yielded a mechanism that was able quantitatively to predict profiles of all nitrogenous species in all coal burning tests. This work is an extension of the previous analysis of Bose and Wendt (1988) to a more general configuration that would allow the prediction of values of all nitrogenous species (NO , HCN and NH_3) in the fuel rich stage, regardless of the overall configuration. Consequently, the kinetic model is used to predict nitrogenous species profiles in the fuel rich reburn zone, as well as in the fuel rich zone of air staging. Following Bose and Wendt (1988), the detailed kinetic mechanism of Glarborg et al. (1986) is used as a basis for determining the reactions that are likely to be most important and for the values of the kinetic parameters that are used. The choice of the reactions is also based on the findings of Section 6.0, where important reaction paths were identified. Partial equilibrium assumptions are made to relate radical species concentrations to those of species that can be measured in the fuel rich zone. Equilibrium data are taken from JANAF tables (1983).

7.2 Calculations of Radical Concentrations

The concentrations of various radical species are calculated using partial and global equilibrium assumptions. These assumptions are used to relate the concentrations of radicals to the concentrations of measurable species in the fuel rich zone. The equilibrium constants, in terms of partial pressures, are taken from the JANAF tables (1983). Table 7.1 shows a list of the equilibrium constants for the species that are relevant in this investigation.

The equilibrium concentrations of O , H and OH are calculated, based on the following equilibria:

Table 7.1.
Equilibrium Constants for Species.

$$K_p = A T^N \exp(-B/T)$$

(units in Kelvins and atm)

Species	A	N	B
N	33.8927	0.5274	56738
NH	11.4811	-0.0047	42351
NH ₂	0.3793	-0.4885	22882
NH ₃	2.2708E-4	-0.6843	-5684
NO	4.1119	0.0135	10860
C	1.3710E6	0.5936	85542
CH	9.8995E6	-0.3412	71677
CH ₂	1.0942E5	-0.6957	46683
CH ₃	126.60	-0.9300	17628
CH ₄	0.0915	-1.3090	-9119
CN	5.4931E6	-0.4339	51510
NCO	24.0660	0.0517	19206
HCN	464.61	-0.2874	16341
HNCO	0.2085	-0.3548	-12191
H	5.7402	0.6377	26061
O	76.4854	0.4332	29912
OH	23.8552	-0.1763	4859
H ₂ O	0.4451	-0.7248	-28983



where K_p is the reaction equilibrium constant, calculated as the product of the equilibrium constants of the product species, divided by the product of the equilibrium constants of the reactant species. Consequently, the free radical concentrations are calculated as:

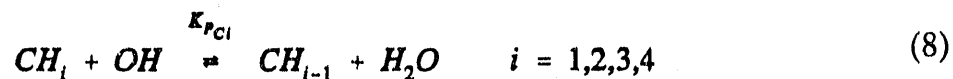
$$(O) = \frac{(OH)^2}{K_{P_1} (H_2O)} \quad (4)$$

$$(H) = \frac{K_{P_2} (OH) (H_2)}{(H_2O)} \quad (5)$$

$$(OH) = (H_2O) \sqrt{\frac{K_{P_3}}{(H_2)/C_T}} \quad (6)$$

where C_T is the total molar concentration, which can be related to pressure and temperature by ideal gas law ($C_T = P/RT$). The molar concentration of a particular species, C_i , is related to the mole fraction, y_i , by $C_i = C_T y_i$.

The concentrations of NH_i and CH_i species are calculated from the partial equilibria:



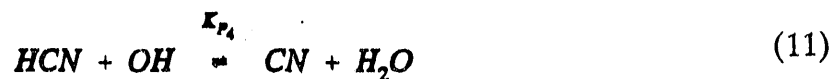
which are used to relate NH_i and CH_i concentrations to those of NH_3 and CH_4 respectively.

These concentrations can be expressed as:

$$(NH_{i-1}) = (NH_3) \left(\prod_i^3 K_{P_{Ni}} \right) \left[\frac{(OH)}{(H_2O)} \right]^{4-i} \quad i = 1,2,3 \quad (9)$$

$$(CH_{i-1}) = (CH_4) \left(\prod_i^4 K_{P_{Ci}} \right) \left[\frac{(OH)}{(H_2O)} \right]^{5-i} \quad i = 1,2,3,4 \quad (10)$$

Assumption of partial equilibrium is made for:



and is used to relate CN radical concentration to that of HCN as:

$$(CN) = K_{P_4} (HCN) \frac{(OH)}{(H_2O)} \quad (12)$$

The partial equilibrium assumptions, described above, are incorporated in the overall mechanism in order to develop a kinetic model that can predict values of NO, HCN and NH₃ in the fuel rich reburn zone.

7.3 NO Destruction Mechanism

Bose and Wendt (1988) proposed that NO decay occurred primarily due to NO reactions with NH_i species and the reduction would be first order with respect to NO and NH₃ concentrations. The destruction of NO by hydrocarbon radicals was judged as a minor contributor to NO decay. Similar conclusions were reported by Knill and Morgan (1989), who used a model that excluded hydrocarbon reactions to predict NO profiles in the reburn zone, for coal reburning data. These works suggest that the contribution of hydrocarbon reactions to NO decay would be minor and limited to short time scales. This is in contrast with the accepted notion that NO destruction by hydrocarbon radicals is the driving force behind the reburning process. Furthermore, the reburning results of Section 6.0 demonstrate the significance of hydrocarbon reactions in destroying NO. This discrepancy can be explained by an examination of hydrocarbon concentrations in the fuel rich zone.

Figure 7.1 compares typical fuel rich zone temperature and species profiles in a reburning configuration (Coal #2) to those in an air staging configuration (Run #15), with time zero starting at the inlet to the fuel rich zone. The results of these experiments are listed in Appendix B. The air staging data are extracted from the work of Bose (1989). Fuel rich zone temperatures in reburning are usually lower than those in an air staging configuration. Furthermore, methane concentrations in the reburn zone are much higher than those in the fuel rich zone of air staging. A comparison of CH₄ profiles (Figure 7.1) suggests that the exclusion of hydrocarbon reactions can be justified in describing nitrogenous species inter-conversion in the fuel rich zone of air staging, where CH₄ values are low. However, this assumption does not hold in the fuel rich reburn zone, where CH₄ values are relatively high.

The coal reburning tests of Sections 6.7 and 6.8 corresponded to methane concentrations that were less than 0.1% in the fuel rich reburn zone. Low hydrocarbon concentrations in the reburn zone might explain the success of a model that included only NO + NH_i reactions (Knill and Morgan, 1989), in describing the fate of NO when coal was used as the reburning fuel.

The success of a kinetic model that excludes hydrocarbon reactions is greatly dependent on the levels of hydrocarbons that are present in the fuel rich zone. These levels depend on stoichiometry, temperature and the overall configuration. If methane concentration in the fuel rich zone is significantly low (less than 0.1%), NO destruction by CH_i species would be of minor significance and NO + NH_i reactions would dominate NO decay. Low hydrocarbon concentrations may exist in the fuel rich zone of air staging and

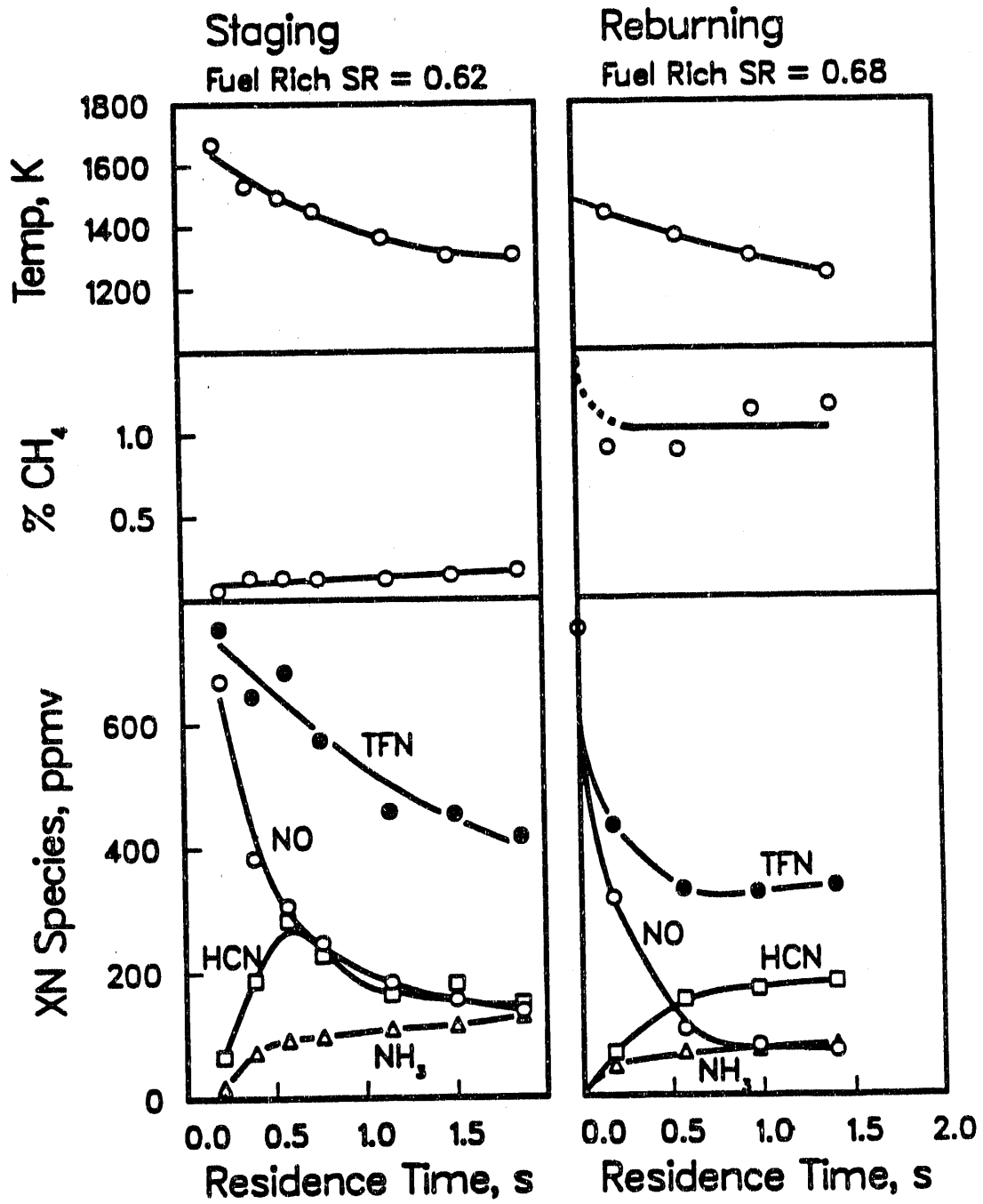
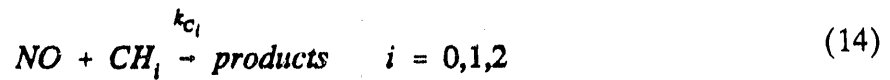
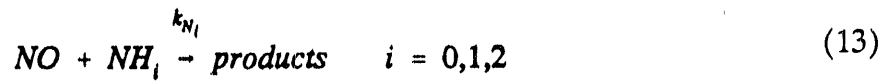


Figure 7.1. Typical Fuel Rich Zone Profiles in Air Staging and Reburning Configurations - Bituminous Coal Primary Flame.

in the fuel rich reburn zone if coal is used as the reburning fuel. An examination of nitrogenous species inter-conversion reactions under these conditions may lead to the false conclusion, with respect to the significance of hydrocarbon reactions in destroying NO.

In natural gas reburning, significant amounts of hydrocarbons are introduced into the reburn zone. Consequently, reactions involving hydrocarbon radicals play a significant role in the mechanism that govern the fate of nitrogenous species. Thus, a successful mechanism must account for reactions involving CH_i species as well as reactions involving NH_i species.

The destruction of NO is the result of the following reactions:



The reversible reaction $N + OH \rightleftharpoons NO + H$ was not included, since it contributed at most 2 ppm NO under fuel rich reburning conditions. In a similar examination, Bose (1989) showed that this reaction had a negligible contribution (less than 1 ppm NO) to the overall destruction of NO in the fuel rich zone. Also, NO formation due to $N + O_2$ reaction was found to be of minor significance. Thus, NO destruction reactions would dominate the change in NO under fuel rich conditions.

The rate of destruction of NO, based on Reactions 13 and 14, is expressed as:

$$\frac{d(NO)}{dt} = - \sum_{i=0}^2 k_{N_i} (NO)(NH_i) - \sum_{i=0}^2 k_{C_i} (NO)(CH_i) \quad (15)$$

The kinetic rate coefficients, k_{N_i} and k_{C_i} , were taken from the work of Glarborg et al. 1986). Table 7.2 shows a list of the reactions and the corresponding rate coefficients that are relevant in the development of the kinetic model.

The concentrations of NH_i and CH_i species are related to those of NH_3 and CH_4 , based on the partial equilibrium assumptions of Reactions 7 and 8, respectively. Combining Equations 9, 10 and 15 yields the following expression for the rate of destruction of NO:

Table 7.2.
 Reaction Mechanism Forward Rate Coefficients.
 (from Glarborg et al., 1986)

$$k = A T^N \exp(-E/RT)$$

(Units in g-moles, cm³, seconds, Kelvins and cal/g-mole)

Reaction	A	N	E
H + OH + M --> H ₂ O + M	7.50E23	-2.60	0
NH ₂ + NO --> NNH + OH	8.80E15	-1.25	0
NH ₂ + NO --> N ₂ + H ₂ O	3.80E15	-1.25	0
NH + NO --> N ₂ O + H	4.30E14	-0.50	0
N + NO --> N ₂ + O	3.30E12	0.30	0
N + OH --> NO + H	3.80E13	0.00	0
CH ₂ + NO --> HCNO + H	1.40E12	0.00	0
CH + NO --> HCN + O	1.10E14	0.00	0
C + NO --> CN + O	6.60E13	0.00	0
HCN + OH --> HOCN + H	9.20E12	0.00	15000
HCN + OH --> HNCO + H	4.80E11	0.00	11000
HCN + O --> NCO + H	1.40E04	2.64	4980
HCN + O --> NH + CO	3.50E03	2.64	4980
CN + OH --> NCO + H	6.00E13	0.00	0
CH + N ₂ --> HCN + N	1.90E11	0.00	13600
CH ₃ + N --> HCN + H + H	5.00E13	0.00	0
NCO + NO --> N ₂ O + CO	1.00E13	0.00	-390
N ₂ O + H --> N ₂ + OH	7.60E13	0.00	15200
NCO + H --> NH + CO	5.00E13	0.00	0

$$\frac{d(NO)}{dt} = -(NO)(NH_3)f_1 - (NO)(CH_4)f_2 \quad (16)$$

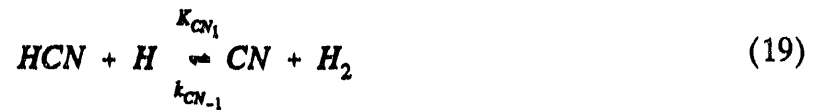
Functions f_i represent groupings of known elementary reaction rate coefficients (Table 7.2), and reaction equilibrium constants (Table 7.1) and are expressed as:

$$f_i = \sum_j A_{ij} T^{N_{ij}} \exp(B_{ij}/T) \left[\frac{(OH)^{m_{ij}}}{(H_2O)^{l_{ij}}} \right]$$

These functions depend on temperature, OH and H₂O concentrations. The values of the parameters are listed in Table 7.3.

7.4 HCN Destruction Mechanism

The destruction of HCN is based on the following reactions:



Then, the rate of destruction of HCN is:

TABLE 7.3
Expressions for Functions f_i .

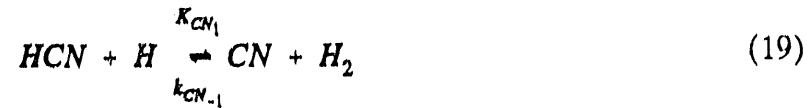
$$f_i = \sum_j f_{ij} \text{ where } f_{ij} = A_{ij} T^{N_{ij}} \exp(B_{ij}/T) \times \left[\frac{(OH)^{m_{ij}}}{(H_2O)^{l_{ij}}} \right]$$

(units in g-moles, cm³, seconds, Kelvins)

i	j	A	N	B	m	l
1	1	3.93E17	-1.603	5277	1	1
	2	7.57E15	-0.917	19650	2	2
	3	3.20E12	-0.134	39105	3	3
2	1	5.83E14	-0.484	12436	2	2
	2	7.73E16	-0.678	20730	3	3
	3	1.20E14	-0.292	40708	4	4
3	1	9.20E12	0.0	-7549	1	0
	2	4.80E11	0.0	-5536	1	0
4	1	1.05E03	2.701	6283	2	1
	2	1.32E16	-0.695	-1327	2	1
5	1	1.34E14	-0.678	13886	3	3
6	1	1.25E15	-0.603	46200	4	4
7	1	1.18E17	-1.603	5277	1	1
	2	7.57E15	-0.917	19650	2	2
	3	3.20E12	-0.134	39105	3	3
8	1	8.03E22	-2.511	7781	2	1
9	1	9.30E02	-1.007	19518	1	1

$$\frac{d(\text{HCN})}{dt} = -k_{\text{O}}(\text{HCN})(\text{O}) - k_{\text{OH}}(\text{HCN})(\text{OH}) - r_{19} \quad (20)$$

where $-r_{19}$ is the contribution of Reaction 19 to the rate of destruction of HCN. This rate is dependent on CN concentration and thus, reactions involving CN must also be included. These reactions are:



Then, the rate of change of CN is:

$$\frac{d(\text{CN})}{dt} = r_{19} - k_{\text{CN}}(\text{CN})(\text{OH}) + k_{\text{C}_0}(\text{C})(\text{NO}) \quad (23)$$

A pseudo steady state assumption is made for CN radical. Thus,

$$\frac{d(\text{CN})}{dt} = 0 \quad ; \quad -r_{19} = -k_{\text{CN}}(\text{CN})(\text{OH}) + k_{\text{C}_0}(\text{C})(\text{NO}) \quad (24)$$

Combining Equations 20 and 24 gives:

$$\frac{d(\text{HCN})}{dt} = -k_o(\text{HCN})(\text{O}) - k_{OH}(\text{HCN})(\text{OH}) - k_{CN}(\text{CN})(\text{OH}) + k_{C_0}(\text{C})(\text{NO}) \quad (25)$$

The term $k_{C_0}(\text{C})(\text{NO})$ in Equation 25 is the contribution of Reaction 22 to HCN formation. This term is separated from the expression for HCN decay and is later included in the expression for HCN formation.

The partial equilibrium assumptions of Reactions 1 and 11 are used to relate O radical concentration to that of OH, and CN concentration to that of HCN, respectively. Combining equations 4, 12 and 25, and excluding the contribution of Reaction 22 to HCN formation, yields the following expression for HCN decay:

$$\frac{d(\text{HCN})}{dt} = -k_{OH}(\text{HCN})(\text{OH}) - k_{CN} K_{P_4} \frac{(\text{HCN})(\text{OH})^2}{(\text{H}_2\text{O})} - \frac{k_o(\text{HCN})(\text{OH})^2}{K_{P_1}(\text{H}_2\text{O})} \quad (26)$$

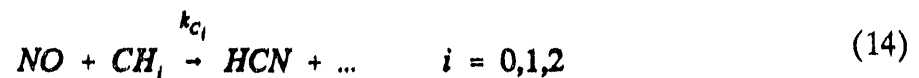
which can be expressed as:

$$\left. \frac{d(\text{HCN})}{dt} \right|_{\text{decay}} = -(\text{HCN})[f_3 + f_4] \quad (27)$$

7.5 HCN Formation Mechanism

Bose and Wendt (1988) proposed a heterogeneous source of HCN formation in the fuel rich coal post flame that would produce HCN as a result of the continued release of nitrogen from the coal residue. As discussed in Section 6.0, the source of HCN formation is most likely the result of reactions involving hydrocarbon radicals. The findings of this study suggest that the carry over of char nitrogen from the primary flame is only a minor contributor to HCN formation in the reburn zone.

The formation of HCN is based on the following reactions:





It should be noted that Reaction set 14 includes Reaction 22, which contributes indirectly to HCN formation by producing CN. The contribution of Reaction 22 was excluded from the HCN destruction expression and is included here. Thus, all reactions involving NO destruction by hydrocarbon radicals contribute to the formation of HCN, although that is partly through the formation of CN intermediate. Reaction 28 was determined to be the dominant Fenimore N₂ fixation reaction. HCN formation due to the fixation of N₂ by CH₂ radicals was several orders of magnitude smaller than that of Equation 28, and was therefore, excluded from HCN formation mechanism. Reaction 29 has received little attention in previous works, but was included in HCN formation mechanism, since it was identified by Glarborg et al. (1986) as an important reaction in NO formation from CH₄ in well stirred reactors. Calculations of the kinetic model verified the significance of this reaction in forming HCN.

The rate of formation of HCN, based on Reactions 14, 28 and 29, is thus,

$$\frac{d(HCN)}{dt} = (NO)(CH_i)f_2 + k_{HCN_1}(CH)(N_2) + k_{HCN_2}(CH_3)(N) \quad (30)$$

The first term on the right hand side of Equation 30 is the contribution of hydrocarbon reactions to NO decay and the subsequent formation of HCN (see Equation 16). The concentrations of CH_i (i=1,3) and N are related to those of CH₄ and NH₃ by the partial equilibrium calculations of Equations 9 and 10, respectively. Substituting for the concentrations of CH, CH₃ and N in Equation 30 and combining the various rate constants, yields the following expression for HCN formation:

$$\left. \frac{d(HCN)}{dt} \right|_{\text{formation}} = CH_4 [(NO)f_2 + (N_2)f_3 + (NH_3)f_4] \quad (31)$$

Functions f_i and the values of the parameters are shown in Table 7.3.

7.6 NH₃ Destruction and Formation Mechanism

A nitrogen balance gives:

$$\text{Fuel Nitrogen in} = \text{Char N} + \text{NO} + \text{HCN} + \text{NH}_3 + 2\text{N}_2 \quad (32)$$

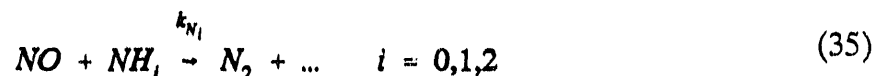
N₂O was not included in the nitrogen balance since in most cases, its concentration was less than 2 ppm in the reburn zone, as seen in Section 3.3. Therefore,

$$\frac{d(\text{Char})}{dt} + \frac{d(\text{NO})}{dt} + \frac{d(\text{HCN})}{dt} + \frac{d(\text{NH}_3)}{dt} + 2\frac{d(\text{N}_2)}{dt} = 0 \quad (33)$$

Heterogeneous processes were shown in Section 6.0 to be of minor significance in the reburn zone. Thus, the rate of change of char nitrogen was assumed to be negligible. Consequently,

$$\frac{d(\text{NH}_3)}{dt} = -\frac{d(\text{NO})}{dt} - \frac{d(\text{HCN})}{dt} - 2\frac{d(\text{N}_2)}{dt} \quad (34)$$

The following reaction set results in the formation of N₂:



It should be noted that Reaction sets 13 and 35 are not identical, since NO + NH₂ reaction may produce N₂ or NNH, as seen in Table 7.2. A reaction path that produces NNH may ultimately produce N₂ or NO and is thus, excluded as an N₂ forming path. The inclusion of reaction NO + NH₂ → NNH + OH requires a detailed examination of various reaction paths, which is contradictory to the simplistic approach that is intended in this work.

The destruction of N₂ is due to Fenimore nitrogen fixation reaction (Reaction 28). Thus the rate of change of N₂ can be expressed as:

$$\frac{d(\text{N}_2)}{dt} = -(\text{CH}_4)(\text{N}_2)f_5 + (\text{NO})(\text{NH}_3)f_7 \quad (36)$$

The rate of change of NH_3 can be determined from Equations 16, 27, 31, 34 and 36. The expressions for functions f_i are presented in Table 7.3.

7.7 OH Decay Mechanism

The decay in OH concentration is based on the following recombination reaction:



This reaction dominates OH decay (Bose, 1989), which justified the exclusion of $\text{O} + \text{OH}$, $\text{H} + \text{OH}$, and $\text{OH} + \text{OH}$ reactions. Thus, the rate of decay of OH is expressed as:

$$\frac{d(\text{OH})}{dt} = -k_{\text{H}_2\text{O}} (\text{OH})(\text{H}) \quad (38)$$

A partial equilibrium assumption is used to relate H radical concentration to that of OH, based on Reaction 2. Combining Equations 5 and 38 gives:

$$\frac{d(\text{OH})}{dt} = -k_{\text{H}_2\text{O}} * K_{P_2} \frac{(\text{OH})^2 (\text{H}_2)}{(\text{H}_2\text{O})} \quad (39)$$

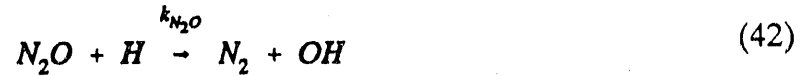
which can be expressed as:

$$\frac{d(\text{OH})}{dt} = -(\text{H}_2)f_8 \quad (40)$$

The values of the parameters, corresponding to function f_8 , are shown in Table 7.3.

7.8 N_2O Destruction and Formation Mechanism

The following reactions are proposed as the dominant reactions affecting N_2O formation and destruction:



The formation of N_2O due to $NCO + NO \rightarrow N_2O + CO$ was of minor significance, with a contribution of less than 3%. Then, the rate of change of N_2O is:

$$\frac{d(N_2O)}{dt} = k_{N_1}(NH)(NO) - k_{N_2O}(N_2O)(H) \quad (43)$$

A pseudo steady state assumption of N_2O allows the evaluation of its concentration.

$$(N_2O) = \frac{k_{N_1}(NH)(NO)}{k_{N_2O}(H)} \quad (44)$$

Using the partial equilibrium assumptions of Reactions 2 and 7, and combining Equations 5, 9 and 44, the expression for N_2O concentration can be expressed as:

$$N_2O = f_9 \frac{(NH_3)(NO)}{(H_2)} \quad (45)$$

The values of the parameters of function f_9 are shown in Table 7.3.

7.9 Kinetic Model: Nitrogenous Species Predictions

A homogeneous gas phase mechanism was proposed to describe the inter-conversion of nitrogenous species in the fuel rich reburn zone. Simultaneous solution of rate Equations 16, 27, 31, 34, 36 and 40 would give predictions of all nitrogenous species values (NO, HCN

and NH_3) in the fuel rich reburn zone. However, the solution required known initial concentrations of OH, NO, HCN and NH_3 . Measured nitrogenous species values at the first port, downstream of the reburning fuel injection point, were used as initial concentrations. In general, these measurements corresponded to residence times 0.15-0.20 seconds in the reburn zone. Thus, the predictions of the kinetic model were restricted to the region of the reburn where mixing complications were of minor significance. No measurements of OH concentrations were made in this study and an empirical correlation was used to estimate the initial OH concentration, as a function of temperature in the reburn zone.

Bose and Wendt (1988) showed that a global equilibrium assumption for OH concentrations produced low predictions of NO decay rates, under fuel rich combustion conditions. Furthermore, the error in the prediction was greater at lower temperatures in the combustor. The researchers suggested that a super equilibrium concentration of OH would be present in the fuel rich post flame. This was attributed to the slow rates of OH radical recombination (Reaction 37), which could not keep up with the axial drop in temperature down the combustor. An empirical correlation was derived to estimate the OH equilibrium overshoot, based on fuel rich gas burning experiments.

A similar analysis to that of Bose and Wendt (1988) is applied here to estimate an initial value of OH entering the reburn zone. The results of five natural gas reburning experiments (Gas #2, 3, 4, 5 and 7) were used for this purpose, corresponding to 19 data points (Appendix B). In these experiments, the primary fuel was natural gas and two experiments (Gas #2 and 3) involved a primary flame doped with NH_3 . Equation 16 was solved for the initial OH concentration using measured values of NH_3 and CH_4 , and a numerical estimate of the slope for NO decay, based on a cubic splines fit. A root finding routine, based on the Secant method, was used to solve the fourth degree polynomial (with respect to OH), taking only the positive root as the solution. Subsequent kinetic concentrations of OH were calculated by solving Equation 40, using Runge-Kutta Fehlberg fifth and sixth order adjustable step size integrating routine. Program OH.FOR was used for these calculations, and is listed in Appendix C. Correlating the calculated OH concentrations (gas flame data only), yielded the following expression for the initial OH concentration, as a function of temperature:

$$R = \frac{(\text{OH})_{\text{initial}}}{(\text{OH})_{\text{equil}}} = 1.65 \times 10^5 \exp\left(\frac{18745}{T}\right) ; T < 1425\text{K} \quad (46)$$

The scatter of the data is shown in Figure 7.2.

Equation 46 was used only in the temperature range of the gas flame data (1160-1425 K). In order to avoid serious errors due to the extrapolation of the exponential function, the initial OH concentration at temperatures higher than 1425 K were estimated by

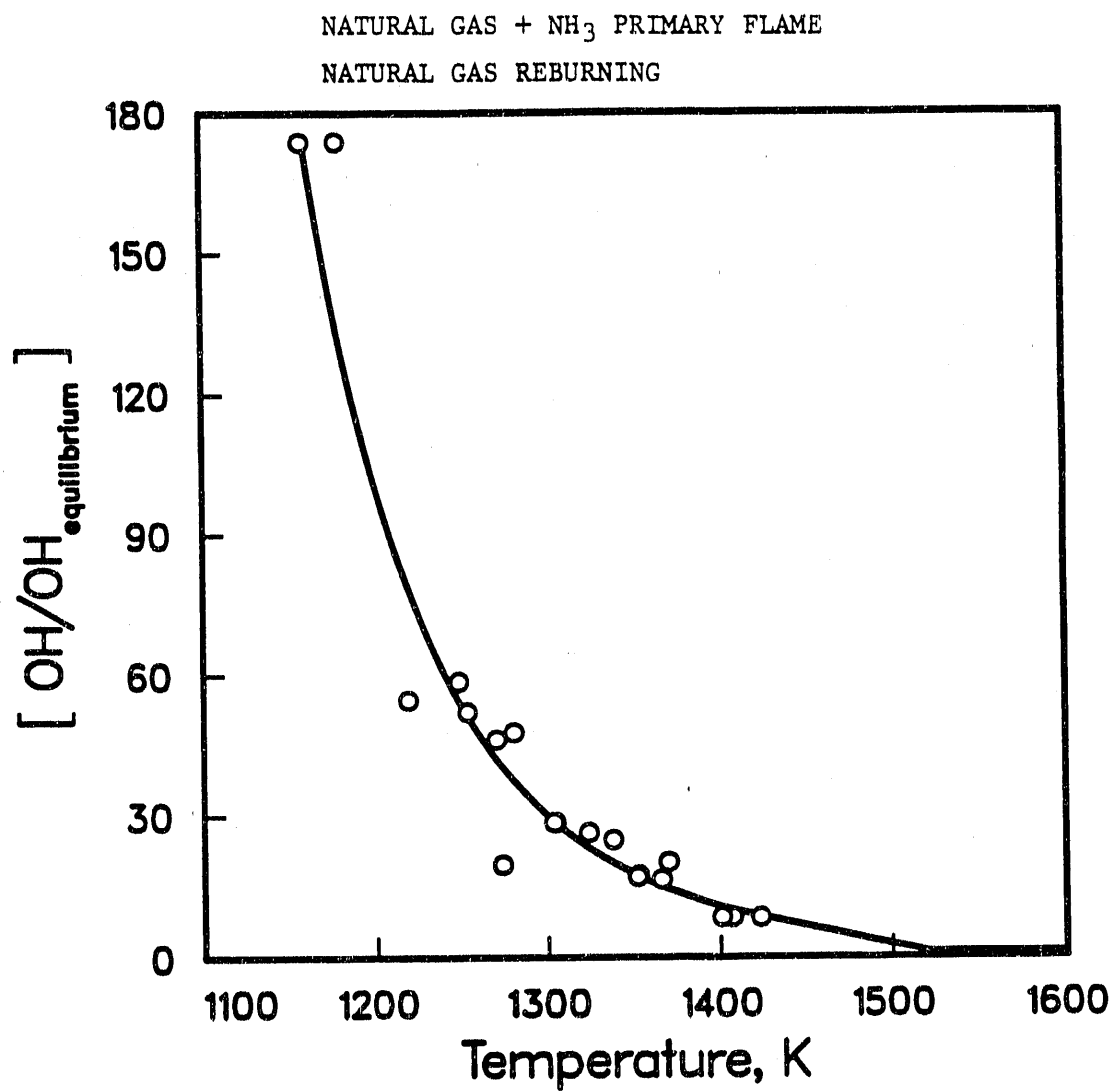


Figure 7.2. Estimation of Initial OH Concentration in the Reburn Zone.

assuming a constant change of R (Equation 46) with temperature (constant dR/dT). Thus, at temperatures greater than 1425 K, a linear correlation was used,

$$R = \frac{(OH)_{initial}}{(OH)_{equil}} = 120.6 - 0.0786 \times T ; T = 1425 - 1520K \quad (47)$$

At temperatures greater than 1520 K, a global equilibrium assumption was made for initial OH concentration.

It should be emphasized that, unlike the analysis of Bose and Wendt (1988), the use of an empirical estimate of OH was restricted **only** to the calculation of an **initial** condition for OH decay. Clearly, less empirical techniques for determining this initial condition would be preferable. The decay in OH concentration was calculated using the kinetic rate Equation (40), solved simultaneously with the rate equations of the nitrogenous species.

Figure 7.3 shows the different stages of development of the kinetic model, where the curves are model predictions for NO and HCN. The dashed curve clearly demonstrates the significance of an initial estimate for OH, where an equilibrium assumption predicts low rates for both NO and HCN. A comparison of the other two curves demonstrates the significance of HCN formation due to the contributions of reactions of hydrocarbon radicals with N_2 and N species.

7.9.1 Model Testing: Reburning

Figure 7.4 shows a comparison between measured and predicted nitrogenous species profiles in the reburn zone for three natural gas reburning experiments, in which the primary fuel was natural gas doped with varying amounts of NH_3 (Gas #2, 3 and 4). This allowed the variation of the primary NO concentration entering the reburn zone. The symbols represent measured values of nitrogenous species, on a wet basis, and the curves are model predictions. Program MODELFOR is used for the calculations of the kinetic model and is listed in Appendix C. Only measured values of CH_4 , H_2 , H_2O and N_2 are used in the prediction of nitrogenous species profiles in the reburn zone, as described earlier. In general, there is good agreement between measurements and predictions over a wide range of primary NO levels (33-715 ppm).

Figure 7.5 shows a similar comparison for three natural gas reburning tests at different reburn zone stoichiometries (Coal #6, 9 and 19), in which bituminous coal was used as the primary fuel. Reasonable predictions are obtained for all nitrogenous species, but the predicted NO values are relatively high in all three cases.

Figure 7.6 shows the effect of temperature on model predictions, where two natural gas reburning experiments of different temperature environments (Coal #7 and 10) are

BITUMINOUS COAL PRIMARY FLAME, NATURAL GAS REBURN
 $\text{NO}_p = 840 \text{ ppm}$, FUEL RICH SR = 0.68

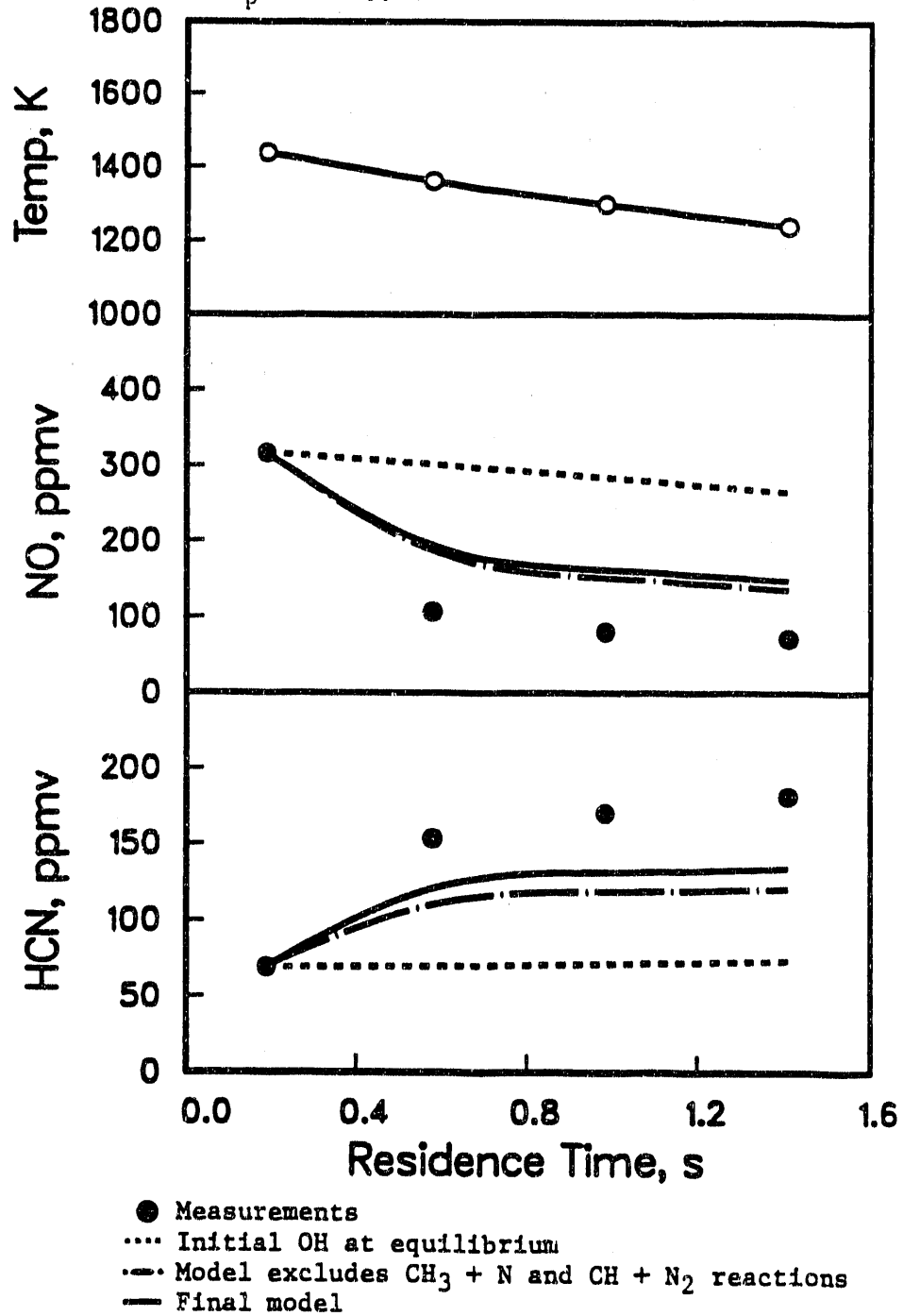


Figure 7.3. Development of a Kinetic Model to Predict Nitrogenous Species Profiles in the Reburn Zone.

NATURAL GAS REBURNING, FUEL RICH SR = 0.86

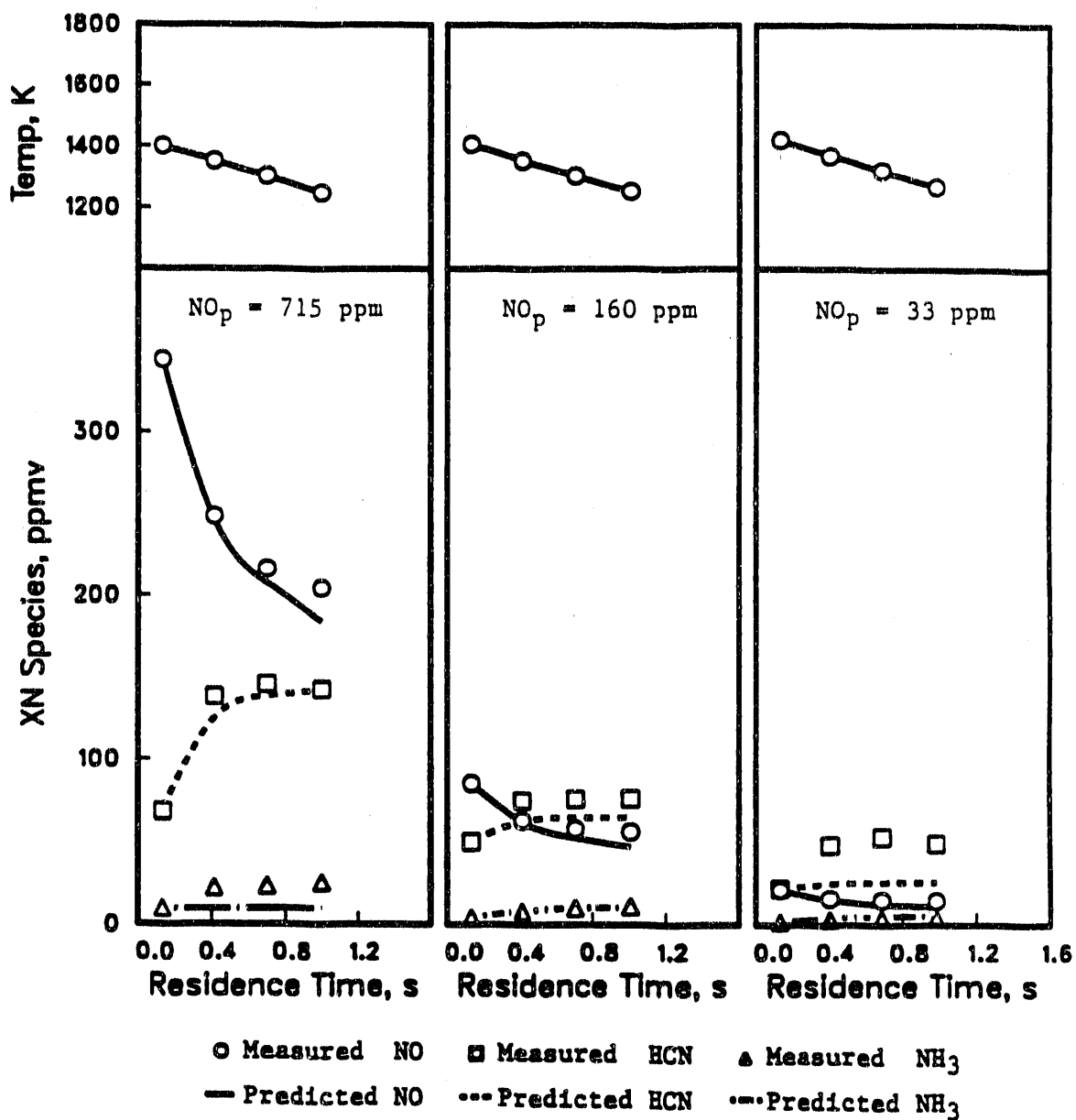


Figure 7.4. Comparison between Measured and Predicted Nitrogenous Species Profiles in the Reburn Zone - Natural Gas + NH₃ Primary Flame.

NATURAL GAS REBURNING

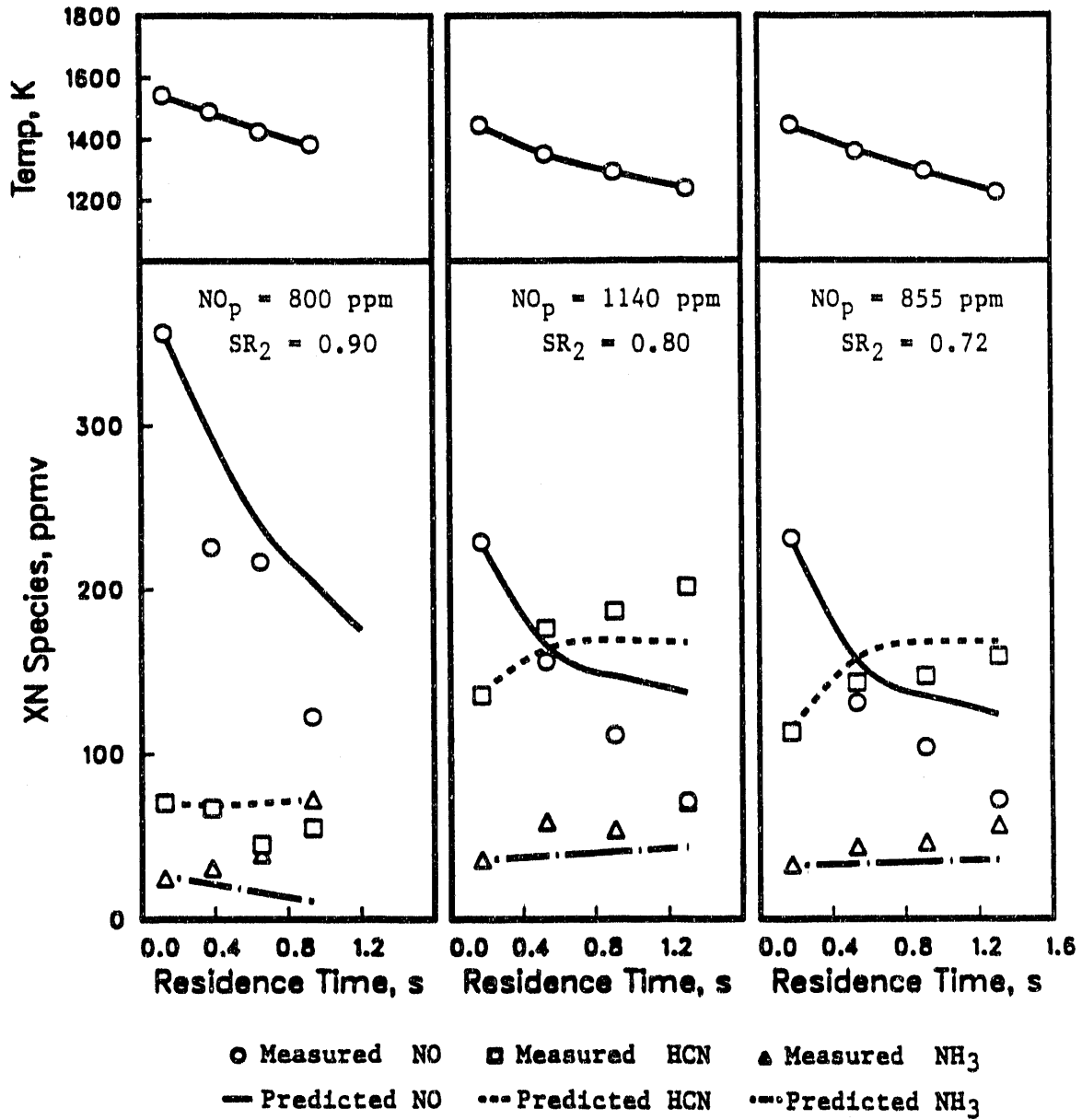


Figure 7.5. Comparison between Measured and Predicted Nitrogenous Species Profiles in the Reburn Zone - Bituminous Coal Primary Flame.

BITUMINOUS COAL PRIMARY FLAME, NATURAL GAS REBURNING

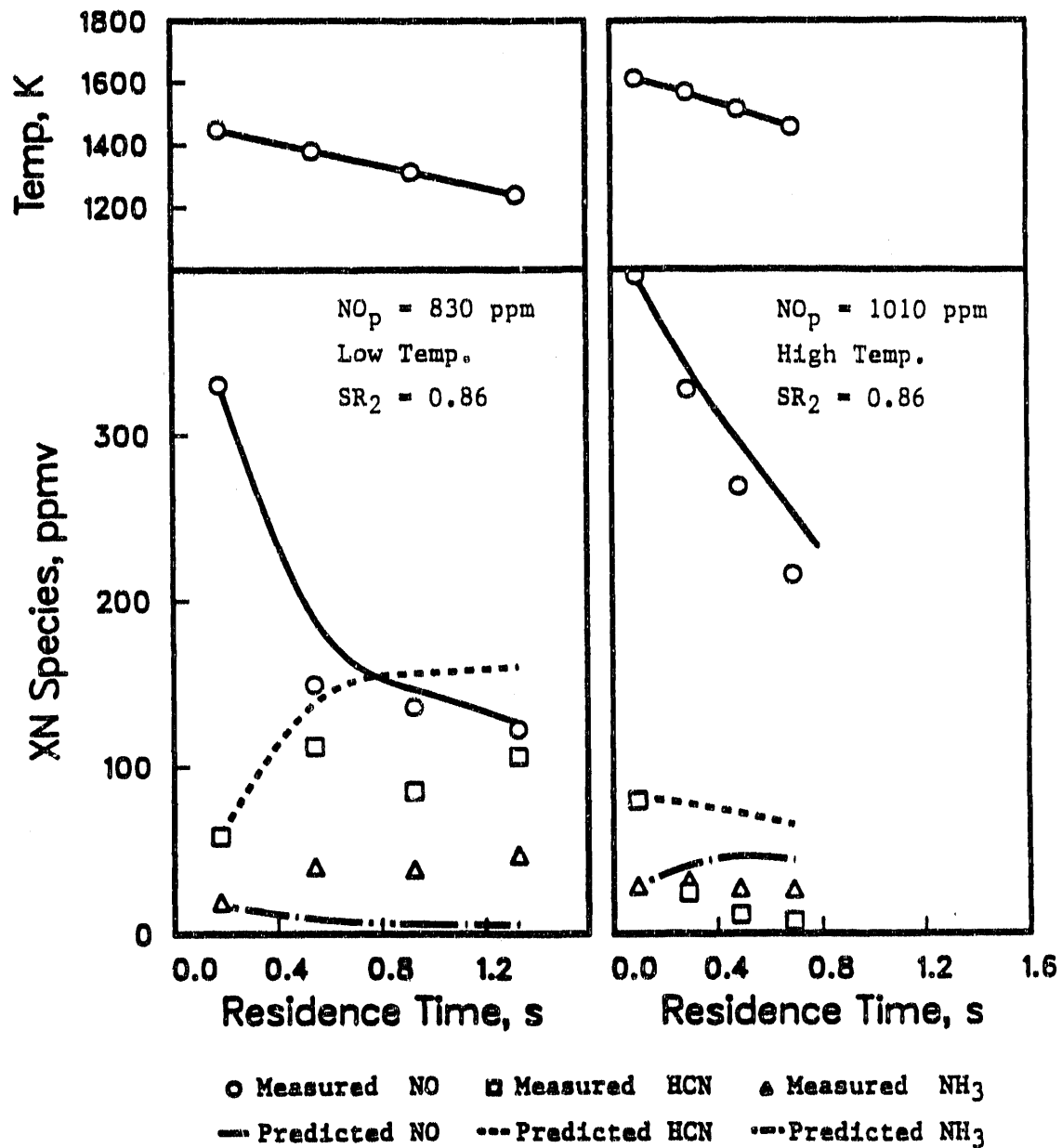


Figure 7.6. Comparison between Measured and Predicted Nitrogenous Species Profiles in the Reburn Zone - Effect of Temperature.

examined. Bituminous coal was the primary fuel in both cases. The model predicted nitrogenous species values well, at different temperature profiles in the reburn zone. However, the model failed to account for the rapid decay in HCN at high temperatures.

Comparisons between model predictions and experimental measurements for all the natural gas reburning experiments of this study are shown in Figure 7.7, where each nitrogenous species is examined separately. These experiments consist of seven natural gas primary flame tests, two of each were doped with NH_3 , and ten bituminous coal primary flame tests, under various conditions. The scatter of the predictions does not indicate bias with respect to a primary fuel type (coal or gas flame), or a certain range of values for a particular nitrogenous species. In general, good predictions for HCN are observed for all runs, but the model predicts high values for NO and low values for NH_3 . The discrepancy between measurements and predictions for NO and NH_3 , is possibly due to an error in the nitrogen balance (Equation 34). A negative error in the prediction of NH_3 would produce higher predictions of NO. Furthermore, higher estimates of the initial OH concentration can greatly improve NO predictions. The effects of the initial OH and the NH_3 rate equation on the predictions of NO and NH_3 is further discussed in a later section.

7.9.2 Model Testing: Air Staging

The validity of the kinetic model was tested using fuel rich coal combustion data, that were extracted from the work of Bose et al. (1989). The data corresponded to the fuel rich zone of an air staging configuration, and are listed in Appendix B. A total of 12 coal burning tests were examined under a wide range of conditions, and involved two coals, a Utah Bituminous coal (9 tests) and a German Brown Lignite coal (3 tests). Fuel rich stoichiometries ranged from 0.6 to 0.8. In some of the tests, temperature changes in the fuel rich zone were achieved by N_2 dilution or by O_2 enrichment of the primary flame. Thus, an examination of the kinetic model using these data would provide valuable information, with respect to the dependence of the proposed mechanism on coal composition, the temperature environment, as well as the overall configuration. The first measurement in the post flame (port 2) was used to establish an initial condition for the concentrations of the nitrogenous species, and an equilibrium assumption was made for the initial OH concentration.

Figures 7.8 and 7.9 show a comparison between experimental measurements and model predictions at two different stoichiometries in the fuel rich combustion of a bituminous coal and a lignite coal, respectively. In both cases, good agreements between measurements and predictions are observed, for all nitrogenous species.

Figure 7.10 examines the effect of dilution of the primary flame on model predictions. Again, the kinetic model was successful in predicting values for all three nitrogenous species, under different temperature environments.

Figure 7.11 shows a comparison between experimental measurements and model

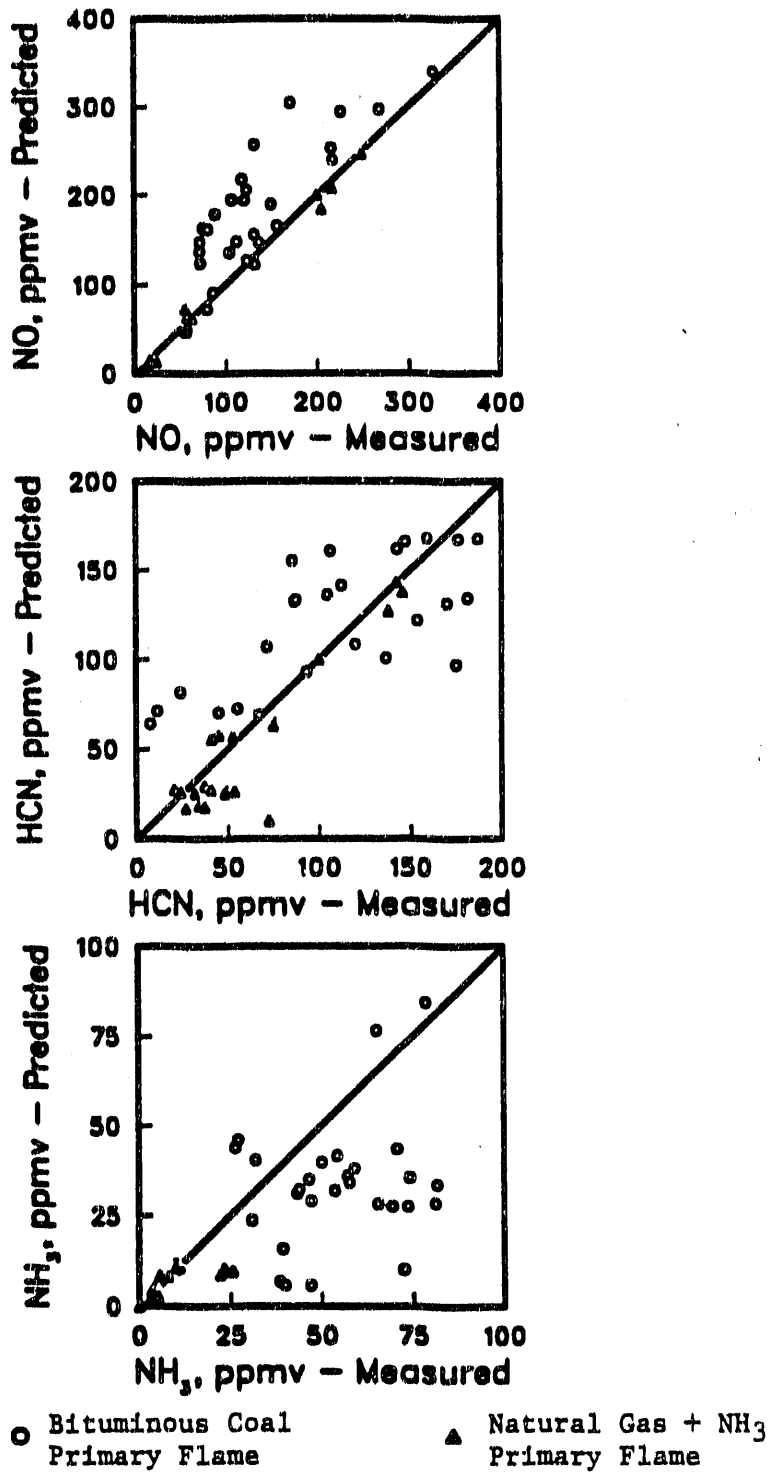


Figure 7.7. Comparison between Model Predictions and Measurements - Natural Gas Reburning.

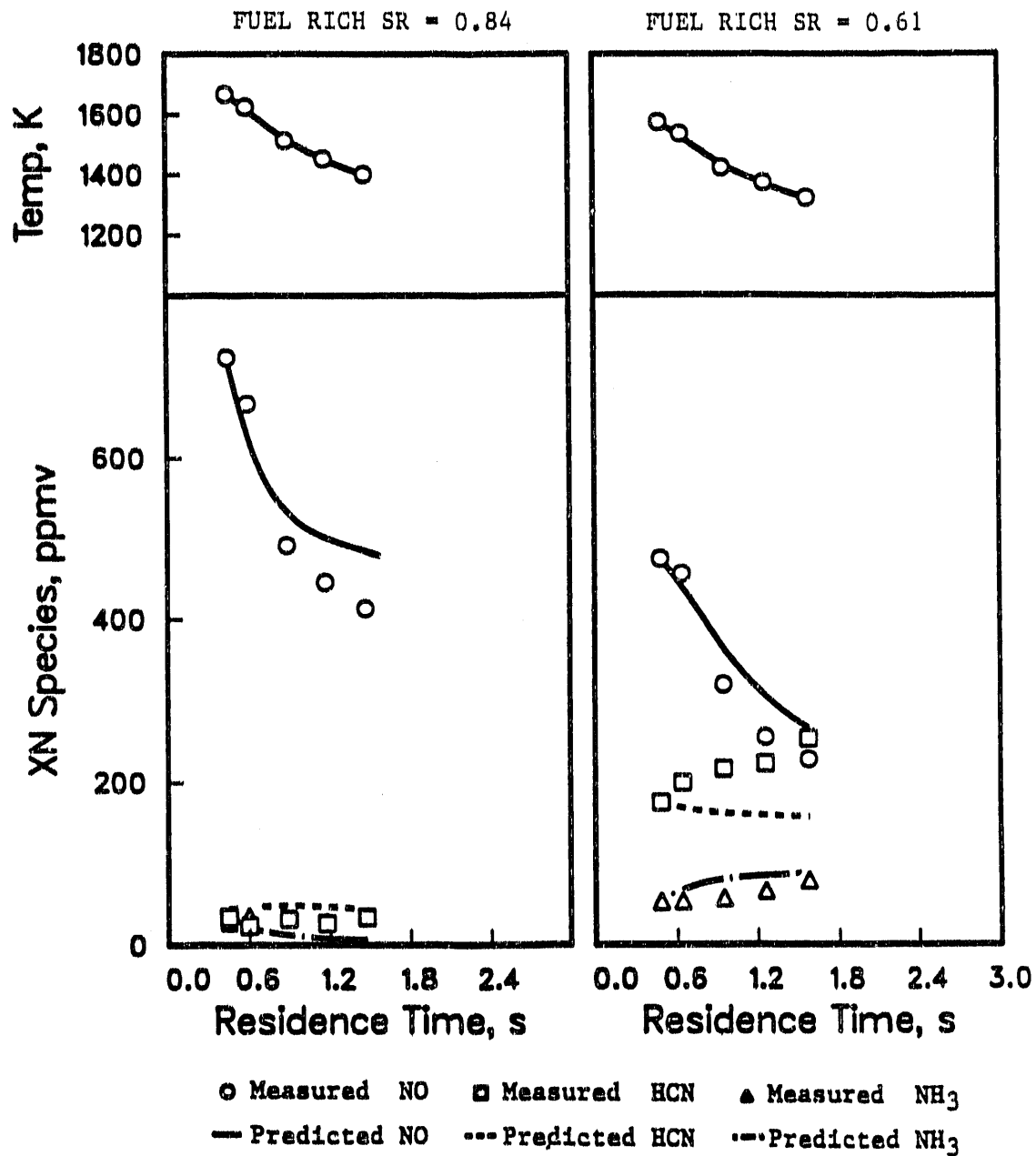


Figure 7.8. Comparison between Measured and Predicted Nitrogenous Species Profiles in the Fuel Rich Combustion of Bituminous Coal - Effect of Stoichiometry.

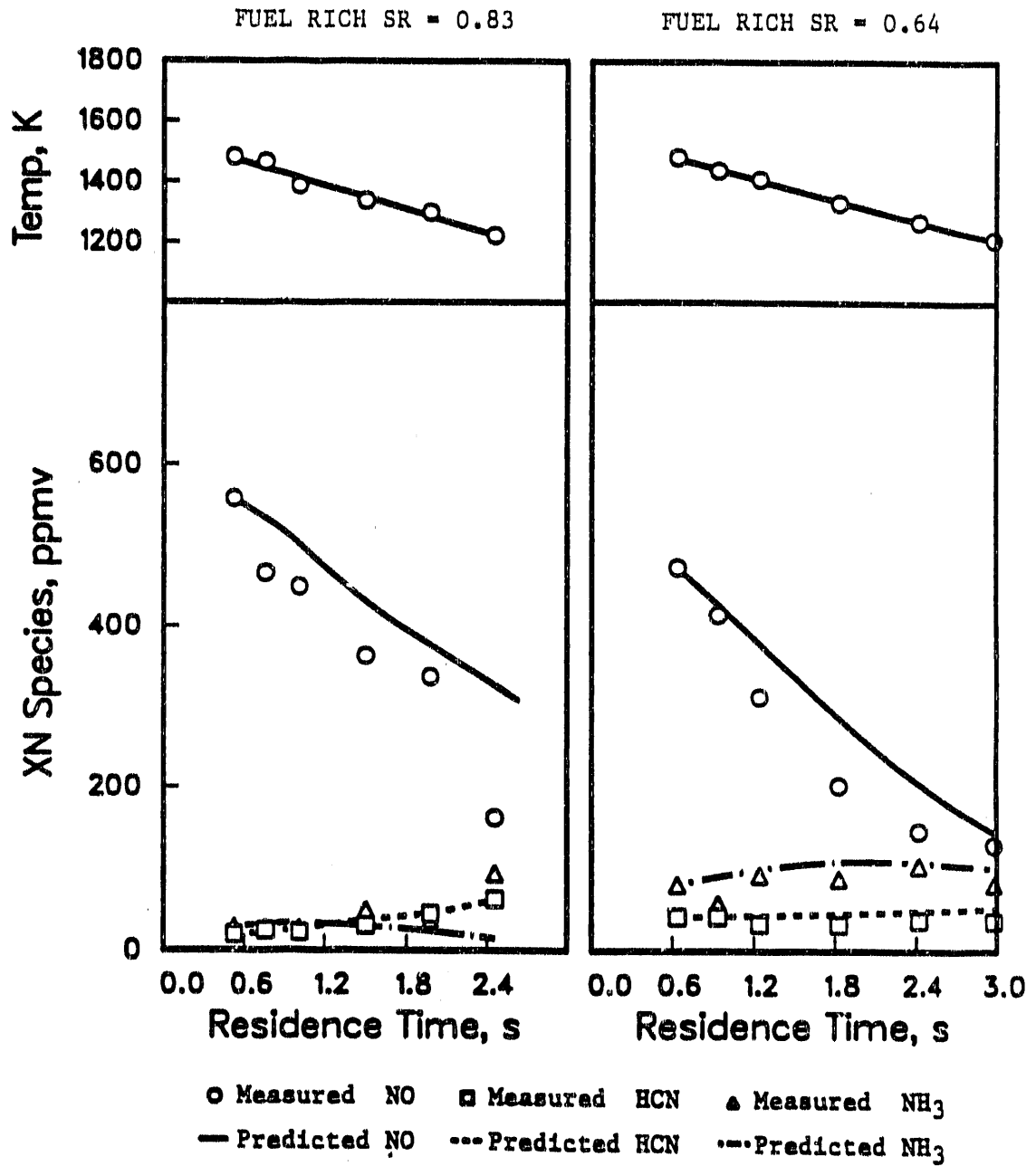


Figure 7.9. Comparison between Measured and Predicted Nitrogenous Species Profiles in the Fuel Rich Combustion of Lignite Coal - Effect of Stoichiometry.

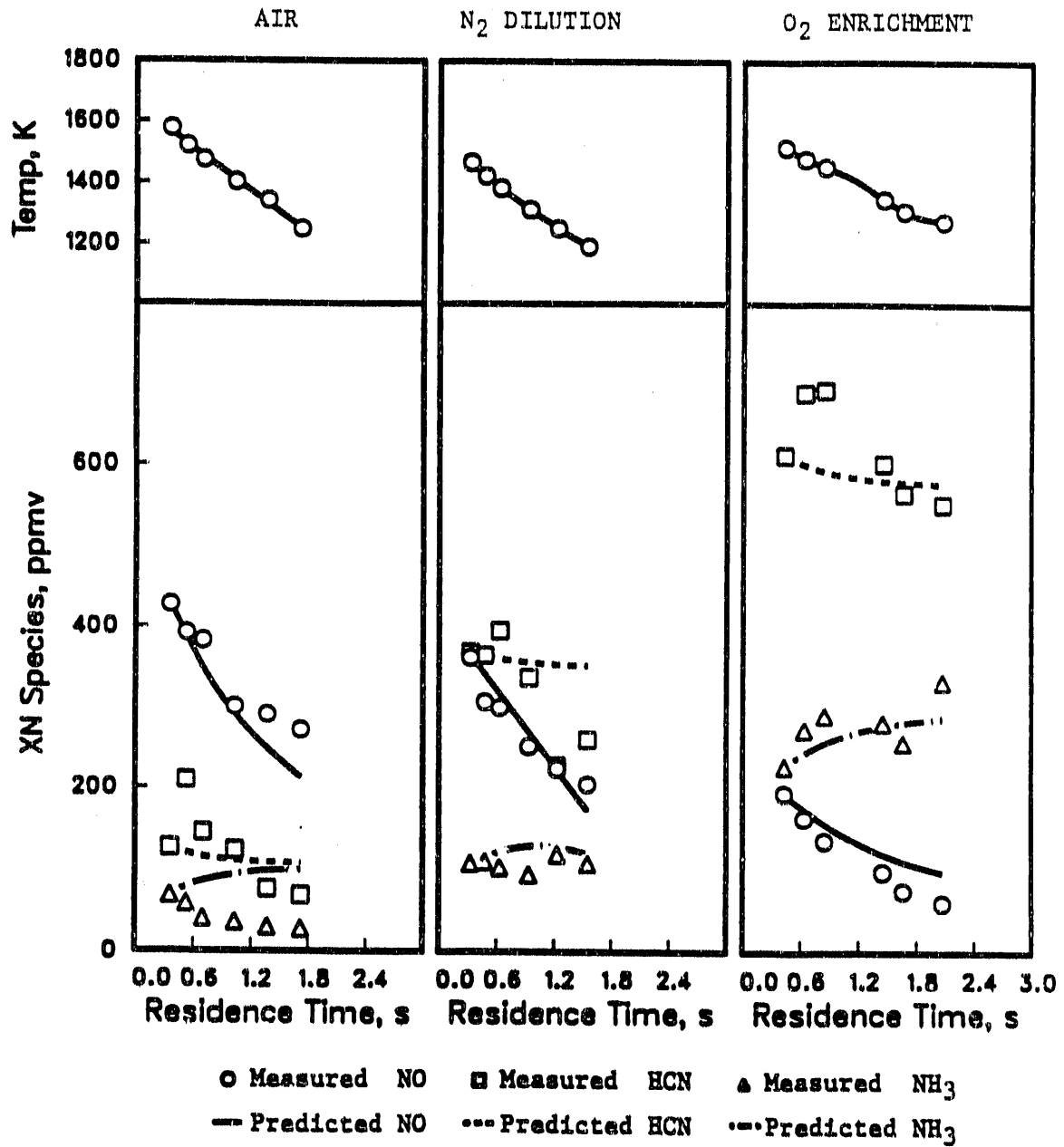


Figure 7.10. Comparison between Measured and Predicted Nitrogenous Species Profiles in the Fuel Rich Combustion of Bituminous Coal at SR of 0.6 - Effect of Dilution of the Primary Flame.

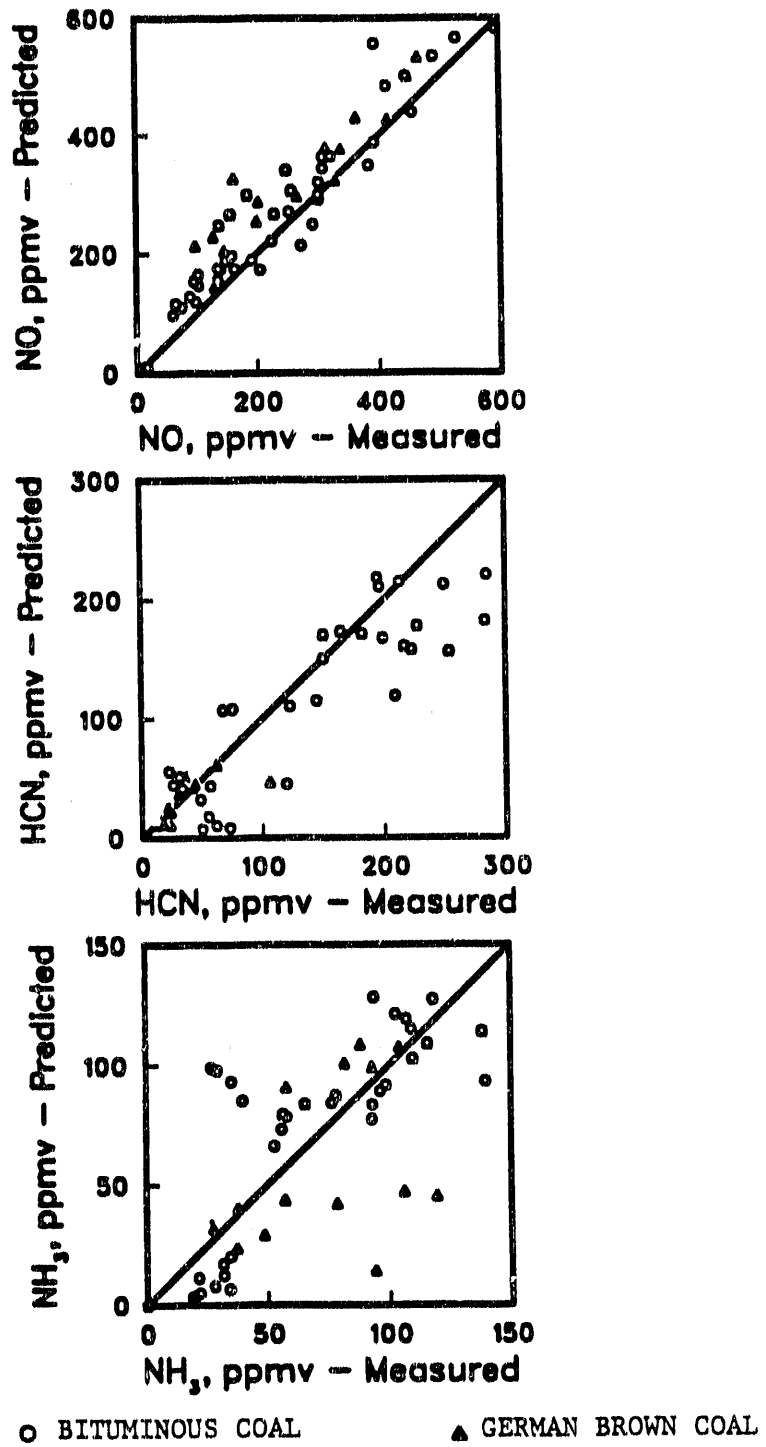


Figure 7.11. Comparison between Model Predictions and Measurements - Fuel Rich Combustion of Coal.

predictions for the twelve fuel rich coal combustion experiments of Bose (1989). The comparison between measurements and predictions for each nitrogenous species is shown separately. Under most conditions, good predictions of all nitrogenous species are observed.

In general, the model was more successful in describing the fate of coal nitrogen in the fuel rich combustion of coal (air staging data), than in the fuel rich stage of reburning. That was partly due to the effects of mixing in early time scales in the reburn zone, and partly due to differences in the temperature environments and the uncertainty in the choice of an initial OH estimate. In a reburning configuration, mixing effects were, in general, limited to a time scale of less than 0.18 seconds in the reburn zone, but might have affected the first measured values, that were used as initial conditions in the prediction of nitrogenous species profiles. The effects of mixing were of minor significance in the fuel rich combustion of coal. In addition, there was more uncertainty in the choice of an initial estimate for OH in the fuel rich zone of reburning, relative to that of an air staging configuration. The equilibrium assumption for the initial OH would be realistic in the fuel rich combustion of coal, where temperatures are relatively high (above 1500 K). The effect of temperature on model predictions is further discussed in the evaluation of the model.

7.9.3 Model Testing: N₂O Predictions

The kinetic model was mainly applied to predict NO, HCN and NH₃ values in the fuel rich zone. Nevertheless, the mechanism also allowed the calculation of N₂O concentrations, based on Reactions 41 and 42. These concentrations would be expected to be less than 5 ppm under fuel rich conditions, as seen in Section 3.3. Equation 45 was used, concurrently with the predictions of the kinetic model for NH₃ and NO values, to calculate N₂O concentrations.

Figure 7.12 compares measured and predicted N₂O concentrations at various temperatures in the combustion of bituminous coal, at a stoichiometry of 0.6. Both measured and predicted values of N₂O are below 2 ppm, which does not allow a proper examination of the proposed N₂O mechanism. However, low concentrations of N₂O (less than 10 ppm) are predicted in most cases under fuel rich conditions (reburning and air staging configurations), which is consistent with the experimental measurements of Section 3.3.

7.10 **Evaluation of the Kinetic Model**

A simple mechanism was proposed to describe the inter-conversion of nitrogenous species in the fuel rich zone of reburning. This mechanism was based on homogeneous gas phase kinetics and consisted of 15 elementary reactions, coupled with simplifying partial equilibrium assumptions to relate the concentrations of radical species to those of measurable species in the fuel rich zone. The values of the kinetic parameters and the equilibrium data were extracted from the literature without any adjustment. The kinetic model allowed the prediction of NO, HCN and NH₃ profiles under fuel rich conditions. The

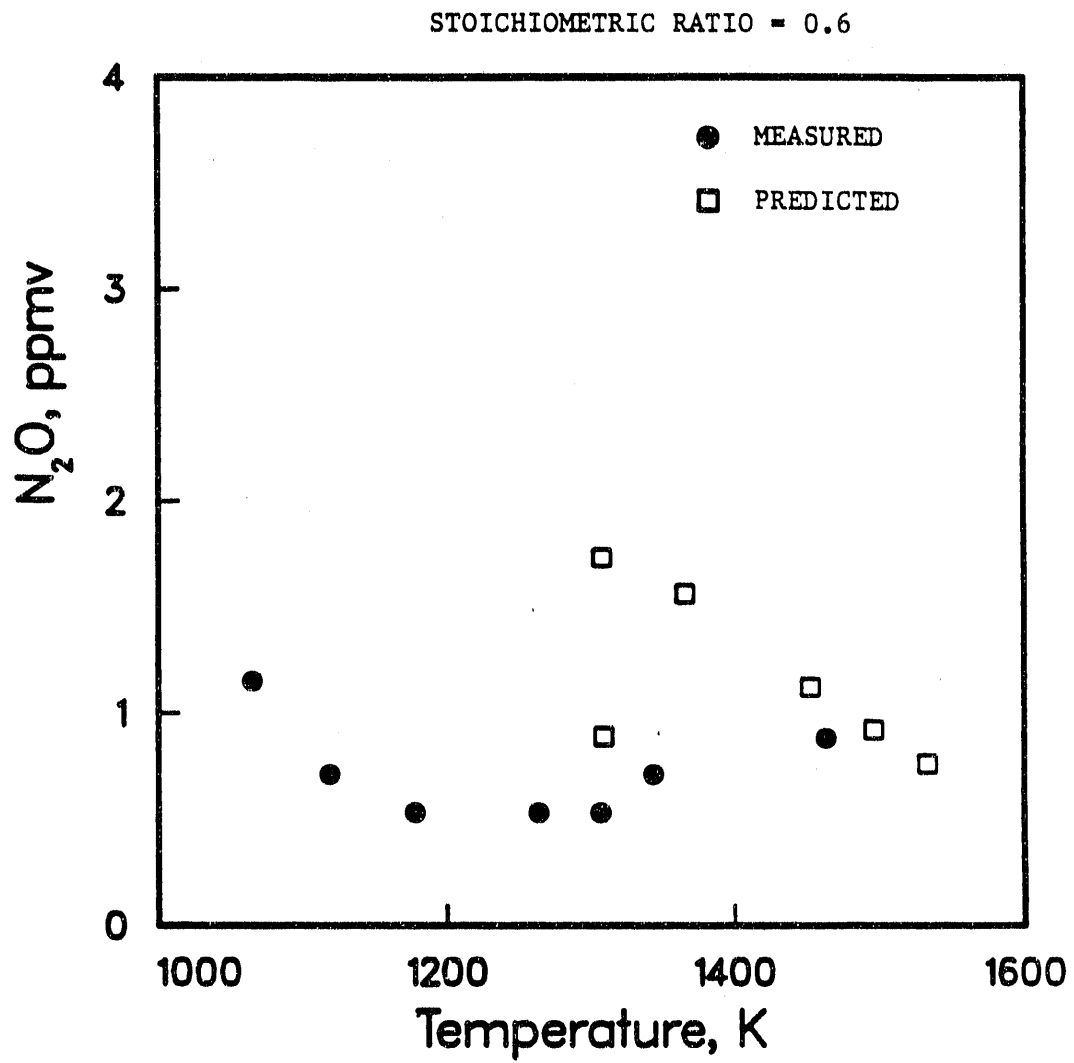
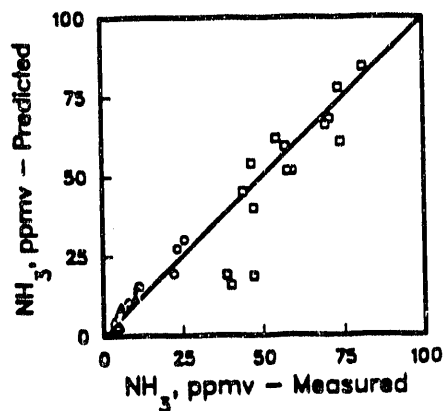
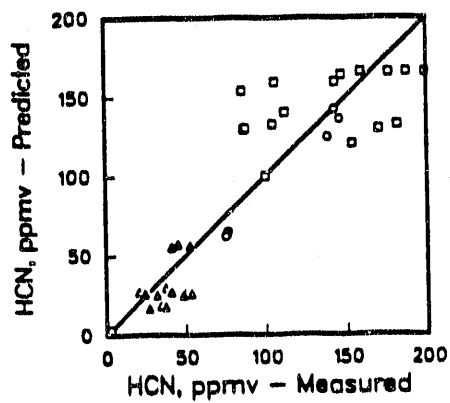
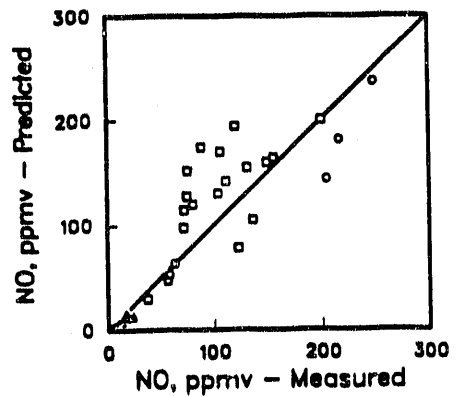


Figure 7.12. Comparison between Measured and Predicted N_2O Concentrations - Bituminous Coal Flame.

predictions were independent of measured values of the nitrogenous species, and used only measured values of CH_4 , H_2 , H_2O and N_2 . However, measured nitrogenous species values were used to establish an initial condition for the predicted profiles of the nitrogenous species. An empirical correlation was used only for an initial estimate of OH concentration.

The validity of the kinetic model was examined using the natural gas reburning results of this study, and the fuel rich coal combustion data of Bose (1989), as seen in Figures 7.7 and 7.11, respectively. In general, the proposed mechanism was successful in describing coal nitrogen kinetics under fuel rich conditions, independently of the overall configuration or the fuel type. However, model predictions were high for NO and low for NH_3 in the reburn zone, and in some cases, in the fuel rich combustion of lignite coal. Further examination of the data suggested that the discrepancy was greater at lower temperatures in the fuel rich zone, roughly below 1500 K at the initial measurement. Two possibilities could create the observed trend at low temperatures. First, a low estimate of the initial OH concentration would have more dramatic effects at lower temperatures. Second, an error in the nitrogen balance (Equation 34) would affect NH_3 predictions and consequently, those of NO. Better predictions of NO and NH_3 values were possible by manipulation of the initial OH estimate, but was not pursued further, since that involved a trial and error examination. Consequently, only the second possibility, namely, an error in the nitrogen balance, was further investigated.

An examination of Reactions 41 and 42, and the temperature dependence of $k_{\text{N}_2\text{O}}$, suggested that a steady state assumption for N_2O concentration might have accounted for the low predictions of NH_3 at low temperatures. This assumption required the inclusion of Reaction 41 ($\text{NO} + \text{NH}$) as an N_2 forming reaction in the overall mechanism. The assumption of steady state for N_2O concentration was not made in the early stages of development of the model (Mereb and Wendt, 1990) and better predictions were obtained for both NO and NH_3 , as seen in Figure 7.13. All the natural gas reburning data of Figure 7.13 correspond to initial temperatures that were below 1500 K in the reburn zone. Therefore, the predictions of the kinetic model can be greatly improved by allowing N_2O formation by NO + NH reaction at temperatures below 1500 K and assuming a steady state behavior of N_2O (to form N_2) at higher temperatures (above 1500 K). However, this selectivity cannot be justified on a theoretical basis, in view of the present mechanism of N_2O formation and destruction.



- Utah Bituminous Coal/Natural Gas
- Natural Gas + NH₃/Natural Gas
- ▲ Natural Gas/Natural Gas

Figure 7.13. Comparison between Model Predictions and Measurements - Natural Gas Reburning - $\text{NH} + \text{NO}$ gives N_2O .

8.0 APPLICATIONS OF THE KINETIC MODEL

The inter-conversion of nitrogenous species in the fuel rich stage of reburning was examined in Section 6.0 and a simple mechanism was proposed in Section 7.0, based on homogeneous gas phase kinetics, known kinetic parameters and partial equilibrium assumptions. This mechanism was successful in predicting nitrogenous species profiles in the fuel rich zone, under reburning and air staging configurations. This Section is concerned with the applications of the kinetic model as a predictive tool. The objectives are to expand the model to predict the overall destruction of NO in a reburning configuration, and to examine hypothetical configurations that would allow further reductions in NO emissions.

In the previous analysis, the use of the kinetic model was limited to the prediction of nitrogenous species profiles in the region of the reburn zone where mixing effects were not important. Furthermore, the model required known initial concentrations of nitrogenous species (NO, HCN and NH₃). In order to apply the model to the prediction of the overall reburning effectiveness, it is necessary to expand the analysis to allow the prediction of nitrogenous species values in the reburn zone from the primary NO level, and then to estimate the conversion of nitrogenous species to NO in the final stage of reburning. Empirical correlations, both derived and taken from the literature, are used for this purpose. The combined model, which describes profiles of nitrogenous species from the start to the end of a reburning process, is then compared to the parametric results of Section 4.0. Thus, the empirical models of the parametric study are reconciled with a model based on mechanisms and major species profiles.

In another application of the kinetic model, hypothetical configurations are examined to identify kinetic limits in achieving low levels of nitrogenous species under fuel rich conditions. The two variables that are manipulated in this examination are temperature and residence time.

8.1 Predictions of Reburn Zone Nitrogenous Species

It is desired to predict the values of nitrogenous species in the reburn zone from primary NO values and known process parameters, such as temperature, reburn zone residence time and stoichiometries. The kinetic model can be used for this purpose, provided an initial value for OH concentration is known, and if the effect of mixing in the vicinity of the reburning fuel flame is accounted for.

8.1.1 Corrections for Mixing Effects in the Reburn Zone

Mixing can limit NO destruction by hydrocarbon radicals, since it affects the interaction between the primary NO and the reburning fuel. Furthermore, oxygen carryover into the reburn zone can create variations in the local stoichiometry, which affects the distribution and the levels of the nitrogenous species. In the region of the reburn zone where mixing effects are important, the presence of oxygen results in the destruction of a

fraction of the hydrocarbon radicals to form neutral products, such as CO and CO₂. Thus, mixing affects NO destruction by hydrocarbon radicals, partly due to limited contact between NO and the reburning fuel, and partly due to the presence of oxygen rich pockets which can reduce the availability of CH_i radicals.

In the vicinity of the reburning fuel flame, mixing can also limit HCN formation from hydrocarbon reactions, partly due to reduced NO destruction by hydrocarbons, and partly due to the enhanced destruction of HCN in the presence of oxygen carryover from the primary zone. Thus, a fraction of the HCN that is formed in the early stage of the reburn zone, is oxidized to form other nitrogenous species and N₂. An examination of nitrogenous species values, under fuel lean reburn zone conditions (Figure 6.3), supports this hypothesis. The profiles (Coal #4) show that the introduction of the reburning fuel corresponds to a destruction of over 400 ppm NO, mostly within 0.18 seconds, but HCN levels are less than 5 ppm throughout the reburn zone. Clearly, a significant amount of NO can be destroyed in the reburn zone without a significant increase in HCN levels, depending on the extent of mixing and oxygen availability.

The development of a fundamentally based theoretical model, to account for mixing at the reburning fuel injection point, is beyond the scope of this investigation. Instead, a simple mixing model is presented to account for mixing effects in short time scales (less than 0.18 seconds) in the reburn zone. In this model, CH₄ values rise linearly from zero at the entrance to the reburn zone to an average measured value. The use of an effective CH₄ value would then, account for mixing effects on NO and hydrocarbon interaction in the vicinity of the reburning fuel flame. To account for reduced HCN formation from hydrocarbons, a correction factor of 0.3 is used. Thus, 70% of HCN formation from hydrocarbons is assumed to be destroyed by oxidation reactions, that result in the formation of N₂. These assumptions are made only in the region between the entrance to the reburn zone and the first measured point downstream of the injection point, corresponding a to residence time of about 0.18 seconds. For the remainder of the reburn zone, the kinetic model is used as before, without any modifications.

The initial OH concentration was estimated by extrapolating calculated OH values in the reburn zone and correlating these values as a function of temperature at the entrance to the reburn zone. Adjustment of this expression was necessary to obtain predictions for all three nitrogenous species in the reburn zone from the primary NO level. The following correlation for initial OH values was used:

$$\text{OH} = 35 \times \exp(-24100/T)$$

To summarize, some modifications were necessary to permit the application of the kinetic model in short residence times in the reburn zone (less than 0.18 seconds), where mixing effects were important. An empirical correlation was used to estimate the initial OH, combined with a model, in which methane concentration rose linearly from zero to an average value, and 70% of HCN formation was destroyed to form N₂. These empirical

modifications were designed to account for the effects of mixing on the inter-conversion of nitrogenous species in the early stage of the reburn zone. The choice of the parameters was mostly based on trial and error and an examination of the predicted values. It should be emphasized that these modifications are empirical and would be valid only in the experimental configuration of this study. The objective of this analysis is to demonstrate that, with proper modifications to account for mixing effects in the early stage of reburning, the kinetic model can be applied to predict nitrogenous species values in the reburn zone from known NO concentrations in the primary zone.

8.1.2 Predictions of the Extended Model

The extended model was used to predict nitrogenous species values in short residence times of less than 0.2 seconds in the reburn zone, as seen in Figure 8.1. The predicted values could then serve as initial concentrations to predict nitrogenous species profiles in the remainder of the reburn zone, using the kinetic model with no limitation. In all these tests (Coal #2, 3, 6, 7, 10, 12 and 19), the primary fuel was bituminous coal and the reburning fuel was natural gas. Reasonable predictions were obtained for all nitrogenous species.

The choice of a CH_4 concentration at the inlet to the reburn zone can greatly affect the predicted NO values, as shown in Figure 8.2. If the initial diluted value for CH_4 is used (assumes instantaneous perfect mixing), the model predicts NO decay rates that are far too rapid. A similar trend for NO decay is observed, if the first measurement downstream of the reburning fuel injection point is used as an initial value for CH_4 (assumes instantaneous oxidation of the reburning fuel). Better predictions are obtained by assuming that CH_4 concentration rises linearly from zero to the measured value below the reburning fuel injection point. This demonstrates the significance of an initial estimate of CH_4 on NO predictions in the reburn zone, and the limitations imposed by mixing on NO reduction by hydrocarbon reactions.

Figure 8.3 shows a comparison between measured and predicted nitrogenous species profiles in the reburn zone, starting from the primary NO values. The predictions are based on the extended model, as described earlier. Again, it is emphasized that for residence times greater than 0.18 seconds, the kinetic model is used with no modifications. The empirical corrections are used only to account for mixing effects that exist in short time scales (less than 0.18 seconds). Comparing the lines to the data shows good agreements between measurements and predictions of NO, HCN and NH_3 values throughout the reburn zone and, under various conditions in the primary zone and in the reburn zone.

To summarize, in natural gas reburning in a practical coal combustor, the inter-conversion of nitrogenous species occurs in two sequential regions in the reburn zone. The first region is in the vicinity of the reburning fuel flame, involves short time scales, and in which mixing effects can limit both NO destruction by hydrocarbon reactions and the formation of HCN. The second region follows downstream, covers the remainder of the

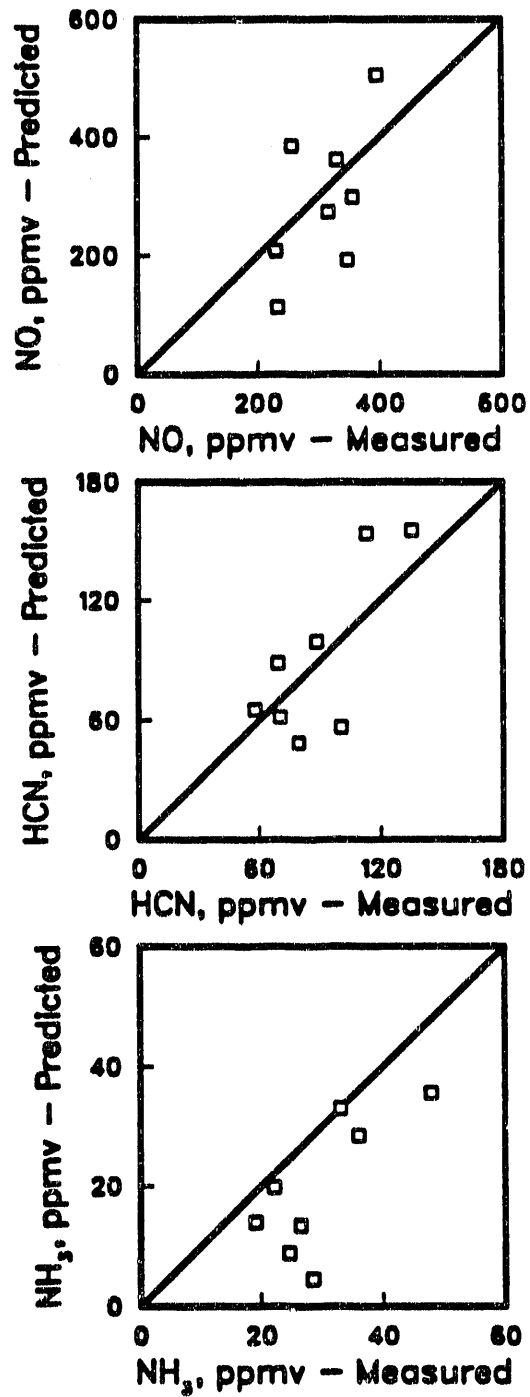


Figure 8.1. Comparison between Model Predictions and Measurements for Reburn Zone Residence Times Less than 0.2 Seconds - Bituminous Coal Primary Flame - Natural Gas Reburning.

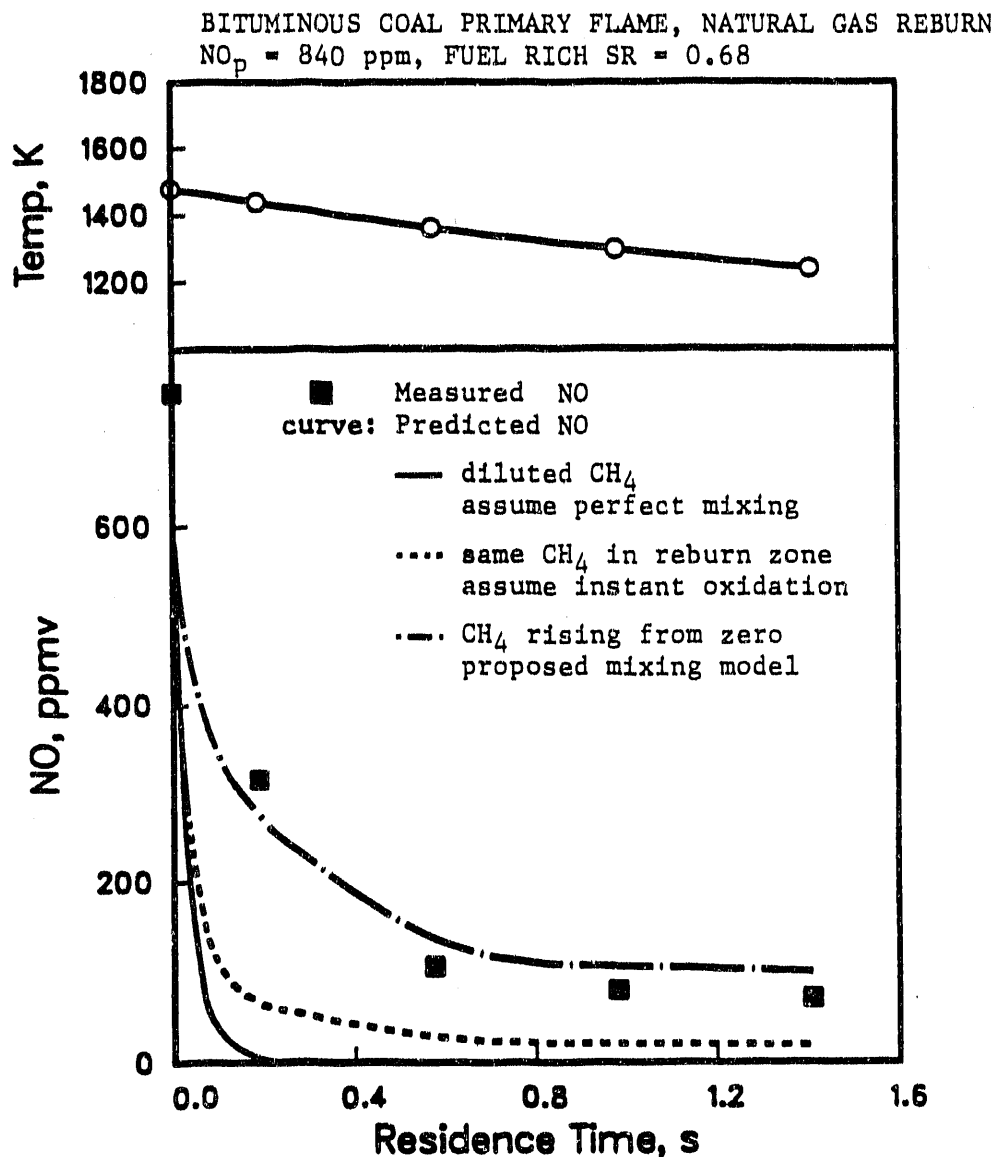


Figure 8.2. Effect of CH₄ Concentration at the Reburning Fuel Injection Point on NO Predictions in the Reburn Zone.

BITUMINOUS COAL PRIMARY FLAME, NATURAL GAS REBURNING

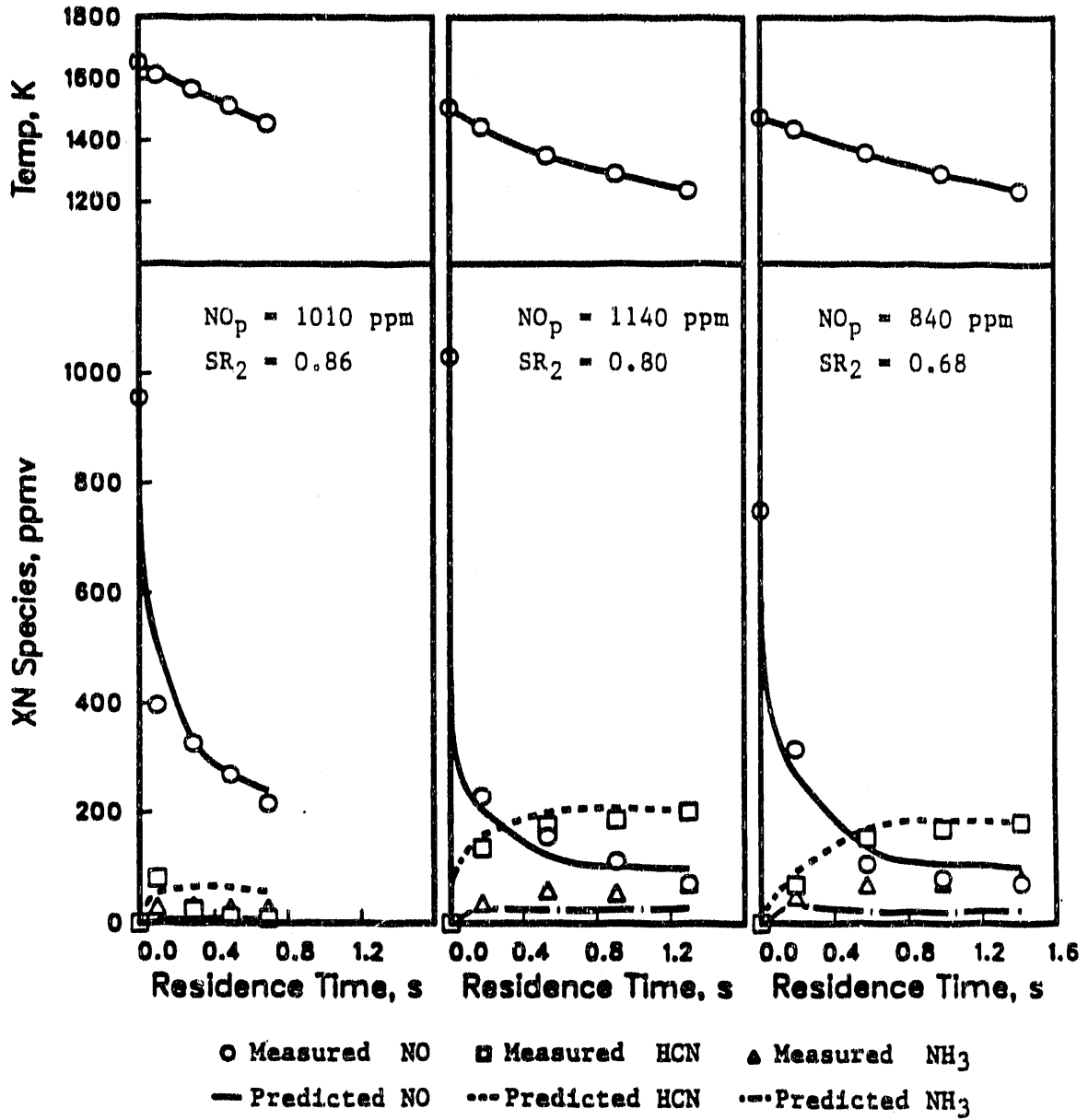


Figure 8.3. Comparison between Measured and Predicted Nitrogenous Species Profiles in the Reburn Zone - Predictions from Primary NO Concentrations.

reburn zone and involves no mixing complications. In the region of the reburn zone, where mixing effects are not important, the inter-conversion of nitrogenous species can be described by a kinetic model, based on homogeneous gas phase kinetics. The kinetic model was combined with empirical corrections to account for mixing effects (first region) in short residence times in the reburn zone (less than 0.18 seconds). The extended model was successful in predicting nitrogenous species values (NO, HCN and NH₃) in the reburn zone from primary NO levels.

8.2 Prediction of Exhaust NO in the Burnout Zone

In the final stage of reburning, air is added and the oxidizable nitrogenous species (HCN and NH₃) are converted to NO and N₂. In this stage, there is no validated detailed mechanism to predict the formation of NO. An empirical correlation (Chen et al., 1986) is used in this study to estimate final NO emissions for known reburn zone values. The correlation is later combined with the extended predictive model to allow the prediction of NO exhaust emissions from primary NO values. The following correlation is used:

$$NO_{ex} = 0.81 * SR_2 * NO + \left[\frac{0.36 (HCN + NH_3)}{1 + 0.0024 (HCN + NH_3)} \right] + 53$$

All concentrations are in ppm, on a dry basis, and corrected to 0% excess O₂. This correlation was developed by Chen et al. (1986) and was used in this study without any adjustments.

Figure 8.4 shows a comparison between measured and predicted NO exhaust values for different reburning fuel types. There is good agreement between measurements and predictions under various conditions.

8.3 Prediction of Overall Reburning Effectiveness

An overall model is derived, consisting of the kinetic model, corrected for mixing effects for residence times shorter than 0.18 seconds in the reburn zone, and incorporating an empirical correlation (Chen et al., 1986) to predict final NO emissions from reburn zone values, as described earlier. The combined model can be used to predict the overall reburning effectiveness from primary NO values, provided the concentrations of H₂, CH₄, H₂O and N₂, and temperature values down the combustor are known.

The results of natural gas reburning experiments were used to estimate the concentrations of H₂, CH₄, H₂O and N₂ in the reburn zone, the primary NO concentration where needed, as well as temperature profiles down the combustor. Only the experiments in which the primary flame was that of bituminous coal in the premixed mode were used for this purpose (Coal #2, 3, 4, 7, 9, 10, 12, 16, 18 and 19). The concentration of H₂

BITUMINOUS COAL PRIMARY FLAME

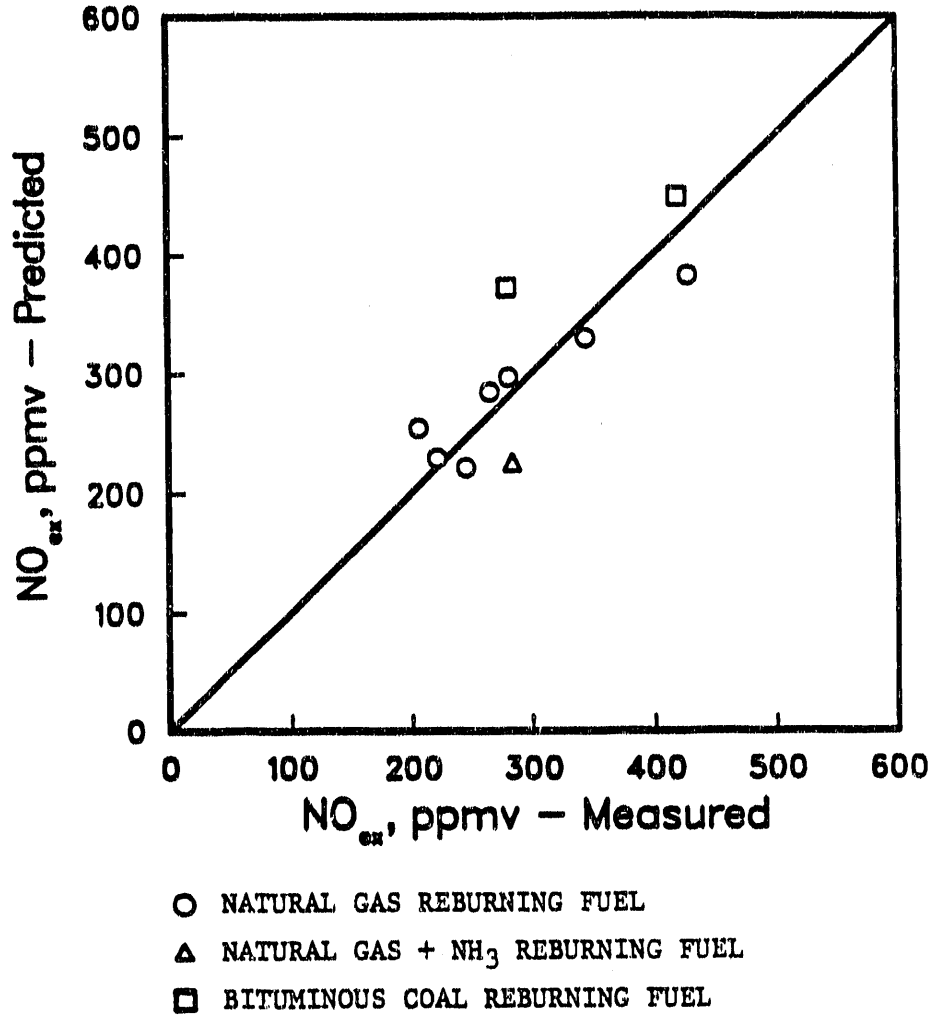


Figure 8.4. Comparison between Measured and Predicted NO Exhaust Emissions (Dry, 0% O₂) in the Final Stage of Reburning.

depended mostly on reburn zone stoichiometry, whereas, the concentration of CH₄ depended on reburn zone stoichiometry and reburn zone inlet temperature. The following empirical correlations were derived to estimate H₂ and CH₄ concentrations, respectively:

$$\begin{aligned} \%H_2 &= 8.0 - 7.9 * SR_2 \quad ; \quad (r^2 = 0.94) \\ \%CH_4 &= 3.5 - 0.0024 * SR_2 * T \quad ; \quad (r^2 = 0.82) \end{aligned}$$

where T is the reburn zone inlet temperature. Temperature values were estimated from known residence times in the reburn zone and the empirical correlation:

$$\text{Temperature Quench Rate} = 178 - 0.000162 * T^2 \quad ; \quad (r^2 = 0.89)$$

In the reburn zone, H₂O concentrations varied from 9% to 11%, whereas, N₂ concentrations varied from 71% to 76%. Average values of 10% and 73.5% were used, respectively. In the primary zone, measured primary NO levels were 680-950 ppm and an average value of 750 ppm (1000 ppm dry, 0% O₂) was used, whenever measured values were not known. The overall reburning effectiveness was calculated in a similar fashion as described in Section 4.2.2. An average correction factor (DCF) of 1.3 was used to convert predicted values (wet) of nitrogenous species in the reburn zone to dry values and 0% excess O₂. Values of the dilution correction factor (DCF) for the various reburning experiments are listed in Appendix B.

Figure 8.5 shows measured and predicted variations of the overall reburning effectiveness with reburn zone stoichiometry. A comparison between the predictions, based on the correlation of Table 4.13, and the predictions of the extended model shows that the latter model is more successful in describing reburning effectiveness in the vicinity of an optimum reburn zone stoichiometry (SR₂). However, the predicted values are relatively high. The overall model predicted an S shaped curve, with a rapid jump at a reburn zone stoichiometry of about 0.9. The shape of the predicted curve is strongly dependent on the estimate of CH₄ values, since the model predicts low values of NH₃ in the reburn zone, as seen in Figures 8.1 and 8.3. Consequently, the model overestimates the significance of NO destruction by hydrocarbon radicals, and low values of reburning effectiveness are predicted at SR₂ values below 0.9, where CH₄ concentrations below 0.05% are estimated.

The effect of reburn zone inlet temperature on predicted reburning effectiveness is shown in Figure 8.6. The curves are based on the predictions of the extended kinetic model and show a greater sensitivity to variations in temperature than the predictions of the parametric study (Figure 4.4). The destruction of NO by hydrocarbon radicals is enhanced at higher temperatures, whereas, the destruction of NO by NH₃ species is favored at lower temperatures. These two opposing effects reduce the overall effect of temperature on reburning effectiveness. Therefore, a greater effect of temperature is predicted, since the model predicts low values of NH₃, in addition to low CH₄ estimates at higher temperatures.

BITUMINOUS COAL PRIMARY FLAME, NATURAL GAS REBURNING
 Reburn Zone: Time = 0.33-0.43 s, Temp = 1550-1600 K
 NO ~ 900 ppm (dry, 0% O₂)

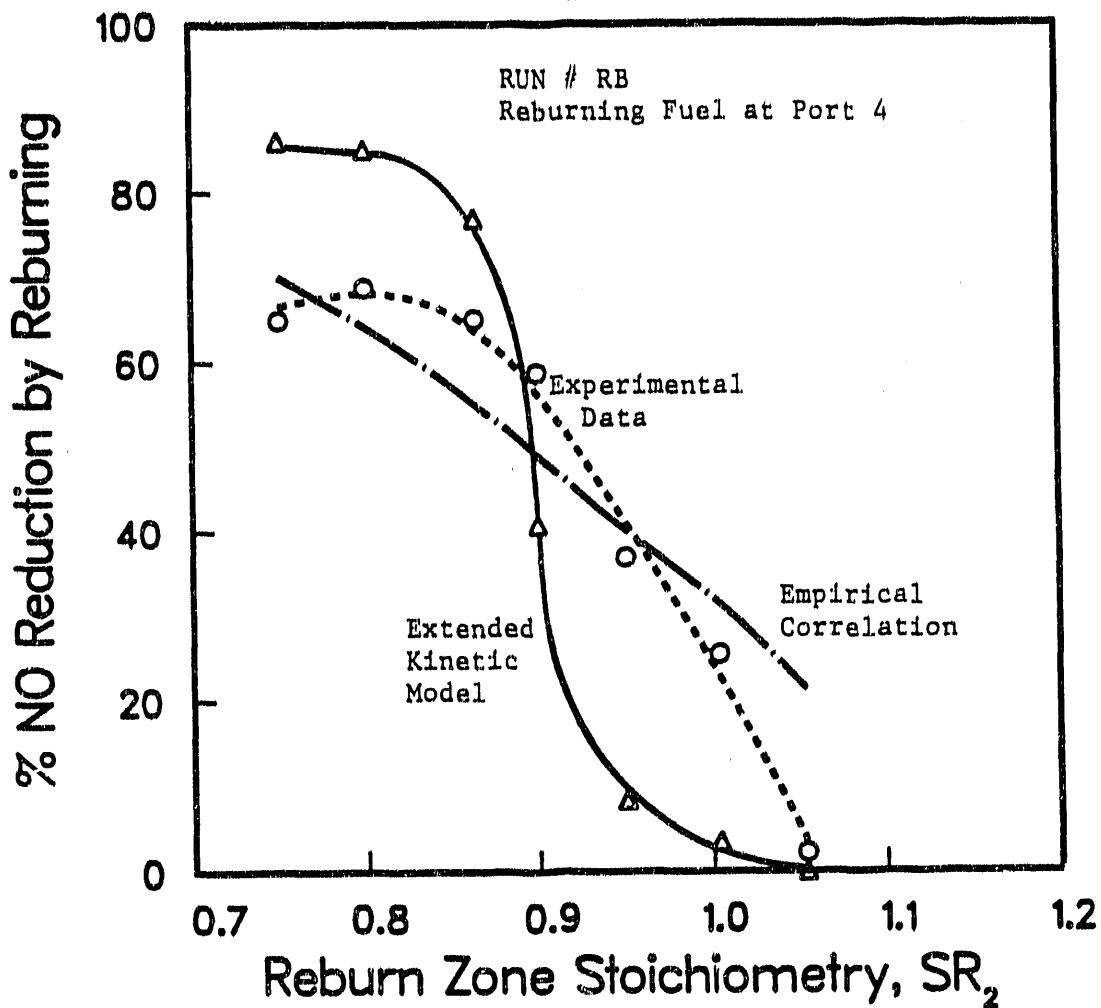


Figure 8.5. Comparison between Measured and Predicted Reburning Effectiveness - Predictions of the Extended Kinetic Model.

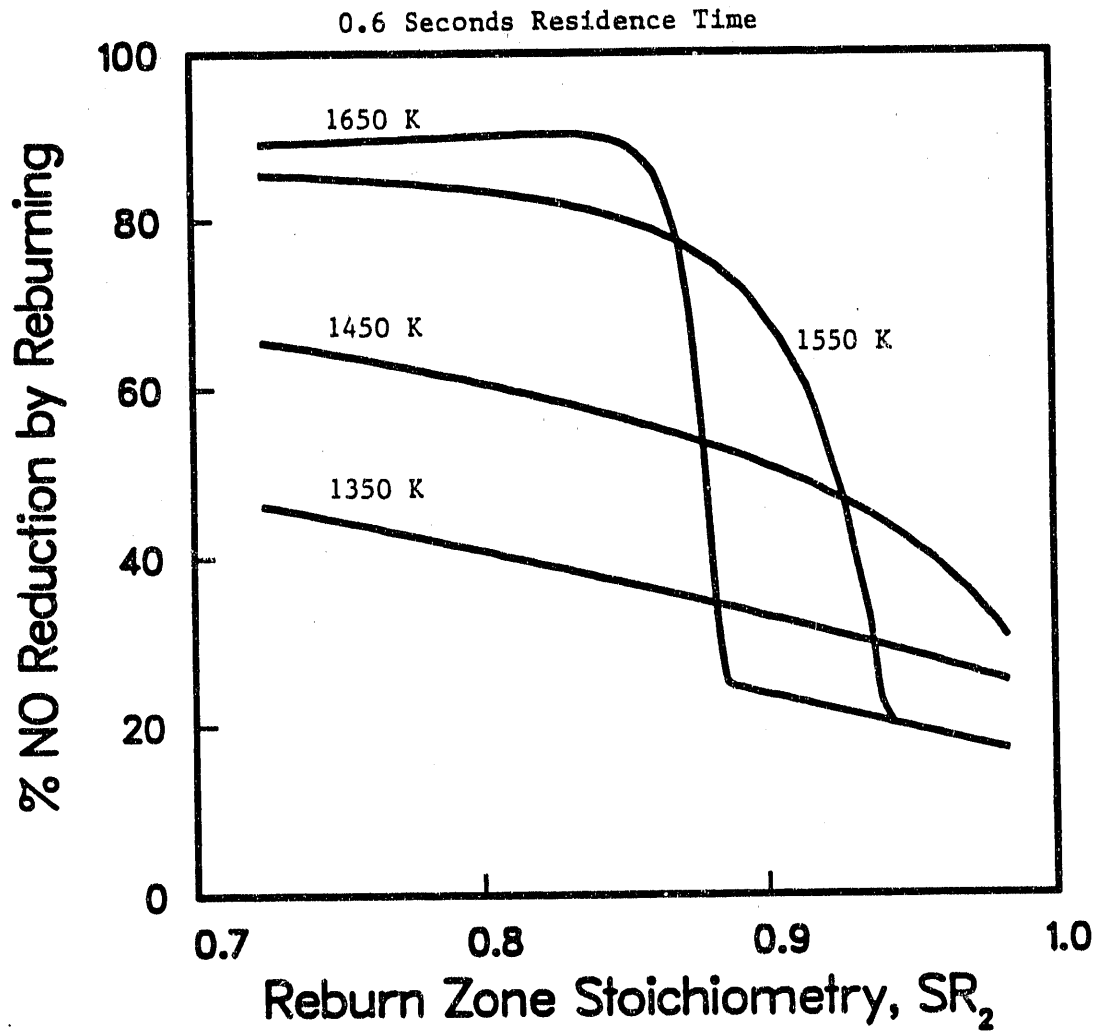


Figure 8.6. Predictions of the Extended Kinetic Model.

The model (Figure 8.6) predicts an improvement in reburning effectiveness at higher temperatures, only at reburn zone stoichiometries (SR_2) richer than 0.86. As the reburn zone approaches the fuel lean side ($SR_2 > 0.94$), temperature effects are reversed, and greater destruction of NO is predicted at lower temperatures. In general, these observations are consistent with the results of the parametric study of Section 4.4 (Figure 4.4). The sensitivity of predicted values of reburning effectiveness to changes in stoichiometry, at SR_2 values 0.86-0.94, depends on temperature, which also determines the shape of the predicted curve. This behavior is caused by the dependence of CH_4 estimates on temperature and stoichiometry. Consequently, the trends in this stoichiometric range ($SR_2 = 0.86-0.94$) cannot be analyzed objectively, since they depend on the choice of a correlation to estimate CH_4 concentrations.

8.4 Prediction of Configurations for Low NO Emissions

The validity of the kinetic model, in describing the inter-conversion of nitrogenous species under fuel rich conditions, was demonstrated in Section 7.9. The model was shown to be relatively insensitive to the overall configuration and could be applied under reburning and air staging configurations. Under practical combustion conditions, final NO emissions would have minor dependence on final stage parameters and would be mostly determined by the levels and the distribution of nitrogenous species leaving the fuel rich stage. In this section, the kinetic model was used to examine hypothetical configurations under reducing conditions that would ultimately produce low levels of final NO emissions after final air addition. The objectives are to identify fuel rich configurations for low total fixed nitrogen concentrations and to determine kinetic limits that would prevent further destruction of nitrogenous species.

In this examination, initial conditions are specified and residence time and temperature in the fuel rich zone are allowed to vary downstream of the initial point. The focus is on the change in the values of the nitrogenous species. The values of the major species are assumed to be independent of residence time and temperature. Four cases are examined, corresponding to the fuel rich zones of two reburning tests and two air staging tests. An equilibrium assumption is made for the initial concentration of OH.

8.4.1 Effect of Temperature Quench

Under fuel rich conditions, the mutual destruction of NO and NH_3 species is favored at lower temperatures. However, high temperatures at early residence times enhance the formation of NH_3 . Therefore, it is expected that temperature quench rate would have a significant effect on the distribution of nitrogenous species in the fuel rich zone. Figure 8.7 and 8.8 show the effect of temperature quench rate on predicted nitrogenous species values, after a residence time of 3 seconds. Figure 8.7 examines two fuel rich reburn zones at different initial temperatures and Figure 8.8 examines the fuel rich combustion of a bituminous coal and a lignite coal. In all four cases, an optimum temperature quench rate is obtained, and corresponds to a minimum value of the total fixed nitrogen concentration.

BITUMINOUS COAL PRIMARY FLAME, NATURAL GAS REBURNING
FUEL RICH SR = 0.86, RESIDENCE TIME = 3 seconds

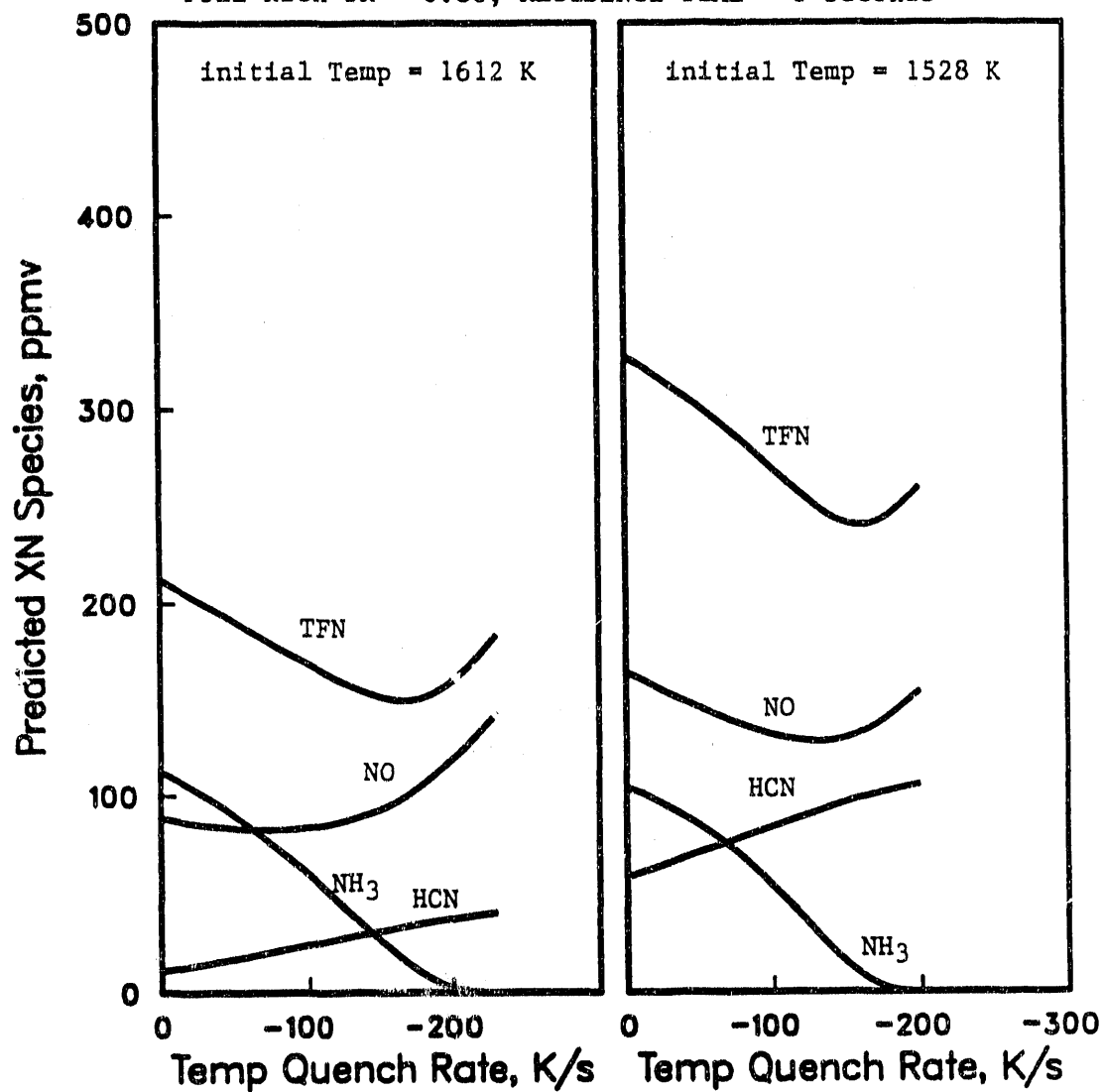


Figure 8.7. Effect of Temperature Quench Rate on Predicted Nitrogenous Species Concentrations in the Reburn Zone.

FUEL RICH SR = 0.6, RESIDENCE TIME = 3 seconds

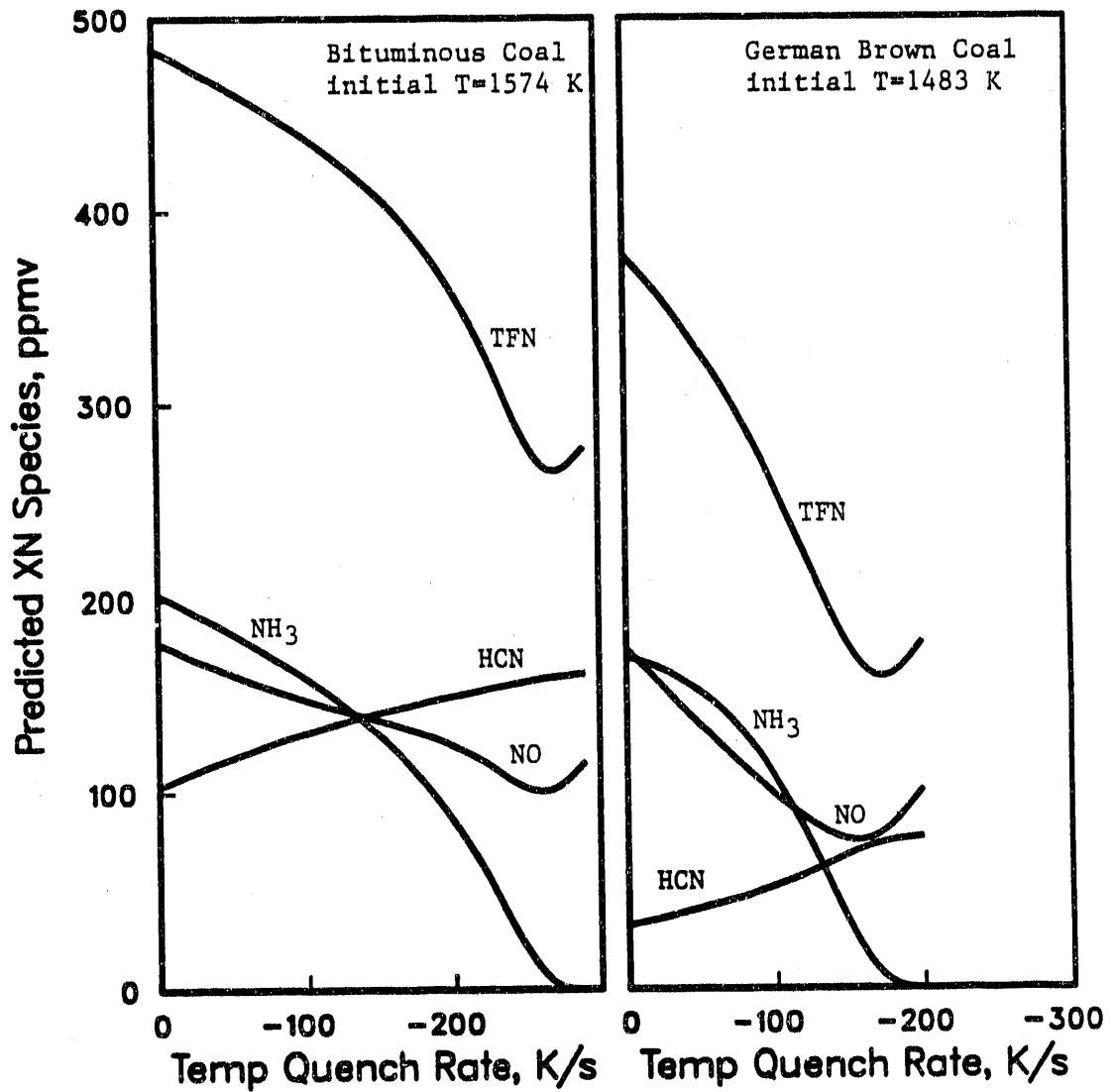


Figure 8.8. Effect of Temperature Quench Rate on Predicted Nitrogenous Species Concentrations in the Fuel Rich Combustion of Coal.

An increase in temperature quench rate corresponds to an increase in HCN concentration, and decrease in NO and NH₃ concentrations, until an optimum quench rate is approached. The increase in HCN concentration is expected since its destruction is less favorable at lower temperatures. The decrease in NO and NH₃ concentration is due to their mutual destruction, which is favored at lower temperatures. However, as NH₃ values approach zero, NO decay rate is reduced and further reduction in the total fixed nitrogen concentration may not be possible. If temperature quench rate is too rapid, NH₃ formation is retarded in the early stage of the fuel rich zone and NH₃ values approach zero in less time. Consequently, the enhanced destruction of NO and NH_i species at short residence times at reduced temperatures is offset by reduced NO decay rates at longer residence times as NH₃ concentration drop to low levels. Furthermore, lower temperatures are accompanied by higher HCN concentrations. On the other hand, if temperature quench rate is too slow, NO + NH_i reactions are less favorable at the higher temperatures in the fuel rich zone. NO destruction by CH_i radicals has weak sensitivity to changes in temperature and is not addressed in this analysis.

8.4.2 Effect of Residence Time

Figures 8.9 and 8.10 show time resolved predicted nitrogenous species profiles for the four cases discussed earlier, at their optimum temperature quench rates. The trends are similar to the experimental results discussed of this study, in which NO decay to lower levels and small changes in HCN concentrations are observed. However, NH₃ profiles show an increase in NH₃ concentrations within residence times of about 1 second, followed by decay to lower levels that approach zero within 3-4 seconds. The profiles suggest that there are two limitations that would prevent significant reductions in the total fixed nitrogen concentration at longer residence times. First, no reduction in HCN levels could be obtained by allowing longer residence times in the fuel rich zone and these levels seem to depend mostly on conditions in the early stage of the fuel rich zone. Second, the mutual destruction of NO and NH₃ could be enhanced by manipulation of the time temperature history in the fuel rich zone, but would also be limited by the decay in NH₃ concentrations to low levels in about three seconds, beyond which only minor reduction in total fixed nitrogen could be further achieved.

To summarize, temperature quench rate affects the distribution and levels of all nitrogenous species in the fuel rich zone. There is an optimum temperature quench rate that corresponds to a minimum concentration of the total fixed nitrogen, mainly due to the effect of temperature on NO + NH_i reactions. The value of this optimum seems to depend on the properties of the fuel rich zone, such as stoichiometry and the temperature profile. Long residence times are effective in reducing NO and NH₃ concentrations, until NH₃ concentrations approach zero. The presence of high levels of HCN in the fuel rich zone limits the decay in the total fixed nitrogen with time. Residence time in the fuel rich zone seems to have a minor effect on HCN concentrations. This suggests that HCN levels at the exit of the fuel rich zone are mostly dependent on conditions at or near the entrance of the fuel rich zone, such as temperature and local concentrations.

BITUMINOUS COAL PRIMARY FLAME, NATURAL GAS REBURNING
FUEL RICH SR = 0.86

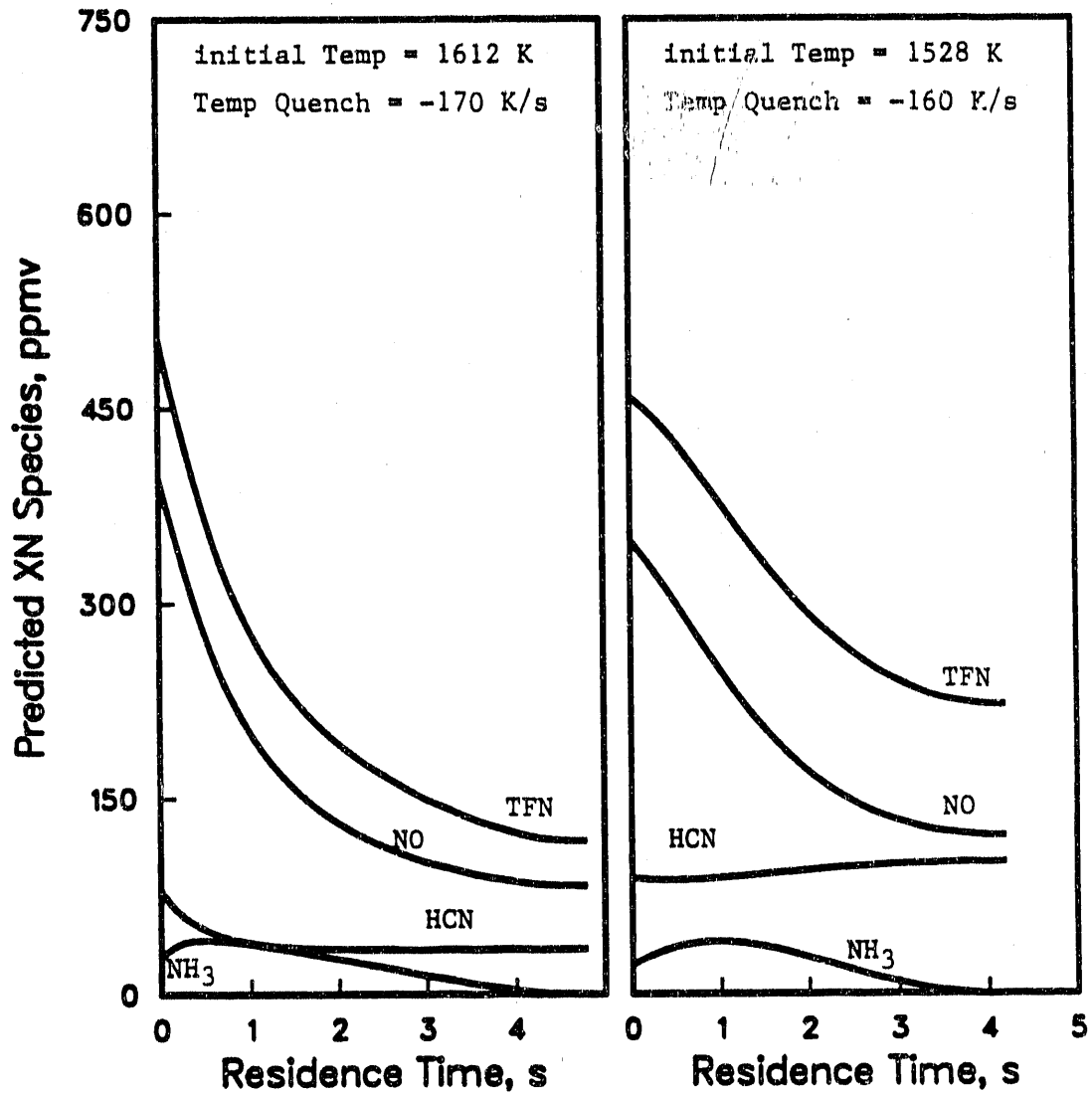


Figure 8.9. Predicted Nitrogenous Species Profiles in the Reburn Zone at Optimum Temperature Quench Rate.

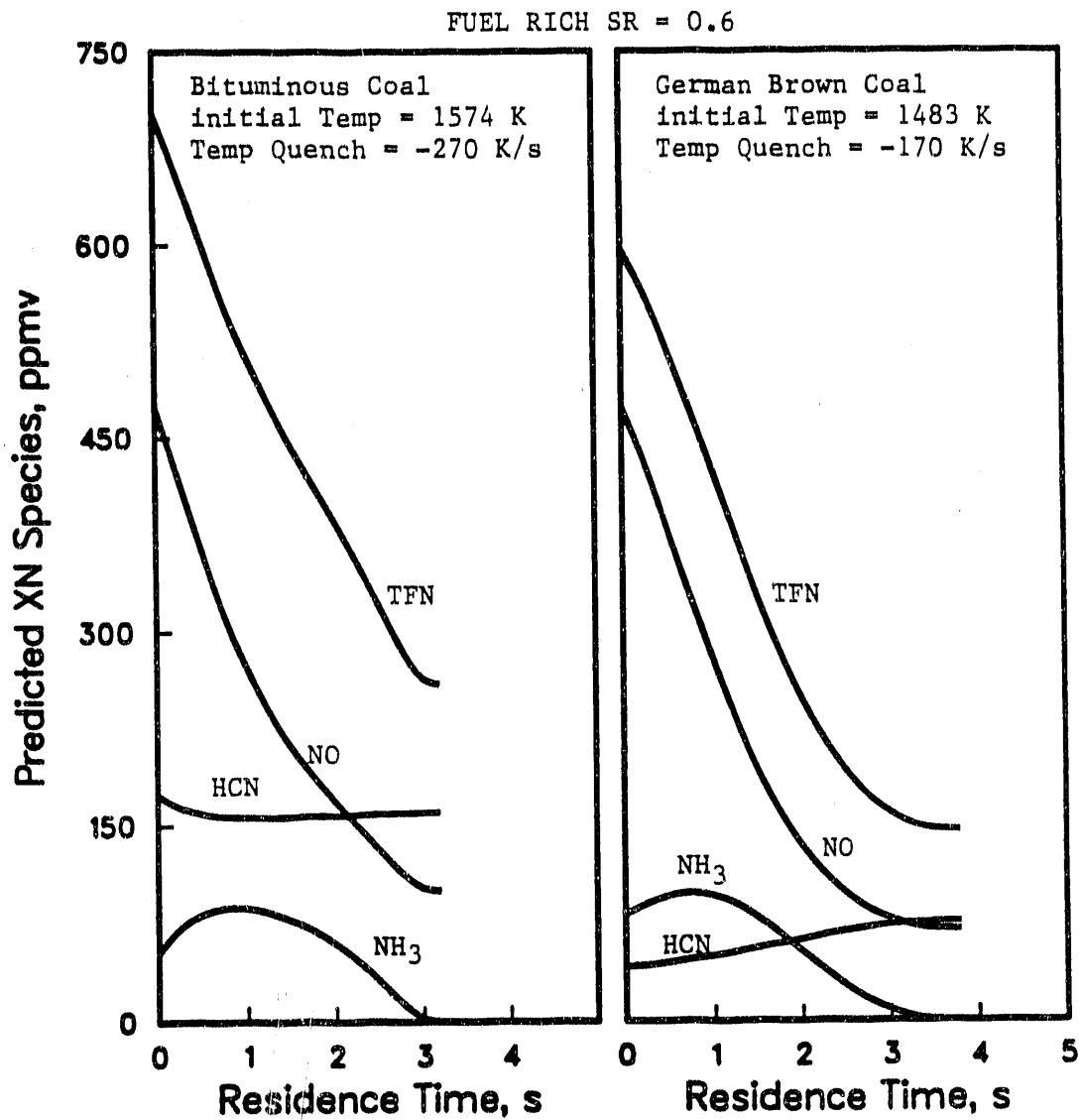


Figure 8.10. Predicted Nitrogenous Species Profiles in the Fuel Rich Combustion of Coal at Optimum Temperature Quench Rate.

9.0 CONCLUSION AND RECOMMENDATIONS

Reburning experiments were conducted on a 17 kW down-fired laboratory combustor to investigate various aspects of the reburning process as a combustion modification technique to reduce NO emissions from coal combustion. The focus was on natural gas reburning and a bituminous coal primary flame in a premixed mode, although other configurations were also examined in various parts of the study.

The following conclusions were derived from this work.

1. On-line measurements of N_2O concentrations in coal combustion flue gases showed that uncontrolled emissions were less than 2 ppm. These levels increased after air addition in air staging and reburning configurations, but were less than 10 ppm. This increase in N_2O levels was higher at richer stoichiometries in the fuel rich zone, which suggested N_2O formation through an HCN intermediate. Therefore, reburning might produce higher levels of N_2O in the exhaust, relative to uncontrolled emissions, but the increase in N_2O would be of minor significance, under practical reburning conditions.
2. A parametric study of reburning was conducted, based on a statistical experimental design. The study showed that the effect of one reburning parameter, could only be examined in view of the effects of the other parameters of the system. Reburn zone variables, namely, stoichiometry, residence time and temperature, dominated the overall destruction of NO. The effect of stoichiometry in the primary zone was of minor significance and depended on the stoichiometry in the fuel rich zone. Furthermore, the effect of temperature in the reburn zone was dependent on residence time and stoichiometry. Temperature effects were dominant at shorter residence times in the reburn zone and higher temperatures enhanced reburning effectiveness, under sufficiently fuel rich conditions. This effect was reversed when the reburn zone was sufficiently fuel lean, where lower temperatures enhanced the destruction of NO. This was attributed to mixing inhomogeneities in the reburn zone and the temperature dependence of reactions that destroyed hydrocarbons to form neutral products (CO and CO_2).
3. In the examination of reburning, the statistical approach failed to predict an optimum configuration. Thus, the parametric study was complemented by tests, in which one variable was varied at a time. These tests identified optimum reburn zone stoichiometries between 0.8 and 0.9, depending on the extent of mixing. Improved mixing conditions in the reburn zone shifted the optimum stoichiometry to the leaner side and produced greater destruction of NO. However, these effects could not be quantified. A parametric study, based on a statistical experimental design, was an efficient method for a qualitative, rather than quantitative, examination of the reburning process.

4. A reburning configuration, in which the reburning fuel was introduced as multiple stream injections into the reburn zone, did not improve reburning effectiveness, relative to single stream injections. The distribution of the reburning fuel down the combustor enhanced the interaction between NO and hydrocarbon radicals. This effect was offset by a decrease in the effectiveness of residence time, temperature and stoichiometry in the reburn zone.
5. Reburning in a premixed primary flame mode, was compared to that in an axial diffusion primary flame mode. The overall destruction of NO was greater when the primary flame was premixed. However, final NO emissions below 250 ppm (dry, 0% O₂) were possible in both flame modes.
6. Residence time resolved nitrogenous species profiles in the reburn zone showed that there are two regimes for NO destruction in the reburn zone. First, in the vicinity of the reburning fuel flame, corresponding to short residence times, there is rapid destruction of NO and mixing effects can limit NO destruction by hydrocarbon reactions. The time scale of this regime is determined by the extent of mixing in the reburn zone. Second, for the remainder of the reburn zone, mixing effects are of minor significance and nitrogen kinetics dominate the destruction of NO.
7. Reburning results, in which various reburning fuels were used, verified the significance of hydrocarbon reactions in governing NO destruction. In addition, HCN formation from hydrocarbons was shown to be a dominant source of HCN in the fuel rich reburn zone. The fixation of N₂ by hydrocarbons (Fenimore, 1971) contributed to HCN formation and presented a serious limitation to the effectiveness of reburning, especially at low primary NO levels. There was no evidence to indicate that heterogeneous processes would be significant under fuel rich natural gas reburning conditions.
8. A simple mechanism was proposed to describe the inter-conversion of nitrogenous species in the fuel rich reburn zone. A kinetic model was developed, based on homogeneous gas phase kinetics, simplifying partial equilibrium assumptions and known kinetic parameters, taken from the literature (Glarborg et al., 1986). The model was used to predict NO, HCN and NH₃ values in the fuel rich zone in reburning and air staging configurations. The proposed mechanism was shown to be independent of the overall configuration and primary fuel type. However, the predictions of the kinetic model in the reburn zone were restricted to the region, where mixing effects were not significant.
9. The kinetic model was combined with empirical corrections to account for mixing effects in early time scales of the reburn zone. Then, the extended model was used to predict values of NO, HCN and NH₃ in the reburn zone, starting from the primary NO level. The success of this analysis demonstrated that the kinetic model could be used to predict the overall reburning effectiveness from known primary NO values,

provided mixing effects in the reburn zone were accounted for. An empirical correlation (Chen et al., 1986) was used to predict final NO emissions from reburn zone values. The combined model was compared to the statistically derived empirical model and served to support the conclusions of the parametric study of reburning.

10. The kinetic model was used to examine hypothetical fuel rich configurations, in which variations in temperature and residence time were not restricted. The study identified temperature quench rate as a significant variable that affected the inter-conversion of nitrogenous species, mainly due to the effect of temperature on NO reactions with NH_i species. Two limitations prevented further destruction of nitrogenous species at long residence times (greater than 3 seconds), namely, the presence of HCN, and the complete destruction of NH_3 that would prevent further destruction of NO by NH_i radicals.

The following recommendations are made for future work:

1. The application of reburning under fuel lean conditions in the reburn zone can be a useful tool in achieving moderate reductions in NO emissions, and needs to be further investigated. In this study, NO reductions, as high as 45%, were possible under fuel lean reburning conditions. Lower temperatures and poor mixing conditions may enhance the overall destruction of NO, if the reburn zone is operated fuel lean.
2. The concentration of the OH radical in the reburn zone was a dominant factor in the generation of CH_i and NH_i radicals, and thus, affected the overall destruction of NO. Measurements of OH concentrations can provide valuable information regarding the validity of the partial equilibrium assumptions that were incorporated in the kinetic model.
3. In this work, an empirical correlation was used to predict final NO emissions from reburn zone values. A fundamental understanding of the mechanisms that govern the inter-conversion of nitrogenous species in the final stage of reburning is lacking.
4. Mixing is a limiting factor in the optimization of the reburning process and needs to be quantified. A theoretical mixing model, combined with a kinetic model, would provide a valuable tool in the design of combustion modification configurations for low NO emissions.

5. The kinetic model showed that temperature quench rate could greatly affect the outcome of reburning. Furthermore, an optimum temperature quench was detected and depended on the conditions of the fuel rich zone. The effect of this variable needs to be further investigated, since its manipulation can be a powerful tool in achieving further destruction of NO in reburning.

10.0 REFERENCES

- Beer, J.M. and N.A. Chigier, Combustion Aerodynamics, Halsted Press Division, John Wiley and Sons, Inc., New York, NY, (1972).
- Bose, A.C., and J.O.L. Wendt, "Pulverized Coal Combustion: Fuel Nitrogen Mechanisms in the Rich Post-Flame," Twenty-Second Symposium (International) on Combustion, The Combustion Institute, Pittsburgh, PA, 1127 (1988).
- Bose, A.C., K.M. Dannecker, and J.O.L. Wendt, "Coal Composition Effects on Mechanisms Governing the Destruction of NO and other Nitrogenous Species During Fuel-Rich Combustion," Journal of Energy and Fuels, 2, 301 (1988).
- Bose, A.C., "Pulverized Coal Combustion: Fuel Nitrogen Mechanisms in the Rich Post-Flame," Ph.D. Dissertation, The University of Arizona, Tucson, AZ, (1989).
- Bradley R. A., "Determination of Optimum Operating Conditions by Experimental Methods; Part I: Mathematics and Statistics Fundamental to the Fitting of Response Surfaces," Industrial Quality Control, 16 (July, 1958).
- Brown, R. A. and W. C. Kuby, "Application of Reburning for NO_x Control in Cogeneration," Proceedings of the 1985 Joint Symposium on Stationary Combustion NO_x Control, Volume 1, Acurex Corporation, Mountain View, CA, 26-1 (1986).
- Chen, S.L., M.P. Heap, D.W. Pershing, and G.B. Martin, "Influence of Coal Composition on the Fate of Volatile and Char Nitrogen During Combustion," Nineteenth Symposium (International) on Combustion, The Combustion Institute, Pittsburgh, PA, 1271 (1982).
- Chen, S. L., W. C. Clark, M. P. Heap, D. W. Pershing and W. R. Seeker, "NO_x Reduction by Reburning with Gas and Coal - Bench Scale Studies," Proceedings of the 1982 Joint Symposium on Stationary Combustion NO_x Control, Volume 1, Electric Power Research Institute, Palo Alto, CA, 16-1 (1983).
- Chen, S. L., J. M. McCarthy, W. D. Clark, M. P. Heap, W. R. Seeker and D. W. Pershing, "Bench and Pilot Scale Process Evaluation of Reburning for In-Furnace NO_x Reduction," Twenty-first Symposium (International) on Combustion, The Combustion Institute, Pittsburgh, PA, 1159 (1986).
- Davies, O. L., ed., Design and Analysis of Industrial Experiments, Hafner Publishing Company, New York, NY, (1956).
- Elliot, M.A., ed. Chemistry of Coal Utilization, 2nd Volume, Wiley-Interscience, New York, NY, (1981).

England, G.C., M.P. Heap, D.W. Pershing, R.K. Nihart and G.B. Martin, "Mechanisms of NO_x Formation and Control: Alternative and Petroleum-Derived Liquid Fuels," Eighteenth Symposium (International) on Combustion, The Combustion Institute, Pittsburgh, PA, 163 (1981).

Fenimore, C.P., "Studies of Fuel Nitrogen Species in Rich Flame Gases," Seventeenth Symposium (International) on Combustion, The Combustion Institute, Pittsburgh, PA, 661 (1979).

Fenimore, C.P., "Reactions of Fuel Nitrogen in Rich Flame Gases," Combustion and Flame, 26, 249 (1976).

Fenimore, C.P., "Formation of Nitric Oxide in Premixed Hydrocarbon Flames," Thirteenth Symposium (International) on Combustion, The Combustion Institute, Pittsburgh, PA, 373 (1971).

Gerber, C.R., "Opening Remarks," Proceedings of the 1985 Joint Symposium of Stationary Combustion NO_x Control, Volume 1, Acurex Corporation, Mountain View, CA, 2-1 (1986).

Glarborg, P., J. A. Miller and R. J. Kee, "Kinetic Modeling and Sensitivity Analysis of Nitrogen Oxide Formation in Well-Stirred Reactors," Combustion and Flame, 65, 177 (1986).

Glass, J.W., and J.O.L. Wendt, "Mechanisms Governing the Destruction of Nitrogenous Species During Fuel-Rich Combustion of Pulverized Coal," Nineteenth Symposium (International) on Combustion, The Combustion Institute, Pittsburgh, PA, 1243 (1982).

Greene, S. B., S. L. Chen, W. D. Clark, M. P. Heap, D. W. Pershing and W. R. Seeker, "Bench-Scale Process Evaluation of Reburning and Sorbent Injection for In-Furnace NO_x/SO_x Reduction," U.S. EPA Report EPA-600/7-85-012, (1985).

Hao, W.M., S.C. Wolfsy, M.B. McElroy, J.M. Beer and M.A. Togan, "Sources of Atmospheric Nitrous Oxide from Combustion," Journal of Geophysical Research, 92, 3098 (1987).

Haynes, B.S., "The Oxidation of Hydrogen Cyanide in Fuel-Rich Flames," Combustion and Flame, 28, 113 (1977a).

Haynes, B.S., D. Iverach, and N.Y. Kirov, "The Behavior of Nitrogenous Species in Fuel Rich Hydrocarbon Flames," Fifteenth Symposium (International) on Combustion, The Combustion Institute, Pittsburgh, PA, 1103 (1975).

Haynes, B.S., "Reactions of Ammonia and Nitric Oxide in the Burnt Gases of Fuel-Rich Hydrocarbon-Air Flames," Combustion and Flame, 28, 81 (1977b).

Hicks, C. R., Fundamental Concepts in the Design of Experiments, 3rd ed., Holt, Rinehart and Winston, New York, NY, (1982).

Hunter, J. S., "Determination of Optimum Operating Conditions by Experimental Methods: Models and Methods," Industrial Quality Control, (Dec-Feb 1958-1959).

JANAF Thermochemical Tables, PB 168 370, Clearinghouse, Springfield, VA, (1983).

Kelly, J. T., R. L. Pam and S. T. Suttman, "Fuel Staging for Pulverized Coal Furnace NO_x Control," Proceedings of the 1982 Joint Symposium on Stationary Combustion NO_x Control, Volume 1, Electric Power Research Institute, Palo Alto, CA, 17-1 (1983).

Knill, K. J. and Morgan, M. E., "The Effect of Process Variables on NO_x and Nitrogen Species Reduction in Coal Fuel Staging," Paper presented at the 1989 Joint Symposium on Stationary Combustion NO_x Control, San Francisco, CA, (March 1989).

Kolb, T., P. Jansohn and W. Leuckel, "Reduction of NO_x Emission in Turbulent Combustion by Fuel-Staging / Effects of Mixing and Stoichiometry in the Reduction Zone," Twenty-second Symposium (International) on Combustion, The Combustion Institute, Pittsburgh, PA, 1193 (1988).

Kramlich, J.C., J.A. Cole, J.M. McCarthy, W.S. Lanier and J.A. McSorley, "Mechanisms of Nitrous Oxide Formation in Coal Flames," Combustion and Flame, 77, 373 (1989).

Kramlich, J.C., R. K. Lyon and W. S. Lanier, "EPA/NOAA/NASA/USDA N₂O Workshop," U.S. EPA Report EPA-68-02-4247, (1987).

Kremer, H., and W. Schulz, "Influence of Temperature on the Formation of NO_x During Pulverized Coal Combustion," Twenty-first Symposium (International) on Combustion, The Combustion Institute, Pittsburgh, PA, 1217 (1986).

La Fond, J. F. and S. L. Chen, "An Investigation to Define the Physical/Chemical Constraints which Limit NO_x Emission Reduction Achievable by Reburning," U.S. DOE Quarterly Report DE-AC22-86PC91025, (1987).

Lanier, W.S., "An Investigation of Chemical and Mixing Phenomena Associated with Reburning Applied to Firetube Package Boilers," Ph.D. Dissertation, University of Virginia, Charlottesville, Virginia, (1984).

Lanier, W.S. and S.B. Robinson, "EPA Workshop on N₂O Emission from Combustion," U.S. EPA Report EPA-600/8-86-035, (1986b).

- Lanier, W. S., J. A. Mulholland and J. T. Beard, "Reburning Thermal and Chemical Processes in a Two-Dimensional Pilot-Scale System," Twenty-first Symposium (International) on Combustion, The Combustion Institute, Pittsburgh, PA, 1171 (1986a).
- Linak, W. P., J. D. Kilgroe, J. A. McSorley, J. O. L. Wendt and J. E. Dunn, "On the Occurrence of Transient Puffs in a Rotary Kiln Incinerator Simulator: I. Prototype Solid Plastic Wastes," JAPCA, 37, 54 (1987).
- Linak, W. P., J.A. Mc Sorley, R.E. Hall, J.V. Ryan, R.K. Srivastava, J.O.L. Wendt and J.B. Mereb, "Nitrous Oxide Emissions from Fossil Fuel Combustion," Journal of Geophysical Research, 95(D6), 7533 (1990).
- Lyon, R.K., "Method for the Reduction of the Concentration of NO in Combustion Effluents Using Ammonia," Exxon Research Company, U.S. Patent 3,900,544, (1975).
- McInnes, R. and M.B. Vanwormer, "Cleaning up NO_x Emissions," Chemical Engineering, 97(9), 131 (1990).
- Mereb, J.B. and J.O.L. Wendt, "Reburning Mechanisms in a Pulverized Coal Combustor," Paper presented at the Twenty-Third Symposium (International) on Combustion, Orleans, France, (July 1990).
- Miller, J.A. and C.T. Bowman, "Mechanism and Modeling of Nitrogen Chemistry in Combustion," Progress in Energy and Combustion Science, 15, 287 (1989).
- Miller, J.A., M.C. Branch, W.J. McLean, D.W. Chandler, M.D. Smooke, and R.J. Kee, "The Conversion of HCN to NO and N₂ in H₂-O₂-HCN-Ar Flames at Low Pressure," Twentieth Symposium (International) on Combustion, The Combustion Institute, Pittsburgh, PA, 673 (1984).
- Miyamae, S., H. Ikebe, K. Makino, K. Suzuki and J. Mogi, "Evaluation of In-Furnace NO_x Reduction," Proceedings of the 1985 Joint Symposium on Stationary Combustion NO_x Control, Volume 1, Acurex Corporation, Mountain View, CA, 24-1 (1986).
- Miyamae, S., T. Kiga, H. Ikebe and K. Suzuki, "Experimental Study on NO_x Destruction Characteristics by Reburning of Pulverized Coal," Paper presented at the 1986 Fall Meeting of Western State Section/ The Combustion Institute, Tucson, AZ, October 1986.
- Morrison, G.F., "Understanding Pulverised Coal Combustion," IEA Coal Research, London, England, (December, 1986).
- Mulholland, J.A., and W.S. Lanier, "Application of Reburning for NO_x Control to a Firetube Package Boiler," Journal of Engineering for Gas Turbines and Power, 107, 739 (1985).

Mulholland, J. A. and R. E. Hall, "The Effect of Fuel Nitrogen in Reburning Application to a Firetube Package Boiler," Proceedings of the 1985 Joint Symposium on Stationary Combustion NO_x Control, Volume 1, Accurex Corporation, Mountain View, CA, 22-1 (1986).

Murakami, N., "Application of the MACT In-Furnace NO_x Removal Process Coupled with a Low-NO_x SGR Burner," Proceedings of the 1985 Joint Symposium of Stationary Combustion NO_x Control, Volume 1, Accurex Corporation, Mountain View, CA, 32-1 (1986).

Muzio, L.J. and J.C. Kramlich, "An Artifact in the Measurement of N₂O from Combustion Sources," Geophysical Research Letters, 15(2), 1369 (1988).

Myerson, A. L., "The Reduction of Nitric Oxide in Simulated Combustion Effluents by Hydrocarbon-Oxygen Mixtures," Fifteenth Symposium (International) on Combustion, The Combustion Institute, Pittsburgh, PA, 1085 (1975).

Myerson, A.L., F.R. Taylor, and B.G. Faunce, "Ignition Limits and Products of the Multistage Flames of Propane-Nitrogen Dioxide Mixtures," Sixth Symposium (International) on Combustion, The Combustion Institute, Pittsburgh, PA, 154 (1957).

Okigami, N., Y. Sekiguchi, Y. Miura, K. Sasaki, and R. Tamaru, "Three-Stage Pulverized Coal Combustion System for In-Furnace NO_x Reduction," Proceedings of the 1985 Joint Symposium of Stationary Combustion NO_x Control, Accurex Corporation, Mountain View, CA, 25-1, (1986).

Overmoe, B. J., J. M. McCarthy, S. L. Chen, W. R. Seeker, G. D. Silcox and D. W. Pershing, "Pilot Scale Evaluation of NO_x Control from Pulverized Coal Combustion by Reburning," Proceedings of the 1985 Joint Symposium on Stationary Combustion NO_x Control, Volume 1, Accurex Corporation, Mountain View, CA, 21-1, (January, 1986).

Pershing, D.W. and J.O.L. Wendt, "Pulverized Coal Combustion: The Influence of Flame Temperature and Coal Composition on Thermal and Fuel NO_x," Sixteenth Symposium (International) on Combustion, The Combustion Institute, Pittsburgh, PA, 389 (1977).

Pohl, J.H., and A.F. Sarofim, "Devolatilization and Oxidation of Coal Nitrogen," Sixteenth Symposium (International) on Combustion, The Combustion Institute, Pittsburgh, PA, 491 (1977).

Radak, L.J., A. Weir, Jr., B.G. Morton, M.N. Manseur, L.L. Smith, and S.E. Kerho, "In-Furnace Control of NO Formation in Gas- and Oil-Fired Utility Boilers," Proceedings of the 1982 Joint Symposium on Stationary Combustion NO_x Control, Volume 1, Electric Power Research Institute, Palo Alto, CA, 18-1 (1983).

Reed, R.D., "Process for the Disposal of Nitrogen Oxide," John Zink Company, U.S. Patent 1,274,637, (1969).

Rees, D.P., L.D. Smoot and P.O. Hedman, "Nitrogen Oxide Formation Inside a Laboratory Pulverized Coal Combustor," Eighteenth Symposium (International) on Combustion, The Combustion Institute, Pittsburgh, PA, 1305 (1981).

Roose, T.R., R.K. Hanson and C.H. Kruger, "A Shock Tube Study of the Decomposition of NO in the presence of NH₃," Eighteenth Symposium (International) on Combustion, The Combustion Institute, Pittsburgh, PA, 853 (1981).

Song, Y.H., J.H. Pohl, J.M. Beer and A.F. Serafim, "Nitric Oxide Formation During Pulverized Coal Combustion," Combustion Science and Technology, 28, 31 (1982b).

Song, Y.H., J.M. Beer, and A.F. Sarofim, "Oxidation and Devolatilization of Nitrogen in Coal Char," Combustion Science and Technology, 28, 177 (1982a).

Song, Y.H., D.W. Blair, V.J. Siminski, and W. Bartok, "Conversion of Fixed Nitrogen to N₂ in Rich Combustion," Eighteenth Symposium (International) on Combustion, The Combustion Institute, Pittsburgh, PA, 53 (1981).

Takahashi, Y., M. Sakai, N. Murakami, T. Sengoku, T. Kawamura, T. Kunimoto, H. Haneda, A. Hirayama, K. Muraishi and S. Kaneko, "Development of Mitsubishi 'MACT' In-Furnace NO_x Removal Process," Paper presented at the U.S.-Japan NO_x Information Exchange, Tokyo, Japan, May 1981.

Takahashi, Y., M. Sakai, T. Kunimoto, S. Ohme, H. Haneda, T. Kawamura, and S. Kaneko, "Development 'MACT' In-Furnace NO_x Removal Process for Steam Generators," Proceedings of the 1982 Joint Symposium on Stationary Combustion NO_x Control, Volume 1, Electric Power Research Institute, Palo Alto, CA, 15-1 (1983).

SPSS-X, 2nd ed., Mc Graw Hill, New York, NY, (1986).

Weiss, R.F., "The Temporal and Spatial Distribution of Tropospheric Nitrous Oxide," Journal of Geophysical Research, 86, 7185 (1981).

Wen, C.Y. and L.T. Fan, Models for Flow Systems and Chemical Reactors, Marcel Dekker, Inc., New York, NY, 68-108 (1975).

Wendt, J.O.L., "Fundamental Coal Combustion Mechanisms and Pollutant Formation in Furnaces," Progress in Energy and Combustion Science, 6, 201 (1980).

Wendt, J.O.L., "Nitrogen Oxide Abatement by Distributed Fuel Addition," Research Proposal submitted to the U.S. Department of Energy, Contract No. DE-AC22-87PC79850, Pittsburgh Energy Technology Center, Pittsburgh, PA, April 1986.

Wendt, J.O.L., D.W. Pershing, J.W. Lee, and J.W. Glass, "Pulverized Coal Combustion: NO_x Formation Mechanisms Under Fuel-Rich and Staged Combustion Conditions," Seventeenth Symposium (International) on Combustion, The Combustion Institute, Pittsburgh, PA, 77 (1979).

Wendt, J.O.L., C.V. Sterling, and M.A. Matovich, "Reduction of Sulfur Trioxide and Nitrogen Oxides by Secondary Fuel Injection," Fourteenth Symposium (International) on Combustion, The Combustion Institute, Pittsburgh, PA, 897 (1973).

Yang, R.J., F.J. Garcia and S.C. Hunter, "Screening and Optimization of In-Furnace NO_x-Reduction Processes for Refinery Process Heater Applications," Proceedings of the 1985 Joint Symposium on Stationary Combustion NO_x Control, Volume 1, Acurex Corporation, Mountain View, CA, 23-1, (January, 1986).

Zeldovich, J., "The Oxidation of Nitrogen in Combustion and Explosions," Acta Physiocochemica, U.R.S.S., 21(4), 577, (1946).

APPENDIX A:

RAW EXPERIMENTAL DATA

NO and N₂O Measurements:

RUN: BL# 1, NO and N₂O vs. SR
 Beulah Lignite coal in kg/h = 0.942

Stoichiometry	% vol			ppmv	
	CO ₂	CO	O ₂	NO	N ₂ O
1.230	15.00	0.50	4.00	625	1.70
1.190	15.70	1.00	3.45	600	0.00
1.160	16.00	1.20	3.00	560	1.00
1.110	16.90	0.80	2.10	545	1.10
1.100	16.80	1.60	2.00	480	0.90
1.060	17.00	2.00	1.25	420	1.20
1.040	17.25	1.15	2.10	445	1.00
0.940	17.90	1.80	0.80	310	0.90
0.840	18.00	2.60	0.30	160	0.40

RUN: UB# 1, NO and N₂O vs. SR
 Utah Bituminous # 2 coal in kg/h = 1.002

Stoichiometry	peak Temp K	% vol			ppmv	
		CO ₂	CO	O ₂	NO	N ₂ O
0.750	1529	16.00	3.75	0.00	265	0.47
0.790	1594	16.45	3.05	0.00	375	0.61
0.840	1605	17.15	2.20	0.00	470	0.69
0.906	1609	17.85	1.03	0.00	690	0.75
0.983	1597	17.85	0.18	0.15	820	0.97
1.044	1600	17.30	0.05	0.90	970	1.50
1.093	1564	16.45	0.05	1.80	985	1.15
1.095	1588	16.45	0.05	1.85	1025	1.22
1.120	1537	15.80	0.04	2.30	920	1.21
1.185	1543	15.30	0.03	3.35	940	0.97
1.250	1518	14.00	0.03	4.25	900	1.03

RUN: UB# 4B, Air Staging
 Utah Bituminous # 2 coal in kg/h = 0.960
 primary stoichiometry = 0.630

PORT	K Temp	% vol			ppmv	
		CO ₂	CO	O ₂	NO	N ₂ O
1	1435	15.50	3.55	0.00	330	0.90
2	1383	15.50	3.30	0.00	360	1.20
3	1333	15.90	2.35	0.40	350	3.40
4	inject 2.050 SCFM air					
5	1204	13.90	0.05	4.30	165	8.70
6	1182	14.00	0.04	3.95	165	8.10
7	1120	14.35	0.04	3.80	155	6.60

RUN: UB# 6A, Air Staging
 Utah Bituminous # 2 coal in kg/h = 1.002
 primary stoichiometry = 0.660

PORT	K Temp	% vol			ppmv	
		CO ₂	CO	O ₂	NO	N ₂ O
2	1398	15.00	4.15	0.00	410	0.55
3	1358	15.15	3.75	0.20	360	0.68
4	inject 1.990 SCFM air					
5	1194	14.90	0.05	3.35	195	5.50
6	1145	14.80	0.05	3.40	195	3.80
7	1073	14.80	0.05	3.50	200	3.50

RUN: UB# 5B, Air Staging
 Utah Bituminous # 2 coal in kg/h = 1.002
 primary stoichiometry = 0.880

PORT	K Temp	% vol			ppmv	
		CO ₂	CO	O ₂	NO	N ₂ O
2	1451	16.60	0.35	1.00	940	0.92
3	1373	16.45	0.50	1.00	865	1.05
4	inject 0.980 SCFM air					
5	1238	14.05	0.04	4.20	555	2.89
6	1228	14.50	0.05	3.75	595	1.71
7	1153	14.35	0.04	3.60	565	1.86

RUN: UB# 3A, Reburning
 Utah Bituminous # 2 coal in kg/h = 0.978
 primary stoichiometry = 1.100

Port	K Temp	% vol			ppmv	
		CO ₂	CO	O ₂	NO	N ₂ O
1	1513	16.00	0.13	1.90	700	1.10
2	1448	16.80	0.09	1.50	830	1.10
3	inject	0.100 SCFM natural gas and 0.000 SCFM N ₂				
4	1373	14.65	2.35	0.60	365	0.60
5	inject	0.835 SCFM air				
6	1223	14.35	0.07	3.15	300	1.80
7	1161	13.75	0.04	3.85	300	3.50

Reburning Tests:

RUN: RS# OA

Utah Bituminous # 2 coal in kg/h = 2.070, primary stoichiometry = 1.35
inject 0.742 SCFM natural gas and 0.000 SCFM N₂ at port 3
inject 5.800 SCFM air at port 6
primary zone: ppmv NO = 895.0, % O₂ = 4.00, % CO₂ = 14.30, % CO = 0.00
exhaust : ppmv NO = 135.0, % O₂ = 4.60, % CO₂ = 11.50, % CO = 0.00
Temp. in K: T₁=1681, T₂=1652, T₃= -- , T₄=1638, T₅=1629, T₆= -- , T₇=1498

RUN: RS# OB

Utah Bituminous # 2 coal in kg/h = 2.070, primary stoichiometry = 1.35
inject 0.742 SCFM natural gas and 0.000 SCFM N₂ at port 5
inject 5.800 SCFM air at port 6
primary zone: ppmv NO = 890.0, % O₂ = 4.15, % CO₂ = 13.90, % CO = 0.00
exhaust : ppmv NO = 285.0, % O₂ = 4.10, % CO₂ = 11.90, % CO = 0.00
Temp. in K: T₁=1661, T₂=1645, T₃=1634, T₄=1618, T₅= -- , T₆= -- , T₇=1507

RUN: RS# 1A

Utah Bituminous # 2 coal in kg/h = 2.100, primary stoichiometry = 1.35
inject 0.828 SCFM natural gas and 0.000 SCFM N₂ at port 3
inject 6.380 SCFM air at port 6
primary zone: ppmv NO = 850.0, % O₂ = 4.90, % CO₂ = 13.45, % CO = 0.00
exhaust : ppmv NO = 120.0, % O₂ = 4.45, % CO₂ = 11.37, % CO = 0.00
Temp. in K: T₁=1681, T₂=1652, T₃= -- , T₄=1638, T₅=1629, T₆= -- , T₇=1498

RUN: RS# 1B

Utah Bituminous # 2 coal in kg/h = 2.100, primary stoichiometry = 1.35
inject 0.828 SCFM natural gas and 0.000 SCFM N₂ at port 5
inject 6.380 SCFM air at port 6
primary zone: ppmv NO = 850.0, % O₂ = 4.90, % CO₂ = 13.45, % CO = 0.00
exhaust : ppmv NO = 250.0, % O₂ = 4.10, % CO₂ = 11.60, % CO = 0.00
Temp. in K: T₁=1661, T₂=1645, T₃=1634, T₄=1618, T₅= -- , T₆= -- , T₇=1507

RUN: RS# 2A

Utah Bituminous # 2 coal in kg/h = 2.070, primary stoichiometry = 1.20
inject 0.393 SCFM natural gas and 0.000 SCFM N₂ at port 3
inject 3.207 SCFM air at port 6
primary zone: ppmv NO = 815.0, % O₂ = 3.20, % CO₂ = 15.15, % CO = 0.00
exhaust : ppmv NO = 230.0, % O₂ = 3.80, % CO₂ = 12.90, % CO = 0.00
Temp. in K: T₁=1705, T₂=1683, T₃= -- , T₄=1671, T₅=1628, T₆= -- , T₇=1456

RUN: RS# 2B

Utah Bituminous # 2 coal in kg/h = 2.070, primary stoichiometry = 1.20
inject 0.393 SCFM natural gas and 0.000 SCFM N₂ at port 5
inject 3.207 SCFM air at port 6
primary zone: ppmv NO = 815.0, % O₂ = 3.20, % CO₂ = 15.15, % CO = 0.00
exhaust : ppmv NO = 410.0, % O₂ = 3.80, % CO₂ = 12.90, % CO = 0.00
Temp. in K: T₁=1709, T₂=1663, T₃=1646, T₄=1626, T₅= -- , T₆= -- , T₇=1512

RUN: RS# 3A

Utah Bituminous # 2 coal in kg/h = 2.070, primary stoichiometry = 1.35
inject 0.828 SCFM natural gas and 0.000 SCFM N₂ at port 3
inject 6.380 SCFM air at port 6
primary zone: ppmv NO = 815.0, % O₂ = 5.50, % CO₂ = 12.80, % CO = 0.00
exhaust : ppmv NO = 110.0, % O₂ = 4.90, % CO₂ = 10.90, % CO = 0.00
Temp. in K: T₁=1604, T₂=1623, T₃= -- , T₄=1621, T₅=1622, T₆= -- , T₇=1469

RUN: RS# 3B

Utah Bituminous # 2 coal in kg/h = 2.070, primary stoichiometry = 1.35
inject 0.828 SCFM natural gas and 0.000 SCFM N₂ at port 5
inject 6.380 SCFM air at port 6
primary zone: ppmv NO = 815.0, % O₂ = 5.50, % CO₂ = 12.80, % CO = 0.00
exhaust : ppmv NO = 220.0, % O₂ = 4.95, % CO₂ = 10.85, % CO = 0.00
Temp. in K: T₁=1574, T₂=1524, T₃=1567, T₄=1576, T₅= -- , T₆= -- , T₇=1533

RUN: RS# 4A

Utah Bituminous # 2 coal in kg/h = 2.100, primary stoichiometry = 1.35
inject 0.368 SCFM natural gas and 0.000 SCFM N₂ at port 3
inject 1.541 SCFM air at port 6
primary zone: ppmv NO = 810.0, % O₂ = 5.50, % CO₂ = 12.90, % CO = 0.00
exhaust : ppmv NO = 420.0, % O₂ = 1.20, % CO₂ = 14.65, % CO = 0.32
Temp. in K: T₁=1613, T₂=1627, T₃= -- , T₄=1646, T₅=1617, T₆= -- , T₇=1455

RUN: RS# 4B

Utah Bituminous # 2 coal in kg/h = 2.100, primary stoichiometry = 1.35
inject 0.368 SCFM natural gas and 0.000 SCFM N₂ at port 5
inject 1.541 SCFM air at port 6
primary zone: ppmv NO = 810.0, % O₂ = 5.50, % CO₂ = 12.90, % CO = 0.00
exhaust : ppmv NO = 515.0, % O₂ = 1.55, % CO₂ = 14.05, % CO = 0.87
Temp. in K: T₁=1561, T₂=1530, T₃=1594, T₄=1542, T₅= -- , T₆= -- , T₇=1504

RUN: RS# 6A

Utah Bituminous # 2 coal in kg/h = 1.980, primary stoichiometry = 1.22
inject 0.398 SCFM natural gas and 0.000 SCFM N₂ at port 3
inject 3.086 SCFM air at port 6
primary zone: ppmv NO = 900.0, % O₂ = 4.10, % CO₂ = 14.20, % CO = 0.00
exhaust : ppmv NO = 245.0, % O₂ = 3.15, % CO₂ = 13.45, % CO = 0.00
Temp. in K: T₁=1635, T₂=1620, T₃= -- , T₄=1621, T₅=1563, T₆= -- , T₇=1385

RUN: RS# 6B

Utah Bituminous # 2 coal in kg/h = 1.980, primary stoichiometry = 1.22
inject 0.398 SCFM natural gas and 0.000 SCFM N₂ at port 5
inject 3.086 SCFM air at port 6
primary zone: ppmv NO = 900.0, % O₂ = 4.10, % CO₂ = 14.20, % CO = 0.00
exhaust : ppmv NO = 440.0, % O₂ = 2.95, % CO₂ = 13.60, % CO = 0.00
Temp. in K: T₁=1601, T₂=1595, T₃=1543, T₄=1560, T₅= -- , T₆= -- , T₇=1497

RUN: RS# 7A

Utah Bituminous # 2 coal in kg/h = 1.980, primary stoichiometry = 1.10
inject 0.466 SCFM natural gas and 0.000 SCFM N₂ at port 3
inject 4.902 SCFM air at port 6
primary zone: ppmv NO = 1035.0, % O₂ = 2.50, % CO₂ = 15.80, % CO = 0.00
exhaust : ppmv NO = 155.0, % O₂ = 4.80, % CO₂ = 12.05, % CO = 0.00
Temp. in K: T₁=1675, T₂=1641, T₃= -- , T₄=1592, T₅=1530, T₆= -- , T₇=1405

RUN: RS# 7B

Utah Bituminous # 2 coal in kg/h = 1.980, primary stoichiometry = 1.10
inject 0.466 SCFM natural gas and 0.000 SCFM N₂ at port 5
inject 4.902 SCFM air at port 6
primary zone: ppmv NO = 1035.0, % O₂ = 2.50, % CO₂ = 15.80, % CO = 0.00
exhaust : ppmv NO = 305.0, % O₂ = 5.00, % CO₂ = 11.90, % CO = 0.00
Temp. in K: T₁=1692, T₂=1674, T₃=1657, T₄=1648, T₅= -- , T₆= -- , T₇=1431

RUN: RS# 8A

Utah Bituminous # 2 coal in kg/h = 1.980, primary stoichiometry = 1.10
inject 0.112 SCFM natural gas and 0.000 SCFM N₂ at port 3
inject 1.184 SCFM air at port 6
primary zone: ppmv NO = 935.0, % O₂ = 2.00, % CO₂ = 16.15, % CO = 0.00
exhaust : ppmv NO = 585.0, % O₂ = 0.95, % CO₂ = 16.00, % CO = 0.10
Temp. in K: T₁=1673, T₂=1639, T₃= -- , T₄=1631, T₅=1568, T₆= -- , T₇=1406

RUN: RS# 8B

Utah Bituminous # 2 coal in kg/h = 1.980, primary stoichiometry = 1.10
inject 0.112 SCFM natural gas and 0.000 SCFM N₂ at port 5
inject 1.184 SCFM air at port 6
primary zone: ppmv NO = 935.0, % O₂ = 2.00, % CO₂ = 16.15, % CO = 0.00
exhaust : ppmv NO = 650.0, % O₂ = 1.20, % CO₂ = 16.35, % CO = 0.13
Temp. in K: T₁=1675, T₂=1647, T₃=1646, T₄=1610, T₅= -- , T₆= -- , T₇=1430

RUN: RS# 9A

Utah Bituminous # 2 coal in kg/h = 1.590, primary stoichiometry = 1.22
inject 0.500 SCFM natural gas and 0.000 SCFM N₂ at port 3
inject 4.381 SCFM air at port 6
primary zone: ppmv NO = 805.0, % O₂ = 3.75, % CO₂ = 14.35, % CO = 0.00
exhaust : ppmv NO = 130.0, % O₂ = 5.40, % CO₂ = 10.85, % CO = 0.00
Temp. in K: T₁=1563, T₂=1541, T₃= -- , T₄=1526, T₅=1515, T₆= -- , T₇=1358

RUN: RS# 9B

Utah Bituminous # 2 coal in kg/h = 1.590, primary stoichiometry = 1.22
inject 0.500 SCFM natural gas and 0.000 SCFM N₂ at port 5
inject 4.381 SCFM air at port 6
primary zone: ppmv NO = 805.0, % O₂ = 3.75, % CO₂ = 14.35, % CO = 0.00
exhaust : ppmv NO = 235.0, % O₂ = 5.15, % CO₂ = 11.10, % CO = 0.00
Temp. in K: T₁=1575, T₂=1569, T₃=1547, T₄=1531, T₅= -- , T₆= -- , T₇=1411

RUN: RS#10A

Utah Bituminous # 2 coal in kg/h = 1.590, primary stoichiometry = 1.22
inject 0.184 SCFM natural gas and 0.000 SCFM N₂ at port 3
inject 1.059 SCFM air at port 6
primary zone: ppmv NO = 810.0, % O₂ = 4.30, % CO₂ = 13.90, % CO = 0.00
exhaust : ppmv NO = 385.0, % O₂ = 1.25, % CO₂ = 15.10, % CO = 0.20
Temp. in K: T₁=1574, T₂=1569, T₃= -- , T₄=1568, T₅=1528, T₆= -- , T₇=1422

RUN: RS#10B

Utah Bituminous # 2 coal in kg/h = 1.590, primary stoichiometry = 1.22
inject 0.184 SCFM natural gas and 0.000 SCFM N₂ at port 5
inject 1.059 SCFM air at port 6
primary zone: ppmv NO = 810.0, % O₂ = 4.30, % CO₂ = 13.90, % CO = 0.00
exhaust : ppmv NO = 500.0, % O₂ = 1.65, % CO₂ = 14.65, % CO = 0.45
Temp. in K: T₁=1584, T₂=1570, T₃=1541, T₄=1521, T₅= -- , T₆= -- , T₇=1462

RUN: RS#11A

Utah Bituminous # 2 coal in kg/h = 1.590, primary stoichiometry = 1.22
inject 0.319 SCFM natural gas and 0.000 SCFM N₂ at port 3
inject 2.478 SCFM air at port 6
primary zone: ppmv NO = 850.0, % O₂ = 4.50, % CO₂ = 13.80, % CO = 0.00
exhaust : ppmv NO = 230.0, % O₂ = 2.90, % CO₂ = 13.30, % CO = 0.00
Temp. in K: T₁=1575, T₂=1562, T₃= -- , T₄=1578, T₅=1572, T₆= -- , T₇=1449

RUN: RS#11B

Utah Bituminous # 2 coal in kg/h = 1.590, primary stoichiometry = 1.22
inject 0.319 SCFM natural gas and 0.000 SCFM N₂ at port 5
inject 2.478 SCFM air at port 6
primary zone: ppmv NO = 850.0, % O₂ = 4.50, % CO₂ = 13.80, % CO = 0.00
exhaust : ppmv NO = 380.0, % O₂ = 3.95, % CO₂ = 12.45, % CO = 0.00
Temp. in K: T₁=1575, T₂=1563, T₃=1553, T₄=1533, T₅= -- , T₆= -- , T₇=1449

RUN: RS#12A

Utah Bituminous # 2 coal in kg/h = 1.554, primary stoichiometry = 1.22
inject 0.180 SCFM natural gas and 0.000 SCFM N₂ at port 3
inject 1.035 SCFM air at port 6
primary zone: ppmv NO = 835.0, % O₂ = 4.70, % CO₂ = 13.60, % CO = 0.00
exhaust : ppmv NO = 430.0, % O₂ = 0.90, % CO₂ = 15.65, % CO = 0.12
Temp. in K: T₁=1477, T₂=1445, T₃= -- , T₄=1460, T₅=1413, T₆= -- , T₇=1256

RUN: RS#12B

Utah Bituminous # 2 coal in kg/h = 1.554, primary stoichiometry = 1.22
inject 0.180 SCFM natural gas and 0.000 SCFM N₂ at port 5
inject 1.035 SCFM air at port 6
primary zone: ppmv NO = 835.0, % O₂ = 4.70, % CO₂ = 13.60, % CO = 0.00
exhaust : ppmv NO = 505.0, % O₂ = 1.00, % CO₂ = 15.45, % CO = 0.40
Temp. in K: T₁=1476, T₂=1440, T₃=1429, T₄=1387, T₅= -- , T₆= -- , T₇=1313

RUN: RS#13A

Utah Bituminous # 2 coal in kg/h = 1.554, primary stoichiometry = 1.22
inject 0.312 SCFM natural gas and 0.000 SCFM N₂ at port 3
inject 2.422 SCFM air at port 6
primary zone: ppmv NO = 850.0, % O₂ = 4.50, % CO₂ = 13.80, % CO = 0.00
exhaust : ppmv NO = 220.0, % O₂ = 2.35, % CO₂ = 14.00, % CO = 0.00
Temp. in K: T₁=1522, T₂=1504, T₃= -- , T₄=1485, T₅=1451, T₆= -- , T₇=1275

RUN: RS#13B

Utah Bituminous # 2 coal in kg/h = 1.554, primary stoichiometry = 1.22
inject 0.312 SCFM natural gas and 0.000 SCFM N₂ at port 5
inject 2.422 SCFM air at port 6
primary zone: ppmv NO = 850.0, % O₂ = 4.50, % CO₂ = 13.80, % CO = 0.00
exhaust : ppmv NO = 375.0, % O₂ = 1.45, % CO₂ = 14.65, % CO = 0.12
Temp. in K: T₁=1515, T₂=1490, T₃=1474, T₄=1451, T₅= -- , T₆= -- , T₇=1317

RUN: RS#14A

Utah Bituminous # 2 coal in kg/h = 1.554, primary stoichiometry = 1.35
inject 0.417 SCFM natural gas and 0.000 SCFM N₂ at port 3
inject 2.670 SCFM air at port 6
primary zone: ppmv NO = 775.0, % O₂ = 5.95, % CO₂ = 12.60, % CO = 0.00
exhaust : ppmv NO = 235.0, % O₂ = 2.85, % CO₂ = 13.30, % CO = 0.00
Temp. in K: T₁=1481, T₂=1468, T₃= -- , T₄=1532, T₅=1511, T₆= -- , T₇=1334

RUN: RS#14B

Utah Bituminous # 2 coal in kg/h = 1.554, primary stoichiometry = 1.35
inject 0.417 SCFM natural gas and 0.000 SCFM N₂ at port 5
inject 2.670 SCFM air at port 6
primary zone: ppmv NO = 775.0, % O₂ = 5.95, % CO₂ = 12.60, % CO = 0.00
exhaust : ppmv NO = 350.0, % O₂ = 2.30, % CO₂ = 13.60, % CO = 0.00
Temp. in K: T₁=1473, T₂=1469, T₃=1442, T₄=1450, T₅= -- , T₆= -- , T₇=1402

RUN: RS#15A

Utah Bituminous # 2 coal in kg/h = 1.554, primary stoichiometry = 1.10
inject 0.207 SCFM natural gas and 0.000 SCFM N₂ at port 3
inject 2.175 SCFM air at port 6
primary zone: ppmv NO = 870.0, % O₂ = 2.50, % CO₂ = 15.80, % CO = 0.00
exhaust : ppmv NO = 185.0, % O₂ = 1.45, % CO₂ = 15.45, % CO = 0.00
Temp. in K: T₁=1549, T₂=1518, T₃= -- , T₄=1492, T₅=1418, T₆= -- , T₇=1301

RUN: RS#15B

Utah Bituminous # 2 coal in kg/h = 1.554, primary stoichiometry = 1.10
inject 0.207 SCFM natural gas and 0.000 SCFM N₂ at port 5
inject 2.175 SCFM air at port 6
primary zone: ppmv NO = 870.0, % O₂ = 2.50, % CO₂ = 15.80, % CO = 0.00
exhaust : ppmv NO = 440.0, % O₂ = 1.75, % CO₂ = 15.15, % CO = 0.00
Temp. in K: T₁=1563, T₂=1555, T₃=1508, T₄=1522, T₅= -- , T₆= -- , T₇=1329

RUN: RS#16A

Utah Bituminous # 2 coal in kg/h = 1.074, primary stoichiometry = 1.35
inject 0.423 SCFM natural gas and 0.000 SCFM N₂ at port 3
inject 3.264 SCFM air at port 6
primary zone: ppmv NO = 720.0, % O₂ = 5.55, % CO₂ = 12.80, % CO = 0.00
exhaust : ppmv NO = 170.0, % O₂ = 2.95, % CO₂ = 12.45, % CO = 0.00
Temp. in K: T₁=1421, T₂=1414, T₃= -- , T₄=1407, T₅=1347, T₆= -- , T₇=1247

RUN: RS#16B

Utah Bituminous # 2 coal in kg/h = 1.074, primary stoichiometry = 1.35
inject 0.423 SCFM natural gas and 0.000 SCFM N₂ at port 5
inject 3.264 SCFM air at port 6
primary zone: ppmv NO = 720.0, % O₂ = 5.55, % CO₂ = 12.80, % CO = 0.00
exhaust : ppmv NO = 250.0, % O₂ = 3.50, % CO₂ = 12.10, % CO = 0.00
Temp. in K: T₁=1412, T₂=1402, T₃=1368, T₄=1337, T₅= -- , T₆= -- , T₇=1283

RUN: RS#17A

Utah Bituminous # 2 coal in kg/h = 1.074, primary stoichiometry = 1.35
inject 0.188 SCFM natural gas and 0.000 SCFM N₂ at port 3
inject 0.789 SCFM air at port 6
primary zone: ppmv NO = 750.0, % O₂ = 4.95, % CO₂ = 13.35, % CO = 0.00
exhaust : ppmv NO = 255.0, % O₂ = 0.50, % CO₂ = 15.15, % CO = 0.45
Temp. in K: T₁=1439, T₂=1432, T₃= -- , T₄=1422, T₅=1355, T₆= -- , T₇=1222

RUN: RS#17B

Utah Bituminous # 2 coal in kg/h = 1.074, primary stoichiometry = 1.35
inject 0.188 SCFM natural gas and 0.000 SCFM N₂ at port 5
inject 0.789 SCFM air at port 6
primary zone: ppmv NO = 750.0, % O₂ = 4.95, % CO₂ = 13.35, % CO = 0.00
exhaust : ppmv NO = 395.0, % O₂ = 1.25, % CO₂ = 14.65, % CO = 0.55
Temp. in K: T₁=1444, T₂=1415, T₃=1389, T₄=1348, T₅= -- , T₆= -- , T₇=1285

RUN: RS#18A
Utah Bituminous # 2 coal in kg/h = 1.164, primary stoichiometry = 1.35
inject 0.459 SCFM natural gas and 0.000 SCFM N₂ at port 3
inject 3.536 SCFM air at port 6
primary zone: ppmv NO = 795.0, % O₂ = 5.55, % CO₂ = 12.80, % CO = 0.00
exhaust : ppmv NO = 165.0, % O₂ = 3.90, % CO₂ = 11.90, % CO = 0.00
Temp. in K: T₁=1437, T₂=1428, T₃= -- , T₄=1422, T₅=1390, T₆= -- , T₇=1244

RUN: RS#18B
Utah Bituminous # 2 coal in kg/h = 1.164, primary stoichiometry = 1.35
inject 0.459 SCFM natural gas and 0.000 SCFM N₂ at port 5
inject 3.536 SCFM air at port 6
primary zone: ppmv NO = 795.0, % O₂ = 5.55, % CO₂ = 12.80, % CO = 0.00
exhaust : ppmv NO = 245.0, % O₂ = 3.80, % CO₂ = 11.90, % CO = 0.00
Temp. in K: T₁=1433, T₂=1414, T₃=1401, T₄=1382, T₅= -- , T₆= -- , T₇=1270

RUN: RS#19A
Utah Bituminous # 2 coal in kg/h = 1.164, primary stoichiometry = 1.35
inject 0.204 SCFM natural gas and 0.000 SCFM N₂ at port 3
inject 0.854 SCFM air at port 6
primary zone: ppmv NO = 820.0, % O₂ = 5.50, % CO₂ = 13.00, % CO = 0.00
exhaust : ppmv NO = 335.0, % O₂ = 1.00, % CO₂ = 14.90, % CO = 0.30
Temp. in K: T₁=1442, T₂=1422, T₃= -- , T₄=1435, T₅=1388, T₆= -- , T₇=1224

RUN: RS#19B
Utah Bituminous # 2 coal in kg/h = 1.164, primary stoichiometry = 1.35
inject 0.204 SCFM natural gas and 0.000 SCFM N₂ at port 5
inject 0.854 SCFM air at port 6
primary zone: ppmv NO = 820.0, % O₂ = 5.50, % CO₂ = 13.00, % CO = 0.00
exhaust : ppmv NO = 380.0, % O₂ = 0.80, % CO₂ = 14.80, % CO = 0.65
Temp. in K: T₁=1424, T₂=1428, T₃=1391, T₄=1358, T₅= -- , T₆= -- , T₇=1299

RUN: RS#20A
Utah Bituminous # 2 coal in kg/h = 1.164, primary stoichiometry = 1.22
inject 0.234 SCFM natural gas and 0.000 SCFM N₂ at port 3
inject 1.814 SCFM air at port 6
primary zone: ppmv NO = 900.0, % O₂ = 3.65, % CO₂ = 14.50, % CO = 0.05
exhaust : ppmv NO = 190.0, % O₂ = 1.00, % CO₂ = 14.80, % CO = 0.25
Temp. in K: T₁=1493, T₂=1454, T₃= -- , T₄=1431, T₅=1370, T₆= -- , T₇=1244

RUN: RS#20B
Utah Bituminous # 2 coal in kg/h = 1.164, primary stoichiometry = 1.22
inject 0.234 SCFM natural gas and 0.000 SCFM N₂ at port 5
inject 1.814 SCFM air at port 6
primary zone: ppmv NO = 900.0, % O₂ = 3.65, % CO₂ = 14.50, % CO = 0.05
exhaust : ppmv NO = 370.0, % O₂ = 1.65, % CO₂ = 14.35, % CO = 0.05
Temp. in K: T₁=1448, T₂=1420, T₃=1392, T₄=1350, T₅= -- , T₆= -- , T₇=1310

RUN: RS#21A
Utah Bituminous # 2 coal in kg/h = 1.170, primary stoichiometry = 1.10
inject 0.276 SCFM natural gas and 0.000 SCFM N₂ at port 3
inject 2.903 SCFM air at port 6
primary zone: ppmv NO = 920.0, % O₂ = 2.25, % CO₂ = 15.60, % CO = 0.13
exhaust : ppmv NO = 190.0, % O₂ = 2.95, % CO₂ = 13.00, % CO = 0.00
Temp. in K: T₁=1504, T₂=1471, T₃= -- , T₄=1406, T₅=1343, T₆= -- , T₇=1213

RUN: RS#21B

Utah Bituminous # 2 coal in kg/h = 1.170, primary stoichiometry = 1.10
inject 0.276 SCFM natural gas and 0.000 SCFM N₂ at port 5
inject 2.903 SCFM air at port 6
primary zone: ppmv NO = 920.0, % O₂ = 2.25, % CO₂ = 15.60, % CO = 0.13
exhaust : ppmv NO = 260.0, % O₂ = 2.85, % CO₂ = 13.10, % CO = 0.00
Temp. in K: T₁=1498, T₂=1447, T₃=1420, T₄=1375, T₅= -- , T₆= -- , T₇=1254

RUN: RS#22A

Utah Bituminous # 2 coal in kg/h = 1.170, primary stoichiometry = 1.10
inject 0.067 SCFM natural gas and 0.000 SCFM N₂ at port 3
inject 0.701 SCFM air at port 6
primary zone: ppmv NO = 915.0, % O₂ = 2.15, % CO₂ = 15.70, % CO = 0.13
exhaust : ppmv NO = 450.0, % O₂ = 1.70, % CO₂ = 15.40, % CO = 0.13
Temp. in K: T₁=1533, T₂=1473, T₃= -- , T₄=1397, T₅=1305, T₆= -- , T₇=1113

RUN: RS#22B

Utah Bituminous # 2 coal in kg/h = 1.170, primary stoichiometry = 1.10
inject 0.067 SCFM natural gas and 0.000 SCFM N₂ at port 5
inject 0.701 SCFM air at port 6
primary zone: ppmv NO = 915.0, % O₂ = 2.15, % CO₂ = 15.70, % CO = 0.13
exhaust : ppmv NO = 490.0, % O₂ = 1.70, % CO₂ = 15.30, % CO = 0.14
Temp. in K: T₁=1528, T₂=1482, T₃=1452, T₄=1400, T₅= -- , T₆= -- , T₇=1140

RUN: UB# 3A

Utah Bituminous # 2 coal in kg/h = 0.978, primary stoichiometry = 1.10
inject 0.100 SCFM natural gas and 0.000 SCFM N₂ at port 3
inject 0.835 SCFM air at port 5
primary zone: ppmv NO = 830.0, % O₂ = 1.50, % CO₂ = 16.80, % CO = 0.09
exhaust : ppmv NO = 300.0, % O₂ = 3.85, % CO₂ = 13.75, % CO = 0.04
Temp. in K: T₁=1513, T₂=1448, T₃= -- , T₄=1373, T₅= -- , T₆=1223, T₇=1161

RUN: MR# 9

Utah Bituminous # 2 coal in kg/h = 1.437, primary stoichiometry = 1.19
inject 0.313 SCFM natural gas and 0.000 SCFM N₂ at port 3
inject 2.718 SCFM air at port 6
primary zone: ppmv NO = 870.0, % O₂ = 3.75, % CO₂ = 14.25, % CO = 0.05
exhaust : ppmv NO = 170.0, % O₂ = 2.10, % CO₂ = 13.90, % CO = 0.05
Temp. in K: T₁=1567, T₂=1538, T₃= -- , T₄=1509, T₅=1473, T₆= -- , T₇=1343

RUN: MR#10

Utah Bituminous # 2 coal in kg/h = 1.437, primary stoichiometry = 1.19
inject 0.313 SCFM natural gas and 0.000 SCFM N₂ at port 4
inject 2.718 SCFM air at port 6
primary zone: ppmv NO = 870.0, % O₂ = 3.75, % CO₂ = 14.25, % CO = 0.05
exhaust : ppmv NO = 195.0, % O₂ = 2.10, % CO₂ = 13.90, % CO = 0.05
Temp. in K: T₁=1571, T₂=1536, T₃=1493, T₄= -- , T₅=1498, T₆= -- , T₇=1397

RUN: MR#11

Utah Bituminous # 2 coal in kg/h = 1.437, primary stoichiometry = 1.19
inject 0.313 SCFM natural gas and 0.000 SCFM N₂ at port 5
inject 2.718 SCFM air at port 6
primary zone: ppmv NO = 870.0, % O₂ = 3.75, % CO₂ = 14.25, % CO = 0.05
exhaust : ppmv NO = 350.0, % O₂ = 2.00, % CO₂ = 14.05, % CO = 0.05
Temp. in K: T₁=1562, T₂=1528, T₃=1480, T₄=1457, T₅= -- , T₆= -- , T₇=1415

RUN: MR#12

Utah Bituminous # 2 coal in kg/h = 1.449, primary stoichiometry = 1.19
inject 0.093 SCFM natural gas and 0.000 SCFM N₂ at port 3
inject 0.367 SCFM air at port 6
primary zone: ppmv NO = 935.0, % O₂ = 3.65, % CO₂ = 14.50, % CO = 0.10
exhaust : ppmv NO = 680.0, % O₂ = 1.55, % CO₂ = 15.65, % CO = 0.10
Temp. in K: T₁=1508, T₂=1472, T₃= -- , T₄=1412, T₅=1324, T₆= -- , T₇=1086

RUN: MR#13

Utah Bituminous # 2 coal in kg/h = 1.449, primary stoichiometry = 1.19
inject 0.093 SCFM natural gas and 0.000 SCFM N₂ at port 5
inject 0.367 SCFM air at port 6
primary zone: ppmv NO = 935.0, % O₂ = 3.65, % CO₂ = 14.50, % CO = 0.10
exhaust : ppmv NO = 540.0, % O₂ = 1.20, % CO₂ = 15.15, % CO = 0.95
Temp. in K: T₁=1491, T₂=1423, T₃=1333, T₄=1374, T₅= -- , T₆= -- , T₇=1064

RUN: MR#14

Utah Bituminous # 2 coal in kg/h = 1.449, primary stoichiometry = 1.19
inject 0.131 SCFM natural gas and 0.000 SCFM N₂ at port 5
inject 0.769 SCFM air at port 6
primary zone: ppmv NO = 950.0, % O₂ = 3.70, % CO₂ = 14.50, % CO = 0.07
exhaust : ppmv NO = 725.0, % O₂ = 1.45, % CO₂ = 15.75, % CO = 0.12
Temp. in K: T₁=1491, T₂=1463, T₃=1353, T₄=1353, T₅= -- , T₆= -- , T₇=1064

RUN: MR#15

Utah Bituminous # 2 coal in kg/h = 1.449, primary stoichiometry = 1.19
inject 0.173 SCFM natural gas and 0.000 SCFM N₂ at port 3
inject 1.214 SCFM air at port 6
primary zone: ppmv NO = 945.0, % O₂ = 3.80, % CO₂ = 14.55, % CO = 0.07
exhaust : ppmv NO = 355.0, % O₂ = 1.00, % CO₂ = 15.70, % CO = 0.09
Temp. in K: T₁=1543, T₂=1476, T₃= -- , T₄=1438, T₅=1420, T₆= -- , T₇=1182

RUN: MR#16

Utah Bituminous # 2 coal in kg/h = 1.449, primary stoichiometry = 1.19
inject 0.173 SCFM natural gas and 0.000 SCFM N₂ at port 5
inject 1.214 SCFM air at port 6
primary zone: ppmv NO = 945.0, % O₂ = 3.80, % CO₂ = 14.55, % CO = 0.07
exhaust : ppmv NO = 540.0, % O₂ = 0.70, % CO₂ = 15.65, % CO = 0.35
Temp. in K: T₁=1520, T₂=1445, T₃=1374, T₄=1328, T₅= -- , T₆= -- , T₇=1242

RUN: MR#17

Utah Bituminous # 2 coal in kg/h = 1.449, primary stoichiometry = 1.19
inject 0.220 SCFM natural gas and 0.000 SCFM N₂ at port 3
inject 1.709 SCFM air at port 6
primary zone: ppmv NO = 940.0, % O₂ = 3.75, % CO₂ = 14.80, % CO = 0.07
exhaust : ppmv NO = 265.0, % O₂ = 1.20, % CO₂ = 15.30, % CO = 0.08
Temp. in K: T₁=1549, T₂=1497, T₃= -- , T₄=1479, T₅=1404, T₆= -- , T₇=1226

RUN: MR#18

Utah Bituminous # 2 coal in kg/h = 1.449, primary stoichiometry = 1.19
inject 0.220 SCFM natural gas and 0.000 SCFM N₂ at port 5
inject 1.709 SCFM air at port 6
primary zone: ppmv NO = 940.0, % O₂ = 3.75, % CO₂ = 14.80, % CO = 0.07
exhaust : ppmv NO = 470.0, % O₂ = 0.90, % CO₂ = 15.45, % CO = 0.25
Temp. in K: T₁=1533, T₂=1495, T₃=1424, T₄=1410, T₅= -- , T₆= -- , T₇=1252

RUN: MR#19

Utah Bituminous # 2 coal in kg/h = 1.449, primary stoichiometry = 1.19
inject 0.273 SCFM natural gas and 0.000 SCFM N₂ at port 3
inject 2.261 SCFM air at port 6
primary zone: ppmv NO = 930.0, % O₂ = 3.80, % CO₂ = 14.55, % CO = 0.07
exhaust : ppmv NO = 210.0, % O₂ = 1.80, % CO₂ = 14.50, % CO = 0.07
Temp. in K: T₁=1543, T₂=1498, T₃= -- , T₄=1488, T₅=1443, T₆= -- , T₇=1312

RUN: MR#20

Utah Bituminous # 2 coal in kg/h = 1.449, primary stoichiometry = 1.19
inject 0.273 SCFM natural gas and 0.000 SCFM N₂ at port 5
inject 2.261 SCFM air at port 6
primary zone: ppmv NO = 930.0, % O₂ = 3.80, % CO₂ = 14.55, % CO = 0.07
exhaust : ppmv NO = 425.0, % O₂ = 1.50, % CO₂ = 14.80, % CO = 0.07
Temp. in K: T₁=1534, T₂=1491, T₃=1451, T₄=1416, T₅= -- , T₆= -- , T₇=1312

RUN: MR#21

Utah Bituminous # 2 coal in kg/h = 1.449, primary stoichiometry = 1.19
inject 0.320 SCFM natural gas and 0.000 SCFM N₂ at port 3
inject 2.757 SCFM air at port 6
primary zone: ppmv NO = 940.0, % O₂ = 3.85, % CO₂ = 14.50, % CO = 0.07
exhaust : ppmv NO = 175.0, % O₂ = 1.95, % CO₂ = 14.20, % CO = 0.07
Temp. in K: T₁=1559, T₂=1504, T₃= -- , T₄=1491, T₅=1449, T₆= -- , T₇=1298

RUN: MR#22

Utah Bituminous # 2 coal in kg/h = 1.449, primary stoichiometry = 1.19
inject 0.320 SCFM natural gas and 0.000 SCFM N₂ at port 4
inject 2.757 SCFM air at port 6
primary zone: ppmv NO = 940.0, % O₂ = 3.85, % CO₂ = 14.50, % CO = 0.07
exhaust : ppmv NO = 225.0, % O₂ = 1.80, % CO₂ = 14.35, % CO = 0.07
Temp. in K: T₁=1552, T₂=1515, T₃=1476, T₄= -- , T₅=1473, T₆= -- , T₇=1337

RUN: MR#23

Utah Bituminous # 2 coal in kg/h = 1.449, primary stoichiometry = 1.19
inject 0.320 SCFM natural gas and 0.000 SCFM N₂ at port 5
inject 2.757 SCFM air at port 6
primary zone: ppmv NO = 940.0, % O₂ = 3.85, % CO₂ = 14.50, % CO = 0.07
exhaust : ppmv NO = 370.0, % O₂ = 1.35, % CO₂ = 14.55, % CO = 0.09
Temp. in K: T₁=1533, T₂=1497, T₃=1470, T₄=1409, T₅= -- , T₆= -- , T₇=1328

RUN: MR#27

Utah Bituminous # 2 coal in kg/h = 1.437, primary stoichiometry = 1.19
inject 0.317 SCFM natural gas and 0.000 SCFM N₂ at port 3
inject 2.730 SCFM air at port 6
primary zone: ppmv NO = 1000.0, % O₂ = 3.80, % CO₂ = 14.35, % CO = 0.07
exhaust : ppmv NO = 200.0, % O₂ = 2.15, % CO₂ = 13.90, % CO = 0.07
Temp. in K: T₁=1567, T₂=1538, T₃= -- , T₄=1509, T₅=1473, T₆= -- , T₇=1343

RUN: MR#28

Utah Bituminous # 2 coal in kg/h = 1.437, primary stoichiometry = 1.19
inject 0.317 SCFM natural gas and 0.000 SCFM N₂ at port 3
inject 2.730 SCFM air at port 5
primary zone: ppmv NO = 1000.0, % O₂ = 3.80, % CO₂ = 14.35, % CO = 0.07
exhaust : ppmv NO = 290.0, % O₂ = 2.15, % CO₂ = 13.90, % CO = 0.07
Temp. in K: T₁=1567, T₂=1538, T₃= -- , T₄=1503, T₅= -- , T₆=1395, T₇=1348

RUN: MR#29

Utah Bituminous # 2 coal in kg/h = 1.437, primary stoichiometry = 1.19
inject 0.317 SCFM natural gas and 0.000 SCFM N₂ at port 4 .
inject 2.730 SCFM air at port 6
primary zone: ppmv NO = 1000.0, % O₂ = 3.80, % CO₂ = 14.35, % CO = 0.07
exhaust : ppmv NO = 215.0, % O₂ = 2.10, % CO₂ = 13.45, % CO = 0.07
Temp. in K: T₁=1571, T₂=1536, T₃=1493, T₄= -- , T₅=1498, T₆= -- , T₇=1397

RUN: MR#30

Utah Bituminous # 2 coal in kg/h = 1.437, primary stoichiometry = 1.19
inject 0.317 SCFM natural gas and 0.000 SCFM N₂ at port 5
inject 2.730 SCFM air at port 6
primary zone: ppmv NO = 1020.0, % O₂ = 3.60, % CO₂ = 14.50, % CO = 0.07
exhaust : ppmv NO = 405.0, % O₂ = 2.10, % CO₂ = 13.90, % CO = 0.07
Temp. in K: T₁=1562, T₂=1528, T₃=1480, T₄=1457, T₅= -- , T₆= -- , T₇=1415

RUN: RV# 1

Utah Bituminous # 2 coal in kg/h = 1.948, primary stoichiometry = 1.07
inject 0.065 SCFM natural gas and 0.000 SCFM N₂ at port 5
inject 0.927 SCFM air at port 6
primary zone: ppmv NO = 925.0, % O₂ = 1.90, % CO₂ = 15.95, % CO = 0.12
exhaust : ppmv NO = 700.0, % O₂ = 1.85, % CO₂ = 15.45, % CO = 0.07
Temp. in K: T₁=1633, T₂=1588, T₃=1543, T₄=1538, T₅= -- , T₆= -- , T₇=1256

RUN: RV# 2

Utah Bituminous # 2 coal in kg/h = 1.948, primary stoichiometry = 1.07
inject 0.116 SCFM natural gas and 0.000 SCFM N₂ at port 5
inject 1.464 SCFM air at port 6
primary zone: ppmv NO = 925.0, % O₂ = 1.90, % CO₂ = 15.95, % CO = 0.12
exhaust : ppmv NO = 615.0, % O₂ = 2.10, % CO₂ = 15.10, % CO = 0.05
Temp. in K: T₁=1638, T₂=1596, T₃=1551, T₄=1521, T₅= -- , T₆= -- , T₇=1321

RUN: RV# 3

Utah Bituminous # 2 coal in kg/h = 1.948, primary stoichiometry = 1.07
inject 0.116 SCFM natural gas and 0.000 SCFM N₂ at port 3
inject 1.464 SCFM air at port 6
primary zone: ppmv NO = 925.0, % O₂ = 1.90, % CO₂ = 15.95, % CO = 0.12
exhaust : ppmv NO = 515.0, % O₂ = 2.95, % CO₂ = 14.50, % CO = 0.05
Temp. in K: T₁=1638, T₂=1589, T₃= -- , T₄=1571, T₅=1493, T₆= -- , T₇=1276

RUN: RV# 4

Utah Bituminous # 2 coal in kg/h = 1.948, primary stoichiometry = 1.07
inject 0.116 SCFM natural gas and 0.000 SCFM N₂ at port 3
inject 1.464 SCFM air at port 5
primary zone: ppmv NO = 925.0, % O₂ = 1.90, % CO₂ = 15.95, % CO = 0.12
exhaust : ppmv NO = 545.0, % O₂ = 2.60, % CO₂ = 14.80, % CO = 0.05
Temp. in K: T₁=1638, T₂=1589, T₃= -- , T₄=1586, T₅= -- , T₆=1376, T₇=1282

RUN: RV# 5

Utah Bituminous # 2 coal in kg/h = 1.948, primary stoichiometry = 1.07
inject 0.116 SCFM natural gas and 0.000 SCFM N₂ at port 4
inject 1.464 SCFM air at port 5
primary zone: ppmv NO = 925.0, % O₂ = 1.90, % CO₂ = 15.95, % CO = 0.12
exhaust : ppmv NO = 545.0, % O₂ = 2.60, % CO₂ = 14.80, % CO = 0.05
Temp. in K: T₁=1641, T₂=1605, T₃=1560, T₄= -- , T₅= -- , T₆=1375, T₇=1275

RUN: RV# 6

Utah Bituminous # 2 coal in kg/h = 1.948, primary stoichiometry = 1.07
inject 0.116 SCFM natural gas and 0.000 SCFM N₂ at port 4
inject 1.464 SCFM air at port 6
primary zone: ppmv NO = 925.0, % O₂ = 1.90, % CO₂ = 15.95, % CO = 0.12
exhaust : ppmv NO = 505.0, % O₂ = 3.00, % CO₂ = 14.50, % CO = 0.05
Temp. in K: T₁=1641, T₂=1605, T₃=1560, T₄= -- , T₅=1526, T₆= -- , T₇=1273

RUN: RV# 7

Utah Bituminous # 2 coal in kg/h = 1.948, primary stoichiometry = 1.07
inject 0.173 SCFM natural gas and 0.000 SCFM N₂ at port 4
inject 2.060 SCFM air at port 6
primary zone: ppmv NO = 885.0, % O₂ = 2.15, % CO₂ = 16.00, % CO = 0.05
exhaust : ppmv NO = 350.0, % O₂ = 2.85, % CO₂ = 14.20, % CO = 0.05
Temp. in K: T₁=1660, T₂=1602, T₃=1577, T₄= -- , T₅=1528, T₆= -- , T₇=1337

RUN: RV# 8

Utah Bituminous # 2 coal in kg/h = 1.948, primary stoichiometry = 1.07
inject 0.173 SCFM natural gas and 0.000 SCFM N₂ at port 3
inject 2.060 SCFM air at port 6
primary zone: ppmv NO = 885.0, % O₂ = 2.15, % CO₂ = 16.00, % CO = 0.05
exhaust : ppmv NO = 320.0, % O₂ = 2.60, % CO₂ = 14.50, % CO = 0.07
Temp. in K: T₁=1647, T₂=1601, T₃= -- , T₄=1576, T₅=1503, T₆= -- , T₇=1317

RUN: RV# 9

Utah Bituminous # 2 coal in kg/h = 1.948, primary stoichiometry = 1.07
inject 0.173 SCFM natural gas and 0.000 SCFM N₂ at port 5
inject 2.060 SCFM air at port 6
primary zone: ppmv NO = 885.0, % O₂ = 2.15, % CO₂ = 16.00, % CO = 0.05
exhaust : ppmv NO = 500.0, % O₂ = 2.50, % CO₂ = 14.70, % CO = 0.10
Temp. in K: T₁=1663, T₂=1627, T₃=1574, T₄=1549, T₅= -- , T₆= -- , T₇=1363

RUN: RV#10

Utah Bituminous # 2 coal in kg/h = 1.948, primary stoichiometry = 1.07
inject 0.449 SCFM natural gas and 0.000 SCFM N₂ at port 4
inject 4.900 SCFM air at port 6
primary zone: ppmv NO = 865.0, % O₂ = 2.05, % CO₂ = 16.00, % CO = 0.10
exhaust : ppmv NO = 150.0, % O₂ = 2.10, % CO₂ = 13.90, % CO = 0.15
Temp. in K: T₁=1643, T₂=1625, T₃=1558, T₄= -- , T₅=1523, T₆= -- , T₇=1440

RUN: RV#11

Utah Bituminous # 2 coal in kg/h = 1.948, primary stoichiometry = 1.07
inject 0.449 SCFM natural gas and 0.000 SCFM N₂ at port 5
inject 4.900 SCFM air at port 6
primary zone: ppmv NO = 865.0, % O₂ = 2.05, % CO₂ = 16.00, % CO = 0.10
exhaust : ppmv NO = 285.0, % O₂ = 2.30, % CO₂ = 13.85, % CO = 0.07
Temp. in K: T₁=1661, T₂=1628, T₃=1584, T₄=1579, T₅= -- , T₆= -- , T₇=1393

RUN: RV#12

Utah Bituminous # 2 coal in kg/h = 1.948, primary stoichiometry = 1.07
inject 0.449 SCFM natural gas and 0.000 SCFM N₂ at port 3
inject 4.900 SCFM air at port 6
primary zone: ppmv NO = 865.0, % O₂ = 2.05, % CO₂ = 16.00, % CO = 0.10
exhaust : ppmv NO = 130.0, % O₂ = 2.05, % CO₂ = 14.15, % CO = 0.07
Temp. in K: T₁=1655, T₂=1601, T₃= -- , T₄=1550, T₅=1498, T₆= -- , T₇=1346

RUN: RV#13

Utah Bituminous # 2 coal in kg/h = 1.948, primary stoichiometry = 1.07
inject 0.388 SCFM natural gas and 0.000 SCFM N₂ at port 5
inject 4.326 SCFM air at port 6
primary zone: ppmv NO = 920.0, % O₂ = 1.65, % CO₂ = 16.30, % CO = 0.10
exhaust : ppmv NO = 290.0, % O₂ = 3.15, % CO₂ = 13.40, % CO = 0.05
Temp. in K: T₁=1655, T₂=1615, T₃=1583, T₄=1571, T₅= -- , T₆= -- , T₇=1418

RUN: RV#14

Utah Bituminous # 2 coal in kg/h = 1.948, primary stoichiometry = 1.07
inject 0.388 SCFM natural gas and 0.000 SCFM N₂ at port 3
inject 4.326 SCFM air at port 6
primary zone: ppmv NO = 920.0, % O₂ = 1.65, % CO₂ = 16.30, % CO = 0.10
exhaust : ppmv NO = 125.0, % O₂ = 3.30, % CO₂ = 13.30, % CO = 0.05
Temp. in K: T₁=1667, T₂=1602, T₃= -- , T₄=1551, T₅=1493, T₆= -- , T₇=1412

RUN: RV#15

Utah Bituminous # 2 coal in kg/h = 1.948, primary stoichiometry = 1.07
inject 0.388 SCFM natural gas and 0.000 SCFM N₂ at port 4
inject 4.326 SCFM air at port 6
primary zone: ppmv NO = 920.0, % O₂ = 1.65, % CO₂ = 16.30, % CO = 0.10
exhaust : ppmv NO = 165.0, % O₂ = 3.20, % CO₂ = 13.30, % CO = 0.05
Temp. in K: T₁=1643, T₂=1632, T₃=1572, T₄= -- , T₅=1503, T₆= -- , T₇=1434

RUN: RV#16

Utah Bituminous # 2 coal in kg/h = 1.948, primary stoichiometry = 1.07
inject 0.292 SCFM natural gas and 0.000 SCFM N₂ at port 4
inject 3.319 SCFM air at port 6
primary zone: ppmv NO = 875.0, % O₂ = 1.80, % CO₂ = 16.25, % CO = 0.09
exhaust : ppmv NO = 170.0, % O₂ = 2.55, % CO₂ = 14.20, % CO = 0.05
Temp. in K: T₁=1682, T₂=1638, T₃=1595, T₄= -- , T₅=1528, T₆= -- , T₇=1461

RUN: RV#17

Utah Bituminous # 2 coal in kg/h = 1.948, primary stoichiometry = 1.07
inject 0.292 SCFM natural gas and 0.000 SCFM N₂ at port 5
inject 3.319 SCFM air at port 6
primary zone: ppmv NO = 875.0, % O₂ = 1.80, % CO₂ = 16.25, % CO = 0.09
exhaust : ppmv NO = 340.0, % O₂ = 2.25, % CO₂ = 14.45, % CO = 0.07
Temp. in K: T₁=1678, T₂=1630, T₃=1603, T₄=1573, T₅= -- , T₆= -- , T₇=1481

RUN: RV#18

Utah Bituminous # 2 coal in kg/h = 1.948, primary stoichiometry = 1.07
inject 0.292 SCFM natural gas and 0.000 SCFM N₂ at port 3
inject 3.319 SCFM air at port 6
primary zone: ppmv NO = 875.0, % O₂ = 1.80, % CO₂ = 16.25, % CO = 0.09
exhaust : ppmv NO = 135.0, % O₂ = 2.80, % CO₂ = 13.90, % CO = 0.05
Temp. in K: T₁=1688, T₂=1623, T₃= -- , T₄=1515, T₅=1507, T₆= -- , T₇=1448

RUN: RV#19

Utah Bituminous # 2 coal in kg/h = 1.948, primary stoichiometry = 1.07
inject 0.292 SCFM natural gas and 0.000 SCFM N₂ at port 3
inject 3.319 SCFM air at port 5
primary zone: ppmv NO = 875.0, % O₂ = 1.80, % CO₂ = 16.25, % CO = 0.09
exhaust : ppmv NO = 200.0, % O₂ = 2.00, % CO₂ = 14.75, % CO = 0.05
Temp. in K: T₁=1688, T₂=1623, T₃= -- , T₄=1615, T₅= -- , T₆=1463, T₇=1434

RUN: RV#20

Utah Bituminous # 2 coal in kg/h = 1.948, primary stoichiometry = 1.07
inject 0.292 SCFM natural gas and 0.000 SCFM N₂ at port 3
inject 3.319 SCFM air at port 4
primary zone: ppmv NO = 875.0, % O₂ = 1.80, % CO₂ = 16.25, % CO = 0.09
exhaust : ppmv NO = 440.0, % O₂ = 1.90, % CO₂ = 14.80, % CO = 0.05
Temp. in K: T₁=1688, T₂=1623, T₃= -- , T₄= -- , T₅=1561, T₆=1506, T₇=1423

RUN: RA#10

Utah Bituminous # 2 coal in kg/h = 1.800, primary stoichiometry = 1.32
inject 0.171 SCFM natural gas and 0.000 SCFM N₂ at port 3
inject 0.481 SCFM air at port 6
primary zone: ppmv NO = 765.0, % O₂ = 5.40, % CO₂ = 12.90, % CO = 0.00
exhaust : ppmv NO = 610.0, % O₂ = 2.50, % CO₂ = 14.85, % CO = 0.00
Temp. in K: T₁=1643, T₂=1633, T₃= -- , T₄=1631, T₅=1551, T₆= -- , T₇=1375

RUN: RA#20

Utah Bituminous # 2 coal in kg/h = 1.800, primary stoichiometry = 1.32
inject 0.199 SCFM natural gas and 0.000 SCFM N₂ at port 5
inject 0.482 SCFM air at port 6
primary zone: ppmv NO = 780.0, % O₂ = 5.55, % CO₂ = 12.90, % CO = 0.00
exhaust : ppmv NO = 545.0, % O₂ = 3.25, % CO₂ = 13.30, % CO = 0.83
Temp. in K: T₁=1643, T₂=1603, T₃= -- , T₄=1496, T₅= -- , T₆= -- , T₇=1436

RUN: RA#21

Utah Bituminous # 2 coal in kg/h = 1.800, primary stoichiometry = 1.32
inject 0.199 SCFM natural gas and 0.000 SCFM N₂ at port 4
inject 0.482 SCFM air at port 6
primary zone: ppmv NO = 780.0, % O₂ = 5.55, % CO₂ = 12.90, % CO = 0.00
exhaust : ppmv NO = 490.0, % O₂ = 2.60, % CO₂ = 14.20, % CO = 0.30
Temp. in K: T₁=1643, T₂= -- , T₃=1579, T₄= -- , T₅=1558, T₆= -- , T₇=1438

RUN: RA#22

Utah Bituminous # 2 coal in kg/h = 1.800, primary stoichiometry = 1.32
inject 0.199 SCFM natural gas and 0.000 SCFM N₂ at port 3
inject 0.482 SCFM air at port 6
primary zone: ppmv NO = 780.0, % O₂ = 5.55, % CO₂ = 12.90, % CO = 0.00
exhaust : ppmv NO = 565.0, % O₂ = 1.80, % CO₂ = 14.85, % CO = 0.15
Temp. in K: T₁=1643, T₂=1583, T₃= -- , T₄=1599, T₅=1581, T₆= -- , T₇=1420

RUN: RA#24

Utah Bituminous # 2 coal in kg/h = 1.800, primary stoichiometry = 1.32
inject 0.289 SCFM natural gas and 0.000 SCFM N₂ at port 5
inject 1.249 SCFM air at port 6
primary zone: ppmv NO = 760.0, % O₂ = 5.65, % CO₂ = 12.75, % CO = 0.00
exhaust : ppmv NO = 540.0, % O₂ = 2.45, % CO₂ = 14.05, % CO = 0.30
Temp. in K: T₁=1643, T₂=1603, T₃= -- , T₄=1495, T₅= -- , T₆= -- , T₇=1510

RUN: RA#26

Utah Bituminous # 2 coal in kg/h = 1.800, primary stoichiometry = 1.32
inject 0.289 SCFM natural gas and 0.000 SCFM N₂ at port 4
inject 1.249 SCFM air at port 6
primary zone: ppmv NO = 760.0, % O₂ = 5.65, % CO₂ = 12.75, % CO = 0.00
exhaust : ppmv NO = 485.0, % O₂ = 2.25, % CO₂ = 14.20, % CO = 0.13
Temp. in K: T₁=1643, T₂= -- , T₃=1575, T₄= -- , T₅=1537, T₆= -- , T₇=1436

RUN: RA#27

Utah Bituminous # 2 coal in kg/h = 1.800, primary stoichiometry = 1.32
inject 0.289 SCFM natural gas and 0.000 SCFM N₂ at port 3
inject 1.249 SCFM air at port 6
primary zone: ppmv NO = 760.0, % O₂ = 5.65, % CO₂ = 12.75, % CO = 0.00
exhaust : ppmv NO = 440.0, % O₂ = 1.95, % CO₂ = 14.45, % CO = 0.13
Temp. in K: T₁=1643, T₂=1585, T₃= -- , T₄=1581, T₅=1553, T₆= -- , T₇=1394

RUN: RB# 1

Utah Bituminous # 2 coal in kg/h = 1.824, primary stoichiometry = 1.09
inject 0.032 SCFM natural gas and 0.000 SCFM N₂ at port 4
inject 0.405 SCFM air at port 6
primary zone: ppmv NO = 795.0, % O₂ = 2.30, % CO₂ = 15.70, % CO = 0.07
exhaust : ppmv NO = 745.0, % O₂ = 2.70, % CO₂ = 15.20, % CO = 0.05
Temp. in K: T₁=1674, T₂= -- , T₃=1578, T₄= -- , T₅=1469, T₆= -- , T₇=1253

RUN: RB# 2

Utah Bituminous # 2 coal in kg/h = 1.824, primary stoichiometry = 1.09
inject 0.076 SCFM natural gas and 0.000 SCFM N₂ at port 4
inject 0.868 SCFM air at port 6
primary zone: ppmv NO = 820.0, % O₂ = 2.25, % CO₂ = 15.80, % CO = 0.10
exhaust : ppmv NO = 560.0, % O₂ = 2.70, % CO₂ = 15.00, % CO = 0.07
Temp. in K: T₁=1674, T₂= -- , T₃=1575, T₄= -- , T₅=1492, T₆= -- , T₇=1290

RUN: RB# 3

Utah Bituminous # 2 coal in kg/h = 1.824, primary stoichiometry = 1.09
inject 0.128 SCFM natural gas and 0.000 SCFM N₂ at port 4
inject 1.396 SCFM air at port 6
primary zone: ppmv NO = 820.0, % O₂ = 2.25, % CO₂ = 15.80, % CO = 0.10
exhaust : ppmv NO = 450.0, % O₂ = 2.60, % CO₂ = 14.95, % CO = 0.06
Temp. in K: T₁=1674, T₂= -- , T₃=1620, T₄= -- , T₅=1536, T₆= -- , T₇=1357

RUN: RB# 4

Utah Bituminous # 2 coal in kg/h = 1.824, primary stoichiometry = 1.09
inject 0.182 SCFM natural gas and 0.000 SCFM N₂ at port 4
inject 1.964 SCFM air at port 6
primary zone: ppmv NO = 820.0, % O₂ = 2.25, % CO₂ = 15.80, % CO = 0.10
exhaust : ppmv NO = 280.0, % O₂ = 3.00, % CO₂ = 14.25, % CO = 0.06
Temp. in K: T₁=1674, T₂= -- , T₃=1630, T₄= -- , T₅=1547, T₆= -- , T₇=1403

RUN: RB# 5

Utah Bituminous # 2 coal in kg/h = 1.824, primary stoichiometry = 1.09
inject 0.225 SCFM natural gas and 0.000 SCFM N₂ at port 4
inject 2.600 SCFM air at port 6
primary zone: ppmv NO = 820.0, % O₂ = 2.25, % CO₂ = 15.80, % CO = 0.10
exhaust : ppmv NO = 225.0, % O₂ = 2.85, % CO₂ = 13.90, % CO = 0.10
Temp. in K: T₁=1674, T₂= -- , T₃=1615, T₄= -- , T₅=1539, T₆= -- , T₇=1421

RUN: RB# 6

Utah Bituminous # 2 coal in kg/h = 1.824, primary stoichiometry = 1.09
inject 0.311 SCFM natural gas and 0.000 SCFM N₂ at port 4
inject 3.322 SCFM air at port 6
primary zone: ppmv NO = 820.0, % O₂ = 2.25, % CO₂ = 15.80, % CO = 0.10
exhaust : ppmv NO = 190.0, % O₂ = 2.25, % CO₂ = 14.20, % CO = 0.14
Temp. in K: T₁=1674, T₂= -- , T₃=1624, T₄= -- , T₅=1537, T₆= -- , T₇=1434

RUN: RB# 7

Utah Bituminous # 2 coal in kg/h = 1.824, primary stoichiometry = 1.09
inject 0.388 SCFM natural gas and 0.000 SCFM N₂ at port 4
inject 4.133 SCFM air at port 6
primary zone: ppmv NO = 820.0, % O₂ = 2.25, % CO₂ = 15.80, % CO = 0.10
exhaust : ppmv NO = 200.0, % O₂ = 2.55, % CO₂ = 13.75, % CO = 0.14
Temp. in K: T₁=1674, T₂= -- , T₃=1642, T₄= -- , T₅=1525, T₆= -- , T₇=1459

RUN: RC# 1

Utah Bituminous # 2 coal in kg/h = 1.732, primary stoichiometry = 1.12
inject 0.054 SCFM natural gas and 0.000 SCFM N₂ at port 3
inject 0.425 SCFM air at port 6
primary zone: ppmv NO = 885.0, % O₂ = 2.10, % CO₂ = 15.80, % CO = 0.17
exhaust : ppmv NO = 660.0, % O₂ = 2.65, % CO₂ = 15.10, % CO = 0.05
Temp. in K: T₁=1645, T₂=1597, T₃= -- , T₄=1553, T₅=1452, T₆= -- , T₇=1251

RUN: RC# 2

Utah Bituminous # 2 coal in kg/h = 1.732, primary stoichiometry = 1.12
inject 0.054 SCFM natural gas and 0.000 SCFM N₂ at port 4
inject 0.425 SCFM air at port 6
primary zone: ppmv NO = 885.0, % O₂ = 2.10, % CO₂ = 15.80, % CO = 0.17
exhaust : ppmv NO = 690.0, % O₂ = 3.25, % CO₂ = 14.65, % CO = 0.07
Temp. in K: T₁=1663, T₂=1622, T₃=1600, T₄= -- , T₅=1509, T₆= -- , T₇=1312

RUN: RC# 3

Utah Bituminous # 2 coal in kg/h = 1.732, primary stoichiometry = 1.12
inject 0.054 SCFM natural gas and 0.000 SCFM N₂ at port 5
inject 0.425 SCFM air at port 6
primary zone: ppmv NO = 885.0, % O₂ = 2.25, % CO₂ = 15.80, % CO = 0.17
exhaust : ppmv NO = 585.0, % O₂ = 2.85, % CO₂ = 14.80, % CO = 0.07
Temp. in K: T₁=1650, T₂=1633, T₃=1594, T₄=1581, T₅= -- , T₆= -- , T₇=1332

RUN: RC# 4

Utah Bituminous # 2 coal in kg/h = 1.732, primary stoichiometry = 1.12
inject 0.087 SCFM natural gas and 0.000 SCFM N₂ at port 5
inject 0.798 SCFM air at port 6
primary zone: ppmv NO = 885.0, % O₂ = 2.30, % CO₂ = 15.80, % CO = 0.17
exhaust : ppmv NO = 500.0, % O₂ = 2.20, % CO₂ = 15.15, % CO = 0.12
Temp. in K: T₁=1663, T₂=1629, T₃=1613, T₄=1589, T₅= -- , T₆= -- , T₇=1350

RUN: RC# 5

Utah Bituminous # 2 coal in kg/h = 1.732, primary stoichiometry = 1.12
inject 0.087 SCFM natural gas and 0.000 SCFM N₂ at port 4
inject 0.798 SCFM air at port 6
primary zone: ppmv NO = 875.0, % O₂ = 2.20, % CO₂ = 15.80, % CO = 0.17
exhaust : ppmv NO = 525.0, % O₂ = 2.75, % CO₂ = 14.85, % CO = 0.07
Temp. in K: T₁=1672, T₂=1643, T₃=1600, T₄= -- , T₅=1625, T₆= -- , T₇=1338

RUN: RC# 6

Utah Bituminous # 2 coal in kg/h = 1.732, primary stoichiometry = 1.12
inject 0.087 SCFM natural gas and 0.000 SCFM N₂ at port 4
inject 0.798 SCFM air at port 5
primary zone: ppmv NO = 885.0, % O₂ = 2.30, % CO₂ = 15.80, % CO = 0.12
exhaust : ppmv NO = 575.0, % O₂ = 2.20, % CO₂ = 15.40, % CO = 0.07
Temp. in K: T₁=1672, T₂=1643, T₃=1612, T₄= -- , T₅= -- , T₆=1304, T₇=1318

RUN: RC# 7
Utah Bituminous # 2 coal in kg/h = 1.732, primary stoichiometry = 1.12
inject 0.087 SCFM natural gas and 0.000 SCFM N₂ at port 3
inject 0.798 SCFM air at port 5
primary zone: ppmv NO = 885.0, % O₂ = 2.30, % CO₂ = 15.80, % CO = 0.12
exhaust : ppmv NO = 550.0, % O₂ = 2.20, % CO₂ = 15.30, % CO = 0.05
Temp. in K: T₁=1663, T₂=1648, T₃= -- , T₄=1597, T₅= -- , T₆= -- , T₇=1319

RUN: RC# 8
Utah Bituminous # 2 coal in kg/h = 1.732, primary stoichiometry = 1.12
inject 0.087 SCFM natural gas and 0.000 SCFM N₂ at port 3
inject 0.798 SCFM air at port 6
primary zone: ppmv NO = 885.0, % O₂ = 2.30, % CO₂ = 15.80, % CO = 0.12
exhaust : ppmv NO = 530.0, % O₂ = 2.60, % CO₂ = 15.15, % CO = 0.05
Temp. in K: T₁=1663, T₂=1643, T₃= -- , T₄=1610, T₅=1499, T₆= -- , T₇=1268

RUN: RH# 1
Utah Bituminous # 2 coal in kg/h = 1.782, primary stoichiometry = 1.10
inject 0.243 SCFM natural gas and 0.000 SCFM N₂ at port 5
inject 2.558 SCFM air at port 6
primary zone: ppmv NO = 885.0, % O₂ = 2.05, % CO₂ = 15.40, % CO = 0.09
exhaust : ppmv NO = 395.0, % O₂ = 1.30, % CO₂ = 14.65, % CO = 0.31
Temp. in K: T₁=1676, T₂=1657, T₃=1634, T₄=1607, T₅= -- , T₆= -- , T₇=1507

RUN: RH# 2
Utah Bituminous # 2 coal in kg/h = 1.782, primary stoichiometry = 1.10
inject 0.243 SCFM natural gas and 0.000 SCFM N₂ at port 4
inject 2.558 SCFM air at port 6
primary zone: ppmv NO = 860.0, % O₂ = 2.15, % CO₂ = 15.40, % CO = 0.10
exhaust : ppmv NO = 210.0, % O₂ = 0.95, % CO₂ = 15.00, % CO = 0.22
Temp. in K: T₁=1676, T₂=1646, T₃=1617, T₄= -- , T₅=1552, T₆= -- , T₇=1510

RUN: RH# 3
Utah Bituminous # 2 coal in kg/h = 1.782, primary stoichiometry = 1.10
inject 0.243 SCFM natural gas and 0.000 SCFM N₂ at port 3
inject 2.558 SCFM air at port 6
primary zone: ppmv NO = 860.0, % O₂ = 2.15, % CO₂ = 15.40, % CO = 0.10
exhaust : ppmv NO = 165.0, % O₂ = 1.35, % CO₂ = 14.70, % CO = 0.22
Temp. in K: T₁=1676, T₂=1630, T₃= -- , T₄=1582, T₅=1543, T₆= -- , T₇=1496

RUN: RH# 4
Utah Bituminous # 2 coal in kg/h = 1.782, primary stoichiometry = 1.10
inject 0.310 SCFM natural gas and 0.000 SCFM N₂ at port 3
inject 3.263 SCFM air at port 6
primary zone: ppmv NO = 910.0, % O₂ = 2.45, % CO₂ = 15.30, % CO = 0.10
exhaust : ppmv NO = 160.0, % O₂ = 1.15, % CO₂ = 14.80, % CO = 0.19
Temp. in K: T₁=1676, T₂=1636, T₃= -- , T₄=1579, T₅=1538, T₆= -- , T₇=1522

RUN: RH# 5
Utah Bituminous # 2 coal in kg/h = 1.782, primary stoichiometry = 1.10
inject 0.310 SCFM natural gas and 0.000 SCFM N₂ at port 4
inject 3.263 SCFM air at port 6
primary zone: ppmv NO = 910.0, % O₂ = 2.45, % CO₂ = 15.30, % CO = 0.10
exhaust : ppmv NO = 175.0, % O₂ = 0.95, % CO₂ = 14.85, % CO = 0.25
Temp. in K: T₁=1676, T₂=1658, T₃=1622, T₄= -- , T₅=1548, T₆= -- , T₇=1531

RUN: RH# 6

Utah Bituminous # 2 coal in kg/h = 1.782, primary stoichiometry = 1.10
inject 0.310 SCFM natural gas and 0.000 SCFM N₂ at port 5
inject 3.263 SCFM air at port 6
primary zone: ppmv NO = 915.0, % O₂ = 2.20, % CO₂ = 15.60, % CO = 0.07
exhaust : ppmv NO = 375.0, % O₂ = 2.15, % CO₂ = 14.20, % CO = 0.14
Temp. in K: T₁=1676, T₂= -- , T₃=1633, T₄=1610, T₅= -- , T₆= -- , T₇=1530

RUN: RH# 7

Utah Bituminous # 2 coal in kg/h = 1.782, primary stoichiometry = 1.10
inject 0.386 SCFM natural gas and 0.000 SCFM N₂ at port 5
inject 4.063 SCFM air at port 6
primary zone: ppmv NO = 925.0, % O₂ = 2.20, % CO₂ = 15.60, % CO = 0.07
exhaust : ppmv NO = 300.0, % O₂ = 2.10, % CO₂ = 13.90, % CO = 0.10
Temp. in K: T₁=1676, T₂= -- , T₃=1633, T₄=1621, T₅= -- , T₆= -- , T₇=1549

RUN: RH# 8

Utah Bituminous # 2 coal in kg/h = 1.782, primary stoichiometry = 1.10
inject 0.386 SCFM natural gas and 0.000 SCFM N₂ at port 4
inject 4.063 SCFM air at port 6
primary zone: ppmv NO = 855.0, % O₂ = 2.50, % CO₂ = 15.15, % CO = 0.07
exhaust : ppmv NO = 170.0, % O₂ = 1.50, % CO₂ = 14.35, % CO = 0.13
Temp. in K: T₁=1676, T₂= -- , T₃=1618, T₄= -- , T₅=1537, T₆= -- , T₇=1533

RUN: RH# 9

Utah Bituminous # 2 coal in kg/h = 1.782, primary stoichiometry = 1.10
inject 0.386 SCFM natural gas and 0.000 SCFM N₂ at port 3
inject 4.063 SCFM air at port 6
primary zone: ppmv NO = 855.0, % O₂ = 2.50, % CO₂ = 15.15, % CO = 0.07
exhaust : ppmv NO = 145.0, % O₂ = 1.45, % CO₂ = 14.20, % CO = 0.33
Temp. in K: T₁=1676, T₂=1632, T₃= -- , T₄=1577, T₅=1542, T₆= -- , T₇=1502

RUN: RH#10

Utah Bituminous # 2 coal in kg/h = 1.782, primary stoichiometry = 1.10
inject 0.122 SCFM natural gas and 0.000 SCFM N₂ at port 4
inject 0.122 SCFM natural gas and 0.000 SCFM N₂ at port 5
inject 2.829 SCFM air at port 6
primary zone: ppmv NO = 925.0, % O₂ = 2.70, % CO₂ = 15.10, % CO = 0.07
exhaust : ppmv NO = 260.0, % O₂ = 3.45, % CO₂ = 13.15, % CO = 0.10
Temp. in K: T₁=1676, T₂= -- , T₃=1584, T₄= -- , T₅= -- , T₆= -- , T₇=1442

RUN: RH#11

Utah Bituminous # 2 coal in kg/h = 1.782, primary stoichiometry = 1.10
inject 0.122 SCFM natural gas and 0.000 SCFM N₂ at port 3
inject 0.122 SCFM natural gas and 0.000 SCFM N₂ at port 5
inject 2.829 SCFM air at port 6
primary zone: ppmv NO = 925.0, % O₂ = 2.70, % CO₂ = 15.10, % CO = 0.07
exhaust : ppmv NO = 260.0, % O₂ = 2.95, % CO₂ = 13.60, % CO = 0.13
Temp. in K: T₁=1676, T₂=1605, T₃= -- , T₄= -- , T₅= -- , T₆= -- , T₇=1412

RUN: RH#12

Utah Bituminous # 2 coal in kg/h = 1.782, primary stoichiometry = 1.10
inject 0.122 SCFM natural gas and 0.000 SCFM N₂ at port 3
inject 0.122 SCFM natural gas and 0.000 SCFM N₂ at port 4
inject 2.829 SCFM air at port 6
primary zone: ppmv NO = 925.0, % O₂ = 2.70, % CO₂ = 15.10, % CO = 0.07
exhaust : ppmv NO = 170.0, % O₂ = 2.55, % CO₂ = 13.90, % CO = 0.13
Temp. in K: T₁=1676, T₂=1591, T₃= -- , T₄= -- , T₅=1503, T₆= -- , T₇=1422

RUN: RH#13

Utah Bituminous # 2 coal in kg/h = 1.782, primary stoichiometry = 1.10
inject 0.155 SCFM natural gas and 0.000 SCFM N₂ at port 3
inject 0.155 SCFM natural gas and 0.000 SCFM N₂ at port 4
inject 3.263 SCFM air at port 6
primary zone: ppmv NO = 920.0, % O₂ = 2.85, % CO₂ = 15.00, % CO = 0.07
exhaust : ppmv NO = 165.0, % O₂ = 1.90, % CO₂ = 14.05, % CO = 0.31
Temp. in K: T₁=1676, T₂=1600, T₃= -- , T₄= -- , T₅=1490, T₆= -- , T₇=1466

RUN: RH#14

Utah Bituminous # 2 coal in kg/h = 1.782, primary stoichiometry = 1.10
inject 0.155 SCFM natural gas and 0.000 SCFM N₂ at port 4
inject 0.155 SCFM natural gas and 0.000 SCFM N₂ at port 5
inject 3.263 SCFM air at port 6
primary zone: ppmv NO = 920.0, % O₂ = 2.85, % CO₂ = 15.00, % CO = 0.07
exhaust : ppmv NO = 240.0, % O₂ = 2.90, % CO₂ = 13.30, % CO = 0.15
Temp. in K: T₁=1676, T₂= -- , T₃=1576, T₄= -- , T₅= -- , T₆= -- , T₇=1436

RUN: RH#15

Utah Bituminous # 2 coal in kg/h = 1.782, primary stoichiometry = 1.10
inject 0.155 SCFM natural gas and 0.000 SCFM N₂ at port 3
inject 0.155 SCFM natural gas and 0.000 SCFM N₂ at port 5
inject 3.263 SCFM air at port 6
primary zone: ppmv NO = 920.0, % O₂ = 2.85, % CO₂ = 15.00, % CO = 0.07
exhaust : ppmv NO = 240.0, % O₂ = 3.95, % CO₂ = 12.55, % CO = 0.07
Temp. in K: T₁=1676, T₂=1602, T₃= -- , T₄= -- , T₅= -- , T₆= -- , T₇=1426

RUN: RH#16

Utah Bituminous # 2 coal in kg/h = 1.782, primary stoichiometry = 1.10
inject 0.193 SCFM natural gas and 0.000 SCFM N₂ at port 3
inject 0.193 SCFM natural gas and 0.000 SCFM N₂ at port 5
inject 4.410 SCFM air at port 6
primary zone: ppmv NO = 915.0, % O₂ = 2.80, % CO₂ = 15.15, % CO = 0.07
exhaust : ppmv NO = 195.0, % O₂ = 4.30, % CO₂ = 12.00, % CO = 0.05
Temp. in K: T₁=1676, T₂=1607, T₃= -- , T₄= -- , T₅= -- , T₆= -- , T₇=1459

RUN: RH#17

Utah Bituminous # 2 coal in kg/h = 1.782, primary stoichiometry = 1.10
inject 0.193 SCFM natural gas and 0.000 SCFM N₂ at port 4
inject 0.193 SCFM natural gas and 0.000 SCFM N₂ at port 5
inject 4.410 SCFM air at port 6
primary zone: ppmv NO = 915.0, % O₂ = 2.80, % CO₂ = 15.15, % CO = 0.07
exhaust : ppmv NO = 220.0, % O₂ = 4.40, % CO₂ = 12.00, % CO = 0.05
Temp. in K: T₁=1676, T₂= -- , T₃=1577, T₄= -- , T₅= -- , T₆= -- , T₇=1479

RUN: RH#18

Utah Bituminous # 2 coal in kg/h = 1.782, primary stoichiometry = 1.10
inject 0.193 SCFM natural gas and 0.000 SCFM N₂ at port 3
inject 0.193 SCFM natural gas and 0.000 SCFM N₂ at port 4
inject 4.410 SCFM air at port 6
primary zone: ppmv NO = 915.0, % O₂ = 2.80, % CO₂ = 15.15, % CO = 0.07
exhaust : ppmv NO = 180.0, % O₂ = 5.05, % CO₂ = 11.50, % CO = 0.03
Temp. in K: T₁=1676, T₂=1593, T₃= -- , T₄= -- , T₅=1475, T₆= -- , T₇=1475

RUN: MR# 1

Utah Bituminous # 2 coal in kg/h = 1.440, primary stoichiometry = 1.19
inject 0.162 SCFM natural gas and 0.000 SCFM N₂ at port 3
inject 0.162 SCFM natural gas and 0.000 SCFM N₂ at port 4
inject 0.162 SCFM natural gas and 0.000 SCFM N₂ at port 5
inject 4.139 SCFM air at port 6
primary zone: ppmv NO = 940.0, % O₂ = 4.10, % CO₂ = 14.20, % CO = 0.05
exhaust : ppmv NO = 215.0, % O₂ = 2.45, % CO₂ = 13.35, % CO = 0.05
Temp. in K: T₁=1577, T₂=1512, T₃= -- , T₄= -- , T₅= -- , T₆= -- , T₇=1313

RUN: MR# 2

Utah Bituminous # 2 coal in kg/h = 1.440, primary stoichiometry = 1.19
inject 0.242 SCFM natural gas and 0.000 SCFM N₂ at port 3
inject 0.242 SCFM natural gas and 0.000 SCFM N₂ at port 4
inject 4.139 SCFM air at port 6
primary zone: ppmv NO = 940.0, % O₂ = 4.10, % CO₂ = 14.20, % CO = 0.05
exhaust : ppmv NO = 175.0, % O₂ = 2.40, % CO₂ = 13.30, % CO = 0.04
Temp. in K: T₁=1577, T₂=1512, T₃= -- , T₄= -- , T₅=1413, T₆= -- , T₇=1313

RUN: MR# 3

Utah Bituminous # 2 coal in kg/h = 1.440, primary stoichiometry = 1.19
inject 0.242 SCFM natural gas and 0.000 SCFM N₂ at port 3
inject 0.242 SCFM natural gas and 0.000 SCFM N₂ at port 5
inject 4.139 SCFM air at port 6
primary zone: ppmv NO = 940.0, % O₂ = 4.10, % CO₂ = 14.20, % CO = 0.05
exhaust : ppmv NO = 195.0, % O₂ = 2.25, % CO₂ = 13.45, % CO = 0.05
Temp. in K: T₁=1577, T₂=1512, T₃= -- , T₄= -- , T₅= -- , T₆= -- , T₇=1313

RUN: MR# 4

Utah Bituminous # 2 coal in kg/h = 1.440, primary stoichiometry = 1.19
inject 0.242 SCFM natural gas and 0.000 SCFM N₂ at port 4
inject 0.242 SCFM natural gas and 0.000 SCFM N₂ at port 5
inject 4.139 SCFM air at port 6
primary zone: ppmv NO = 940.0, % O₂ = 4.10, % CO₂ = 14.20, % CO = 0.05
exhaust : ppmv NO = 225.0, % O₂ = 2.10, % CO₂ = 13.60, % CO = 0.05
Temp. in K: T₁=1577, T₂=1512, T₃=1487, T₄= -- , T₅= -- , T₆= -- , T₇=1313

RUN: MR# 6

Utah Bituminous # 2 coal in kg/h = 1.437, primary stoichiometry = 1.19
inject 0.156 SCFM natural gas and 0.000 SCFM N₂ at port 3
inject 0.156 SCFM natural gas and 0.000 SCFM N₂ at port 4
inject 2.718 SCFM air at port 6
primary zone: ppmv NO = 870.0, % O₂ = 3.75, % CO₂ = 14.25, % CO = 0.05
exhaust : ppmv NO = 180.0, % O₂ = 1.50, % CO₂ = 14.15, % CO = 0.05
Temp. in K: T₁=1548, T₂=1504, T₃= -- , T₄= -- , T₅=1448, T₆= -- , T₇=1352

RUN: MR# 7

Utah Bituminous # 2 coal in kg/h = 1.437, primary stoichiometry = 1.19
inject 0.156 SCFM natural gas and 0.000 SCFM N₂ at port 3
inject 0.156 SCFM natural gas and 0.000 SCFM N₂ at port 5
inject 2.718 SCFM air at port 6
primary zone: ppmv NO = 870.0, % O₂ = 3.75, % CO₂ = 14.25, % CO = 0.05
exhaust : ppmv NO = 220.0, % O₂ = 1.55, % CO₂ = 14.20, % CO = 0.05
Temp. in K: T₁=1556, T₂=1512, T₃= -- , T₄= -- , T₅= -- , T₆= -- , T₇=1343

RUN: MR# 8

Utah Bituminous # 2 coal in kg/h = 1.437, primary stoichiometry = 1.19
inject 0.156 SCFM natural gas and 0.000 SCFM N₂ at port 4
inject 0.156 SCFM natural gas and 0.000 SCFM N₂ at port 5
inject 2.718 SCFM air at port 6
primary zone: ppmv NO = 870.0, % O₂ = 3.75, % CO₂ = 14.25, % CO = 0.05
exhaust : ppmv NO = 255.0, % O₂ = 1.35, % CO₂ = 14.35, % CO = 0.05
Temp. in K: T₁=1548, T₂=1511, T₃=1457, T₄= -- , T₅= -- , T₆= -- , T₇=1310

RUN: MR#24

Utah Bituminous # 2 coal in kg/h = 1.437, primary stoichiometry = 1.19
inject 0.158 SCFM natural gas and 0.000 SCFM N₂ at port 3
inject 0.158 SCFM natural gas and 0.000 SCFM N₂ at port 4
inject 2.730 SCFM air at port 6
primary zone: ppmv NO = 925.0, % O₂ = 3.85, % CO₂ = 13.90, % CO = 0.07
exhaust : ppmv NO = 200.0, % O₂ = 1.80, % CO₂ = 13.60, % CO = 0.07
Temp. in K: T₁=1548, T₂=1504, T₃= -- , T₄= -- , T₅=1448, T₆= -- , T₇=1352

RUN: MR#25

Utah Bituminous # 2 coal in kg/h = 1.437, primary stoichiometry = 1.19
inject 0.158 SCFM natural gas and 0.000 SCFM N₂ at port 3
inject 0.158 SCFM natural gas and 0.000 SCFM N₂ at port 5
inject 2.730 SCFM air at port 6
primary zone: ppmv NO = 925.0, % O₂ = 3.85, % CO₂ = 13.90, % CO = 0.07
exhaust : ppmv NO = 280.0, % O₂ = 1.70, % CO₂ = 13.90, % CO = 0.07
Temp. in K: T₁=1556, T₂=1512, T₃= -- , T₄= -- , T₅= -- , T₆= -- , T₇=1343

RUN: MR#26

Utah Bituminous # 2 coal in kg/h = 1.437, primary stoichiometry = 1.19
inject 0.158 SCFM natural gas and 0.000 SCFM N₂ at port 4
inject 0.158 SCFM natural gas and 0.000 SCFM N₂ at port 5
inject 2.730 SCFM air at port 6
primary zone: ppmv NO = 925.0, % O₂ = 3.85, % CO₂ = 13.90, % CO = 0.07
exhaust : ppmv NO = 310.0, % O₂ = 1.65, % CO₂ = 13.90, % CO = 0.07
Temp. in K: T₁=1548, T₂=1511, T₃=1457, T₄= -- , T₅= -- , T₆= -- , T₇=1310

RUN: RA# 9

Utah Bituminous # 2 coal in kg/h = 1.800, primary stoichiometry = 1.32
inject 0.171 SCFM natural gas and 0.000 SCFM N₂ at port 3
inject 0.000 SCFM air
primary zone: ppmv NO = 765.0, % O₂ = 5.40, % CO₂ = 12.90, % CO = 0.00
exhaust : ppmv NO = 655.0, % O₂ = 1.95, % CO₂ = 15.45, % CO = 0.07
Temp. in K: T₁=1643, T₂=1610, T₃= -- , T₄=1630, T₅= -- , T₆= -- , T₇=1406

RUN: RA#10

Utah Bituminous # 2 coal in kg/h = 1.800, primary stoichiometry = 1.32
inject 0.171 SCFM natural gas and 0.000 SCFM N₂ at port 3
inject 0.481 SCFM air at port 6
primary zone: ppmv NO = 765.0, % O₂ = 5.40, % CO₂ = 12.90, % CO = 0.00
exhaust : ppmv NO = 610.0, % O₂ = 2.50, % CO₂ = 14.85, % CO = 0.00
Temp. in K: T₁=1643, T₂=1633, T₃= -- , T₄=1631, T₅=1551, T₆= -- , T₇=1375

RUN: RA#13

Utah Bituminous # 2 coal in kg/h = 1.800, primary stoichiometry = 1.32
inject 0.171 SCFM natural gas and 0.000 SCFM N₂ at port 3
inject 0.962 SCFM air at port 6
primary zone: ppmv NO = 765.0, % O₂ = 5.40, % CO₂ = 12.90, % CO = 0.00
exhaust : ppmv NO = 580.0, % O₂ = 3.45, % CO₂ = 14.05, % CO = 0.00
Temp. in K: T₁=1643, T₂=1633, T₃= -- , T₄= -- , T₅= -- , T₆= -- , T₇=1375

RUN: RA#14

Utah Bituminous # 2 coal in kg/h = 1.800, primary stoichiometry = 1.32
inject 0.171 SCFM natural gas and 0.000 SCFM N₂ at port 3
inject 1.444 SCFM air at port 6
primary zone: ppmv NO = 765.0, % O₂ = 5.40, % CO₂ = 12.90, % CO = 0.00
exhaust : ppmv NO = 555.0, % O₂ = 4.40, % CO₂ = 13.30, % CO = 0.00
Temp. in K: T₁=1643, T₂=1633, T₃= -- , T₄= -- , T₅= -- , T₆= -- , T₇=1375

RUN: RA#15

Utah Bituminous # 2 coal in kg/h = 1.800, primary stoichiometry = 1.32
inject 0.171 SCFM natural gas and 0.000 SCFM N₂ at port 3
inject 1.925 SCFM air at port 6
primary zone: ppmv NO = 765.0, % O₂ = 5.40, % CO₂ = 12.90, % CO = 0.00
exhaust : ppmv NO = 540.0, % O₂ = 4.90, % CO₂ = 12.90, % CO = 0.00
Temp. in K: T₁=1643, T₂=1633, T₃= -- , T₄= -- , T₅= -- , T₆= -- , T₇=1375

RUN: RR# 1

Utah Bituminous # 3 coal in kg/h = 1.302, primary stoichiometry = 1.23
inject 0.107 SCFM natural gas and 0.443 SCFM N₂ at port 4
inject 0.350 SCFM air at port 6
primary zone: ppmv NO = 875.0, % O₂ = 2.80, % CO₂ = 15.15, % CO = 0.10
exhaust : ppmv NO = 572.0, % O₂ = 1.50, % CO₂ = 12.93, % CO = 0.07
Temp. in K: T₁=1673, T₂= -- , T₃=1592, T₄= -- , T₅=1440, T₆= -- , T₇=1285

RUN: RR# 2

Utah Bituminous # 3 coal in kg/h = 1.302, primary stoichiometry = 1.23
inject 0.144 SCFM natural gas and 0.406 SCFM N₂ at port 4
inject 0.736 SCFM air at port 6
primary zone: ppmv NO = 875.0, % O₂ = 2.80, % CO₂ = 15.15, % CO = 0.10
exhaust : ppmv NO = 332.0, % O₂ = 1.45, % CO₂ = 13.03, % CO = 0.08
Temp. in K: T₁=1673, T₂= -- , T₃=1595, T₄= -- , T₅=1472, T₆= -- , T₇=1281

RUN: RR# 3

Utah Bituminous # 3 coal in kg/h = 1.302, primary stoichiometry = 1.23
inject 0.185 SCFM natural gas and 0.365 SCFM N₂ at port 4
inject 1.168 SCFM air at port 6
primary zone: ppmv NO = 875.0, % O₂ = 2.80, % CO₂ = 15.15, % CO = 0.10
exhaust : ppmv NO = 205.0, % O₂ = 1.50, % CO₂ = 13.25, % CO = 0.10
Temp. in K: T₁=1673, T₂= -- , T₃=1599, T₄= -- , T₅=1493, T₆= -- , T₇=1318

RUN: RR# 4

Utah Bituminous # 3 coal in kg/h = 1.302, primary stoichiometry = 1.23
inject 0.230 SCFM natural gas and 0.320 SCFM N₂ at port 4
inject 1.642 SCFM air at port 6
primary zone: ppmv NO = 875.0, % O₂ = 2.80, % CO₂ = 15.15, % CO = 0.10
exhaust : ppmv NO = 155.0, % O₂ = 1.65, % CO₂ = 13.15, % CO = 0.10
Temp. in K: T₁=1673, T₂= -- , T₃=1598, T₄= -- , T₅=1523, T₆= -- , T₇=1380

RUN: RR# 5

Utah Bituminous # 3 coal in kg/h = 1.302, primary stoichiometry = 1.23
inject 0.280 SCFM natural gas and 0.270 SCFM N₂ at port 4
inject 2.168 SCFM air at port 6
primary zone: ppmv NO = 875.0, % O₂ = 2.80, % CO₂ = 15.15, % CO = 0.10
exhaust : ppmv NO = 180.0, % O₂ = 2.10, % CO₂ = 12.80, % CO = 0.10
Temp. in K: T₁=1673, T₂= -- , T₃=1602, T₄= -- , T₅=1562, T₆= -- , T₇=1436

RUN: RR# 6

Utah Bituminous # 3 coal in kg/h = 1.302, primary stoichiometry = 1.23
inject 0.337 SCFM natural gas and 0.213 SCFM N₂ at port 4
inject 2.768 SCFM air at port 6
primary zone: ppmv NO = 875.0, % O₂ = 2.80, % CO₂ = 15.15, % CO = 0.10
exhaust : ppmv NO = 185.0, % O₂ = 2.30, % CO₂ = 12.75, % CO = 0.15
Temp. in K: T₁=1673, T₂= -- , T₃=1602, T₄= -- , T₅=1561, T₆= -- , T₇=1449

RUN: RR# 7

Utah Bituminous # 3 coal in kg/h = 1.302, primary stoichiometry = 1.23
inject 0.401 SCFM natural gas and 0.149 SCFM N₂ at port 4
inject 3.442 SCFM air at port 6
primary zone: ppmv NO = 875.0, % O₂ = 2.80, % CO₂ = 15.15, % CO = 0.10
exhaust : ppmv NO = 200.0, % O₂ = 3.35, % CO₂ = 12.15, % CO = 0.05
Temp. in K: T₁=1673, T₂= -- , T₃=1603, T₄= -- , T₅=1556, T₆= -- , T₇=1466

RUN: RR# 8

Utah Bituminous # 3 coal in kg/h = 1.302, primary stoichiometry = 1.23
inject 0.550 SCFM natural gas and 0.000 SCFM N₂ at port 4
inject 4.000 SCFM air at port 6
primary zone: ppmv NO = 875.0, % O₂ = 2.80, % CO₂ = 15.15, % CO = 0.10
exhaust : ppmv NO = 165.0, % O₂ = 1.80, % CO₂ = 12.70, % CO = 0.10
Temp. in K: T₁=1673, T₂= -- , T₃=1604, T₄= -- , T₅=1560, T₆= -- , T₇=1536

RUN: RR# 9

Utah Bituminous # 3 coal in kg/h = 1.302, primary stoichiometry = 1.23
inject 0.043 SCFM natural gas and 0.507 SCFM N₂ at port 4
inject 0.320 SCFM air at port 6
primary zone: ppmv NO = 875.0, % O₂ = 2.80, % CO₂ = 15.15, % CO = 0.10
exhaust : ppmv NO = 730.0, % O₂ = 3.60, % CO₂ = 11.80, % CO = 0.03
Temp. in K: T₁=1673, T₂= -- , T₃=1583, T₄= -- , T₅=1362, T₆= -- , T₇=1202

RUN: RR#10

Utah Bituminous # 3 coal in kg/h = 1.302, primary stoichiometry = 1.23
inject 0.073 SCFM natural gas and 0.477 SCFM N₂ at port 4
inject 0.330 SCFM air at port 6
primary zone: ppmv NO = 875.0, % O₂ = 2.80, % CO₂ = 15.15, % CO = 0.10
exhaust : ppmv NO = 675.0, % O₂ = 2.90, % CO₂ = 12.60, % CO = 0.03
Temp. in K: T₁=1673, T₂= -- , T₃=1588, T₄= -- , T₅=1394, T₆= -- , T₇=1252

RUN: RR#11

Utah Bituminous # 3 coal in kg/h = 1.302, primary stoichiometry = 1.23
inject 0.105 SCFM natural gas and 0.445 SCFM N₂ at port 4
inject 0.340 SCFM air at port 6
primary zone: ppmv NO = 875.0, % O₂ = 2.80, % CO₂ = 15.15, % CO = 0.10
exhaust : ppmv NO = 570.0, % O₂ = 2.15, % CO₂ = 13.15, % CO = 0.04
Temp. in K: T₁=1673, T₂= -- , T₃=1592, T₄= -- , T₅=1432, T₆= -- , T₇=1275

RUN: RR#12

Utah Bituminous # 3 coal in kg/h = 1.302, primary stoichiometry = 1.23
inject 0.141 SCFM natural gas and 0.409 SCFM N₂ at port 4
inject 0.710 SCFM air at port 6
primary zone: ppmv NO = 875.0, % O₂ = 2.80, % CO₂ = 15.15, % CO = 0.10
exhaust : ppmv NO = 405.0, % O₂ = 1.55, % CO₂ = 13.60, % CO = 0.07
Temp. in K: T₁=1673, T₂= -- , T₃=1593, T₄= -- , T₅=1447, T₆= -- , T₇=1294

RUN: RR#13

Utah Bituminous # 3 coal in kg/h = 1.302, primary stoichiometry = 1.23
inject 0.181 SCFM natural gas and 0.369 SCFM N₂ at port 4
inject 1.140 SCFM air at port 6
primary zone: ppmv NO = 875.0, % O₂ = 2.80, % CO₂ = 15.15, % CO = 0.10
exhaust : ppmv NO = 290.0, % O₂ = 1.95, % CO₂ = 13.50, % CO = 0.05
Temp. in K: T₁=1673, T₂= -- , T₃=1597, T₄= -- , T₅=1504, T₆= -- , T₇=1337

RUN: RR#14

Utah Bituminous # 3 coal in kg/h = 1.302, primary stoichiometry = 1.23
inject 0.226 SCFM natural gas and 0.324 SCFM N₂ at port 4
inject 1.610 SCFM air at port 6
primary zone: ppmv NO = 875.0, % O₂ = 2.80, % CO₂ = 15.15, % CO = 0.10
exhaust : ppmv NO = 215.0, % O₂ = 1.80, % CO₂ = 13.60, % CO = 0.07
Temp. in K: T₁=1673, T₂= -- , T₃=1597, T₄= -- , T₅=1527, T₆= -- , T₇=1376

RUN: RR#15

Utah Bituminous # 3 coal in kg/h = 1.302, primary stoichiometry = 1.23
inject 0.245 SCFM natural gas and 0.305 SCFM N₂ at port 4
inject 1.810 SCFM air at port 6
primary zone: ppmv NO = 875.0, % O₂ = 2.80, % CO₂ = 15.15, % CO = 0.10
exhaust : ppmv NO = 205.0, % O₂ = 1.45, % CO₂ = 13.90, % CO = 0.10
Temp. in K: T₁=1673, T₂= -- , T₃=1602, T₄= -- , T₅=1542, T₆= -- , T₇=1383

RUN: RR#16

Utah Bituminous # 3 coal in kg/h = 1.302, primary stoichiometry = 1.23
inject 0.302 SCFM natural gas and 0.248 SCFM N₂ at port 4
inject 2.410 SCFM air at port 6
primary zone: ppmv NO = 875.0, % O₂ = 2.80, % CO₂ = 15.15, % CO = 0.10
exhaust : ppmv NO = 205.0, % O₂ = 2.05, % CO₂ = 13.60, % CO = 0.07
Temp. in K: T₁=1673, T₂= -- , T₃=1602, T₄= -- , T₅=1544, T₆= -- , T₇=1431

RUN: RR#17

Utah Bituminous # 3 coal in kg/h = 1.302, primary stoichiometry = 1.23
inject 0.355 SCFM natural gas and 0.195 SCFM N₂ at port 4
inject 2.970 SCFM air at port 6
primary zone: ppmv NO = 875.0, % O₂ = 2.80, % CO₂ = 15.15, % CO = 0.10
exhaust : ppmv NO = 175.0, % O₂ = 2.20, % CO₂ = 13.45, % CO = 0.07
Temp. in K: T₁=1673, T₂= -- , T₃=1604, T₄= -- , T₅=1560, T₆= -- , T₇=1462

RUN: C# 22A, diffusion primary flame (type A)

Utah Bituminous # 3 coal in kg/h = 1.218, primary stoichiometry = 1.18
inject 0.100 SCFM natural gas and 0.500 SCFM N₂ at port 4
inject 0.514 SCFM air at port 6
primary zone: ppmv NO = 640.0, % O₂ = 4.70, % CO₂ = 12.75, % CO = 0.58
exhaust : ppmv NO = 415.0, % O₂ = 1.95, % CO₂ = 12.30, % CO = 0.32
Temp. in K: T₁=1548, T₂= -- , T₃=1598, T₄= -- , T₅=1487, T₆= -- , T₇=1347

RUN: C# 22B, diffusion primary flame (type A)

Utah Bituminous # 3 coal in kg/h = 1.218, primary stoichiometry = 1.18
inject 0.129 SCFM natural gas and 0.470 SCFM N₂ at port 4
inject 1.079 SCFM air at port 6
primary zone: ppmv NO = 575.0, % O₂ = 4.10, % CO₂ = 12.60, % CO = 0.92
exhaust : ppmv NO = 295.0, % O₂ = 2.00, % CO₂ = 12.30, % CO = 0.32
Temp. in K: T₁=1548, T₂= -- , T₃=1618, T₄= -- , T₅=1512, T₆= -- , T₇=1387

RUN: C# 22C, diffusion primary flame (type A)

Utah Bituminous # 3 coal in kg/h = 1.218, primary stoichiometry = 1.18
inject 0.149 SCFM natural gas and 0.455 SCFM N₂ at port 4
inject 1.428 SCFM air at port 6
primary zone: ppmv NO = 585.0, % O₂ = 3.30, % CO₂ = 13.00, % CO = 1.15
exhaust : ppmv NO = 225.0, % O₂ = 1.85, % CO₂ = 12.45, % CO = 0.50
Temp. in K: T₁=1548, T₂= -- , T₃=1627, T₄= -- , T₅=1529, T₆= -- , T₇=1411

RUN: C# 22D, diffusion primary flame (type A)

Utah Bituminous # 3 coal in kg/h = 1.218, primary stoichiometry = 1.18
inject 0.186 SCFM natural gas and 0.417 SCFM N₂ at port 4
inject 2.069 SCFM air at port 6
primary zone: ppmv NO = 595.0, % O₂ = 4.05, % CO₂ = 12.50, % CO = 1.03
exhaust : ppmv NO = 210.0, % O₂ = 2.55, % CO₂ = 12.30, % CO = 0.25
Temp. in K: T₁=1548, T₂= -- , T₃=1636, T₄= -- , T₅=1548, T₆= -- , T₇=1427

RUN: C# 22E, diffusion primary flame (type A)

Utah Bituminous # 3 coal in kg/h = 1.218, primary stoichiometry = 1.18
inject 0.234 SCFM natural gas and 0.367 SCFM N₂ at port 4
inject 2.485 SCFM air at port 6
primary zone: ppmv NO = 615.0, % O₂ = 3.35, % CO₂ = 13.00, % CO = 1.29
exhaust : ppmv NO = 165.0, % O₂ = 2.75, % CO₂ = 12.15, % CO = 0.21
Temp. in K: T₁=1548, T₂= -- , T₃=1645, T₄= -- , T₅=1552, T₆= -- , T₇=1459

RUN: C# 22F, diffusion primary flame (type A)

Utah Bituminous # 3 coal in kg/h = 1.218, primary stoichiometry = 1.18
inject 0.301 SCFM natural gas and 0.301 SCFM N₂ at port 4
inject 2.916 SCFM air at port 6
primary zone: ppmv NO = 610.0, % O₂ = 3.40, % CO₂ = 13.05, % CO = 1.32
exhaust : ppmv NO = 140.0, % O₂ = 3.50, % CO₂ = 11.90, % CO = 0.12
Temp. in K: T₁=1548, T₂= -- , T₃=1645, T₄= -- , T₅=1559, T₆= -- , T₇=1495

Detailed Measurements:

RUN: GAS# 1

SCFM natural gas = 0.600, primary stoichiometry = 1.10

PORT	K	% vol						ppm vol NO	ml/min WATER	ml/min GAS SAMPLE	ppmw N QUENCH	ppmw CN QUENCH	ppmw CN GAS*
		Temp	CO ₂	CO	H ₂	O ₂	CH ₄						
2	1498	9.70	0.05	0.00	2.00	0.00	0.00	38					
3	inject	0.175 SCFM natural gas and						0.300	SCFM	N ₂			
4	1402	8.85	1.17	1.02	0.10	1.39	0.11	26	62	2921	0.12	1.80	2.85
5	1348	8.80	1.48	1.59	0.00	0.98	0.16	20	61	2921	0.17	1.55	2.08
6	1302	8.50	1.90	1.87	0.00	0.73	0.14	28	62	2811	0.29	1.90	2.03
7	1250	8.55	1.92	1.82	0.10	0.64	0.12	26	60	3182	0.34	1.68	1.71

*bubbled for 5 minutes in 100 ml of 0.1 M NaOH solution

RUN: GAS# 2

SCFM natural gas = 0.600, primary stoichiometry = 1.10

PORT	K	% vol						ppm vol NO	ml/min WATER	ml/min GAS SAMPLE	ppmw N QUENCH	ppmw CN QUENCH	ppmw CN GAS*
		Temp	CO ₂	CO	H ₂	O ₂	CH ₄						
2	1478	9.58	0.05	0.04	2.18	0.00	0.00	863					
3	inject	0.175 SCFM natural gas and						0.300	SCFM	N ₂			
4	1401	9.05	1.05	0.88	0.15	1.08	0.08	420	53	3247	0.38	3.48	2.42
5	1352	9.00	1.40	1.32	0.10	0.61	0.10	305	56	3247	0.83	7.60	3.40
6	1304	8.95	1.45	1.39	0.15	0.64	0.10	265	55	3074	0.84	7.80	3.42
7	1249	8.90	1.50	1.45	0.15	0.67	0.11	250	56	3074	0.90	8.00	2.43

*bubbled for 5 minutes in 100 ml of 0.1 M NaOH solution

RUN: GAS# 3

SCFM natural gas = 0.600, primary stoichiometry = 1.10

PORT	K	% vol						ppm vol NO	ml/min WATER	ml/min GAS SAMPLE	ppmw N QUENCH	ppmw CN QUENCH	ppmw CN GAS*
		Temp	CO ₂	CO	H ₂	O ₂	CH ₄						
2	1503	9.75	0.05	0.00	2.08	0.00	0.00	193					
3	inject	0.169 SCFM natural gas and						0.300	SCFM	N ₂			
4	1407	9.10	1.15	0.98	0.10	1.19	0.09	104	48	3247	0.18	2.39	2.38
5	1353	9.00	1.50	1.40	0.10	0.70	0.11	77	50	3247	0.33	3.81	3.03
6	1305	8.95	1.55	1.52	0.10	0.68	0.11	71	54	3247	0.39	3.72	2.81
7	1254	8.95	1.60	1.56	0.10	0.63	0.10	69	45	3290	0.53	4.60	2.77

*bubbled for 5 minutes in 100 ml of 0.1 M NaOH solution

RUN: GAS# 4

SCFM natural gas = 0.600, primary stoichiometry = 1.11

PORT	K	% vol						ppm vol	ml/min QUENCH	ml/min GAS	ppmw N	ppmw CN	ppmw CN*	
		Temp	CO ₂	CO	H ₂	O ₂	CH ₄							C ₂ H ₂
2	1509	9.70	0.06	0.00	2.25	0.00	0.00	39						
3	inject	0.172 SCFM natural gas and						0.300	SCFM	N ₂				
4	1423	9.60	0.93	0.69	0.20	0.47	0.05	26	52	3204	0.07	0.90	1.19	
5	1370	9.10	1.45	1.51	0.10	0.75	0.14	19	51	3160	0.13	1.95	2.55	
6	1324	9.05	1.55	1.55	0.15	0.69	0.12	18	52	3247	0.16	2.15	2.85	
7	1271	9.00	1.60	1.61	0.15	0.67	0.12	18	52	3247	0.17	2.07	2.52	

*bubbled for 5 minutes in 100 ml of 0.1 M NaOH solution

RUN: GAS# 5

SCFM natural gas = 0.500, primary stoichiometry = 1.13

PORT	K	% vol						ppm vol	ml/min QUENCH	ml/min GAS	ppmw N	ppmw CN	ppmw CN*	
		Temp	CO ₂	CO	H ₂	O ₂	CH ₄							C ₂ H ₂
3	1393	9.45	0.05	0.01	2.68	0.00	0.00	29						
4	inject	0.151 SCFM natural gas and						0.333	SCFM	N ₂				
5	1274	9.10	0.88	0.79	0.20	0.84	0.09	15	47	3589	0.10	1.08	1.48	
6	1219	8.97	0.87	0.83	0.18	0.92	0.09	14	48	3589	0.14	1.06	1.42	
7	1158	8.97	0.87	0.80	0.13	0.95	0.08	14	50	3716	0.11	0.91	1.18	

*bubbled for 5 minutes in 100 ml of 0.1 M NaOH solution

RUN: GAS# 6

SCFM natural gas = 0.500, primary stoichiometry = 1.13

PORT	K	% vol						ppm vol	ml/min QUENCH	ml/min GAS	ppmw N	ppmw CN	ppmw CN*	
		Temp	CO ₂	CO	H ₂	O ₂	CH ₄							C ₂ H ₂
2	1415	9.45	0.05	0.01	2.68	0.00	0.00	29						
3	inject	0.151 SCFM natural gas and						0.333	SCFM	N ₂				
4	1349	9.00	0.84	0.72	0.15	0.92	0.04	14	52	3461	0.12	0.66	0.72	
5	1297	9.00	1.00	0.92	0.10	0.59	0.05	11	52	3461	0.23	1.18	1.43	
6	1246	8.95	1.00	0.88	0.10	0.70	0.08	15	55	3461	0.11	1.60	1.87	
7	1191	8.97	0.96	0.83	0.10	0.67	0.08	14	54	3504	0.10	1.47	1.80	

*bubbled for 5 minutes in 100 ml of 0.1 M NaOH solution

RUN: GAS# 7

SCFM natural gas = 0.500, primary stoichiometry = 1.13

PORT	K	% vol						ppm vol	ml/min QUENCH	ml/min GAS	ppmw N	ppmw CN	ppmw CN*	
		Temp	CO ₂	CO	H ₂	O ₂	CH ₄							C ₂ H ₂
1	1417	9.45	0.05	0.01	2.68	0.00	0.00	29						
2	inject	0.151 SCFM natural gas and						0.333	SCFM	N ₂				
3	1366	9.40	0.96	0.70	0.15	0.54	0.05	23	57	3461	0.08	1.11	1.05	
4	1338	9.10	1.07	0.87	0.10	0.67	0.07	19	60	2590	0.13	1.14	1.15	
5	1281	8.97	1.14	0.96	0.10	0.68	0.08	16	62	3461	0.09	1.63	1.92	
7	1179	8.95	1.16	1.05	0.10	0.89	0.09	16	64	3461	0.09	1.31	1.96	

*bubbled for 5 minutes in 100 ml of 0.1 M NaOH solution

RUN: COAL# 2

Utah Bituminous # 3 coal in kg/h = 0.918, primary stoichiometry = 1.06

PORT	K	% vol						ppm NO	ml/min WATER	ml/min GAS SAMPLE	ppmw N QUENCH	ppmw CN QUENCH	ppmw CN GAS*
		Temp	CO ₂	CO	H ₂	O ₂	CH ₄						
2	1518	16.33	0.08	0.00	1.25	0.00	0.00	908					
3	inject	0.248	SCFM	natural	gas	and	0.301	SCFM	N ₂				
4	1438	13.75	2.65	1.64	0.05	1.03	0.18	360	59	4092	2.00	3.58	2.50
5	1361	11.70	4.15	2.64	0.00	1.00	0.20	120	58	4502	3.21	8.70	5.61
6	1296	11.90	4.05	2.97	0.00	1.26	0.19	90	52	4298	3.59	10.20	6.13
7	1240	11.60	4.50	3.07	0.00	1.29	0.18	80	50	3988	3.81	10.80	6.12

*bubbled for 5 minutes in 100 ml of 0.1 M NaOH solution

RUN: COAL# 3

Utah Bituminous # 3 coal in kg/h = 0.930, primary stoichiometry = 1.26

PORT	K	% vol						ppm NO	ml/min WATER	ml/min GAS SAMPLE	ppmw N QUENCH	ppmw CN QUENCH	ppmw CN GAS*
		Temp	CO ₂	CO	H ₂	O ₂	CH ₄						
2	1488	13.68	0.05	0.00	4.35	0.00	0.00	835					
3	inject	0.248	SCFM	natural	gas	and	0.301	SCFM	N ₂				
4	1439	11.40	2.85	2.02	0.00	2.49	0.30	275	50	3988	1.20	5.83	3.19
5	1411	11.15	4.00	2.15	0.00	0.44	0.15	135	52	4092	2.20	6.29	3.40
6	1331	11.60	3.60	1.87	0.00	0.38	0.10	100	53	4298	2.78	5.62	2.64
7	1269	11.35	3.65	1.86	0.00	0.44	0.10	85	57	3461	2.67	4.73	1.70

*bubbled for 5 minutes in 100 ml of 0.1 M NaOH solution

RUN: COAL# 4

Utah Bituminous # 3 coal in kg/h = 0.930, primary stoichiometry = 1.24

PORT	K	% vol						ppm NO	ml/min WATER	ml/min GAS SAMPLE	ppmw N QUENCH	ppmw CN QUENCH	ppmw CN GAS*
		Temp	CO ₂	CO	H ₂	O ₂	CH ₄						
2	1464	13.90	0.05	0.00	4.20	0.00	0.00	870					
3	inject	0.089	SCFM	natural	gas	and	0.462	SCFM	N ₂				
4	1383	12.35	0.45	0.20	0.90	0.10	0.02	450	45	4196	0.12	0.15	0.25
5	1347	12.55	0.20	0.15	0.65	0.01	0.00	395	47	4092	0.12	0.19	0.15
6	1287	12.60	0.18	0.17	0.65	0.01	0.00	420	47	4092	0.08	0.18	0.19
7	1208	12.70	0.15	0.12	0.65	0.01	0.00	450	50	3884	0.09	0.23	0.13

*bubbled for 5 minutes in 100 ml of 0.1 M NaOH solution

RUN: COAL# 5

Utah Bituminous # 3 coal in kg/h = 0.840, primary stoichiometry = 1.24

PORT	K	% vol						ppm NO	ml/min WATER	ml/min GAS SAMPLE	ppmw N QUENCH	ppmw CN QUENCH	ppmw CN GAS*
		Temp	CO ₂	CO	H ₂	O ₂	CH ₄						
2	1505	14.02	0.05	0.00	4.15	0.00	0.00	825					
3	inject	0.583	SCFM	CO	and	0.194	SCFM	N ₂					
4	1567	19.50	5.55	0.61	0.00	0.00	0.00	695	47	3884	0.17	0.64	0.18
5	1442	20.40	3.60	0.44	0.00	0.00	0.00	670	47	4092	0.24	0.40	0.14
6	1354	20.50	3.05	0.43	0.00	0.00	0.00	625	45	4196	0.34	0.29	0.15
7	1274	20.30	2.95	0.45	0.00	0.00	0.00	540	47	4196	0.61	0.11	0.18

*bubbled for 5 minutes in 100 ml of 0.1 M NaOH solution

RUN: COAL# 6

Utah Bituminous # 3 coal in kg/h = 1.092, stoichiometry = 0.93
 add 0.254 SCFM O₂, primary stoichiometry = 1.18

PORT	K	% vol						ppm vol	ml/min QUENCH NO	ml/min GAS WATER	ml/min SAMPLE	ppmw N	ppmw CN	ppmw CN*
		Temp	CO ₂	CO	H ₂	O ₂	CH ₄							
2	1582	19.02	0.13	0.00	3.22	0.00	0.00	1240						
3	inject 0.248 SCFM natural gas and 0.301 SCFM N ₂													
4	1446	14.40	4.25	2.74	0.00	2.60	0.26	250	51	3547	1.44	7.55	3.50	
5	1352	14.20	4.95	3.10	0.00	0.99	0.22	175	48	3568	2.60	11.10	4.30	
6	1293	13.90	5.15	3.30	0.00	0.92	0.21	125	50	3461	2.22	11.00	4.50	
7	1238	13.85	5.10	3.43	0.00	0.94	0.20	80	55	3461	2.63	10.50	5.30	

*bubbled for 5 minutes in 100 ml of 0.1 M NaOH solution

RUN: COAL# 7

Utah Bituminous # 3 coal in kg/h = 1.660, primary stoichiometry = 1.12

PORT	K	% vol						ppm vol	ml/min QUENCH NO	ml/min GAS WATER	ml/min SAMPLE	ppmw N	ppmw CN	ppmw CN*
		Temp	CO ₂	CO	H ₂	O ₂	CH ₄							
2	1702	15.60	0.04	0.00	2.30	0.00	0.00	1085						
3	inject 0.234 SCFM natural gas and 0.246 SCFM N ₂													
4	1612	12.95	3.55	1.54	0.10	0.56	0.19	435	50	3359	1.10	4.32	2.00	
5	1568	13.00	3.75	1.14	0.05	0.05	0.03	365	55	3461	1.17	1.33	0.51	
6	1513	13.00	3.95	1.18	0.00	0.03	0.01	300	52	3547	1.08	0.67	0.24	
7	1456	12.80	4.15	1.43	0.00	0.02	0.01	240	50	3547	1.10	0.44	0.21	

*bubbled for 5 minutes in 100 ml of 0.1 M NaOH solution

RUN: COAL# 8

Utah Bituminous # 3 coal in kg/h = 0.960, primary stoichiometry = 1.23

PORT	K	% vol						ppm vol	ml/min QUENCH NO	ml/min GAS WATER	ml/min SAMPLE	ppmw N	ppmw CN	ppmw CN*
		Temp	CO ₂	CO	H ₂	O ₂	CH ₄							
2	1543	13.98	0.05	0.00	3.92	0.00	0.00	870						
3	inject 0.659 SCFM H ₂ and 0.211 SCFM N ₂													
4	1481	7.90	4.50	5.84	0.05	0.00	0.00	760	49	3419	0.34	0.31	0.24	
5	1448	9.75	3.50	2.40	0.00	0.00	0.00	805	50	3504	0.28	0.30	0.09	
6	1371	9.80	3.35	2.44	0.00	0.00	0.00	790	57	3504	0.30	0.20	0.11	
7	1286	10.25	3.10	2.64	0.00	0.00	0.00	755	47	3568	0.74	0.26	0.11	

*bubbled for 5 minutes in 100 ml of 0.1 M NaOH solution

RUN: COAL# 9

Utah Bituminous # 3 coal in kg/h = 0.973, primary stoichiometry = 1.11

PORT	K	% vol						ppm vol	ml/min QUENCH NO	ml/min GAS WATER	ml/min SAMPLE	ppmw N	ppmw CN	ppmw CN*
		Temp	CO ₂	CO	H ₂	O ₂	CH ₄							
2	1517	15.55	0.09	0.00	2.08	0.00	0.00	920						
3	inject 0.253 SCFM natural gas and 0.301 SCFM N ₂													
4	1447	11.75	3.00	2.39	0.00	2.94	0.27	250	47	3247	1.30	6.61	2.34	
5	1361	11.70	3.65	2.68	0.00	1.48	0.27	145	49	3247	1.70	8.33	2.85	
6	1298	11.65	3.70	2.93	0.00	1.48	0.25	115	49	3247	1.80	8.09	3.62	
7	1228	11.85	3.65	2.83	0.00	1.45	0.20	80	52	3354	2.15	8.85	3.43	

*bubbled for 5 minutes in 100 ml of 0.1 M NaOH solution

RUN: COAL#10

Utah Bituminous # 3 coal in kg/h = 0.973, primary stoichiometry = 1.10

PORT	K	% vol						ppm vol NO	ml/min QUENCH WATER	ml/min GAS SAMPLE	ppmw N QUENCH	ppmw CN QUENCH	ppmw CN GAS*
		Temp	CO ₂	CO	H ₂	O ₂	CH ₄						
2	1521	15.75	0.09	0.00	2.03	0.00	0.00	895					
3	inject 0.129 SCFM natural gas and 0.425 SCFM N ₂												
4	1448	12.60	1.60	0.57	0.20	0.49	0.06	365	59	3290	0.62	2.82	1.20
5	1380	12.05	2.30	1.03	0.05	0.39	0.07	165	50	3290	1.53	6.71	1.89
6	1312	12.15	2.35	1.08	0.00	0.39	0.06	150	50	3268	1.45	4.70	1.91
7	1239	12.15	2.35	1.07	0.00	0.45	0.06	135	55	3247	1.60	5.42	2.14

*bubbled for 5 minutes in 100 ml of 0.1 M NaOH solution

RUN: COAL#11

Utah Bituminous # 3 coal in kg/h = 1.148, primary stoichiometry = 0.93

PORT	K	% vol						ppm vol NO	ml/min QUENCH WATER	ml/min GAS SAMPLE	ppmw N QUENCH	ppmw CN QUENCH	ppmw CN GAS*
		Temp	CO ₂	CO	H ₂	O ₂	CH ₄						
2	1469	16.45	1.35	0.00	0.00	0.00	0.00	590					
3	inject 0.186 SCFM natural gas and 0.403 SCFM N ₂												
4	1307	11.90	2.40	1.33	0.00	2.81	0.08	295	68	3247	1.15	3.30	12.50
5	1247	11.65	2.85	2.14	0.00	2.62	0.13	185	46	3504	2.52	8.70	20.20
6	1204	11.80	3.15	2.44	0.00	2.29	0.13	120	49	3884	2.95	12.70	20.50
7	1156	11.90	3.10	2.03	0.00	0.82	0.13	90	49	3030	2.60	11.90	19.10

*bubbled for 5 minutes in 100 ml of 0.1 M NaOH solution

RUN: COAL#12

Utah Bituminous # 3 coal in kg/h = 1.077, primary stoichiometry = 1.12

PORT	K	% vol						ppm vol NO	ml/min QUENCH WATER	ml/min GAS SAMPLE	ppmw N QUENCH	ppmw CN QUENCH	ppmw CN GAS*
		Temp	CO ₂	CO	H ₂	O ₂	CH ₄						
2	1577	15.23	0.09	0.00	2.30	0.00	0.00	980					
3	inject 0.158 SCFM natural gas and 0.403 SCFM N ₂												
4	1528	12.85	1.80	0.73	0.15	0.54	0.08	385	66	2811	0.55	2.70	3.20
5	1457	12.45	2.50	0.98	0.00	0.21	0.07	190	47	2478	1.34	3.40	3.60
6	1393	12.30	2.80	1.26	0.00	0.38	0.09	145	48	2366	1.54	5.90	6.80
7	1333	12.30	2.55	1.17	0.00	0.33	0.07	130	48	2366	1.89	5.50	3.60

*bubbled for 5 minutes in 100 ml of 0.1 M NaOH solution

RUN: COAL#13

Utah Bituminous # 3 coal in kg/h = 1.077, primary stoichiometry = 1.10

PORT	K	% vol						ppm vol NO	ml/min QUENCH WATER	ml/min GAS SAMPLE	ppmw N QUENCH	ppmw CN QUENCH	ppmw CN GAS*
		Temp	CO ₂	CO	H ₂	O ₂	CH ₄						
2	1578	15.50	0.13	0.00	2.00	0.00	0.00	945					
3	inject 0.158 SCFM natural gas and 0.403 SCFM N ₂ and 0.0021 SCFM NH ₃												
4	1524	11.90	2.65	1.15	0.05	0.78	0.11	260	67	2254	2.40	4.50	7.80
5	1485	12.20	3.15	1.15	0.00	0.18	0.06	165	65	2478	1.36	2.90	8.90
6	1432	12.05	3.20	1.17	0.00	0.17	0.05	115	66	2701	2.06	4.40	9.80
7	1364	12.30	3.10	1.37	0.00	0.16	0.04	85	54	2478	2.44	3.00	7.20

*bubbled for 5 minutes in 100 ml of 0.1 M NaOH solution

RUN: C# 14A

Utah Bituminous # 3 coal in kg/h = 1.074, primary stoichiometry = 1.18

PORT	K	% vol						ppm NO	ml/min WATER	ml/min GAS	ppmw N	ppmw CN	ppmw CN*
		CO ₂	CO	H ₂	O ₂	CH ₄	C ₂ H ₂						
2	1605	14.45	0.07	0.00	3.20	0.00	0.00	885					
3		inject 0.115 SCFM natural gas and 0.440 SCFM N ₂											
5	1452	13.05	1.05	0.27	0.25	0.04	0.01	330	59	2366	0.44	0.39	0.31
6		inject 0.889 SCFM air											
7	1303	12.60	0.10	0.00	1.80	0.00	0.00	305					

*bubbled for 5 minutes in 100 ml of 0.1 M NaOH solution

RUN: C# 14B

Utah Bituminous # 3 coal in kg/h = 1.074, primary stoichiometry = 1.18

PORT	K	% vol						ppm NO	ml/min WATER	ml/min GAS	ppmw N	ppmw CN	ppmw CN*
		CO ₂	CO	H ₂	O ₂	CH ₄	C ₂ H ₂						
2	1605	14.45	0.07	0.00	3.20	0.00	0.00	885					
3		inject 0.132 SCFM natural gas and 0.417 SCFM N ₂											
5	1450	12.85	1.35	0.40	0.20	0.07	0.02	275	51	2501	0.57	1.45	0.56
6		inject 1.079 SCFM air											
7	1310	12.60	0.08	0.00	1.90	0.00	0.00	240					

*bubbled for 5 minutes in 100 ml of 0.1 M NaOH solution

RUN: C# 14C

Utah Bituminous # 3 coal in kg/h = 1.074, primary stoichiometry = 1.18

PORT	K	% vol						ppm NO	ml/min WATER	ml/min GAS	ppmw N	ppmw CN	ppmw CN*
		CO ₂	CO	H ₂	O ₂	CH ₄	C ₂ H ₂						
2	1605	14.45	0.07	0.00	3.20	0.00	0.00	885					
3		inject 0.172 SCFM natural gas and 0.381 SCFM N ₂											
5	1480	12.30	2.70	0.83	0.05	0.13	0.05	205	50	2366	1.09	5.45	1.18
6		inject 1.506 SCFM air											
7	1352	12.05	0.07	0.00	2.70	0.00	0.00	175					

*bubbled for 5 minutes in 100 ml of 0.1 M NaOH solution

RUN: C# 14D

Utah Bituminous # 3 coal in kg/h = 1.074, primary stoichiometry = 1.18

PORT	K	% vol						ppm NO	ml/min WATER	ml/min GAS	ppmw N	ppmw CN	ppmw CN*
		CO ₂	CO	H ₂	O ₂	CH ₄	C ₂ H ₂						
2	1605	14.45	0.07	0.00	3.20	0.00	0.00	885					
3		inject 0.207 SCFM natural gas and 0.347 SCFM N ₂											
5	1488	12.05	3.55	1.23	0.03	0.15	0.07	180	49	2254	1.03	4.20	2.60
6		inject 1.906 SCFM air											
7	1362	12.45	0.15	0.00	2.25	0.00	0.00	130					

*bubbled for 5 minutes in 100 ml of 0.1 M NaOH solution

RUN: C# 14E

Utah Bituminous # 3 coal in kg/h = 1.074, primary stoichiometry = 1.18

PORT	K	% vol						vol NO	ml/min QUENCH WATER	ml/min GAS SAMPLE	ppmw N QUENCH	ppmw CN QUENCH	ppmw CN GAS*	
		Temp	CO ₂	CO	H ₂	O ₂	CH ₄							C ₂ H ₂
2	1605	14.45	0.07	0.00	3.20	0.00	0.00	885						
3	inject	0.271 SCFM natural gas and 0.278 SCFM N ₂												
5	1490	10.60	5.40	2.57	0.00	0.41	0.19	120	62	2254	1.09	9.60	6.80	
6	inject	2.570 SCFM air												
7	1408	12.15	0.07	0.00	2.90	0.00	0.00	130						

*bubbled for 5 minutes in 100 ml of 0.1 M NaOH solution

RUN: COAL#15

Utah Bituminous # 3 coal in kg/h = 1.068, primary stoichiometry = 1.29

PORT	K	% vol						vol NO	ml/min QUENCH WATER	ml/min GAS SAMPLE	ppmw N QUENCH	ppmw CN QUENCH	ppmw CN GAS*	
		Temp	CO ₂	CO	H ₂	O ₂	CH ₄							C ₂ H ₂
2	1582	13.13	0.03	0.00	4.75	0.00	0.00	825						
3	inject	0.643 kg/h Utah Bituminous # 3 coal and 0.591 SCFM N ₂												
4	1526	12.20	2.30	0.98	0.25	0.08	0.07	405	57	2140	1.32	13.50	8.65	
5	1486	13.80	2.40	0.97	0.20	0.05	0.02	285	60	2276	1.21	3.00	3.50	
6	1432	13.95	2.40	0.69	0.00	0.04	0.01	270	61	2545	0.98	2.30	7.00	
7	1376	14.20	2.40	0.70	0.00	0.02	0.01	170	43	2701	1.24	1.70	4.95	
6	inject	2.275 SCFM air												
7	--	12.85	0.05	0.00	3.60	0.00	0.00	150						

*bubbled for 5 minutes in 100 ml of 0.1 M NaOH solution

RUN: COAL#16

Utah Bituminous # 3 coal in kg/h = 1.068, primary stoichiometry = 1.23

PORT	K	% vol						vol NO	ml/min QUENCH WATER	ml/min GAS SAMPLE	ppmw N QUENCH	ppmw CN QUENCH	ppmw CN GAS*	
		Temp	CO ₂	CO	H ₂	O ₂	CH ₄							C ₂ H ₂
2	1588	13.53	0.05	0.00	4.05	0.00	0.00	885						
3	inject	0.291 SCFM natural gas and 0.301 SCFM N ₂												
4	1530	13.75	1.80	0.48	0.55	0.07	0.03	470	52	2276	0.40	2.30	2.90	
5	1452	10.95	4.95	2.62	0.00	0.55	0.18	110	46	2276	1.83	6.80	10.90	
6	1401	10.95	4.95	2.47	0.00	0.35	0.12	90	49	2276	1.80	7.70	8.30	
7	1343	10.95	5.10	2.34	0.00	0.30	0.09	65	56	2276	1.90	8.20	7.15	
6	inject	2.234 SCFM air												
7	--	12.00	0.06	0.00	2.50	0.00	0.00	145						

*bubbled for 5 minutes in 100 ml of 0.1 M NaOH solution

RUN: COAL#17

Utah Bituminous # 3 coal in kg/h = 1.331, primary stoichiometry = 1.12

PORT	K	% vol						ppm NO	ml/min WATER	ml/min SAMPLE	ppmw QUENCH N	ppmw QUENCH CN	ppmw GAS* CN
		Temp	CO ₂	CO	H ₂	O ₂	CH ₄						
2	1621	15.23	0.12	0.00	2.35	0.00	0.00	818					
3	inject 0.314 kg/h Utah Bituminous # 3 coal and 0.725 SCFM N ₂												
4	1533	14.55	1.00	0.22	0.70	0.01	0.01	510	56	2140	0.58	1.75	0.44
5	1466	14.20	1.35	0.26	0.30	0.01	0.01	405	58	2140	0.58	1.34	0.43
6	1419	14.10	1.15	0.29	0.30	0.01	0.00	395	57	2276	0.33	0.47	0.24
7	1351	14.50	1.05	0.32	0.10	0.01	0.00	305	56	2276	0.59	0.24	0.25
6	inject 1.585 SCFM air												
7	--	12.80	0.05	0.00	3.50	0.00	0.00	280					

*bubbled for 5 minutes in 100 ml of 0.1 M NaOH solution

RUN: COAL#18

Utah Bituminous # 3 coal in kg/h = 1.331, primary stoichiometry = 1.10

PORT	K	% vol						ppm NO	ml/min WATER	ml/min SAMPLE	ppmw QUENCH N	ppmw QUENCH CN	ppmw GAS* CN
		Temp	CO ₂	CO	H ₂	O ₂	CH ₄						
2	1621	15.45	0.15	0.00	2.15	0.00	0.00	795					
3	inject 0.149 SCFM natural gas and 0.440 SCFM N ₂												
5	1466	12.30	2.95	1.19	0.00	0.22	0.06	200	56	2276	1.20	3.90	2.10
6	1419	12.30	2.95	1.11	0.00	0.22	0.06	145	57	2276	1.16	4.32	2.04
7	1351	12.40	3.00	1.14	0.00	0.19	0.03	95	58	2276	1.86	2.77	0.64

*bubbled for 5 minutes in 100 ml of 0.1 M NaOH solution

RUN: COAL#19

Utah Bituminous # 3 coal in kg/h = 1.315, primary stoichiometry = 1.10

PORT	K	% vol						ppm NO	ml/min WATER	ml/min SAMPLE	ppmw QUENCH N	ppmw QUENCH CN	ppmw GAS* CN
		Temp	CO ₂	CO	H ₂	O ₂	CH ₄						
2	1622	15.28	0.14	0.00	1.95	0.00	0.00	865					
3	inject 0.138 SCFM natural gas and 0.440 SCFM N ₂												
4	1543	13.30	1.45	0.35	0.30	0.10	0.02	395	57	2254	0.57	2.53	1.20
5	1490	12.80	1.65	0.63	0.10	0.14	0.03	250	59	2254	0.69	2.25	1.34
6	1425	12.85	1.60	0.66	0.15	0.13	0.03	240	60	2140	0.82	1.43	0.86
7	1384	12.50	2.25	0.91	0.00	0.15	0.02	135	57	2366	1.75	2.27	0.50
6	inject 1.467 SCFM air												
7	--	12.05	0.10	0.00	2.20	0.00	0.00	205					

*bubbled for 5 minutes in 100 ml of 0.1 M NaOH solution

RUN: COAL#20

Utah Bituminous # 3 coal in kg/h = 1.315, primary stoichiometry = 1.08

PORT	K	% vol						vol	ml/min	ml/min	ppmw	ppmw	ppmw
		CO ₂	CO	H ₂	O ₂	CH ₄	C ₂ H ₂						
Temp							NO	WATER	SAMPLE	QUENCH	QUENCH	GAS*	
2	1621	15.53	0.21	0.00	1.65	0.00	0.00	895					
3	inject	0.138	SCFM	natural gas	and	0.440	SCFM	N ₂	and	0.0023	SCFM	NH ₃	
4	1558	13.35	1.60	0.48	0.40	0.12	0.02	425	57	2254	0.61	0.91	1.05
5	1509	12.50	2.45	0.78	0.00	0.11	0.02	160	55	2276	1.27	2.80	1.00
6	1444	12.45	2.35	0.78	0.00	0.13	0.04	185	55	2276	0.75	1.65	1.73
7	1391	12.45	2.40	0.70	0.05	0.10	0.02	160	57	2254	1.49	2.95	0.67
6	inject	1.467	SCFM	air									
7	--	11.90	0.10	0.00	2.20	0.00	0.00	210					

*bubbled for 5 minutes in 100 ml of 0.1 M NaOH solution

RUN: COAL#21

Utah Bituminous # 3 coal in kg/h = 1.369, primary stoichiometry = 1.10

PORT	K	% vol						vol	ml/min	ml/min	ppmw	ppmw	ppmw
		CO ₂	CO	H ₂	O ₂	CH ₄	C ₂ H ₂						
Temp							NO	WATER	SAMPLE	QUENCH	QUENCH	GAS*	
2	1690	15.00	0.30	0.00	2.50	0.00	0.00	650					
3	inject	0.158	SCFM	natural gas	and	0.410	SCFM	N ₂					
4	1634	12.85	3.00	1.15	0.20	0.22	0.05	355	67	2276	1.14	3.42	0.97
5	1554	12.45	3.90	1.58	0.05	0.12	0.04	215	46	2276	1.61	2.95	0.93
6	1502	12.70	3.30	1.15	0.15	0.06	0.01	235	43	2276	1.80	3.17	0.45
7	1448	13.00	2.55	0.84	0.25	0.04	0.01	270	41	2276	1.32	2.40	0.42

*bubbled for 5 minutes in 100 ml of 0.1 M NaOH solution

APPENDIX B:

REDUCED EXPERIMENTAL DATA

Graphical Presentation of the Results

Figure 3.3	BL# 1, UB# 1
Figure 3.4	UB# 2, UB# 5A, UB# 4
Figure 3.5	UB# 6A, UB# 5B
Figure 3.6	UB# 3A
Figure 3.7	UB# 5A, UB# 4, UB# 4B, UB# 6A, UB# 5B, UB# 3A
Figure 4.1	Table 4.5, Table 4.9
Figure 4.2	Table 4.9
Figure 4.3	Table 4.5, Table 4.13
Figure 4.4	Table 4.13
Figure 4.5	MR# 9-23
Figure 4.6	RV# 1-20
Figure 4.7	RB# 1-7, Table 4.9
Figure 4.8	RB# 1-7, Table 4.13
Figure 4.9	RH# 1-18
Figure 5.1	RR# 1-17
Figure 5.2	RB# 1-7
Figure 5.3	Coal # 14 (C# 14)
Figure 5.4	Coal # 7, Coal # 21
Figure 5.5	Coal # 22 (C# 22)
Figure 6.1	Coal # 2, Coal # 9
Figure 6.2	Coal # 10, Coal # 12, Coal # 7
Figure 6.3	Coal # 3, Coal # 6
Figure 6.4	Coal # 4, Coal # 10, Coal # 2
Figure 6.5	Coal # 5, Coal # 8
Figure 6.6	Gas # 7, Gas # 4
Figure 6.7	Gas # 7, Gas # 4
Figure 6.8	Coal # 10, Gas # 2
Figure 6.9	Coal # 12, Coal # 13
Figure 6.10	Coal # 3, Coal # 15
Figure 6.11	Coal # 19, Coal # 20, Coal # 17
Figure 7.1	Run # 15 (Bose, 1989), Coal # 2
Figure 7.2	Gas # 2, Gas # 3, Gas # 4, Gas # 5, Gas # 7
Figure 7.3	Coal # 2
Figure 7.4	Gas # 2, Gas # 3, Gas # 4
Figure 7.5	Coal # 19, Coal # 6, Coal # 9
Figure 7.6	Coal # 10, Coal # 7
Figure 7.7	Gas # 1-7, Coal # 2,3,6,7,9,10,12,16,18,19
Figure 7.8	Run # 1, Run # 2 (Bose, 1989)
Figure 7.9	Run # 3, Run # 4 (Bose, 1989)
Figure 7.10	Run # 13, Run # 9, Run # 11 (Bose, 1989)
Figure 7.11	Run # 1-4, 7-11, 13, 15, 22 (Bose, 1989)
Figure 7.12	UB# 5A, Run # 13 (Bose, 1989)
Figure 7.13	Gas # 1-7, Coal # 2,3,6,7,9,10
Figure 8.1	Coal # 2,3,6,7,9,10,12,19
Figure 8.2	Coal # 2
Figure 8.3	Coal # 7, Coal # 6, Coal # 2
Figure 8.4	Coal # 14 (C# 14), Coal # 15,16,17,19,20
Figure 8.5	RB# 1-7, Table 4.13, FINAL.FOR
Figure 8.6	FINAL.FOR
Figure 8.7	Coal # 7, Coal # 12
Figure 8.8	Run # 2, Run # 4 (Bose, 1989)
Figure 8.9	Coal # 7, Coal # 12
Figure 8.10	Run # 7, Run # 4 (Bose, 1989)

NO AND N₂O MEASUREMENTS

RUN: BL# 1, NO and N₂O vs. SR for Beulah Lignite Coal Flame

SR	% vol					ppmv wet		ppmv dry, 0% O ₂	
	CO ₂	CO	H ₂ O	O ₂	N ₂	NO	N ₂ O	NO	N ₂ O
1.230	13.46	0.45	10.25	3.59	72.25	560.9	1.53	761.9	2.07
1.190	14.05	0.90	10.49	3.09	71.48	537.1	0.00	713.4	0.00
1.160	14.28	1.07	10.72	2.68	71.24	500.0	0.89	649.5	1.16
1.110	15.01	0.71	11.20	1.86	71.22	484.0	0.98	601.9	1.21
1.100	14.92	1.42	11.21	1.78	70.67	426.2	0.80	529.3	0.99
1.060	15.03	1.77	11.61	1.10	70.49	371.2	1.06	445.4	1.27
1.040	15.22	1.01	11.77	1.85	70.14	392.6	0.88	464.5	1.04
0.940	15.60	1.57	12.86	0.70	69.28	270.1	0.78	292.5	0.85
0.840	15.46	2.23	14.11	0.26	67.94	137.4	0.34	135.6	0.34

RUN: UB# 1, NO and N₂O vs. SR for Utah Bituminous # 2 Coal Flame

SR	K peak Temp	% vol					ppmv wet		ppmv dry, 0% O ₂	
		CO ₂	CO	H ₂ O	O ₂	N ₂	NO	N ₂ O	NO	N ₂ O
0.750	1529	14.40	3.37	10.00	0.00	72.22	238.5	0.42	200.8	0.36
0.790	1594	14.88	2.76	9.57	0.00	72.80	339.1	0.55	298.4	0.49
0.840	1605	15.59	2.00	9.07	0.00	73.34	427.4	0.63	396.9	0.58
0.906	1609	16.33	0.94	8.51	0.00	74.22	631.3	0.69	624.7	0.68
0.983	1597	16.43	0.17	7.96	0.14	75.31	754.7	0.89	798.4	0.94
1.044	1600	16.00	0.05	7.53	0.83	75.60	897.0	1.39	1003.8	1.55
1.093	1564	15.26	0.05	7.21	1.67	75.81	914.0	1.07	1067.7	1.25
1.095	1588	15.27	0.05	7.19	1.72	75.78	951.3	1.13	1113.8	1.33
1.120	1537	14.68	0.04	7.06	2.14	76.08	855.0	1.12	1019.8	1.34
1.185	1543	14.28	0.03	6.66	3.13	75.91	877.4	0.91	1109.7	1.15
1.250	1518	13.11	0.03	6.36	3.98	76.52	842.7	0.96	1115.2	1.28

RUN: UB# 2, Utah Bituminous # 2 Coal, Stoichiometry = 1.15

sec RT	K Temp	% vol					ppmv wet		ppmv dry, 0% O ₂	
		CO ₂	CO	H ₂ O	O ₂	N ₂	NO	N ₂ O	NO	N ₂ O
0.240	1513	15.64	0.09	6.88	1.21	76.17	689.1	1.12	842.9	1.37
0.447	1477	15.32	0.08	6.89	1.44	76.26	744.9	1.12	910.0	1.36
0.660	1403	14.90	0.07	6.88	2.05	76.11	745.0	1.12	912.0	1.37
0.882	1364	14.71	0.07	6.87	2.33	76.01	786.9	1.12	964.6	1.37
1.315	1282	14.71	0.08	6.87	2.33	76.00	810.2	1.86	993.2	2.28
1.751	1173	14.85	0.08	6.87	2.24	75.96	805.6	1.86	988.1	2.28
2.226	1075	14.67	0.07	6.87	2.44	75.95	791.6	0.93	971.1	1.14

RUN: UB# 5A, Utah Bituminous # 2 Coal, Stoichiometry = 0.86

sec	K	% vol					ppmv wet		ppmv dry, 0% O ₂	
		RT	Temp	CO ₂	CO	H ₂ O	O ₂	N ₂	NO	N ₂ O
0.303	1548	15.10	0.36	9.03	0.73	74.78	727.7	0.76	678.5	0.70
0.560	1510	15.47	0.52	9.00	0.50	74.51	846.3	0.86	791.9	0.80
0.824	1468	15.61	0.52	9.01	0.32	74.55	837.2	0.79	782.9	0.74
1.094	1428	15.74	0.61	8.99	0.23	74.43	810.0	0.77	758.7	0.72
1.627	1320	15.93	0.55	8.99	0.14	74.40	773.6	1.40	724.9	1.31
2.163	1231	15.79	0.68	8.99	0.09	74.44	705.3	0.74	660.5	0.69
2.731	1173	15.61	0.82	9.00	0.09	74.49	605.2	1.15	566.4	1.07

RUN: UB# 4A, Utah Bituminous # 2 Coal, Stoichiometry = 0.64

sec	K	% vol					ppmv wet		ppmv dry, 0% O ₂	
		RT	Temp	CO ₂	CO	H ₂ O	O ₂	N ₂	NO	N ₂ O
0.425	1463	13.03	3.31	11.67	0.00	71.99	278.2	0.88	200.7	0.64
0.803	1344	13.08	3.53	11.64	0.00	71.75	335.8	0.71	243.0	0.51
1.203	1307	13.08	3.49	11.64	0.00	71.79	344.6	0.53	249.2	0.38
1.615	1264	13.17	3.58	11.62	0.00	71.63	327.0	0.53	237.0	0.38
2.423	1178	13.17	3.58	11.62	0.00	71.63	282.8	0.53	205.0	0.38
3.236	1119	12.35	3.31	11.77	0.00	72.57	242.6	0.71	173.6	0.51
4.089	1065	12.53	3.27	11.75	0.00	72.45	220.6	1.15	158.1	0.82

RUN: UB# 4B, Utah Bituminous # 2, Air Staging

sec	K	% vol					ppmv wet		ppmv dry, 0% O ₂		
		RT	Temp	CO ₂	CO	H ₂ O	O ₂	N ₂	NO	N ₂ O	NO
Stoichiometry = 0.63											
0.435	1435	13.68	3.13	11.77	0.00	71.42	291.2	0.79	208.4	0.57	
0.816	1383	13.67	2.91	11.80	0.00	71.62	317.5	1.06	226.6	0.76	
1.212	1333	14.02	2.07	11.82	0.35	71.74	308.6	3.00	219.9	2.14	
Stoichiometry = 1.11											
1.943	1204	12.91	0.05	7.10	3.99	75.94	153.3	8.08	181.7	9.58	
2.417	1182	13.00	0.04	7.12	3.67	76.17	153.2	7.52	181.2	8.89	
2.907	1120	13.33	0.04	7.11	3.53	76.00	144.0	6.13	170.6	7.26	

RUN: UB# 6A, Utah Bituminous # 2, Air Staging

sec	K	% vol					ppmv wet		ppmv dry, 0% O ₂		
		RT	Temp	CO ₂	CO	H ₂ O	O ₂	N ₂	NO	N ₂ O	NO
Stoichiometry = 0.66											
0.406	1403	13.31	3.68	11.28	0.00	71.73	363.7	0.49	271.5	0.36	
0.757	1398	13.31	3.68	11.28	0.00	71.73	363.7	0.49	271.5	0.36	
1.115	1358	13.44	3.33	11.29	0.18	71.77	319.4	0.60	238.3	0.45	
Stoichiometry = 1.11											
1.812	1194	13.84	0.05	7.12	3.11	75.88	181.1	5.11	214.2	6.04	
2.275	1145	13.75	0.05	7.12	3.16	75.93	181.1	3.53	214.1	4.17	
2.763	1073	13.75	0.05	7.12	3.25	75.84	185.8	3.25	219.8	3.85	

RUN: UB# 5B, Utah Bituminous # 2, Air Staging

sec	K	% vol					ppmv wet		ppmv dry, 0% O ₂		
		RT	Temp	CO ₂	CO	H ₂ O	O ₂	N ₂	NO	N ₂ O	NO
Stoichiometry = 0.88											
0.307	1473	15.13	0.32	8.83	0.91	74.80	857.0	0.84	817.2	0.80	
0.570	1451	15.13	0.32	8.83	0.91	74.80	857.0	0.84	817.2	0.80	
0.843	1373	15.00	0.46	8.83	0.91	74.80	788.6	0.96	752.0	0.91	
Stoichiometry = 1.10											
1.530	1238	13.04	0.04	7.16	3.90	75.86	515.2	2.68	605.6	3.15	
1.971	1228	13.46	0.05	7.16	3.48	75.85	552.4	1.59	649.4	1.87	
2.430	1153	13.32	0.04	7.19	3.34	76.11	524.4	1.73	614.3	2.02	

RUN: UB# 3A, Utah Bituminous # 2, Reburning with Natural Gas

sec	K	% vol					ppmv wet		ppmv dry, 0% O ₂		
		RT	Temp	CO ₂	CO	H ₂ O	O ₂	N ₂	NO	N ₂ O	NO
Stoichiometry = 1.10											
0.251	1513	14.85	0.12	7.19	1.76	76.08	649.7	1.02	761.1	1.20	
0.467	1448	15.60	0.08	7.16	1.39	75.77	770.6	1.02	906.4	1.20	
Stoichiometry = 0.90											
0.907	1373	13.06	2.10	10.83	0.54	73.48	325.5	0.54	394.8	0.65	
Stoichiometry = 1.06											
1.654	1223	13.01	0.06	9.37	2.85	74.70	271.9	1.63	381.0	2.29	
2.046	1161	12.46	0.04	9.36	3.49	74.65	271.9	3.17	381.3	4.45	

Description of the Variables.

- X_1 = Length of Reburn Zone in Meters
- SR_1 = Primary Zone Stoichiometry
- SR_2 = Reburn Zone Stoichiometry
- X_2 = Primary Fuel Load in kg/h (Utah Bituminous #2 Coal)
- SR_3 = Final Stoichiometry
- RT = Residence Time in the Reburn Zone
- NO_p = Primary NO Concentration in ppmv (dry, 0% O_2)
- T_1 = Peak Temperature in the Primary Zone in K
- T_2 = Temperature in Inlet to Reburn Zone in K
- T_3 = Temperature at Inlet to Burnout Zone in K
- RE = Percent NO Destruction by Reburning (Y)
- DCF = Dilution Correction Factor
converts wet values to dry values and 0% excess O_2

REBURNING TESTS

Bituminous Coal Primary Flame (Premixed)
Natural Gas Reburning, no N₂ Transport

RUN	X ₁	SR ₁	SR ₂	X ₂	SR ₃	RT	NO _p	T ₁	T ₂	T ₃	RE
RS# 0A	0.762	1.350	0.761	2.070	1.12	0.295	1197	1668	1658	1565	78.5
RS# 0B	0.305	1.350	0.761	2.070	1.12	0.095	1187	1660	1584	1547	54.2
RS# 1A	0.762	1.350	0.730	2.100	1.10	0.287	1138	1668	1658	1565	79.4
RS# 1B	0.305	1.350	0.730	2.100	1.10	0.091	1138	1660	1584	1547	57.1
RS# 2A	0.762	1.200	0.851	2.070	1.10	0.354	970	1696	1685	1552	64.3
RS# 2B	0.305	1.200	0.851	2.070	1.10	0.122	970	1702	1576	1540	36.4
RS# 3A	0.762	1.350	0.725	2.070	1.10	0.293	1090	1602	1631	1557	80.2
RS# 3B	0.305	1.350	0.725	2.070	1.10	0.093	1090	1554	1561	1551	60.4
RS# 4A	0.762	1.350	0.980	2.100	1.10	0.337	1085	1610	1641	1555	43.3
RS# 4B	0.305	1.350	0.980	2.100	1.10	0.126	1085	1553	1548	1530	30.3
RS# 6A	0.762	1.225	0.855	1.980	1.10	0.377	1093	1629	1625	1489	65.7
RS# 6B	0.305	1.225	0.855	1.980	1.10	0.129	1093	1602	1523	1506	38.4
RS# 7A	0.762	1.100	0.730	1.980	1.10	0.392	1129	1672	1617	1469	77.8
RS# 7B	0.305	1.100	0.730	1.980	1.10	0.121	1129	1688	1589	1519	56.4
RS# 8A	0.762	1.100	0.980	1.980	1.10	0.452	1018	1664	1640	1497	30.7
RS# 8B	0.305	1.100	0.980	1.980	1.10	0.165	1018	1672	1562	1501	22.4
RS# 9A	0.762	1.225	0.730	1.590	1.10	0.452	975	1551	1547	1441	76.2
RS# 9B	0.305	1.225	0.730	1.590	1.10	0.142	975	1577	1496	1455	57.0
RS#10A	0.762	1.225	0.980	1.590	1.10	0.516	982	1572	1569	1485	47.7
RS#10B	0.305	1.225	0.980	1.590	1.10	0.189	982	1587	1492	1472	31.9
RS#11A	0.762	1.225	0.855	1.590	1.10	0.474	1032	1563	1582	1519	66.1
RS#11B	0.305	1.225	0.855	1.590	1.10	0.164	1032	1575	1507	1478	43.8
RS#12A	0.762	1.225	0.980	1.554	1.10	0.574	1014	1464	1462	1347	43.3
RS#12B	0.305	1.225	0.980	1.554	1.10	0.214	1014	1475	1354	1327	33.3
RS#13A	0.762	1.225	0.855	1.554	1.10	0.521	1032	1514	1504	1372	67.5
RS#13B	0.305	1.225	0.855	1.554	1.10	0.181	1032	1513	1407	1362	44.7
RS#14A	0.762	1.350	0.855	1.554	1.10	0.459	1040	1463	1515	1444	62.1
RS#14B	0.305	1.350	0.855	1.554	1.10	0.159	1040	1473	1427	1413	43.7
RS#15A	0.762	1.100	0.855	1.554	1.10	0.585	949	1546	1503	1366	73.1
RS#15B	0.305	1.100	0.855	1.554	1.10	0.196	949	1562	1459	1400	36.0
RS#16A	0.762	1.350	0.730	1.074	1.10	0.665	964	1422	1406	1308	65.7
RS#16B	0.305	1.350	0.730	1.074	1.10	0.214	964	1419	1310	1289	49.4
RS#17A	0.762	1.350	0.980	1.074	1.10	0.771	1003	1440	1424	1302	62.8
RS#17B	0.305	1.350	0.980	1.074	1.10	0.287	1003	1447	1314	1291	42.2
RS#18A	0.762	1.350	0.730	1.164	1.10	0.604	1064	1432	1431	1327	69.7
RS#18B	0.305	1.350	0.730	1.164	1.10	0.195	1064	1432	1346	1309	55.0
RS#19A	0.762	1.350	0.980	1.164	1.10	0.705	1100	1432	1436	1320	55.4
RS#19B	0.305	1.350	0.980	1.164	1.10	0.262	1100	1435	1335	1311	49.4
RS#20A	0.762	1.225	0.855	1.164	1.10	0.726	1091	1485	1446	1311	73.5
RS#20B	0.305	1.225	0.855	1.164	1.10	0.253	1091	1452	1320	1304	48.5
RS#21A	0.762	1.100	0.729	1.170	1.10	0.755	999	1503	1438	1277	69.6
RS#21B	0.305	1.100	0.729	1.170	1.10	0.242	999	1496	1319	1278	58.4
RS#22A	0.762	1.100	0.980	1.170	1.10	0.904	994	1526	1438	1209	45.3
RS#22B	0.305	1.100	0.980	1.170	1.10	0.337	994	1527	1317	1230	40.5

Bituminous Coal Primary Flame (Premixed)
 Natural Gas Reburning, no N₂ Transport

RUN	X ₁	SR ₁	SR ₂	X ₂	SR ₃	RT	NO _p	T ₁	T ₂	T ₃	RE
UB# 3A	0.457	1.100	0.901	0.978	1.06	0.608	906	1506	1412	1290	57.9
MR# 9	0.762	1.195	0.813	1.437	1.10	0.551	1027	1559	1530	1410	74.1
MR#10	0.610	1.195	0.813	1.437	1.10	0.426	1027	1554	1508	1439	70.3
MR#11	0.305	1.195	0.813	1.437	1.10	0.185	1027	1564	1415	1402	46.7
MR#12	0.762	1.195	1.050	1.449	1.10	0.690	1107	1504	1446	1214	24.7
MR#13	0.305	1.195	1.050	1.449	1.10	0.279	1107	1475	1242	1153	40.2
MR#14	0.305	1.195	1.000	1.449	1.10	0.267	1125	1495	1238	1148	17.0
MR#15	0.762	1.195	0.950	1.449	1.10	0.626	1121	1517	1483	1300	57.4
MR#16	0.305	1.195	0.950	1.449	1.10	0.240	1121	1519	1252	1224	35.2
MR#17	0.762	1.195	0.900	1.449	1.10	0.600	1118	1536	1495	1323	66.4
MR#18	0.305	1.195	0.900	1.449	1.10	0.219	1118	1534	1333	1284	40.4
MR#19	0.762	1.195	0.850	1.449	1.10	0.570	1103	1530	1502	1381	71.5
MR#20	0.305	1.195	0.850	1.449	1.10	0.202	1103	1534	1362	1327	42.3
MR#21	0.762	1.195	0.809	1.449	1.10	0.555	1115	1542	1510	1376	75.4
MR#22	0.610	1.195	0.809	1.449	1.10	0.430	1115	1533	1489	1400	68.3
MR#23	0.305	1.195	0.809	1.449	1.10	0.192	1115	1538	1369	1338	48.1
MR#27	0.762	1.195	0.810	1.437	1.10	0.545	1183	1559	1530	1410	73.5
MR#28	0.457	1.195	0.810	1.437	1.10	0.327	1183	1565	1520	1449	61.6
MR#29	0.610	1.195	0.810	1.437	1.10	0.423	1183	1554	1508	1439	71.7
MR#30	0.305	1.195	0.810	1.437	1.10	0.184	1206	1564	1415	1402	47.4
RV# 1	0.305	1.070	0.998	1.948	1.10	0.193	977	1625	1443	1354	17.4
RV# 2	0.305	1.070	0.948	1.948	1.10	0.180	977	1636	1445	1380	23.7
RV# 3	0.762	1.070	0.948	1.948	1.10	0.489	977	1624	1589	1396	35.9
RV# 4	0.457	1.070	0.948	1.948	1.10	0.287	977	1629	1590	1489	32.2
RV# 5	0.305	1.070	0.948	1.948	1.10	0.187	977	1637	1530	1452	32.2
RV# 6	0.610	1.070	0.948	1.948	1.10	0.384	977	1621	1569	1403	37.1
RV# 7	0.610	1.070	0.898	1.948	1.10	0.367	938	1638	1570	1431	52.3
RV# 8	0.762	1.070	0.898	1.948	1.10	0.470	938	1636	1595	1418	56.4
RV# 9	0.305	1.070	0.898	1.948	1.10	0.166	938	1663	1475	1415	31.7
RV#10	0.610	1.070	0.715	1.948	1.09	0.319	916	1641	1557	1472	74.1
RV#11	0.305	1.070	0.715	1.948	1.09	0.130	916	1657	1509	1451	50.8
RV#12	0.762	1.070	0.715	1.948	1.09	0.419	916	1644	1584	1420	77.5
RV#13	0.305	1.070	0.748	1.948	1.10	0.135	973	1650	1510	1462	54.6
RV#14	0.762	1.070	0.748	1.948	1.10	0.425	973	1656	1580	1445	80.4
RV#15	0.610	1.070	0.748	1.948	1.10	0.328	973	1650	1553	1462	74.2
RV#16	0.610	1.070	0.808	1.948	1.10	0.337	926	1677	1572	1484	74.0
RV#17	0.305	1.070	0.808	1.948	1.10	0.143	926	1674	1524	1493	48.1
RV#18	0.762	1.070	0.808	1.948	1.10	0.441	926	1679	1579	1453	79.4
RV#19	0.457	1.070	0.808	1.948	1.10	0.254	926	1677	1619	1534	69.5
RV#20	0.152	1.070	0.808	1.948	1.10	0.077	926	1668	1629	1607	32.8

Bituminous Coal Primary Flame (Premixed)
 Natural Gas Reburning, no N₂ Transport

RUN	X ₁	SR ₁	SR ₂	X ₂	SR ₃	RT	NO _p	T ₁	T ₂	T ₃	RE
RA# 9	1.067	1.325	1.100	1.800	1.10	0.593	1004	1629	1630	1406	15.2
RA#10	0.762	1.325	1.100	1.800	1.15	0.422	1004	1642	1631	1481	17.6
RA#13	0.762	1.325	1.100	1.800	1.20	0.409	1004	1643	1617	1469	18.1
RA#14	0.762	1.325	1.100	1.800	1.25	0.395	1004	1643	1617	1469	18.2
RA#15	0.762	1.325	1.100	1.800	1.30	0.382	1004	1643	1617	1469	17.1
RA#20	0.305	1.325	1.070	1.800	1.12	0.167	1026	1649	1444	1422	27.9
RA#21	0.610	1.325	1.070	1.800	1.12	0.338	1026	1632	1583	1495	35.4
RA#22	0.762	1.325	1.070	1.800	1.12	0.426	1026	1617	1612	1505	25.8
RA#24	0.305	1.325	0.984	1.800	1.10	0.152	999	1650	1458	1460	22.1
RA#26	0.610	1.325	0.984	1.800	1.10	0.328	999	1635	1569	1482	30.2
RA#27	0.762	1.325	0.984	1.800	1.10	0.417	999	1621	1600	1476	36.7
RB# 1	0.610	1.094	1.054	1.824	1.10	0.431	860	1667	1549	1361	2.2
RB# 2	0.610	1.094	1.004	1.824	1.10	0.414	888	1664	1558	1389	25.4
RB# 3	0.610	1.094	0.950	1.824	1.10	0.388	888	1671	1598	1451	36.9
RB# 4	0.610	1.094	0.900	1.824	1.10	0.371	888	1673	1604	1479	58.7
RB# 5	0.610	1.094	0.864	1.824	1.12	0.361	888	1672	1591	1479	65.1
RB# 6	0.610	1.094	0.800	1.824	1.10	0.347	888	1675	1593	1486	68.8
RB# 7	0.610	1.094	0.750	1.824	1.10	0.334	888	1683	1592	1494	65.0
RC# 1	0.762	1.118	1.047	1.732	1.10	0.560	978	1639	1576	1361	22.0
RC# 2	0.610	1.118	1.047	1.732	1.10	0.432	978	1654	1574	1415	18.3
RC# 3	0.305	1.118	1.047	1.732	1.10	0.208	980	1650	1508	1427	31.1
RC# 4	0.305	1.118	1.009	1.732	1.10	0.198	980	1658	1520	1441	38.9
RC# 5	0.610	1.118	1.009	1.732	1.10	0.406	968	1641	1640	1487	34.8
RC# 6	0.305	1.118	1.009	1.732	1.10	0.209	980	1700	1517	1422	29.5
RC# 7	0.457	1.118	1.009	1.732	1.10	0.317	980	1663	1624	1526	32.6
RC# 8	0.762	1.118	1.009	1.732	1.10	0.533	980	1664	1623	1402	34.9
RH# 1	0.305	1.100	0.850	1.782	1.10	0.157	956	1678	1570	1536	43.2
RH# 2	0.610	1.100	0.850	1.782	1.10	0.363	930	1676	1592	1524	69.0
RH# 3	0.762	1.100	0.850	1.782	1.10	0.468	930	1670	1608	1511	75.6
RH# 4	0.762	1.100	0.800	1.782	1.10	0.453	987	1675	1604	1519	76.3
RH# 5	0.610	1.100	0.800	1.782	1.10	0.350	987	1683	1592	1532	74.1
RH# 6	0.305	1.100	0.800	1.782	1.10	0.145	993	1676	1576	1549	44.6
RH# 7	0.305	1.100	0.750	1.782	1.10	0.135	1003	1675	1589	1565	53.4
RH# 8	0.610	1.100	0.750	1.782	1.10	0.338	926	1680	1581	1526	71.5
RH# 9	0.762	1.100	0.750	1.782	1.10	0.440	926	1671	1606	1512	75.7

Bituminous Coal Primary Flame (Premixed)
 Natural Gas Reburning, Multiple Reburning Streams

RUN	X ₁	SR ₁	SR ₂	X ₂	SR ₃	RT	NO _p	T ₁	T ₂	T ₃	RE
RH#10	0.305	1.100	0.850	1.782	1.13	0.152	1003	1676	1488	1454	63.3
RH#11	0.305	1.100	0.850	1.782	1.13	0.149	1003	1676	1424	1397	63.3
RH#12	0.610	1.100	0.850	1.782	1.13	0.369	1003	1657	1547	1451	76.0
RH#13	0.610	1.100	0.800	1.782	1.10	0.358	999	1665	1535	1461	75.8
RH#14	0.305	1.100	0.800	1.782	1.10	0.145	999	1675	1476	1442	64.8
RH#15	0.305	1.100	0.800	1.782	1.10	0.139	999	1676	1421	1400	64.7
RH#16	0.305	1.100	0.750	1.782	1.13	0.121	994	1676	1442	1428	68.5
RH#17	0.305	1.100	0.750	1.782	1.13	0.128	994	1675	1487	1467	64.5
RH#18	0.610	1.100	0.750	1.782	1.13	0.342	994	1665	1520	1454	70.9
MR# 1	0.305	1.195	0.692	1.440	1.07	0.144	1114	1576	1340	1308	65.8
MR# 2	0.610	1.195	0.692	1.440	1.07	0.400	1114	1564	1463	1356	72.2
MR# 3	0.305	1.195	0.692	1.440	1.07	0.144	1114	1576	1340	1308	69.0
MR# 4	0.305	1.195	0.692	1.440	1.07	0.155	1114	1571	1379	1336	64.2
MR# 6	0.610	1.195	0.813	1.437	1.10	0.430	1027	1537	1481	1399	72.7
MR# 7	0.305	1.195	0.813	1.437	1.10	0.172	1027	1556	1386	1354	66.6
MR# 8	0.305	1.195	0.813	1.437	1.10	0.185	1027	1551	1365	1327	61.3
MR#24	0.610	1.195	0.810	1.437	1.10	0.430	1089	1537	1481	1399	71.5
MR#25	0.305	1.195	0.810	1.437	1.10	0.172	1089	1556	1386	1354	60.0
MR#26	0.305	1.195	0.810	1.437	1.10	0.185	1089	1551	1365	1327	55.7

Bituminous Coal Primary Flame (Premixed)
Natural Gas Reburning, N₂ Transport

RUN	X ₁	SR ₁	SR ₂	X ₂	SR ₃	RT	NO _p	T ₁	T ₂	T ₃	RE
RR# 1	0.610	1.230	1.048	1.302	1.10	0.495	1068	1677	1535	1362	29.5
RR# 2	0.610	1.230	0.997	1.302	1.10	0.479	1068	1672	1556	1379	57.3
RR# 3	0.610	1.230	0.946	1.302	1.10	0.459	1068	1671	1566	1407	72.4
RR# 4	0.610	1.230	0.895	1.302	1.10	0.437	1068	1667	1578	1449	78.1
RR# 5	0.610	1.230	0.845	1.302	1.10	0.416	1068	1664	1597	1495	73.3
RR# 6	0.610	1.230	0.795	1.302	1.10	0.402	1068	1664	1596	1500	71.0
RR# 7	0.610	1.230	0.745	1.302	1.10	0.389	1068	1666	1592	1505	66.7
RR# 8	0.610	1.230	0.649	1.302	1.01	0.374	1068	1669	1588	1537	71.9
RR# 9	0.610	1.230	1.149	1.302	1.20	0.513	1068	1686	1493	1283	8.4
RR#10	0.610	1.230	1.099	1.302	1.15	0.503	1068	1683	1510	1322	15.5
RR#11	0.610	1.230	1.051	1.302	1.10	0.496	1068	1678	1532	1354	29.1
RR#12	0.610	1.230	1.001	1.302	1.10	0.480	1068	1677	1539	1370	47.7
RR#13	0.610	1.230	0.950	1.302	1.10	0.455	1068	1669	1570	1421	60.7
RR#14	0.610	1.230	0.899	1.302	1.10	0.437	1068	1666	1580	1450	69.5
RR#15	0.610	1.230	0.880	1.302	1.10	0.429	1068	1665	1591	1462	70.4
RR#16	0.610	1.230	0.825	1.302	1.10	0.412	1068	1667	1587	1483	68.7
RR#17	0.610	1.230	0.780	1.302	1.10	0.396	1068	1666	1595	1506	71.9
C# 14A	0.762	1.176	0.959	1.074	1.11	0.731	1029	1638	1563	1376	58.5
C# 14B	0.762	1.176	0.933	1.074	1.11	0.724	1029	1638	1557	1375	66.5
C# 14C	0.762	1.176	0.878	1.074	1.11	0.691	1029	1635	1571	1414	74.3
C# 14D	0.762	1.176	0.835	1.074	1.11	0.670	1029	1635	1577	1426	80.0
C# 14E	0.762	1.176	0.767	1.074	1.11	0.642	1029	1636	1575	1448	78.5
C# 16	0.762	1.234	0.783	1.068	1.08	0.641	1078	1620	1554	1399	77.3
C# 19	0.762	1.100	0.900	1.315	1.10	0.611	936	1648	1580	1433	70.1

Bituminous Coal Primary Flame (Premixed)
C# 15 and 17: Coal Reburning, N₂ Transport
C# 20: Natural Gas + NH₃ Reburning, N₂ Transport

RUN	X ₁	SR ₁	SR ₂	X ₂	SR ₃	RT	NO _p	T ₁	T ₂	T ₃	RE
C# 15	0.762	1.286	0.803	1.068	1.10	0.610	1051	1603	1556	1429	73.4
C# 17	0.762	1.123	0.908	1.331	1.12	0.578	908	1651	1572	1405	53.9
C# 20	0.762	1.083	0.888	1.315	1.09	0.613	954	1652	1592	1447	70.3

Bituminous Coal Primary Diffusion Flame (Type A)
Natural Gas Reburning, N₂ Transport

RUN	X ₁	SR ₁	SR ₂	X ₂	SR ₃	RT	NO _p	T ₁	T ₂	T ₃	RE
C# 22A	0.610	1.183	1.008	1.218	1.09	0.523	751	1563	1553	1440	26.9
C# 22B	0.610	1.183	0.966	1.218	1.13	0.496	671	1566	1573	1475	37.8
C# 22C	0.610	1.183	0.940	1.218	1.15	0.480	682	1566	1585	1496	51.3
C# 22D	0.610	1.183	0.894	1.218	1.18	0.458	694	1566	1598	1515	52.1
C# 22E	0.610	1.183	0.841	1.218	1.16	0.444	718	1569	1602	1533	62.2
C# 22F	0.610	1.183	0.777	1.218	1.12	0.429	713	1569	1602	1552	66.4

Bituminous Coal (Premixed) Flame, Natural Gas Reburning, no N₂ Transport

RUN	X ₁	SR ₁	SR ₂	X ₂	SR ₃	RT	NO _y	T ₁	T ₂	T ₃	RE
RA# 1	0.610	1.325	1.250	1.800	1.25	0.360	1037	1642	1483	1317	0.0
RA# 2	0.610	1.325	1.200	1.800	1.20	0.353	1037	1642	1488	1350	6.3
RA# 3	0.915	1.325	1.200	1.800	1.20	0.534	1036	1643	1551	1359	0.4
RA# 4	1.067	1.325	1.200	1.800	1.20	0.635	1037	1643	1515	1353	1.7
RA# 5	1.067	1.325	1.150	1.800	1.15	0.623	1004	1643	1545	1373	8.6
RA# 6	0.915	1.325	1.150	1.800	1.15	0.523	1004	1642	1563	1393	6.5
RA# 7	0.610	1.325	1.150	1.800	1.15	0.342	1004	1643	1525	1392	18.3
RA# 8	0.610	1.325	1.100	1.800	1.10	0.333	1004	1642	1545	1423	26.8
RA#16	0.915	1.325	1.100	1.800	1.10	0.522	1004	1649	1557	1397	17.6
RD# 1	1.067	1.185	1.095	1.737	1.10	0.725	1019	1631	1595	1317	7.7
RD# 4	0.915	1.185	1.095	1.737	1.10	0.610	1019	1625	1585	1269	7.8
RE# 1	0.305	0.873	0.830	1.902	1.10	0.202	298	1656	1364	1318	10.1
RE# 2	0.610	0.873	0.830	1.902	1.10	0.408	298	1658	1500	1360	19.8
RE# 3	0.762	0.873	0.830	1.902	1.10	0.517	298	1640	1498	1307	21.5
RE# 4	0.457	0.873	0.830	1.902	1.10	0.329	298	1640	1498	1349	15.8
RE# 5	0.457	0.873	0.800	1.902	1.10	0.318	298	1646	1512	1375	13.1
RE# 6	0.762	0.873	0.800	1.902	1.10	0.495	298	1646	1512	1328	26.8
RE# 7	0.610	0.873	0.800	1.902	1.10	0.395	298	1643	1500	1368	20.8
RE# 8	0.305	0.873	0.800	1.902	1.10	0.212	298	1642	1516	1441	11.1
RE# 9	0.305	0.873	0.800	1.902	1.10	0.188	298	1658	1460	1385	9.1
RE#10	0.305	0.873	0.750	1.902	1.10	0.176	298	1658	1460	1385	14.1
RE#11	0.610	0.873	0.750	1.902	1.10	0.374	298	1643	1500	1368	26.5
RE#12	0.762	0.873	0.750	1.902	1.10	0.468	298	1646	1512	1328	24.5
RF# 1	0.305	0.948	0.850	1.890	1.10	0.182	381	1669	1483	1414	11.5
RF# 2	0.610	0.948	0.850	1.890	1.10	0.384	381	1660	1507	1375	41.7
RF# 3	0.762	0.948	0.850	1.890	1.10	0.480	381	1649	1533	1357	43.3
RF# 4	0.762	0.948	0.800	1.890	1.10	0.447	381	1661	1535	1385	45.1
RF# 5	0.457	0.948	0.800	1.890	1.10	0.292	381	1646	1536	1418	43.3
RF# 6	0.305	0.948	0.800	1.890	1.10	0.194	381	1657	1512	1444	29.9
RF# 7	0.610	0.948	0.800	1.890	1.10	0.353	381	1675	1545	1436	38.3
RF# 8	0.305	0.948	0.800	1.890	1.10	0.166	381	1681	1519	1463	16.5
RF# 9	0.305	0.948	0.749	1.890	1.10	0.153	381	1692	1517	1476	21.8
RF#10	0.610	0.948	0.749	1.890	1.10	0.326	381	1679	1567	1480	38.1
RF#11	0.762	0.948	0.749	1.890	1.10	0.413	381	1665	1586	1448	39.6
RG# 1	0.305	0.993	0.814	1.824	1.11	0.166	534	1682	1521	1460	35.2
RG# 2	0.610	0.993	0.814	1.824	1.11	0.351	534	1670	1545	1440	50.6
RG# 3	0.305	0.993	0.814	1.824	1.11	0.190	534	1665	1567	1504	50.6
RG# 4	0.762	0.993	0.814	1.824	1.11	0.432	534	1676	1602	1466	57.9
RG# 5	0.457	0.993	0.814	1.824	1.11	0.282	534	1672	1611	1518	60.5

Runs RA and RD are reburning tests, in which the reburn zone is operated fuel lean, and no air is added in a final reburning stage. These results are not reliable, because exhaust values would be affected by the poor mixing conditions of the reburn zone.

Runs RE, RF and RG are reburning tests, in which the primary zone is fuel rich. NO_y is the exhaust value of staging tests, in which only staged air is added (no reburning fuel). Thus, NO_y represent exhaust emissions of air staging tests (or blank reburning). The results are difficult to interpret, since a comparison between reburning and air staging must be made at their optimum configurations. Nevertheless, the results of these tests are presented here.

DETAILED MEASUREMENTS IN THE REBURN ZONE

GAS# 1, Natural Gas Primary Flame, Natural Gas Reburning

sec	K	% vol								ppmv					
		RT	Temp	CO ₂	CO	H ₂	H ₂ O	O ₂	CH ₄	C ₂ H ₂	N ₂	NO	HCN	NH ₃	DCF
Stoichiometry = 1.10															
0.286	1498	8.02	0.04	0.00	17.29	1.65	0.00	0.00	73.0	31.4	0.0	0.0	1.329		
Stoichiometry = 0.85															
0.553	1402	7.30	0.97	0.84	17.49	0.08	1.15	0.09	72.0	21.5	56.8	4.0	1.426		
0.833	1348	7.25	1.22	1.31	17.62	0.00	0.81	0.13	71.7	16.9	45.2	5.5	1.434		
1.123	1302	6.99	1.56	1.54	17.76	0.00	0.60	0.12	71.4	23.4	52.7	10.0	1.439		
1.424	1250	7.02	1.58	1.49	17.93	0.08	0.53	0.10	71.3	21.3	41.3	10.0	1.442		

GAS# 2, Natural Gas + NH₃ Primary Flame, Natural Gas Reburning

sec	K	% vol								ppmv					
		RT	Temp	CO ₂	CO	H ₂	H ₂ O	O ₂	CH ₄	C ₂ H ₂	N ₂	NO	HCN	NH ₃	DCF
Stoichiometry = 1.10															
0.289	1478	7.93	0.04	0.03	17.20	1.81	0.00	0.00	73.0	714.6	5.7	1.2	1.334		
Stoichiometry = 0.86															
0.556	1401	7.42	0.86	0.72	18.06	0.12	0.88	0.07	71.8	344.2	68.3	9.7	1.435		
0.834	1352	7.34	1.14	1.08	18.40	0.08	0.50	0.08	71.4	248.9	138.3	22.3	1.444		
1.122	1304	7.31	1.18	1.14	18.28	0.12	0.52	0.08	71.4	216.5	145.8	23.3	1.445		
1.422	1249	7.28	1.23	1.19	18.18	0.12	0.55	0.09	71.4	204.6	142.6	25.6	1.445		

GAS# 3, Natural Gas + NH₃ Primary Flame, Natural Gas Reburning

sec	K	% vol								ppmv					
		RT	Temp	CO ₂	CO	H ₂	H ₂ O	O ₂	CH ₄	C ₂ H ₂	N ₂	NO	HCN	NH ₃	DCF
Stoichiometry = 1.10															
0.286	1503	8.06	0.04	0.00	17.28	1.72	0.00	0.00	72.9	159.6	0.0	0.0	1.330		
Stoichiometry = 0.86															
0.552	1407	7.49	0.95	0.81	17.71	0.08	0.98	0.07	71.9	85.6	50.3	4.1	1.428		
0.831	1353	7.37	1.23	1.15	18.11	0.08	0.57	0.09	71.4	63.1	75.1	7.9	1.438		
1.120	1305	7.34	1.27	1.25	18.03	0.08	0.56	0.09	71.4	58.2	76.0	10.1	1.438		
1.420	1254	7.33	1.31	1.28	18.07	0.08	0.52	0.08	71.3	56.5	76.4	11.2	1.439		

GAS# 4, Natural Gas Primary Flame, Natural Gas Reburning
% vol

sec		% vol								ppmv			
RT	K Temp	CO ₂	CO	H ₂	H ₂ O	O ₂	CH ₄	C ₂ H ₂	N ₂	NO	HCN	NH ₃	DCF
Stoichiometry = 1.11													
0.282	1509	8.04	0.05	0.00	17.15	1.86	0.00	0.00	72.9	32.7	0.0	0.0	1.340
Stoichiometry = 0.86													
0.542	1423	7.78	0.75	0.56	19.00	0.16	0.38	0.04	71.3	21.5	22.2	1.8	1.451
0.816	1370	7.48	1.19	1.24	17.81	0.08	0.62	0.12	71.5	16.0	48.4	3.3	1.448
1.098	1324	7.43	1.27	1.27	17.89	0.12	0.57	0.10	71.3	15.2	53.5	3.9	1.450
1.392	1271	7.39	1.31	1.32	17.87	0.12	0.55	0.10	71.3	14.8	49.5	4.3	1.450

GAS# 5, Natural Gas Primary Flame, Natural Gas Reburning
% vol

sec		% vol								ppmv			
RT	K Temp	CO ₂	CO	H ₂	H ₂ O	O ₂	CH ₄	C ₂ H ₂	N ₂	NO	HCN	NH ₃	DCF
Stoichiometry = 1.13													
0.525	1393	7.86	0.04	0.01	16.81	2.23	0.00	0.00	73.0	24.0	1.0	1.1	1.366
Stoichiometry = 0.87													
1.026	1274	7.46	0.72	0.65	17.97	0.16	0.69	0.07	72.3	12.3	24.6	2.1	1.488
1.384	1219	7.37	0.71	0.68	17.84	0.15	0.76	0.07	72.4	11.9	24.2	3.0	1.485
1.761	1158	7.37	0.71	0.66	17.84	0.11	0.78	0.07	72.4	11.5	20.5	2.2	1.483

GAS# 6, Natural Gas Primary Flame, Natural Gas Reburning
% vol

sec		% vol								ppmv			
RT	K Temp	CO ₂	CO	H ₂	H ₂ O	O ₂	CH ₄	C ₂ H ₂	N ₂	NO	HCN	NH ₃	DCF
Stoichiometry = 1.13													
0.351	1415	7.86	0.04	0.01	16.81	2.23	0.00	0.00	73.0	24.0	1.0	1.1	1.366
Stoichiometry = 0.87													
0.674	1349	7.38	0.69	0.59	17.98	0.12	0.75	0.03	72.4	11.5	14.5	2.7	1.484
1.011	1297	7.35	0.82	0.75	18.33	0.08	0.48	0.04	72.1	9.4	27.0	5.2	1.490
1.361	1246	7.32	0.82	0.72	18.18	0.08	0.57	0.07	72.2	12.7	37.3	2.7	1.488
1.727	1191	7.33	0.78	0.68	18.27	0.08	0.55	0.07	72.2	11.9	34.3	2.5	1.488

GAS# 7, Natural Gas Primary Flame, Natural Gas Reburning
% vol

sec		% vol								ppmv			
RT	K Temp	CO ₂	CO	H ₂	H ₂ O	O ₂	CH ₄	C ₂ H ₂	N ₂	NO	HCN	NH ₃	DCF
Stoichiometry = 1.13													
0.178	1417	7.86	0.04	0.01	16.81	2.23	0.00	0.00	73.0	24.0	1.0	1.1	1.366
Stoichiometry = 0.87													
0.497	1366	7.66	0.78	0.57	18.50	0.12	0.44	0.04	71.9	18.7	24.2	2.0	1.495
0.661	1338	7.44	0.88	0.71	18.20	0.08	0.55	0.06	72.1	16.0	31.9	4.6	1.491
1.001	1281	7.35	0.93	0.79	18.11	0.08	0.56	0.07	72.1	13.1	40.9	2.4	1.490
1.726	1179	7.37	0.95	0.86	17.71	0.08	0.73	0.07	72.2	13.2	37.3	2.6	1.488

COAL# 2, Bituminous Coal Primary Flame, Natural Gas Reburning
% vol

sec	K	% vol									ppmv				
		RT	Temp	CO ₂	CO	H ₂	H ₂ O	O ₂	CH ₄	C ₂ H ₂	N ₂	NO	HCN	NH ₃	DCF
Stoichiometry = 1.06															
0.418	1518	15.11	0.07	0.00	7.42	1.16	0.00	0.00	76.2	840.6	0.0	0.0	1.133		
Stoichiometry = 0.68															
0.782	1438	12.08	2.33	1.44	12.16	0.04	0.90	0.16	70.9	316.2	69.3	48.0	1.324		
1.169	1361	10.37	3.68	2.34	11.37	0.00	0.89	0.18	71.2	106.4	153.6	69.5	1.319		
1.576	1296	10.64	3.62	2.66	10.58	0.00	1.13	0.17	71.2	80.5	170.2	73.6	1.318		
2.002	1240	10.39	4.03	2.75	10.42	0.00	1.16	0.16	71.1	71.7	181.4	81.2	1.320		

COAL# 3, Bituminous Coal Primary Flame, Natural Gas Reburning
% vol

sec	K	% vol									ppmv				
		RT	Temp	CO ₂	CO	H ₂	H ₂ O	O ₂	CH ₄	C ₂ H ₂	N ₂	NO	HCN	NH ₃	DCF
Stoichiometry = 1.26															
0.361	1488	12.81	0.05	0.00	6.32	4.08	0.00	0.00	76.7	782.2	0.0	0.0	1.331		
Stoichiometry = 0.80															
0.691	1439	10.60	2.65	1.88	7.02	0.00	2.32	0.28	75.2	255.7	100.5	26.5	1.457		
1.021	1411	9.94	3.57	1.92	10.86	0.00	0.39	0.13	73.2	120.3	104.6	47.2	1.496		
1.364	1331	10.29	3.19	1.66	11.26	0.00	0.34	0.09	73.2	88.7	87.4	57.7	1.497		
1.727	1269	10.08	3.24	1.65	11.20	0.00	0.39	0.09	73.3	75.5	86.5	74.1	1.493		

COAL# 4, Bituminous Coal Primary Flame, Natural Gas Reburning, Fuel Lean
% vol

sec	K	% vol									ppmv				
		RT	Temp	CO ₂	CO	H ₂	H ₂ O	O ₂	CH ₄	C ₂ H ₂	N ₂	NO	HCN	NH ₃	DCF
Stoichiometry = 1.24															
0.368	1464	13.01	0.05	0.00	6.39	3.93	0.00	0.00	76.6	814.4	0.0	0.0	1.316		
Stoichiometry = 1.03															
0.715	1383	11.30	0.41	0.18	8.54	0.82	0.09	0.02	78.6	411.6	3.9	2.2	1.426		
1.078	1347	11.44	0.18	0.14	8.81	0.59	0.01	0.00	78.8	360.2	3.5	2.4	1.423		
1.453	1287	11.49	0.16	0.16	8.79	0.59	0.01	0.00	78.8	383.1	3.7	1.6	1.423		
1.850	1208	11.58	0.14	0.11	8.83	0.59	0.01	0.00	78.7	410.3	4.0	2.0	1.424		

COAL# 5, Bituminous Coal Primary Flame, CO Reburning
% vol

sec	K	% vol									ppmv				
		RT	Temp	CO ₂	CO	H ₂	H ₂ O	O ₂	CH ₄	C ₂ H ₂	N ₂	NO	HCN	NH ₃	DCF
Stoichiometry = 1.24															
0.400	1505	13.13	0.05	0.00	6.38	3.89	0.00	0.00	76.6	772.4	0.0	0.0	1.319		
Stoichiometry = 0.91															
0.737	1567	18.52	5.27	0.58	5.02	0.00	0.00	0.00	70.6	660.1	9.3	3.7	1.504		
1.087	1442	19.33	3.41	0.42	5.26	0.00	0.00	0.00	71.6	634.8	5.9	4.9	1.483		
1.465	1354	19.41	2.89	0.41	5.30	0.00	0.00	0.00	72.0	591.9	4.5	6.5	1.475		
1.868	1274	19.22	2.79	0.43	5.30	0.00	0.00	0.00	72.3	511.4	2.9	12.3	1.470		

COAL# 6, Bituminous Coal + O₂ Primary Flame, Natural Gas Reburning
 % vol ppmv

sec	K	% vol								ppmv			
RT	Temp	CO ₂	CO	H ₂	H ₂ O	O ₂	CH ₄	C ₂ H ₂	N ₂	NO	HCN	NH ₃	DCF
Stoichiometry = 1.18													
0.362	1582	17.52	0.12	0.00	7.93	2.97	0.00	0.00	71.5	1141.7	0.0	0.0	1.061
Stoichiometry = 0.80													
0.697	1446	13.22	3.90	2.52	8.19	0.00	2.39	0.24	69.5	229.5	135.5	36.1	1.181
1.054	1352	12.67	4.42	2.77	10.79	0.00	0.88	0.20	68.3	156.1	176.3	59.1	1.203
1.431	1293	12.41	4.60	2.95	10.75	0.00	0.82	0.19	68.3	111.6	187.0	54.3	1.203
1.825	1238	12.38	4.56	3.07	10.61	0.00	0.84	0.18	68.3	71.5	202.0	70.8	1.201

COAL# 7, Bituminous Coal Primary Flame, Natural Gas Reburning
 % vol ppmv

sec	K	% vol								ppmv			
RT	Temp	CO ₂	CO	H ₂	H ₂ O	O ₂	CH ₄	C ₂ H ₂	N ₂	NO	HCN	NH ₃	DCF
Stoichiometry = 1.12													
0.202	1702	14.50	0.04	0.00	7.04	2.14	0.00	0.00	76.3	1008.6	0.0	0.0	1.195
Stoichiometry = 0.86													
0.388	1612	11.79	3.23	1.40	8.96	0.09	0.51	0.17	73.8	396.0	79.5	28.6	1.280
0.581	1568	11.65	3.36	1.02	10.38	0.04	0.04	0.03	73.5	327.1	24.3	31.9	1.286
0.780	1513	11.65	3.54	1.06	10.38	0.00	0.03	0.01	73.3	268.9	11.3	27.2	1.288
0.986	1456	11.50	3.73	1.28	10.16	0.00	0.02	0.01	73.3	215.6	7.6	26.4	1.289

COAL# 8, Bituminous Coal Primary Flame, H₂ Reburning
 % vol ppmv

sec	K	% vol								ppmv			
RT	Temp	CO ₂	CO	H ₂	H ₂ O	O ₂	CH ₄	C ₂ H ₂	N ₂	NO	HCN	NH ₃	DCF
Stoichiometry = 1.22													
0.352	1543	13.07	0.05	0.00	6.48	3.67	0.00	0.00	76.7	813.6	0.0	0.0	1.299
Stoichiometry = 0.90													
0.664	1481	7.00	3.99	5.17	11.43	0.04	0.00	0.00	72.4	673.1	6.3	8.2	1.446
0.985	1448	8.34	2.99	2.05	14.49	0.00	0.00	0.00	72.1	688.3	4.5	6.6	1.451
1.319	1371	8.38	2.87	2.09	14.47	0.00	0.00	0.00	72.2	675.7	3.8	8.0	1.449
1.672	1286	8.79	2.66	2.26	14.26	0.00	0.00	0.00	72.0	647.3	4.0	15.9	1.453

COAL# 9, Bituminous Coal Primary Flame, Natural Gas Reburning
 % vol ppmv

sec	K	% vol								ppmv			
RT	Temp	CO ₂	CO	H ₂	H ₂ O	O ₂	CH ₄	C ₂ H ₂	N ₂	NO	HCN	NH ₃	DCF
Stoichiometry = 1.11													
0.380	1517	14.44	0.08	0.00	7.13	1.93	0.00	0.00	76.4	854.4	0.0	0.0	1.180
Stoichiometry = 0.71													
0.725	1447	10.90	2.78	2.22	7.25	0.00	2.73	0.25	73.8	231.9	113.3	33.1	1.316
1.082	1361	10.57	3.30	2.42	9.68	0.00	1.34	0.24	72.4	131.0	143.0	43.9	1.341
1.459	1298	10.55	3.35	2.65	9.45	0.00	1.34	0.23	72.4	104.1	147.2	46.6	1.342
1.855	1228	10.71	3.30	2.56	9.63	0.00	1.31	0.18	72.3	72.3	159.1	57.1	1.344

COAL#10, Bituminous Coal Primary Flame, Natural Gas Reburning

sec	K	% vol								ppmv					
		RT	Temp	CO ₂	CO	H ₂	H ₂ O	O ₂	CH ₄	C ₂ H ₂	N ₂	NO	HCN	NH ₃	DCF
Stoichiometry = 1.10															
0.382	1521	14.62	0.09	0.00	7.14	1.88	0.00	0.00	76.3	831.1	0.0	0.0	1.178		
Stoichiometry = 0.86															
0.729	1448	11.39	1.45	0.52	9.57	0.18	0.44	0.05	76.4	330.1	58.1	19.1	1.306		
1.093	1380	10.93	2.09	0.93	9.33	0.05	0.35	0.06	76.3	149.6	112.3	40.0	1.308		
1.475	1312	11.02	2.13	0.98	9.28	0.00	0.35	0.05	76.2	136.1	85.5	38.6	1.309		
1.878	1239	11.03	2.13	0.97	9.19	0.00	0.41	0.05	76.2	122.6	106.3	47.1	1.309		

COAL#11, Bituminous Coal Primary Flame (Fuel Rich), Natural Gas Reburning

sec	K	% vol								ppmv					
		RT	Temp	CO ₂	CO	H ₂	H ₂ O	O ₂	CH ₄	C ₂ H ₂	N ₂	NO	HCN	NH ₃	DCF
Stoichiometry = 0.93															
0.386	1469	15.07	1.24	0.00	8.37	0.00	0.00	0.00	75.3	540.6	0.0	0.0	1.005		
Stoichiometry = 0.69															
0.756	1307	11.01	2.22	1.23	7.50	0.00	2.60	0.07	75.3	272.9	186.7	42.3	1.111		
1.156	1247	10.83	2.65	1.99	7.03	0.00	2.44	0.12	74.9	172.0	305.6	58.3	1.117		
1.570	1204	10.94	2.92	2.26	7.30	0.00	2.12	0.12	74.3	111.2	351.2	65.4	1.126		
1.994	1156	10.66	2.78	1.82	10.42	0.00	0.73	0.12	73.5	80.6	355.6	71.4	1.139		

COAL#12, Bituminous Coal Primary Flame, Natural Gas Reburning

sec	K	% vol								ppmv					
		RT	Temp	CO ₂	CO	H ₂	H ₂ O	O ₂	CH ₄	C ₂ H ₂	N ₂	NO	HCN	NH ₃	DCF
Stoichiometry = 1.12															
0.332	1577	14.15	0.08	0.00	7.07	2.14	0.00	0.00	76.6	910.7	0.0	0.0	1.190		
Stoichiometry = 0.85															
0.630	1528	11.60	1.63	0.66	9.70	0.14	0.49	0.07	75.7	347.7	88.8	22.1	1.316		
0.938	1457	11.19	2.25	0.88	10.08	0.00	0.19	0.06	75.3	170.8	93.2	43.3	1.322		
1.260	1393	11.13	2.53	1.14	9.48	0.00	0.34	0.08	75.3	131.2	175.2	53.6	1.323		
1.598	1333	11.11	2.30	1.06	9.71	0.00	0.30	0.06	75.5	117.4	137.0	65.6	1.320		

COAL#13, Bituminous Coal Primary Flame, Natural Gas + NH₃ Reburning

sec	K	% vol								ppmv					
		RT	Temp	CO ₂	CO	H ₂	H ₂ O	O ₂	CH ₄	C ₂ H ₂	N ₂	NO	HCN	NH ₃	DCF
Stoichiometry = 1.10															
0.335	1578	14.39	0.12	0.00	7.17	1.86	0.00	0.00	76.5	877.3	0.0	0.0	1.174		
Stoichiometry = 0.84															
0.637	1524	10.83	2.41	1.05	9.00	0.05	0.71	0.10	75.8	236.6	198.8	123.1	1.296		
0.945	1485	10.97	2.83	1.03	10.06	0.00	0.16	0.05	74.9	148.4	153.9	60.8	1.312		
1.263	1432	10.84	2.88	1.05	10.08	0.00	0.15	0.04	75.0	103.4	191.3	85.8	1.311		
1.595	1364	11.08	2.79	1.23	9.90	0.00	0.14	0.04	74.8	76.6	128.2	90.8	1.313		

COAL#15, Bituminous Coal Primary Flame, Bituminous Coal Reburning
 % vol ppmv

sec	K	% vol								ppmv			
RT	Temp	CO ₂	CO	H ₂	H ₂ O	O ₂	CH ₄	C ₂ H ₂	N ₂	NO	HCN	NH ₃	DCF
Stoichiometry = 1.29													
0.293	1582	12.32	0.03	0.00	6.19	4.46	0.00	0.00	77.0	773.9	0.0	0.0	1.358
Stoichiometry = 0.80													
0.554	1526	11.25	2.12	0.90	7.80	0.23	0.07	0.06	77.6	373.4	422.1	61.4	1.512
0.819	1486	12.73	2.21	0.89	7.75	0.18	0.05	0.02	76.2	262.9	108.4	55.8	1.540
1.092	1432	12.83	2.21	0.63	8.04	0.00	0.04	0.01	76.2	248.3	119.4	40.9	1.538
1.375	1376	13.06	2.21	0.64	8.05	0.00	0.02	0.01	76.0	156.3	73.2	34.4	1.542

COAL#16, Bituminous Coal Primary Flame, Natural Gas Reburning
 % vol ppmv

sec	K	% vol								ppmv			
RT	Temp	CO ₂	CO	H ₂	H ₂ O	O ₂	CH ₄	C ₂ H ₂	N ₂	NO	HCN	NH ₃	DCF
Stoichiometry = 1.23													
0.304	1588	12.66	0.05	0.00	6.46	3.79	0.00	0.00	77.1	827.8	0.0	0.0	1.303
Stoichiometry = 0.78													
0.569	1530	11.90	1.56	0.42	13.47	0.48	0.06	0.03	72.1	406.7	72.8	15.0	1.481
0.848	1452	9.80	4.43	2.34	10.55	0.00	0.49	0.16	72.2	98.4	227.8	62.7	1.478
1.138	1401	9.74	4.40	2.20	11.09	0.00	0.31	0.11	72.1	80.0	228.0	65.3	1.480
1.439	1343	9.71	4.52	2.07	11.33	0.00	0.27	0.08	72.0	57.6	249.2	78.6	1.483

COAL#17, Bituminous Coal Primary Flame, Bituminous Coal Reburning
 % vol ppmv

sec	K	% vol								ppmv			
RT	Temp	CO ₂	CO	H ₂	H ₂ O	O ₂	CH ₄	C ₂ H ₂	N ₂	NO	HCN	NH ₃	DCF
Stoichiometry = 1.12													
0.262	1621	14.16	0.11	0.00	7.05	2.18	0.00	0.00	76.5	760.4	0.0	0.0	1.194
Stoichiometry = 0.91													
0.494	1533	13.46	0.92	0.20	7.51	0.65	0.01	0.01	77.2	471.7	47.5	26.6	1.343
0.739	1466	13.13	1.25	0.24	7.51	0.28	0.01	0.01	77.6	374.6	38.5	27.6	1.338
0.995	1419	13.04	1.06	0.27	7.51	0.28	0.01	0.00	77.8	365.3	13.4	14.5	1.333
1.261	1351	13.42	0.97	0.30	7.48	0.09	0.01	0.00	77.7	282.2	8.0	25.4	1.335

COAL#18, Bituminous Coal Primary Flame, Natural Gas Reburning
 % vol ppmv

sec	K	% vol								ppmv			
RT	Temp	CO ₂	CO	H ₂	H ₂ O	O ₂	CH ₄	C ₂ H ₂	N ₂	NO	HCN	NH ₃	DCF
Stoichiometry = 1.10													
0.267	1621	14.34	0.14	0.00	7.18	2.00	0.00	0.00	76.3	737.9	0.0	0.0	1.172
Stoichiometry = 0.89													
0.765	1466	11.19	2.68	1.08	9.01	0.00	0.20	0.05	75.8	182.0	109.2	51.0	1.280
1.031	1419	11.18	2.68	1.01	9.08	0.00	0.20	0.05	75.8	131.8	119.9	50.1	1.280
1.308	1351	11.27	2.73	1.04	9.12	0.00	0.17	0.03	75.7	86.3	71.6	81.7	1.282

COAL#19, Bituminous Coal Primary Flame, Natural Gas Reburning

sec		% vol								ppmv			
RT	K Temp	CO ₂	CO	H ₂	H ₂ O	O ₂	CH ₄	C ₂ H ₂	N ₂	NO	HCN	NH ₃	DCF
Stoichiometry = 1.10													
0.272	1622	14.18	0.13	0.00	7.21	1.81	0.00	0.00	76.7	802.6	0.0	0.0	1.167
Stoichiometry = 0.90													
0.518	1543	11.99	1.31	0.32	9.83	0.27	0.09	0.02	76.2	356.2	70.2	24.6	1.275
0.777	1490	11.58	1.49	0.57	9.54	0.09	0.13	0.03	76.6	226.1	67.1	30.9	1.268
1.047	1425	11.63	1.45	0.60	9.53	0.14	0.12	0.03	76.5	217.1	45.2	39.4	1.269
1.326	1384	11.34	2.04	0.83	9.25	0.00	0.14	0.02	76.4	122.5	55.4	72.5	1.271

COAL#20, Bituminous Coal Primary Flame, Natural Gas + NH₃ Reburning

sec		% vol								ppmv			
RT	K Temp	CO ₂	CO	H ₂	H ₂ O	O ₂	CH ₄	C ₂ H ₂	N ₂	NO	HCN	NH ₃	DCF
Stoichiometry = 1.08													
0.274	1621	14.39	0.19	0.00	7.31	1.53	0.00	0.00	76.6	829.6	0.0	0.0	1.151
Stoichiometry = 0.89													
0.523	1558	12.05	1.44	0.43	9.76	0.36	0.11	0.02	75.8	383.5	31.1	26.4	1.262
0.781	1509	11.31	2.22	0.71	9.54	0.00	0.10	0.02	76.1	144.7	72.0	52.6	1.258
1.049	1444	11.27	2.13	0.71	9.51	0.00	0.12	0.04	76.2	167.4	53.3	31.1	1.256
1.329	1391	11.25	2.17	0.63	9.64	0.05	0.09	0.02	76.2	144.6	75.2	64.5	1.257

COAL#21, Bituminous Coal Primary Diffusion Flame, Type A, Natural Gas Reburning

sec		% vol								ppmv			
RT	K Temp	CO ₂	CO	H ₂	H ₂ O	O ₂	CH ₄	C ₂ H ₂	N ₂	NO	HCN	NH ₃	DCF
Stoichiometry = 1.10													
0.259	1690	13.92	0.28	0.00	7.17	2.32	0.00	0.00	76.3	603.4	0.0	0.0	1.173
Stoichiometry = 0.88													
0.484	1634	11.68	2.73	1.04	9.14	0.18	0.20	0.05	75.0	322.5	102.6	57.8	1.284
0.716	1554	11.34	3.55	1.44	8.88	0.05	0.11	0.04	74.6	195.9	64.3	56.2	1.291
0.959	1502	11.50	2.99	1.04	9.45	0.14	0.05	0.01	74.8	212.8	59.7	58.4	1.287
1.212	1448	11.72	2.30	0.76	9.82	0.23	0.04	0.01	75.1	243.5	43.7	40.7	1.282

RUN: COAL#14, SR₁ = 1.18, SR₃ = 1.11, Primary NO = 1029 (dry, 0% O₂)
 % vol (Reburn Zone) ppmv (dry, 0% O₂)

SR ₂	CO ₂	CO	H ₂	H ₂ O	O ₂	CH ₄	C ₂ H ₂	NO	HCN	NH ₃	NO _{ex}
0.96	11.82	0.95	0.24	9.45	0.23	0.04	0.01	406.0	16.2	25.6	427.5
0.93	11.59	1.22	0.36	9.78	0.18	0.06	0.02	337.6	44.3	27.0	344.3
0.88	11.03	2.42	0.74	10.36	0.04	0.12	0.04	253.3	160.5	54.0	264.8
0.84	10.74	3.16	1.10	10.89	0.03	0.13	0.06	223.6	149.7	52.8	205.9
0.77	9.45	4.81	2.29	10.88	0.00	0.37	0.17	150.8	428.4	71.5	221.4

RUN: COAL#15, SR₁=1.29, SR₂=0.80, SR₃=1.10, Coal Reburning
 RUN: COAL#16, SR₁=1.23, SR₂=0.78, SR₃=1.08, Natural Gas Reburning
 RUN: COAL#17, SR₁=1.12, SR₂=0.91, SR₃=1.12, Coal Reburning
 RUN: COAL#19, SR₁=1.10, SR₂=0.90, SR₃=1.10, Natural Gas Reburning
 RUN: COAL#20, SR₁=1.08, SR₂=0.89, SR₃=1.09, Natural Gas + NH₃ Reburning

COAL RUN	% vol (Reburn Zone)								ppmv (dry, 0% O ₂)				
	SR ₂	CO ₂	CO	H ₂	H ₂ O	O ₂	CH ₄	C ₂ H ₂	NO _p	NO	HCN	NH ₃	NO _{ex}
15	0.80	12.73	2.21	0.89	7.75	0.18	0.05	0.02	1051	404.8	166.9	85.9	279.4
16	0.78	9.80	4.43	2.34	10.55	0.00	0.49	0.16	1079	145.5	336.8	92.7	245.0
17	0.91	13.13	1.25	0.24	7.51	0.28	0.01	0.01	908	501.1	51.5	36.9	418.9
19	0.90	11.58	1.49	0.57	9.54	0.09	0.13	0.03	937	286.7	85.1	39.2	280.4
20	0.89	11.31	2.22	0.71	9.54	0.00	0.10	0.02	955	182.0	90.6	66.2	283.4

FUEL RICH COAL COMBUSTION DATA
(from Bose, 1989)

RT	Temp	H ₂	NH ₃	CH ₄	H ₂ O	N ₂	NO	HCN
RUN #1: UTAH BITUMINOUS #2; SR=0.84								
0.451	1666.8	1.65	28.0	0.186	7.16	71.41	724.1	33.6
0.599	1625.1	1.46	34.9	0.074	7.38	71.67	666.8	22.9
0.887	1512.8	1.55	32.0	0.000	7.26	71.37	491.5	31.3
1.170	1451.8	1.63	28.2	0.000	7.18	71.36	445.6	26.2
1.470	1401.1	1.65	34.4	0.000	7.16	71.41	413.1	33.5
RUN #2: UTAH BITUMINOUS #2; SR=0.61								
0.483	1574.3	2.48	52.6	0.292	8.75	66.56	474.5	174.3
0.642	1536.3	2.44	53.0	0.282	8.82	66.82	455.9	199.2
0.952	1423.0	2.67	56.5	0.219	8.55	66.55	320.1	216.9
1.260	1372.5	2.63	65.4	0.219	8.62	66.74	255.9	222.9
1.580	1323.0	2.55	78.1	0.209	8.72	66.84	228.2	253.8
RUN #3: RWE GERMAN BROWN; SR=0.83								
0.522	1481.9	0.63	28.5	0.329	15.53	66.31	557.5	19.1
0.762	1466.0	0.69	27.7	0.279	15.36	65.87	465.5	24.3
1.010	1387.4	0.68	27.1	0.338	15.38	65.89	448.5	22.0
1.500	1337.1	0.57	48.8	0.371	15.57	66.25	363.0	30.4
1.980	1298.0	0.58	37.5	0.371	15.68	66.72	337.3	44.3
2.460	1222.0	1.28	94.1	1.110	14.63	65.30	162.2	62.7
RUN #4: RWE GERMAN BROWN; SR=0.64								
0.638	1482.5	1.16	81.1	0.440	18.46	62.06	472.9	41.6
0.934	1439.2	1.03	57.8	0.521	18.67	62.30	414.8	41.9
1.240	1410.4	1.01	92.9	0.412	18.77	62.56	312.7	33.0
1.830	1332.0	0.88	88.3	0.461	19.00	62.86	202.5	32.5
2.420	1271.1	0.92	104.2	0.584	18.87	62.58	146.0	37.2
3.030	1212.6	0.71	81.8	0.541	19.21	63.01	129.3	36.5
RUN #7: UTAH BITUMINOUS #2; SR=0.38, N2 DILUTION								
0.517	1451.1	1.91	68.2	0.250	9.88	77.13	203.0	223.9
0.753	1399.9	2.43	56.0	0.330	9.34	77.06	58.6	285.0
0.998	1370.3	2.09	92.9	0.270	9.74	77.43	148.9	194.7
1.460	1358.0	2.47	76.3	0.230	9.32	77.16	136.0	213.3
1.890	1318.4	2.58	96.3	0.250	9.22	77.18	102.6	249.9
2.350	1272.9	2.51	139.8	0.220	9.25	76.93	95.3	196.6
RUN #8: UTAH BITUMINOUS #2; SR=0.77, O2 ENRICHMENT								
0.439	1732.8	2.11	40.4	0.017	10.06	67.55	877.9	73.3
0.643	1677.7	1.62	31.8	0.000	10.57	67.76	778.0	48.8
0.855	1614.6	1.53	21.4	0.000	10.65	67.65	723.7	55.4
1.270	1501.5	1.68	22.0	0.000	10.44	67.34	595.6	62.3
1.680	1456.8	1.04	19.9	0.000	10.35	67.32	529.0	73.3
2.100	1396.1	1.54	18.7	0.000	10.51	66.95	393.7	50.1
RUN #9: UTAH BITUMINOUS #2; SR=0.62, N2 DILUTION								
0.326	1466.7	1.13	107.4	0.149	6.90	79.50	363.1	369.2
0.477	1422.5	1.22	109.4	0.102	6.84	79.76	307.4	366.1
0.632	1383.8	1.85	102.9	0.093	6.17	79.30	300.3	396.1
0.935	1314.1	1.36	94.0	0.088	6.86	79.58	252.0	337.7
1.230	1251.2	1.53	118.5	0.065	6.55	79.94	224.3	228.2
1.550	1190.6	1.30	107.4	0.075	6.77	79.79	205.1	260.5

RT	Temp	H ₂	NH ₃	CH ₄	H ₂ O	N ₂	NO	HCN
RUN #10: UTAH BITUMINOUS #2; SR=0.59, O2 ENRICHMENT								
0.434	1520.0	6.47	194.3	0.224	6.71	63.81	205.2	714.8
0.638	1488.0	6.52	220.5	0.214	6.67	63.89	191.3	652.4
0.847	1451.0	6.82	199.7	0.178	6.34	63.77	140.5	615.4
1.260	1321.0	6.84	218.4	0.169	6.28	63.55	103.1	609.2
1.670	1284.0	6.37	203.5	0.158	6.85	64.03	88.5	464.1
2.090	1248.0	6.09	203.0	0.102	7.08	63.81	65.1	326.0
RUN #11: UTAH BITUMINOUS #2; SR=0.60, O2 ENRICHMENT								
0.435	1519.0	5.69	228.0	0.176	7.38	64.29	194.5	612.3
0.639	1481.0	6.33	273.4	0.196	6.61	63.65	163.4	689.3
0.848	1456.0	6.55	291.1	0.187	6.39	63.69	135.7	692.7
1.450	1351.0	6.80	282.1	0.188	6.15	63.67	98.5	602.8
1.660	1311.0	6.60	257.2	0.201	6.37	63.82	74.9	565.8
2.070	1278.0	6.20	333.7	0.149	6.69	63.39	60.6	553.4
RUN #13: UTAH BITUMINOUS #2; SR=0.62								
0.356	1577.0	2.65	67.9	0.130	9.11	69.83	427.2	125.7
0.524	1520.0	2.97	58.0	0.139	8.74	69.51	392.4	209.2
0.698	1475.0	2.96	40.1	0.125	8.76	69.55	383.2	144.4
1.030	1403.0	2.76	35.5	0.120	8.96	69.51	300.4	122.7
1.370	1343.0	2.65	29.7	0.128	9.12	69.81	290.8	76.1
1.720	1249.0	2.39	27.3	0.140	9.44	70.22	271.7	68.2
RUN #15: UTAH BITUMINOUS #2; SR=0.62								
0.384	1533.0	3.16	73.5	0.131	8.60	69.75	383.9	188.0
0.570	1496.0	3.38	93.1	0.132	8.32	69.42	307.1	283.6
0.762	1452.2	3.54	98.8	0.126	8.16	69.40	248.0	227.6
1.140	1366.0	3.82	109.9	0.125	7.82	69.01	184.4	164.5
1.500	1308.0	3.76	116.1	0.147	7.91	69.21	156.6	182.2
1.870	1309.0	3.65	138.5	0.174	10.59	69.52	137.9	150.1
RUN #22: RWE GERMAN BROWN; SR=0.81, O2 ENRICHMENT								
0.528	1580.0	1.83	36.7	0.040	16.15	60.47	352.1	14.3
0.776	1551.0	1.99	38.0	0.049	15.95	60.34	327.8	18.2
1.030	1485.0	2.24	78.5	0.055	15.73	60.44	265.4	24.0
1.540	1391.0	2.73	57.2	0.075	15.12	60.02	199.5	17.4
2.030	1327.0	3.05	119.7	0.094	14.77	59.93	127.8	14.3
2.550	1281.0	2.68	106.2	0.108	15.16	60.00	97.6	18.1

APPENDIX C:
PROGRAM LISTINGS

FAC.SPS: SPSS Multiple Regression Program

FILE HANDLE FAC/NAME='FAC.DAT'
DATA LIST FILE=FAC/RUN 5-11(A) DIST 13-17(3) SRONE 19-23(3)
SRTWO 25-29(3) COAL 31-35(3) SRF 37-40(2) TIME 42-46(3)
NOIN 49-52 TONE 54-57 TTWO 59-62 TF 64-67 Y 69-72(1)

COMPUTE X1=(DIST-0.5335)/0.2285
COMPUTE SR1=(SRONE-1.225)/0.125
COMPUTE SR2=(SRTWO-0.855)/0.125
COMPUTE X4=(COAL-1.575)/0.425
COMPUTE RT=(TIME-0.35)/0.25
COMPUTE NOP=(NOIN-1040.0)/95.0
COMPUTE T1=(TONE-1550.0)/150.0
COMPUTE T2=(TTWO-1490.0)/180.0
COMPUTE T3=(TF-1405.0)/170.0

COMPUTE X1X1=X1*X1
COMPUTE X1SR1=X1*SR1
COMPUTE X1SR2=X1*SR2
COMPUTE X1X4=X1*X4
COMPUTE X4X4=X4*X4
COMPUTE X4SR1=X4*SR1
COMPUTE X4SR2=X4*SR2
COMPUTE SR1SR1=SR1*SR1
COMPUTE SR1SR2=SR1*SR2
COMPUTE SR1RT=SR1*RT
COMPUTE SR1T2=SR1*T2
COMPUTE SR2SR2=SR2*SR2
COMPUTE SR2RT=SR2*RT
COMPUTE SR2T2=SR2*T2
COMPUTE RTRT=RT*RT
COMPUTE RTT2=RT*T2
COMPUTE T2T2=T2*T2

REGRESSION VARIABLES=Y SR1 SR2 RT NOP T1 T2 T3
/STATISTICS=DEFAULTS CI F
/DEPENDENT=Y
/METHOD=BACKWARD SR1 SR2 RT NOP T1 T2 T3

REGRESSION VARIABLES=Y X1 SR1 SR2 X4 X1X1 SR1SR1 SR2SR2 X4X4
X1SR1 X1SR2 X1X4 SR1SR2 X4SR1 X4SR2
/CRITERIA=PIN(0.099) POUT(0.1)
/STATISTICS=DEFAULTS CI F
/DEPENDENT=Y
/METHOD=STEPWISE X1 SR1 SR2 X4 X1X1 SR1SR1 SR2SR2 X4X4
X1SR1 X1SR2 X1X4 SR1SR2 X4SR1 X4SR2

REGRESSION VARIABLES=Y SR1 SR2 RT T2 SR1SR1 SR2SR2 RTRT T2T2
SR1SR2 SR1RT SR1T2 SR2RT SR2T2 RTT2
/CRITERIA=PIN(0.099) POUT(0.1)
/STATISTICS=DEFAULTS CI F
/DEPENDENT=Y
/METHOD=STEPWISE SR1 SR2 RT T2 SR1SR1 SR2SR2 RTRT T2T2
SR1SR2 SR1RT SR1T2 SR2RT SR2T2 RTT2

MASS.FOR: Mass Balance Program

```

C ***      Furnace mass balance, updated OCTOBER, 1990
C -- coal burning, staging with air, reburning with fuel
C      detailed species analysis
C      also used to generate tables of experimental data
C -- input file REB.DAT
C -- output files:
C      REB.RES : all information
C      FOR021.DAT: times and T, intermediate use data only
C      FOR040.DAT: raw data, all flows, primary and exhaust, T
C      FOR050.DAT: run ID, RZ length, SR1, SR2, coal feed, SR3,
C                  time, NOP, T1, T2, T3, RE, RP, BP, RT1, NOex
C      FOR060.DAT: data file for MODEL program
C      FOR065.DAT: data for N-species (dry, 0% O2), conversions
C      FOR070.DAT: detailed measurements raw data
C      FOR080.DAT: wet values, reduced data
C      PROGRAM MASS
C -- data entry guide: # runs, then for each run,
C title and explanation of run
C ICODE, coal type code, coal feed rate in g/min, SR1
C      ICODE=1, one stream reburning fuel
C      ICODE=2, multiple reburning fuel streams
C      ICODE=3, effect of SR3
C      ICODE=4, N2O data follow other concentration data
C      ICODE=5, and higher: new construction of furnace
C      ICODE=6, and higher: detailed species (except N2O)
C      ICODE=7, O2 enrichment in feed
C      ICODE=8, gas flame
C port number, ISTAT: a number indicating what the port is used for
C      ISTAT=0, port not used
C      ISTAT=1, sample, data follow: T(C), ppm NO, %O2, %CO2, %CO..
C      ISTAT=2, air staging port, SCFM staged air follow
C      ISTAT=3, reburning port: 5 entries
C          1. M=1 coal reburn, M=2 gas reburn
C          2. MN=1 CH4/NH3 REBURN FUEL
C             MN=4 OTHER, next line enter # atoms
C          3. ZW1=g/min reburn coal or SCFM reburn gas
C          4. TRN2 SCFM of transport N2
C          5. ZW2 fraction of N-species gas doped
C      ICODE < 6, M=2, enter only ZW1 and TRN2
C -- end of data entry guide
C watch for NPORTS and VOL, depend on furnace used

REAL N2AIR
CHARACTER RID*80,ANS
DIMENSION TEMP(0:16),VOL(16),VOLEFF(16),VOLONE(7),VOLTWO(16),
+          VOLNEW(7),X(9),Y1(9),Y2(9),DIST(7),REG(7),ITEMP(7)

C -- 3rd generation 16-port furnace
C DATA VOLTWO/0.0709,0.1963,0.1963,0.1963,0.1759,0.2209,0.3722,
C      2 0.2291,0.1963,0.1963,0.1963,0.1963,0.1963,0.1963,0.2004,0.1963/
C -- 2nd generation 7-port furnace
C for the newly constructed furnace
C DATA VOLNEW/0.0653,0.0886,0.0886,0.0886,0.1772,0.1772,0.1772/
C old values: for all data before RR# runs, February 1989
C DATA VOLONE/0.0806,0.0982,0.0982,0.0982,0.1832,0.171,0.171/

OPEN (UNIT=9,FILE='REB.DAT',STATUS='OLD')
OPEN (UNIT=10,FILE='REB.RES',STATUS='NEW')
OPEN (UNIT=12,FILE='FOR021.DAT',STATUS='NEW')

```

```

          NPORTS=7
C ... get number of runs
  READ (9,*) NRUNS
  DO 400 IR=1,NRUNS
***** initialize
          SRONE =0.0
          IREBP =0
          IBZP  =0
          SRTWO =0.0
          SROAIR=0.0
          ANO   =0.0
          PNO   =0.0
          STAGNO=0.0
          ZW1   =0.0
          TRN2  =0.0
          SAIR  =0.0

C ... input run data
C ... run title
  READ (9,500) RID
  500   FORMAT (A80)
  WRITE (12,902) RID
  902   FORMAT (1X,A75)
C ...   ICODE, coal type, coal feed (g/min), initial stoichiometry
  READ (9,*) ICODE,MCOAL,WCLWA,SRONE
  FO2=0.0
  IF (ICODE .EQ. 7) READ (9,*) FO2
C ...   kg/h coal feed
  GKPHR=WCLWA*60.0/1000.0
  FN2=0.0
C ...   T of preheat air is 600 F
  TEMP(0)=589.0

  DO 700 IAM=1,NPORTS
  IF (NPORTS .EQ. 16) VOL(IAM)=VOLTWO(IAM)
  IF (NPORTS .EQ. 7 .AND. ICODE .LT. 5) VOL(IAM)=VOLONE(IAM)
  IF (NPORTS .EQ. 7 .AND. ICODE .GE. 5) VOL(IAM)=VOLNEW(IAM)
  700   CONTINUE
  IF (ICODE .GE. 6) WRITE (60,902) RID
  IF (ICODE .GE. 6) WRITE (65,902) RID
  IF (ICODE .GE. 6) WRITE (70,906) RID,GKPHR,SRONE
  906   FORMAT ('/RUN: ',A7/'Utah Bituminous # 2 coal feed in kg/h =',
  1       F6.3,', primary stoichiometry =',F5.2/
  2       'PORT',1X,'Temp',2X,'CO2',3X,'CO',3X,'H2',
  3       3X,'O2',2X,'CH4 C2H2',3X,'NO'/
  4       '-----',1X,'-----',2X,'---',3X,'---',3X,'---',
  5       3X,'---',2X,'---' '-----',3X,'---')
  WRITE (80,*) ' '
  WRITE (80,902) RID

C ... fuel analysis:
C ... wt % C, H, O, N, S, ASH (dry basis), MOISTURE (wet basis)
C AIRREQ = theoretical SCFM air/ grams per min of coal
C TOTFLU = theoretical moles of flue gas/mass of coal at SR=1
C IF (MCOAL .EQ. 1) THEN
C '(1) UTAH BITUMINOUS #3'
  WPC=70.58
  WPH=5.09
  WPO=11.84
  WPN=1.3
  WPS=0.27
  WPASH=10.46

```



```

WPMOIS=2.07
AIRREQ=0.2713
TOTFLU=0.3099
ELSEIF (MCOAL .EQ. 2) THEN
C '(2) ILLINOIS BITUMINOUS #2'
WPC=60.31
WPH=3.87
WPO=9.52
WPN=1.52
WPS=2.4
WPASH=21.6
WPMOIS=5.06
AIRREQ=0.2235
TOTFLU=0.2563
ELSEIF (MCOAL .EQ. 3) THEN
C '(3) TEXAS LIGNITE, SAN MIGUEL'
WPC=39.05
WPH=3.11
WPO=18.18
WPN=0.82
WPS=2.28
WPASH=36.56
WPMOIS=23.2
AIRREQ=0.1107
TOTFLU=0.1285
ELSEIF (MCOAL .EQ. 4) THEN
C '(4) UTAH BITUMINOUS #2'
WPC=70.42
WPH=5.04
WPO=16.25
WPN=1.47
WPS=0.62
WPASH=6.91
WPMOIS=1.71
AIRREQ=0.2662
TOTFLU=0.3054
ELSEIF (MCOAL .EQ. 5) THEN
C '(5) BEULAH LIGNITE, LOW NA'
WPC=54.93
WPH=3.86
WPO=24.47
WPN=0.72
WPS=2.09
WPASH=11.07
WPMOIS=18.64
AIRREQ=0.1607
TOTFLU=0.1871
ELSEIF (MCOAL .EQ. 6) THEN
C '(6) NATURAL GAS, HOUSE'
WPC=71.75
WPH=23.27
WPO=0.000001
WPN=0.000001
WPS=0.000001
WPASH=0.000001
WPMOIS=0.000001
AIRREQ=0.4812
TOTFLU=0.5063
WCLWA=WCLWA/0.04963
C 'FOR NATURAL GAS, 0.04963 SCFM PER EACH g/min
ENDIF

```

```

C ... fuel flow rate in pounds per hour
WCLW=WCLWA/7.56
C ... air feed in SCFM
FAIR=SRONE*AIRREQ*WCLWA

C ... output run data
C WRITE (10,510) RID,IR
510 FORMAT ('1',' Mass balance for: ',A75,I3/)
C WRITE (10,520) WPC,WPH,WPO,WPS,WPN,WPAsh,WPMOIS
520 FORMAT (' FUEL ANALYSIS '/' C wt % dry ',F6.2/
1 ' H wt % dry ',F6.2/
2 ' O wt % dry ',F6.2/' S wt % dry ',F6.2/
3 ' N wt % dry ',F6.2/' ASH wt % dry ',F6.2/
4 ' MOISTURE wt % (wet basis) ',F6.2/)
C WRITE (10,525) MCOAL,WCLWA,FAIR,FO2
525 FORMAT (1X,'INLET: Coal Type',I2,2X,F5.2,' g/min with ',
1 F6.3,' SCFM Air and ',F6.3,' SCFM O2')

C ... coal flow, dry basis
WCL=WCLW*(1.0-0.01*WPMOIS)
C ... total lb-moles in, basis minute
CIN=WCL/60.*WPC/100./12.
HIN=WCL/60.*WPH/100. + WCLW/60.*WPMOIS/100./18.*2.
OINF=WCL/60.*WPO/100./16. + WCLW/60.*WPMOIS/100./18.
SIN=WCL/60.*WPS/100./32.
FNIN=WCL/60.*WPN/100./14.
C note: 386.72 is molar volume (SCFM/lb-mol)
O2AIR=(FO2+0.209*FAIR)/386.72
N2AIR=(FN2+0.791*FAIR)/386.72
C ... calculate SR, stoichiometric ratio
O2TH=CIN+(WCL/60.*WPH/100.)/4.+SIN-(WCL/60.*WPO/100./16.)/2.
SR=O2AIR/O2TH
C WRITE (10,530) SR
SRONE=SR
530 FORMAT (' The stoichiometric ratio = ',F5.3)

C ... initialize VOLEFF
DO 100 I=1,NPORTS
VOLEFF(I)=0.0
100 CONTINUE

TAU = 0.0
VOLEFF(1)=VOL(1)

WRITE (80,701)
701 FORMAT (1X,' RT',2X,'Temp',2X,'CO2',3X,'CO',3X,'H2',
+ 3X,'H2O O2 CH4 C2H2 N2 NO HCN NH3 DCF '/
+ ' --- ---- --- -- --',
+ 3X,'--- -- --- ---- -- -- --- --- --- ')
WRITE (80,806) SR
806 FORMAT (1X,'Stoichiometry = ',F4.2)
C ... for each port
DO 200 IPORT=1,NPORTS

READ (9,*) NPORT,ISTAT
IF (IPORT.NE.NPORT) THEN
WRITE (6,*) 'RUN # ',IR
WRITE (6,*) 'IPORT = ',IPORT,' ; NPORT = ',NPORT
WRITE (6,*) 'PLEASE CHECK DATA ; PROGRAM TERMINATING'
STOP
ENDIF

```

```

                                DONT=0.0
                                IF (ISTAT .NE. 1) WRITE (12,606) IPORT,DONT,DONT
                                IF (ISTAT .NE. 1) ITEMP(IPORT)=0
606                                FORMAT (1X,I2,1X,F5.3,1X,F6.1)

C ...                                ISTAT gives status of IPORT:
C ...                                ISTAT=0 ==> IPORT not used
C ...                                ISTAT=1 ==> IPORT used for data collection
C ...                                ISTAT=2 ==> IPORT is air staging port
C ...                                ISTAT=3 ==> IPORT is reburning port
C ...                                if this is not a data port ...
                                IF (ISTAT .NE. 1) THEN
                                    TEMP(IPORT)=TEMP(IPORT-1)
                                    VOLEFF(IPORT+1)=VOLEFF(IPORT)+VOL(IPORT+1)
C ...                                if this is a staging port ...
                                IF (ISTAT .EQ. 2) THEN
                                    READ (9,*) SAIR
                                        SN2=0.0
                                        SO2=0.0
C ...                                WRITE (10,532) IPORT,SAIR
532                                FORMAT (' STAGING PORT ',I2,' with ',F6.3,' SCFM air')
C ...                                figure O2 and N2 additions, convert to lb-mols/min
                                    SN2=(SN2+0.791*SAIR)/386.72
                                    SO2=(SO2+0.209*SAIR)/386.72
C ...                                total N2 and O2 fed, recalculate SR
                                    N2AIR=N2AIR+SN2
                                    O2AIR=O2AIR+SO2
                                    SR=O2AIR/O2TH
                                WRITE (80,806) SR
907                                IF (ICODE .GE. 6) WRITE (70,907) IPORT,SAIR
                                    FORMAT (1X,I1,3X,'inject ',F5.3,' SCFM air')
                                        IBZP=IPORT
                                        SROAIR=SR
                                        STAGNO=ANO
C ...                                WRITE (10,530) SR
                                ENDIF

C ...                                if this is a reburning port ...
                                IF (ISTAT .EQ. 3) THEN
                                    XYZ1=0.01*(1.0-0.01*WPMOIS)
                                    C1=WPC*XYZ1
                                    H1=WPH*XYZ1
                                    O1=WPO*XYZ1
                                    AN1=WPN*XYZ1
                                    S1=WPS*XYZ1

                                    IF (ICODE .LT. 6) READ (9,*) ZW1,TRN2
                                        to cut down on data in file if only exhaust is of interest
                                        natural gas reburning, no N- additives
C ...                                M =2
C ...                                MN=1
                                    ZW2=0.0
                                    IF (ICODE .GE. 6) READ (9,*) M,MN,ZW1,TRN2,ZW2
                                        TRAIR=0.0
                                        TRO2=0.0
                                        KLM1=2

C ...                                M=1 for coal reburning, M=2 for gas reburning
C ...                                TRAIR=air added at reburning port in SCFM
C ...                                ZW1=g/min reburn coal if M=1 or SCFM reburn gas if M=2
C ...                                rest of data relevant to gas reburning only
C ...                                KLM1= (1 for mass), (2 for volume) fraction of N-species

```

```

C ...      ZW2 is fraction
C ...      MN=1 for CH4/NH3 combination reburn gas
C ...      MN=2 for H2 -NH3 REBURN FUEL
C ...      MN=3 for CO -NH3 REBURN FUEL
C ...      MN=4 for OTHER, most general
C ...      rest of data relevent only in case of MN=4: next line
C ...      # of atoms: 1 for reburn fuel gas, 2 for N-species

      IF (M .EQ. 1) THEN
          R2=60.0*O2TH/WCLW
          C2=C1
          H2=H1
          S2=S1
          O2=O1
          AN2=AN1
          REBF=ZW1/453.6
          REBFV=0.0
          XYZ2=(WCLWA+ZW1)/WCLWA
          CIN=CIN*XYZ2
          HIN=HIN*XYZ2
          OINF=OINF*XYZ2
          SIN=SIN*XYZ2
          FNIN=FNIN*XYZ2
      ELSEIF (M .EQ. 2) THEN
          NC1=0
          NH1=0
          NO1=0
          NS1=0
          NC2=0
          NH2=3
          NO2=0
          NN2=1
C      (1) CH4-NH3 REBURN FUEL
C      (2) H2 -NH3 REBURN FUEL
C      (3) CO -NH3 REBURN FUEL
C      (4)          OTHER
      IF (MN .EQ. 1) THEN
          NC1=1
          NH1=4
      ELSEIF (MN .EQ. 2) THEN
          NH1=2
      ELSEIF (MN .EQ. 3) THEN
          NC1=1
          NO1=1
      ELSEIF (MN .EQ. 4) THEN
          READ (9,*) NC1,NH1,NS1,NO1,NC2,NH2,NO2,NN2
      ENDIF

          GM2=NC2*12.0+NH2*1.0+NO2*16.0+NN2*14.0
          GM1=NC1*12.0+NH1*1.0+NS1*32.0+NO1*16.0
C ...      (GM1) IS MW OF REBURN GAS
C ...      (GM2) IS MW OF N-SPECIES
      IF (ZW2 .EQ. 0.0) GM2=1.0
          IF (KLM1 .EQ. 1) THEN
              FNS=ZW2
          ELSEIF (KLM1 .EQ. 2) THEN
              FNSV=ZW2
              FNS=FNSV*GM2/(FNSV*GM2+(1.0-FNSV)*GM1)
          ENDIF
C ...      (GMOL1) IS MOLES OF REBURN GAS
C ...      (GMOL2) IS MOLES OF N-SPECIES
C ...      (TGMOL) IS 1/MW OF REBURN GAS MIXTURE

```

```

GMOL1=(1.0-FNS)/GM1
GMOL2=FNS/GM2
TGMOL=GMOL1+GMOL2
FNSV=GMOL2/TGMOL
C ... (FNSV) IS VOLUME FRACTION OF N-SPECIES

C2=NC1*12.0*GMOL1+NC2*12.0*GMOL2
H2=NH1*1.0 *GMOL1+NH2*1.0 *GMOL2
S2=NS1*32.0*GMOL1
O2=NO1*16.0*GMOL1+NO2*16.0*GMOL2
AN2= NN2*14.0*GMOL2
R2=(C2/12.0)+(H2/4.0)+(S2/32.0)-(O2/32.0)

REBFV=ZW1
REBF=REBFV/(386.72*TGMOL)
CIN=CIN+(C2*REBF/12.0)
HIN=HIN+(H2*REBF/1.0)
OINF=OINF+(O2*REBF/16.0)
SIN=SIN+(S2*REBF/32.0)
FNIN=FNIN+(AN2*REBF/14.0)

ENDIF
C ... the ENDIF is for reburn fuel type check (M)

N2AIR=N2AIR+0.791*TRAIR/386.72+TRN2/386.72
O2AIR=O2AIR+0.209*TRAIR/386.72+TRO2/386.72
O2TH=O2TH+R2*REBF
SR=O2AIR/O2TH
WRITE (80,806) SR
802 IF (ICODE .GE. 6) WRITE (70,802) IPORT,REBFV,TRN2
      FORMAT (1X,I1,3X,'inject ',F5.3,' SCFM natural gas and ',
      F5.3,' SCFM N2')
      1
      IREBP=IPORT
      SRTWO=SR
      PNO=ANO
      PNOW=YNOW
      RNO =YNO
      RO2 =YO2 *100.0
      RCO2=YCO2*100.0
      RCO =YCO *100.0

C ... dilution factor due to N2 and gas addition
ddd=386.72*fwet/(zwl+trn2+386.72*fwet)
pcto2=vo2w*ddd
pctch4=zwl*100.0/(zwl+trn2+386.72*fwet)
c pctch4=(zwl*100.0/(zwl+trn2+386.72*fwet))-0.5*pcto2
pcth2o=vh2ow*ddd
pctn2=(trn2*100.0+386.72*fwet*vn2w)/(zwl+trn2+386.72*fwet)
pctno=ynow*ddd
du=0.0
IF (ICODE .GE. 6) WRITE (60,705)
+ du,du,du,du,pctch4,pcth2o,pctn2,pctno,du
705 FORMAT(1X,F5.3,F8.1,F7.3,F7.1,F7.3,2(F7.2),2(F7.1))

C WRITE (10,533) IPORT,TRN2,REBFV,ZW1
533 FORMAT (' REBURNING PORT ',I2,' with ',F6.3,' SCFM N2 and ',
      F6.3,' SCFM REBURN FUEL or ',F8.4)
      1
C IF (M .EQ. 1) WRITE (10,*) ' COAL REBURNING'
C IF (M .EQ. 2) WRITE (10,*) ' GAS REBURNING'
C IF (M .EQ. 2 .AND. MN .EQ. 1) WRITE (10,*) ' CH4/NH3 GAS'
C IF (M .EQ. 2 .AND. MN .EQ. 2) WRITE (10,*) ' H2/NH3 GAS'
C IF (M .EQ. 2 .AND. MN .EQ. 3) WRITE (10,*) ' CO/NH3 GAS'

```

```

C          WRITE (10,534) ZW2,AN2
534  FORMAT (' Fractions N-species and -N- in reburn fuel',F6.4,F9.4)
C          WRITE (10,530) SR
C          recalculate SR
C          ...
C          ENDIF
C          the ENDIF is for ISTAT check
C          ...
C          no data to read, so go to next port
C          GOTO 200
C          ENDIF
C          the ENDIF is for ISTAT .NE. 1 check
C          ...
C          initialize to avoid errors if not entered
YHCN =0.0
YNH3 =0.0
YH2  =0.0
YCH4 =0.0
YC2H6=0.0
YC2H2=0.0
YN2O =0.0
C          ...
C          get data for this port
      IF (ICODE .LT. 6) READ (9,*) TMPINC,YNO,YO2,YCO2,YCO
      IF (ICODE .GE. 6) READ (9,*)
+      TMPINC,YNO,YO2,YCO2,YCO,YHCN,YNH3,YH2,YCH4,YC2H6,YC2H2
      IF (ICODE .EQ. 4) READ (9,*) YN2O
      TMP=TMPINC+273.0
      ITEMP(IPORT)=INT(TMP)
      IYNO=INT(YNO)
      IF (ICODE .GE. 6) WRITE (70,801) IPORT,ITEMP(IPORT),YCO2,YCO,
+      YH2,YO2,YCH4,YC2H2,IYNO
801  FORMAT (1X,I1,3X,I4,F6.2,5(F5.2),I5)
C          WRITE (10,535) IPORT,TMP,YCO2,YCO,YH2,YO2,YNO,YN2O,YHCN,
C          YNH3,YCH4,YC2H6,YC2H2
535  FORMAT (//' PORT',I3/' Temp K= ',F8.2/' YCO2 dry %= ',F7.3/
2      ' YCO dry %= ',F7.3/' YH2 dry %= ',F7.3/
3      ' YO2 dry %= ',F7.3/' NO ppmv= ',F6.2/
4      ' N2O ppmv= ',F6.2/
5      ' HCN ppmv= ',F6.2/' YNH3 ppmv= ',F6.2/
6      ' CH4 dry %= ',F7.3/' C2H6 dry %= ',F7.3/
7      ' C2H2 dry %= ',F7.3)
      TEMP(IPORT)=TMP
      XNO =YNO
      XO2 =YO2
      XCO2=YCO2
      XCO =YCO
C          ...
C          dry flue gas rate in lb-moles/min from N balance
      YN2=(100.0-YCO2-YCO-YO2-YH2-YCH4-YC2H6-YC2H2)/100.0
      FDRY=(N2AIR+FNIN/2.)/YN2
C          ...
C          convert vol% to mole fraction
      YH2=YH2/100.0
      YCO2=YCO2/100.0
      YCO=YCO/100.0
      YO2=YO2/100.0
      YCH4=YCH4/100.0
      YC2H6=YC2H6/100.0
      YC2H2=YC2H2/100.0

```

```

C ... mole fraction water by H balance
  YH2O=(HIN-FDRY*(2.0*(YH2+YC2H2)+
+       4.0*YCH4+6.0*YC2H6))/(2.0*FDRY)
C ... lb-moles wet flue gas
  FWET=FDRY*(1.0+YH2O)
C ... moles carbon remaining in residue
  CS=CIN-FDRY*(YCO2+YCO+YCH4+2.*YC2H2+2.*YC2H6)
C ... % carbon remaining in residue
  FCS=(CS/CIN)*100.0
C ... moles of O unaccounted for
  ODEFML=2.0*O2AIR+OINF-FDRY*(2.*(YO2+YCO2)+YCO+YH2O)
C ... % oxygen deficit
  ODEF=(ODEFML/(2.0*O2AIR+OINF))*100.0
C ... fuel nitrogen conversions
  CNO=(1.0E-6*YNO*FDRY/FNIN)*100.0
  CN2O=(1.0E-6*YN2O*FDRY/FNIN)*100.0
  CHCN=(1.0E-6*YHCN*FDRY/FNIN)*100.0
  CNH3=(1.0E-6*YNH3*FDRY/FNIN)*100.0
  CXN=100.0-CNO-CN2O-CHCN-CNH3
IF (ICODE .EQ. 8) THEN
  CNO =0.0
  CHCN=0.0
  CNH3=0.0
ENDIF

C ... wet percentages
  XSI=FDRY/FWET
  YN2W=YN2*XSI
  YCO2W=YCO2*XSI
  YCOW=YCO*XSI
  YH2W=YH2*XSI
  YH2OW=YH2O*XSI
  YO2W=YO2*XSI
  YNOW=YNO*XSI
  YN2OW=YN2O*XSI
  YHCNW=YHCN*XSI
  YNH3W=YNH3*XSI
  YCH4W=YCH4*XSI
  YC2H6W=YC2H6*XSI
  YC2H2W=YC2H2*XSI

C ... dilution correction
C ... dry values correction to 0% O2
  DCF=FDRY/(TOTFLU*(WCLW/60.0))
C ... wet values correction to dry and 0% O2
  DCFA=DCF/XSI

  ANO=YNO*DCF
  AN2O=YN2O*DCF
  AHCN=YHCN*DCF
  ANH3=YNH3*DCF
  ANOW=ANO*XSI
  AN2OW=AN2O*XSI
  AHCNW=AHCN*XSI
  ANH3W=ANH3*XSI

C ... residence time from top to port
  TAV=(TEMP(IPORT)+TEMP(IPORT-1))/2.0
  VRAT=(760.0/700)*FWET*386.72*TAV/(530.0*60.0/1.8)
  TAU=TAU+VOLEFF(IPORT)/VRAT

```

```

C ... write answers
WRITE (12,606) IPORT,TAU,TMP
C WRITE (10,541) IPORT,TAU,TMPINC
541 FORMAT (1X'PORT',I3,' with',F6.3,' sec and',F7.1,' C'//
4 ' Mole Fractions Dry',9X,'Wet',9X,'Dry, Stoichiometric')

C ... convert dry mole fraction to vol%
VCO2=YCO2*100.0
VCO=YCO*100.0
VH2=YH2*100.0
VH2O=YH2O*100.0
VO2=YO2*100.0
VCH4=YCH4*100.0
VC2H6=YC2H6*100.0
VC2H2=YC2H2*100.0
VN2=YN2*100.0

C ... convert wet mole fraction to vol%
VCO2W=YCO2W*100.0
VCOW=YCOW*100.0
VH2W=YH2W*100.0
VH2OW=YH2OW*100.0
VO2W=YO2W*100.0
VCH4W=YCH4W*100.0
VC2H6W=YC2H6W*100.0
VC2H2W=YC2H2W*100.0
VN2W=YN2W*100.0

C WRITE(10,545) VN2,VN2W,du,VCO2,VCO2W,du,VCO,VCOW,du,VH2,VH2W,du,
C 1 VH2O,VH2OW,du,VO2,VO2W,du,VCH4,VCH4W,du,VC2H6,VC2H6W,du,
C 2 VC2H2,VC2H2W,du,
C 3 YNO,YNOW,ANO,YN2O,YN2OW,AN2O,YHCN,YHCNW,AHCN,YNH3,YNH3W,ANH3
545 FORMAT (/ ' N2 ',10X,3(F10.3,3X)/' CO2 ',10X,3(F10.3,3X)/
1 ' CO ',10X,3(F10.3,3X)/' H2 ',10X,3(F10.3,3X)/
2 ' H2O ',10X,3(F10.3,3X)/' O2 ',10X,3(F10.3,3X)/
6 ' CH4 ',10X,3(F10.3,3X)/' C2H6 ',10X,3(F10.3,3X)/
7 ' C2H2 ',10X,3(F10.3,3X)/
3 ' NO ',10X,3(F10.3,3X)/
4 ' N2O ',10X,3(F10.3,3X)/
5 ' HCN ',10X,3(F10.3,3X)/' NH3 ',10X,3(F10.3,3X))

C ... if this data port is not the last port, assign VOLEFF
C for the next port
IF (IPORT .LT. NPORTS) VOLEFF(IPORT+1)=VOL(IPORT+1)

WRITE (80,702) TAU,ITEMP(IPORT),VCO2W,VCOW,VH2W,
+ VH2OW,VO2W,VCH4W,VC2H2W,VN2W,YNOW,YHCNW,YNH3W,DCFA
702 FORMAT (1X,F5.3,I5,F6.2,2(F5.2),F6.2,3(F5.2),
+ F5.1,F7.1,2(F6.1),F6.3)
QNO =100.0
QHCH= 0.0
QNH3= 0.0
IF (PNO .EQ. 0.0) GO TO 808
QNO =100.0*ANO /PNO
QHCH=100.0*AHCN/PNO
QNH3=100.0*ANH3/PNO
808 IF (ICODE .GE. 6) WRITE (65,809)
+ TAU,TMP,VH2W,VCH4W,ANO,AHCN,ANH3,QNO,QHCH,QNH3
809 FORMAT (1X,F5.3,F8.1,2(F7.3),F8.1,2(F7.1),3(F7.2))
IF (ICODE .GE. 6) WRITE (60,704)
+ TAU,TMP,VH2W,YNH3W,VCH4W,VH2OW,VN2W,YNOW,YHCNW
704 FORMAT(1X,F5.3,F8.1,F7.3,F7.1,F7.3,2(F7.2),2(F7.1))
200 CONTINUE

```



```

WRITE(40,901)RID,GKPHR,SRONE,REBFV,TRN2,IREBP,SAIR,IBZP,RNO,
+   RO2,RCO2,RCO,XNO,XO2,XCO2,XCO,ITEMP(1),ITEMP(2),ITEMP(3),
+   ITEMP(4),ITEMP(5),ITEMP(6),ITEMP(7)
901  FORMAT (1X,'RUN: ',A7/'Utah Bituminous # 2 coal feed in kg/h =',
+   F6.3,', primary stoichiometry =',F5.2/
+   'inject ',F5.3,' SCFM natural gas and ',
+   F5.3,' SCFM N2 at port ',I1/
+   'inject ',F5.3,' SCFM air at port ',I1/
+   'primary zone: ppmv NO = ',F6.1,', % O2 = ',F4.2,
+   ', % CO2 = ',F5.2,', % CO = ',F4.2/
+   'exhaust : ppmv NO = ',F6.1,', % O2 = ',F4.2,
+   ', % CO2 = ',F5.2,', % CO = ',F4.2/
+   'Temp. in K: T1=',I4,', T2=',I4,', T3=',I4,', T4=',I4,
+   ', T5=',I4,', T6=',I4,', T7=',I4/)

WRITE(12,399)GKPHR,SRONE,IREBP,SRTWO,IBZP,SROAIR,ANO,PNO,STAGNO
399  FORMAT (1X,F8.3,F8.3,I4,F8.3,I4,F8.3,F9.1,F9.1,F9.1)
IF (ICODE .GE. 6) WRITE (70,*)
+   '*bubbled for 5 minutes in 100 ml of 0.1 M NaOH solution'

400  CONTINUE

CLOSE(9)
CLOSE(12)

C      LEAST SQUARES USED TO ESTIMATE RT IN REBURN ZONE
DIST(1)= 22.9
DIST(2)= 38.1
DIST(3)= 53.4
DIST(4)= 68.6
DIST(5)= 99.1
DIST(6)=129.6
DIST(7)=160.1

WRITE (50,499)
499  FORMAT(1X,' RUN',5X,'X1',4X,'SR1',3X,'SR2',2X,'kg/h',2X,'SR3',
+ 3X,'RT',4X,'NOP',2X,'T1',3X,'T2',3X,'T3',2X,'RE', ' RP BP RTp')
WRITE (50,905)
905  FORMAT(1X,' -----',3X,'-----',3X,'----',3X,'--- ---- ----',
+ 2X,'-----',3X,'----',1X,'-----',1X,'-----',1X,'-----')
DO 101 KSOY=1,NRUNS
904  READ (21,904) RID
FORMAT (A60)
M=0
DO 1 ISOY=1,7
READ (21,*) IPORT,REST,TINK
IF (REST .NE. 0.0) THEN
M=M+1
X(M)=DIST(IPORT)
Y1(M)=REST
Y2(M)=TINK
ENDIF
1  CONTINUE
READ (21,*) GKPHR,SRONE,IREBP,SRTWO,IBZP,SROAIR,ANO,PNO,STAGNO
IF (M .EQ. 2) N=1
IF (M .GT. 2) N=2
IF (IBZP .EQ. 0 .AND. IREBP .EQ. 0) PNO=ANO
IF (IBZP .EQ. 0 .AND. IREBP .EQ. 0) STAGNO=ANO
IF (IBZP .EQ. 0) IBZP=7
IF (IREBP .EQ. 0) PNO=STAGNO
IF (IREBP .EQ. 0) IREBP=IBZP

```

```

CALL REGR (N,M,X,Y1,DIST,REG)
RTPRIM=REG(IREBP)
RTREBZ=REG(IBZP) - REG(IREBP)
REBDIS=(DIST(IBZP)-DIST(IREBP))/100.0
CALL REGR (N,M,X,Y2,DIST,REG)
ITEMPZ=INT(REG(1))
ITEMRZ=INT(REG(IREBP))
ITEMBZ=INT(REG(IBZP))
IANO =INT(ANO)
IPNO =INT(PNO)
PCTRED=100.0-(ANO*100.0/PNO)
WRITE (50,903) RID,REBDIS,SRONE,SRTWO,GKPHR,SROAIR,RTREBZ,
1 IPNO,ITEMPZ,ITEMRZ,ITEMBZ,PCTRED,IREBP,IBZP,RTPRIM,KSOY,IANO
903 1 FORMAT (1X,A8,1X,F5.3,1X,2(F5.3,1X),F5.3,1X,F4.2,1X,
1 F5.3,1X,I4,1X,I4,1X,I4,1X,I4,1X,F4.1,I2,I2,1X,F5.3,I4,I5)

101 CONTINUE

STOP
END

```

```

C ... a regression routine
SUBROUTINE REGR (N,M,X,Y,DIST,REG)
DIMENSION X(9),Y(9),S(0:9),A(9,9),B(9),Z(9),DIST(7),REG(7)
DO 3 J=1,2*N
3 S(J)=0.0
DO 4 J=1,N+1
4 B(J)=0.0
DO 5 I=1,M
DO 6 J=1,2*N
6 S(J)=S(J)+X(I)**FLOAT(J)
DO 7 J=1,N+1
7 B(J)=B(J)+Y(I)*(X(I)**(J-1.0))
5 CONTINUE
DO 8 I=1,N+1
Z(I)=B(I)
DO 8 J=1,N+1
A(I,J)=S(I+J-2)
8 CONTINUE
A(1,1)=FLOAT(M)
DO 30 I=1,N
DO 30 J=I+1,N+1
IF (A(J,I) .EQ. 0.0) GO TO 30
C=-A(J,I)/A(I,I)
DO 25 K=I+1,N+1
25 A(J,K)=A(J,K)+C*A(I,K)
Z(J)=Z(J)+C*Z(I)
30 CONTINUE
DO 50 I=2,N+1
L=N+3-I
DO 50 J=1,L-1
C=-A(J,L)/A(L,L)
Z(J)=Z(J)+C*Z(L)
50 CONTINUE
DO 60 I=1,N+1
Z(I)=Z(I)/A(I,I)
60 CONTINUE
DO 97 J=1,7
97 REG(J)=Z(1)+DIST(J)*Z(2)+DIST(J)*DIST(J)*Z(3)
RETURN
END

```

OH.FOR: Calculates Initial OH Concentration

```

C ... finds yOH for gas runs in two ways:
C 1) data fit: solve NO decay rate eq for YOH based on rxns:
C      cubic splines to calculate NO decay rate from data
C      NO + NH2 ==> N2 + H2O
C      NO + NH  ==> N2O + H
C      NO + N   ==> N2 + O
C      NO + CH2 ==> HCNO + H
C      NO + CH  ==> HCN + O
C      NO + C   ==> CN + O
C 2) kinetic: solve OH decay rate eq for YOH based on rxn:
C      H + OH + M ---> H2O + M and assumes partial equil
C      OH + H2 == H2O + H
C HAS COEFFICIENTS OPTION FOR:
C (1) GLARBORG, MILLER & KEE (1986) (2) MILLER & BOWMAN (1990)

PROGRAM OH
PARAMETER (NEQ=1)
IMPLICIT REAL (K)
      DIMENSION TIMDAT(7),TMPDAT(7),H2DAT(7),H2ODAT(7),TINV(7),X7(7)
DIMENSION YOHEQ(7),YOHNUM(7),YOHKIN(7),RATNUM(7),RATKIN(7)
logical intrns
real ydata(7),xout(7),yout(7),yprime(7),YDP(7),z2(7),z5(7)
integer errcod
CHARACTER*75 RUNID
COMMON /BASIS/ TEMP, YNO, YNH3, DYNO, YH2O, YH2, YCH4
COMMON /RUNDAT/ NPTS, TIMDAT, TMPDAT, H2DAT, H2ODAT
COMMON /OHEQ/ YH
EXTERNAL FRATE
DATA H/0.02/, ITMAX/1000/, EMIN/1.0E-7/, EMAX/1.0E-5/
DATA TOL/1.0E-6/

OPEN (UNIT=7, FILE='OH.DAT', STATUS='OLD')
OPEN (UNIT=8, FILE='OH.RES', STATUS='NEW')
READ (7, *) NRUNS
DO 100 IRUN=1, NRUNS
  READ (7, 151) RUNID
151  FORMAT (A75)
  WRITE (8, 152) RUNID
152  FORMAT (1X, A75)
  WRITE (8, 500)
500  FORMAT (4X, 'RT', 2X, 'TEMP', 3X, 'ppm NO', 1X, 'NO(fit)',
           2X, 'dyNO/dt', 2X, 'YOH EQ', 5X, '1/TEMP', 3X, '(YOH)/(YOH EQ)')
  READ (7, *) NPTS
  nout=NPTS

  DO 55 IPT=1, NPTS
  READ (7, *) TIMDAT(IPT), TMPDAT(IPT), X1, X2, X3, X4, X5, X6, X7(IPT)
  YDATA(IPT)=X6/1000000.0
  xout(IPT)=TIMDAT(IPT)
  Z2(IPT)=X2/1000000.0
  H2ODAT(IPT)=X4/100.0
  H2DAT(IPT)=X1/100.0
  Z5(IPT)=X3/100.0
55  CONTINUE
*****
IF (NPTS .GE. 4) NPBS=NPTS
IF (NPTS .EQ. 2) THEN
yprime(1)=(ydata(2)-ydata(1))/(TIMDAT(2)-TIMDAT(1))
yprime(2)=yprime(1)

```

```

GO TO 53
ELSEIF (NPTS .EQ. 3) THEN
NPBS=4
TIMDAT(4)=TIMDAT(3)+(TIMDAT(3)-TIMDAT(2))/4.0
YDATA(4) =YDATA(3) +( YDATA(3)-YDATA(2) )/4.0
ENDIF
call smooth (.false., 10, NPBS, TIMDAT, ydata, nout, xout, yout,
1 yprime, YDP, errcod)
*****

53 DO 50 IPT=1, NPTS
Y1=1.E-7
Y2=1.E-5
RT =TIMDAT(IPT)
TEMP=TMPDAT(IPT)
YNO =YDATA(IPT)
YNH3=Z2(IPT)
YH2O=H2ODAT(IPT)
YH2 =H2DAT(IPT)
YCH4=Z5(IPT)
DYNO=yprime(IPT)

CALL SECRF (FRATE, Y1, Y2, TOL, YOHR)
KPH2=1.0
KPH2O=0.4451429*TEMP**(-0.72481)*EXP(28983.0/TEMP)
KPOH=23.85515*TEMP**(-0.17626)*EXP(-4859.2/TEMP)
KP4 = KPH2*KPOH**2/(KPH2O*KPH2O)
YOHEQ(IPT)=SQRT(KP4/YH2)*YH2O
YOHNUM(IPT)=YOHR
RATNUM(IPT)=YOHNUM(IPT)/YOHEQ(IPT)
TINV(IPT)=1.0/TEMP
50 CONTINUE

IT=1
C ... at initial TIME:
YOH=YOHNUM(IT)
IF (YOH .LT. YOHEQ(IT)) YOH=YOHEQ(IT)
TIME=TIMDAT(IT)

DO 52 I=IT, NPTS
C ... for each interval:
TIMFIN=TIMDAT(I)
IF (I.NE.IT) CALL RKF56 (NEQ, TIME, YOH, H, EMIN, EMAX, ITMAX, TIMFIN)
CALL RATES (TIME, YOH, ROH)
YOHKIN(I)=YOH
RATKIN(I)=YOHKIN(I)/YOHEQ(I)
G1=YDATA(I)*1000000.0
G2=YOUT(I)*1000000.0
G3=YPRIME(I)*1000000.0
WRITE (8, 510) TIME, TEMP, G1, G2, G3,
2 YOHEQ(I), TINV(I), RATNUM(I), RATKIN(I)
510 FORMAT (1X, F6.3, 3(F7.1), F8.1, 1X, 4(1PE10.3))
52 CONTINUE

100 CONTINUE

CLOSE(7)
CLOSE(8)

STOP
END

```


 REAL FUNCTION FRATE(YOH)

IMPLICIT REAL (K)
 COMMON /BASIS/ TEMP, YNO, YNH3, DYNO, YH2O, YH2, YCH4
 DATA PATM, RGAS /0.9205, 82.057/

KPH2=1.0
 KPH2O=0.4451429*TEMP**(-0.72481)*EXP(28983.0/TEMP)
 KPN=33.89271*TEMP**(0.52741)*EXP(-56738.0/TEMP)
 KPNH=11.48107*TEMP**(-0.004682)*EXP(-42351.0/TEMP)
 KPNH2=0.3792992*TEMP**(-0.48854)*EXP(-22882.0/TEMP)
 KPNH3=2.27082E-4*TEMP**(-0.68432)*EXP(5683.7/TEMP)
 KPOH=23.85515*TEMP**(-0.17626)*EXP(-4859.2/TEMP)
 KPC=1.371E6*TEMP**(0.5936)*EXP(-85542.0/TEMP)
 KPCH=9.8996E6*TEMP**(-0.34124)*EXP(-71677.0/TEMP)
 KPCH2=1.0943E5*TEMP**(-0.69568)*EXP(-46683.0/TEMP)
 KPCH3=126.6*TEMP**(-0.93)*EXP(-17628.0/TEMP)
 KPCH4=9.1501E-2*TEMP**(-1.309)*EXP(9119.3/TEMP)

KP1N=KPNH2*KPH2O/(KPNH3*KPOH)
 KP2N=KPNH*KPH2O/(KPNH2*KPOH)
 KP3N=KPN*KPH2O/(KPNH*KPOH)

KP1C=KPCH3*KPH2O/KPCH4/KPOH
 KP2C=KPCH2*KPH2O/KPCH3/KPOH
 KP3C=KPCH*KPH2O/KPCH2/KPOH
 KP4C=KPC*KPH2O/KPCH/KPOH

*****GLARBORG MILLER AND KEE*****

KN1=3.8E15*TEMP**(-1.25)
 KN1P=8.8E15*TEMP**(-1.25)
 KN2=4.3E14*TEMP**(-0.5)
 KN3=3.3E12*TEMP**0.3
 KC1=1.4E12*EXP(553.6/TEMP)
 KC2=1.1E14
 KC3=6.6E13

*****MILLER AND BOWMAN*****

C KN1=6.2E15*TEMP**(-1.25)
 C KN1P=6.4E15*TEMP**(-1.25)
 C KN2=2.4E15*TEMP**(-0.8)
 C KN3=3.27E12*TEMP**0.3
 C KC1=1.39E12*EXP(553.6/TEMP)
 C KC2=1.1E14
 C KC3=6.6E13

CTOT=PATM/(RGAS*TEMP)
 FRATE = YNH3*((KN1+KN1P)*KP1N*YOH/YH2O +
 2 KN2*KP1N*KP2N*(YOH/YH2O)**2 +
 3 KN3*KP1N*KP2N*KP3N*(YOH/YH2O)**3) +
 4 YCH4*(KC1*KP1C*KP2C*(YOH/YH2O)**2 +
 5 KC2*KP1C*KP2C*KP3C*(YOH/YH2O)**3 +
 6 KC3*KP1C*KP2C*KP3C*KP4C*(YOH/YH2O)**4) + DYNO/(CTOT*YNO)

RETURN
 END

```

*****
*****
C ... root finding routine
SUBROUTINE SECRF (F, XA, XB, TOL, XNEW)
  FA=F(XA)
  FB=F(XB)
  DO 100 I=1, 10000
    XNEW=XB-FB*(XB-XA)/(FB-FA)
    FN=F(XNEW)
    XA=XB
    FA=FB
    XB=XNEW
    FB=FN
    IF (ABS((XA-XB)/XB) .LT. TOL) GO TO 200
  100 CONTINUE
  WRITE (*,*) 'NO ANSWER AFTER 10000 ITERATIONS'
  STOP
  200 CONTINUE
  RETURN
  END
*****
*****
* routine for smoothing discrete experimental data by cubic spline
* and to calculate first and second derivatives at specified points
SUBROUTINE SMOOTH (INTRES, MAXIT, NDATA, XDATA, YDATA, NOUT, XOUT,
  1 YOUT, YPRIME, YDPRIM, ERRCOD)
  INTEGER ERRCOD, MAX, MAXM1, IBREAK
  PARAMETER (MAX=101, MAXM1=MAX-1)
  PARAMETER (IR=10, II=20, ID=30)
  PARAMETER (DIS=1.0, SC=0.0)
  LOGICAL INTRES
  REAL XDATA (NDATA), YDATA (NDATA), XOUT (NOUT), YOUT (NOUT)
  REAL YPRIME (NOUT), YDPRIM (NOUT), YSMTH1 (MAX)
  REAL BREAK (MAX), CSCOE (4, MAX)
  IF (NDATA.GT.MAX) THEN
    ERRCOD = 1
    RETURN
  END IF
C call imsl subroutine CSSCV for cubic spline smoothing
CALL CSSCV (NDATA, XDATA, YDATA, 2, break, cscoef)
C now perform the interpolation, imsl function will be used
DO 30 IOUT=1, NOUT
  T=XOUT(IOUT)
  YOUT(IOUT)= CSVAL (T, NDATA-1, BREAK, CSCOE)
  yprime(iout)=csder (1, t, ndata-1, break, cscoef)
  30 ydprim(iout)=csder (2, t, ndata-1, break, cscoef)
  ERRCOD=0
  RETURN
  END
*****
*****
SUBROUTINE RATES (TIME, YOH, R)
  IMPLICIT REAL (K)
  DIMENSION TIMDAT (7), TMPDAT (7), H2DAT (7), H2ODAT (7)
  COMMON /RUNDAT/ NPTS, TIMDAT, TMPDAT, H2DAT, H2ODAT
  COMMON /BASIS/ TEMP, YNO, YNH3, DYNO, YH2O, YH2, YCH4
  COMMON /OHEQ/ YH
  DATA PATM, RGAS /0.9205, 82.057/
  TEMP=FINTLN (TIMDAT, TMPDAT, TIME, NPTS)
  YH2=FINTLN (TIMDAT, H2DAT, TIME, NPTS)
  YH2O=FINTLN (TIMDAT, H2ODAT, TIME, NPTS)

```

```

CTOT=PATM/(RGAS*TEMP)
C *** YH, based on partial equil: OH + H2 == H2O + H eq const KP3
  KPH=5.740234*TEMP**(0.63772)*EXP(-26061.0/TEMP)
  KPH2=1.0
  KPOH=23.85515*TEMP**(-0.17626)*EXP(-4859.2/TEMP)
  KPH2O=0.4451429*TEMP**(-0.72481)*EXP(28983.0/TEMP)
  KP3=KPH2O*KPH/(KPH2*KPOH)
  YH=KP3*YOH*YH2/YH2O

C      reaction                rate      rate constant
C      H + OH + M --> H2O + M      R          KOH

*****GLARBORG MILLER AND KEE*****
  KOH=7.5E23*TEMP**(-2.6)
*****MILLER AND BOWMAN*****
C      KOH=1.6E22*TEMP**(-2.0)

  R=-CTOT*CTOT*KOH*YH*YOH
  RETURN
  END
*****
*****
C *** Linearly interpolates between data points (XDAT,YDAT)
  to give a value of Y at XVAL
C      REAL FUNCTION FINTLN (XDAT,YDAT,XVAL,N)
      DIMENSION XDAT(N),YDAT(N)
      DO 10 I=N-1,2,-1
        DIFF=XVAL-XDAT(I)
        IF (DIFF .GE. 0.0) GOTO 20
10      CONTINUE
        I=1
        DIFF=XVAL-XDAT(1)
20      CONTINUE
        SLOPE = (YDAT(I+1)-YDAT(I))/(XDAT(I+1)-XDAT(I))
        FINTLN = YDAT(I)+SLOPE*DIFF
      RETURN
      END
*****
*****
C *** Subroutine to solve a system of D.E.'s (20 max)
  SUBROUTINE RKF56(N,X,Y,HOPTM,EMIN,EMAX,ITMAX,XEND)
C ... note: same subroutine as in MODEL.FOR
  ...
  ...
  ...

```

MODEL.FOR: Kinetic Model Calculations

```

C *** gives NO, HCN and NH3 profiles in reburn zone, given
C T, %H2, %CH4, %H2O, %N2 change with RT and initial values for
C NO, HCN, NH3 and OH, correcting equilibrium assumption for
C 2H2O = H2 + 2OH for initial OH and T < 1521 K
C OH decay rate based on rxn: H + OH + M --> H2O + M
C solves OH simultaneously with other decay rates (NO, HCN and NH3)
C and assumes partial equil OH + H2 == H2O + H
C ... uses RKF56 adjustable step size integrating routine
C ... reads from MODEL.DAT, writes to MODEL.RES and RATES.RES
C This version concentrates only on reburn zone

PROGRAM MODEL
PARAMETER (NEQ=4)
C ... NEQ is the number of rate equations to be solved
IMPLICIT REAL (K)
REAL NH3DAT,N2DAT
CHARACTER*80 RUNID
      DIMENSION TIMDAT(7),TMPDAT(7),H2DAT(7),NH3DAT(7),CH4DAT(7),
      2 H2ODAT(7),N2DAT(7),ACTNO(7),ACTHCN(7),Y(NEQ),RATE(NEQ)
C ... array Y holds YNO,YHCN,YNH3 and YOH values, RATE holds rates
      COMMON /RUNDAT/ NPTS,TIMDAT,TMPDAT,H2DAT,NH3DAT,CH4DAT,H2ODAT,
      2 N2DAT,ACTNO,ACTHCN
      COMMON /INTDAT/ TEMP,YH2,YNH3,YCH4,YH2O,YN2
      COMMON /NORXN/ RN0,RN1,RN2,RN3,RN4,FN,RC1,RC2,RC3,FC
      COMMON /HCNRXN/ RO,ROH,RCN1,RNIT1,RNIT2,RNIT3,RNIT,RHC
      COMMON /OHEXP/ A,B,IEQ,IN2,YN2O1
      DATA H/0.02/,ITMAX/1000/,EMIN/1.0E-7/,EMAX/1.0E-5/

      OPEN (UNIT=7,FILE='MODEL.DAT',STATUS='OLD')
      OPEN (UNIT=8,FILE='MODEL.RES',STATUS='NEW')
      OPEN (UNIT=9,FILE='RATES.RES',STATUS='NEW')

C ... get number of runs
      READ (7,*) NRUNS
      DO 20 J=1,NRUNS
C ... 26 is number of reburning experiments
      IF (J .LE. 26) ITM=2
      IF (J .GT. 26) ITM=1
C ... input time, temp., mole fraction data and initial conditions
C time, temp and mole fraction data stored in common block RUNDAT
*****
C *** input data (time, temp, yH2, yNH3, yCH4, yH2O, yN2)
      READ (7,50) RUNID
      50 FORMAT (A80)
      READ (7,*) NPTS
      DO 49 I=1,NPTS
      READ (7,*)TIMDAT(I),TMPDAT(I),X1,X2,X3,X4,X5,ACTNO(I),ACTHCN(I)
      H2DAT(I)=X1/100.0
      NH3DAT(I)=X2/1000000.0
      CH4DAT(I)=X3/100.0
      H2ODAT(I)=X4/100.0
      N2DAT(I)=X5/100.0
      49 CONTINUE
      IF (CH4DAT(1) .LE. 0.0) CH4DAT(1)=0.0
      TIMONE=TIMDAT(1)
      IF (J. LE. 26) THEN
      DO 51 I=1,NPTS
      51 TIMDAT(I)=TIMDAT(I)-TIMONE
      ENDDIF

```



```

Y(1)=ACTNO(ITM)/1000000.0
Y(2)=ACTHCN(ITM)/1000000.0
Y(3)=NH3DAT(ITM)
*****
C gets initial value of yOH
  KPH2=1.0
  KPH2O=0.4451429*TMPDAT(ITM)**(-0.72481)*EXP(28983.0/TMPDAT(ITM))
  KPOH=23.85515*TMPDAT(ITM)**(-0.17626)*EXP(-4859.2/TMPDAT(ITM))
C *** YOH, correct partial equil for: 2H2O == 2OH + H2 eq const KP1
  KP1 = KPH2*KPOH*KPOH/(KPH2O*KPH2O)
C ... yOH based on partial equilibrium and corrected yOH
  IF (J .GT. 26 .OR. TMPDAT(ITM) .GE. 1521.6) THEN
  Y(4)=(H2ODAT(ITM)*SQRT(KP1/H2DAT(ITM)))
  GO TO 11
  ENDIF
  IF (TMPDAT(ITM) .LT. 1425.0) THEN
  A=1.65E-5
  B=18745.0
  Y(4)=(H2ODAT(ITM)*SQRT(KP1/H2DAT(ITM)))*A*EXP(B/TMPDAT(ITM))
  ELSEIF (TMPDAT(ITM).GE.1425.0 .AND. TMPDAT(ITM).LT.1521.6) THEN
  A=120.6
  B=-0.0786
  Y(4)=(H2ODAT(ITM)*SQRT(KP1/H2DAT(ITM)))* ( A + B * TMPDAT(ITM) )
  ELSEIF (J .GT. 26 .OR. TMPDAT(ITM) .GE. 1521.6) THEN
  WRITE (6,*) 'ERROR'
  ELSE
  WRITE (6,*) 'ERROR'
  ENDIF
*****
11 WRITE (8,103) RUNID,J
  WRITE (9,*)
  WRITE (9,*) RUNID
  103 FORMAT (1X,'N-species: ',A65,' J=',I3)
  WRITE (8,101)
  101 FORMAT(1X,'time TEMP ex NO pr NO',
+ ' ex HCN pr HCN ex NH3 pr NH3 N2O',8X,'OH'/
+ ' -----',
+ ' -----',8X,'---')

  NPORT=NPTS+1-ITM
  WRITE (8,*) NPORT
  WRITE(9,106)
  106 FORMAT (1X,'TIME NHi rx Chi rx NO rate O rx ',
+ 'OH rx',' CN rx N/N2 rx HCN rate NH3 rate')
*****
C ... at initial TIME:
  TIME=TIMDAT(ITM)
  DO 10 IPR=ITM,NPTS
C ... for each interval:
  TIMFIN=TIMDAT(IPR)
  IF(IPR.NE.ITM)CALL RKF56(NEQ,TIME,Y,H,EMIN,EMAX,ITMAX,TIMFIN)
  CALL RATES (TIME,Y,RATE)

  YOFNO=Y(1)*1000000.0
  YOFHCN=Y(2)*1000000.0
  YOFNH3=Y(3)*1000000.0
  EXPNH3=NH3DAT(IPR)*1000000.0

  WRITE (8,100) TIME,TEMP,ACTNO(IPR),YOFNO,ACTHCN(IPR),
+ YOFHCN,EXPNH3,YOFNH3,YN2O1,Y(4)
  100 FORMAT(1X,F5.3,F6.0,6(F8.1),F5.1,1PE13.2)

```

```

WRITE(9,105) TIME, FN, FC, RATE(1), RO, ROH, RCN1, RNIT, RATE(2), RATE(3)
105  FORMAT (1X, F5.3, 2(1PE9.1), 1X, 1PE10.3, 4(1PE9.1), 2(1X, 1PE10.3))
WRITE (9,110) RN1, RN2, RN3, RN4, FN, RC1, RC2, RC3, FC
WRITE (9,120) RO, ROH, RCN1, RNIT1, RNIT2, RNIT3, RHC
WRITE (9,130) RATE(1), RATE(2), RATE(3)
110  FORMAT (/1X, 'NO REACTION RATES: '/10X, 'RN1: ', E11.4/10X,
        'RN2: ', E11.4/10X, 'RN3: ', E11.4/10X, 'RN4: ', E11.4/5X,
        'TOTAL NHi: ', E11.4/10X, 'RC1: ', E11.4/10X,
        'RC2: ', E11.4/10X, 'RC3: ', E11.4/
        5X, 'TOTAL CHi: ', E11.4)
120  FORMAT (1X, 'HCN REACTION RATES: '/
        10X, 'RO : ', E11.4/10X, 'ROH : ', E11.4/
        10X, 'RCN1 : ', E11.4/10X, 'RNIT1: ', E11.4/
        10X, 'RNIT2: ', E11.4/10X, 'RNIT3: ', E11.4/
        10X, 'RHC : ', E11.4)
130  FORMAT (1X, 'NET NO REACTION RATE: ', E11.4/
        4      'NET HCN REACTION RATE: ', E11.4/
        4      'NET NH3 REACTION RATE: ', E11.4//)

```

```

10  CONTINUE
20  CONTINUE

```

```

CLOSE(7)
CLOSE(8)
CLOSE(9)

```

```

STOP
END

```

```

*****
*****

```

```

C *** computes rate of change of vector Y with TIME
C -- linearly interpolates to get T, YH2, YNH3, YCH4, YH2O and YN2
SUBROUTINE RATES(TIME, Y, G)

```

```

IMPLICIT REAL(K)
REAL NH3DAT, N2DAT

```

```

DIMENSION Y(4), G(4)
DIMENSION H2DAT(7), TMPDAT(7), NH3DAT(7), TIMDAT(7), CH4DAT(7),
2      H2ODAT(7), N2DAT(7), ACTNO(7), ACTHCN(7)

```

```

COMMON /RUNDAT/ NPTS, TIMDAT, TMPDAT, H2DAT, NH3DAT, CH4DAT, H2ODAT,
2      N2DAT, ACTNO, ACTHCN
COMMON /INTDAT/ TEMP, YH2, YNH3, YCH4, YH2O, YN2
COMMON /NORXN/ RNO, RN1, RN2, RN3, RN4, FN, RC1, RC2, RC3, FC
COMMON /HCNRXN/ RO, ROH, RCN1, RNIT1, RNIT2, RNIT3, RNIT, RHC
COMMON /OHEXP/ A, B, IEQ, IN2, YN2O1

```

```

DATA PATM, RGAS /0.9205, 82.057/

```

```

TEMP=FINTLN (TIMDAT, TMPDAT, TIME, NPTS)
YH2 =FINTLN (TIMDAT, H2DAT ,TIME, NPTS)
YCH4=FINTLN (TIMDAT, CH4DAT, TIME, NPTS)
YH2O=FINTLN (TIMDAT, H2ODAT, TIME, NPTS)
YN2 =FINTLN (TIMDAT, N2DAT ,TIME, NPTS)

```

```

YNO =Y(1)
YHCN=Y(2)
YNH3=Y(3)
YCH =Y(4)

```

```
C *** calculate species KP values
KPC=1.371E6*TEMP**(0.5936)*EXP(-85542.0/TEMP)
KPCH=9.8996E6*TEMP**(-0.34124)*EXP(-71677.0/TEMP)
KPCH2=1.0943E5*TEMP**(-0.69568)*EXP(-46683.0/TEMP)
KPCH3=126.6*TEMP**(-0.93)*EXP(-17628.0/TEMP)
KPCH4=9.1501E-2*TEMP**(-1.309)*EXP(9119.3/TEMP)
KPCN=5.493082E6*TEMP**(-0.43393)*EXP(-51510.0/TEMP)
KPH=5.740234*TEMP**(0.63772)*EXP(-26061.0/TEMP)
KPHCN=464.6108*TEMP**(-0.28741)*EXP(-16341.0/TEMP)
KPHNCO=0.2084825*TEMP**(-0.35489)*EXP(12191.0/TEMP)
KPH2=1.0
KPH2O=0.4451429*TEMP**(-0.72481)*EXP(28983.0/TEMP)
KPN=33.89271*TEMP**(0.52741)*EXP(-56738.0/TEMP)
KPNCO=24.06600*TEMP**(0.051735)*EXP(-19206.0/TEMP)
KPNH=11.48107*TEMP**(-0.004682)*EXP(-42351.0/TEMP)
KPNH2=0.3792992*TEMP**(-0.48854)*EXP(-22882.0/TEMP)
KPNH3=2.27082E-4*TEMP**(-0.68432)*EXP(5683.7/TEMP)
KPN0=4.11196*TEMP**(0.01346)*EXP(-10860.0/TEMP)
KPO=76.48541*TEMP**(0.43322)*EXP(-29912./TEMP)
KPOH=23.85515*TEMP**(-0.17626)*EXP(-4859.2/TEMP)
```

```
C *** Gives the value of dYNO/dt
```

C	reaction	rate	rate constant
C	NO + NH2 --> N2 + H2O	RNO } SUM=RN1	KN1
C	NO + NH2 --> NNH + OH	RNOP}	KN1P
C	NO + NH --> N2O + H	RN2	KN2
C	N + NO --> N2 + O	RN3	KN3
C	CH2+ NO --> HCNO + H	RC1	KC1
C	CH + NO --> HCN + O	RC2	KC2
C	C + NO --> CN + O	RC3	KC3

```
C ... rate constants
222 KN1=3.8E15*TEMP**(-1.25)
KN1P=8.8E15*TEMP**(-1.25)
KN2=4.3E14*TEMP**(-0.5)
KN3=3.3E12*TEMP**0.3
KC1=1.4E12*EXP(553.6/TEMP)
KC2=1.1E14
KC3=6.6E13
```

C	reaction	equilibrium constant
C	OH + NH3 == NH2 + H2O	KP1N
C	OH + NH2 == NH + H2O	KP2N
C	OH + NH == N + H2O	KP3N
C	OH + CH4 == CH3 + H2O	KP1C
C	OH + CH3 == CH2 + H2O	KP2C
C	OH + CH2 == CH + H2O	KP3C
C	OH + CH == C + H2O	KP4C

```
C ... equilibrium constants
KP1N=KPNH2*KPH2O/(KPNH3*KPOH)
KP2N=KPNH *KPH2O/(KPNH2*KPOH)
KP3N=KPN *KPH2O/(KPNH *KPOH)
KP1C=KPCH3*KPH2O/(KPCH4*KPOH)
KP2C=KPCH2*KPH2O/(KPCH3*KPOH)
KP3C=KPCH *KPH2O/(KPCH2*KPOH)
KP4C=KPC *KPH2O/(KPCH *KPOH)
```

```
C *** YH, based on partial equil: OH + H2 == H2O + H eq const KP3
KP3=KPH2O*KPH/(KPH2*KPOH)
YH=KP3*YOH*YH2/YH2O
```

C ... NHi and CHi species concentrations

223 YNH2=KP1N*YNH3*YOH/YH2O
YNH =KP2N*YNH2*YOH/YH2O
YN =KP3N*YNH *YOH/YH2O
YCH3=KP1C*YCH4*YOH/YH2O
YCH2=KP2C*YCH3*YOH/YH2O
YCH =KP3C*YCH2*YOH/YH2O
YC =KP4C*YCH *YOH/YH2O

CTOT=PATM/(RGAS*TEMP)

C ... rates of reactions involving NO

RNO=-CTOT*YNO*YNH2* KN1
RNOF=-CTOT*YNO*YNH2*KN1P
RN1=-CTOT*YNO*YNH2*(KN1+KN1P)
RN2=-CTOT*YNO*YNH * KN2
RN3=-CTOT*YNO*YN *KN3
FN=RN1+RN2+RN3
RC1=-CTOT*YNO*YCH2*KC1
RC2=-CTOT*YNO*YCH *KC2
RC3=-CTOT*YNO*YC *KC3
FC=RC1+RC2+RC3
FNO=FN+FC
G(1) = FNO

C *** Gives the value of dYHCN/dt

C	reaction	rate	rate constant
C	HCN + O --> NCO + H	RO	KO1
C	HCN + O --> NH + CO	RO	KO2
C	HCN + OH --> HOCN + H	ROH	KOH1
C	HCN + OH --> HNCO + H	ROH	KOH2
C	CH2 + NO --> HCN + OH	RC1	KC1
C	CH + NO --> HCN + O	RC2	KC2
C	C + NO --> CN + O	RC3	KC3
C	CN + OH --> NCO + H	RCN1	KCN1
C	CH + N2 --> HCN + N	RNIT1	KNIT1
C	CH3 + N --> HCN + H + H	RNIT3	KNIT3

C reactions whose terms cancel out due to partial equil of CN and HCN
C HCN + H == CN + H2 reversible rxn
C HCN + OH == CN + H2O partial equilibrium

C ... rate constants
KO1 = 1.4E04*TEMP**(2.64)*EXP(-2506.3/TEMP)
KO2 = 3.5E03*TEMP**(2.64)*EXP(-2506.3/TEMP)
KOH1 = 9.2E12*EXP(-7549.1/TEMP)
KOH2 = 4.8E11*EXP(-5536.0/TEMP)
KCN1 = 6.0E13
KNIT1 = 1.9E11*EXP(-6844.5/TEMP)
KNIT3 = 5.0E13

C *** YCN, based on partial equil: HCN + OH == CN + H2O eq const KP3
KEQCN = (KPCN*KPH2O)/(KPOH*KPHCN)
YCN =KEQCN*YOH*YHCN/YH2O

C *** YO, based on partial equil: O + H2O == OH + OH eq const KP2
KP2 = (KPOH*KPOH)/(KPO*KPH2O)
YO = YOH*YOH/(KP2*YH2O)

C ... rates of reactions involving HCN

RO = -CTOT*YHCN*YO *(KO1 +KO2)
ROH = -CTOT*YHCN*YOH*(KOH1+KOH2)
RCN1 = -CTOT*YCN *YOH* KCN1
RNIT1 = CTOT*YCH *YN2* KNIT1
RNIT3 = CTOT*YCH3*YN * KNIT3
RNIT = RNIT1+RNIT3
RHC = -FC
FHCN = RO+ROH+RCN1+RNIT+RHC
G(2) = FHCN

C *** Gives the value of dYN2/dt

reaction	rate	rate constant
NO + NH2 --> N2 + H2O	RNO	KN1
NO+NH --> N2O+H --> N2+OH	RN2	KN2
NO + N --> N2 + O	RN3	KN3
CH + N2 --> HCN + N	RNIT1	KNIT1

C rates above are for N-species rates, for N2 rate need -ve sign
C dYN2/dt = -RNO -RN2 -RN3 -RNIT1

C *** Gives the value of dYNH3/dt

C dNO/dt + dHCN/dt + dNH3/dt + 2*dN2/dt = 0

G(3) = -G(2) - G(1) + 2.0*(RNO+RN2+RN3+RNIT1)

C *** Gives the value of dYOH/dt

reaction	rate	rate constant
H + OH + M --> H2O + M	G(4)	KOH

KOH = 7.5E23*TEMP**(-2.6)
G(4) = -CTOT*CTOT*KOH*YH*YOH

IF (IEQ .EQ. 5) THEN
RATIO = YOH/YH2O

F1 = 3.93E17*TEMP**(-1.603)*EXP(5277.0/TEMP)*RATIO**1.0
+ 7.57E15*TEMP**(-0.917)*EXP(19650.0/TEMP)*RATIO**2.0
+ 3.20E12*TEMP**(-0.134)*EXP(39105.0/TEMP)*RATIO**3.0
F2 = 5.83E14*TEMP**(-0.484)*EXP(12436.0/TEMP)*RATIO**2.0
+ 7.73E16*TEMP**(-0.678)*EXP(20730.0/TEMP)*RATIO**3.0
+ 1.20E14*TEMP**(-0.292)*EXP(40708.0/TEMP)*RATIO**4.0
F3 = 9.20E12*TEMP**(-0.000)*EXP(-7549.0/TEMP)*RATIO*YH2O
+ 4.80E11*TEMP**(-0.000)*EXP(-5536.0/TEMP)*RATIO*YH2O
F4 = 1.05E03*TEMP**(2.701)*EXP(6283.0/TEMP)*RATIO*YOH
+ 1.32E16*TEMP**(-0.695)*EXP(-1327.0/TEMP)*RATIO*YOH
F5 = 1.34E14*TEMP**(-0.678)*EXP(13886.0/TEMP)*RATIO**3.0
F6 = 1.25E15*TEMP**(-0.603)*EXP(46200.0/TEMP)*RATIO**4.0
F7 = 1.18E17*TEMP**(-1.603)*EXP(5277.0/TEMP)*RATIO**1.0
+ 7.57E15*TEMP**(-0.917)*EXP(19650.0/TEMP)*RATIO**2.0
+ 3.20E12*TEMP**(-0.134)*EXP(39105.0/TEMP)*RATIO**3.0
F8 = 8.03E22*TEMP**(-2.511)*EXP(7781.0/TEMP)*RATIO*YOH
G(1) = -CTOT*YNO*(YNH3*F1+YCH4*F2)
G(2) = CTOT*(-YHCN*(F3+F4)+YCH4*(YNO*F2+YN2*F5+YNH3*F6))
G(3) = -G(1)-G(2)-2.0*CTOT*(YNO*YNH3*F7-CH4*YN2*F5)
G(4) = -YH2*F8*CTOT*CTOT

ENDIF

```

*****
C SECTION FOR N2O
C NO + NH --> N2O + H KN2
C N2O + H --> N2 + OH KN2O1
KN2O1=7.6E13*EXP(-7649.7/TEMP)
YN2O1=(YNO*YNH*KN2/(YH*KN2O1))*1000000.0
*****
RETURN
END
*****
*****
C *** Linearly interpolates between data points (XDAT,YDAT)
C to give a value of Y at XVAL
REAL FUNCTION FINTLN (XDAT,YDAT,XVAL,N)

DIMENSION XDAT(N),YDAT(N)
DO 10 I=N-1,2,-1
DIFF=XVAL-XDAT(I)
IF (DIFF .GE. 0.0) GOTO 20
10 CONTINUE
I=1
DIFF=XVAL-XDAT(1)
20 CONTINUE
SLOPE = (YDAT(I+1)-YDAT(I))/(XDAT(I+1)-XDAT(I))
FINTLN = YDAT(I)+SLOPE*DIFF
RETURN
END
*****
*****
C *** Subroutine to solve a system of D.E.'s (20 max)
SUBROUTINE RKF56(N,X,Y,HOPTM,EMIN,EMAX,ITMAX,XEND)

REAL K1(20),K2(20),K3(20),K4(20),K5(20),K6(20),K7(20),K8(20)
LOGICAL LINCR,LDECR
DIMENSION Y(N),YK(20),YNEXT5(20),YNEXT6(20),EABS(20),EREL(20)

NSTEP=0
H=HOPTM
IFLAG=0
C ... initialize X and Y's
XK=X
DO 10 I=1,N
10 YK(I)=Y(I)
5 CONTINUE
IF(NSTEP.GT.ITMAX) THEN
WRITE (6,*) 'MAX NO OF ITERATIONS EXCEEDED'
RETURN
ENDIF
15 CONTINUE
DO 17 I=1,N
17 Y(I)=YK(I)
C ... GET K1
CALL RATES(X,Y,K1)
DO 20 I=1,N
20 Y(I)=YK(I)+H*K1(I)/6.0
C ... GET K2
CALL RATES(X+H/6.0,Y,K2)
DO 30 I=1,N
30 Y(I)=YK(I)+H*(4.0*K1(I)/75.0+16.0*K2(I)/75.0)
C ... GET K3
CALL RATES(X+4.0*H/15.0,Y,K3)

```

```

DO 40 I=1,N
40 Y(I)=YK(I)+H*(5.0*K1(I)/6.0-8.0*K2(I)/3.0+5.0*K3(I)/2.0)
C ... GET K4
CALL RATES(X+2.0*H/3.0,Y,K4)
DO 50 I=1,N
50 Y(I)=YK(I)+H*(-8.0*K1(I)/5.0+144.0*K2(I)/25.0
1 -4.0*K3(I)+16.0*K4(I)/25.0)
C ... GET K5
CALL RATES(X+4.0*H/5.0,Y,K5)
DO 60 I=1,N
60 Y(I)=YK(I)+H*(361.0*K1(I)/320.0-18.0*K2(I)/5.0
1 +407.0*K3(I)/128.0-11.0*K4(I)/80.0
2 +55.0*K5(I)/128.0)
C ... GET K6
CALL RATES(X+H,Y,K6)
DO 70 I=1,N
70 Y(I)=YK(I)+H*(-11.0*K1(I)/640.0+11.0*K3(I)/256.0
1 -11.0*K4(I)/160.0+11.0*K5(I)/256.0)
C ... GET K7
CALL RATES(X,Y,K7)
DO 80 I=1,N
80 Y(I)=YK(I)+H*(93.0*K1(I)/640.0-18.0*K2(I)/5.0
1 +803.0*K3(I)/256.0-11.0*K4(I)/160.0
2 +99.0*K5(I)/256.0+K7(I))
C ... GET K8
CALL RATES(X+H,Y,K8)
C ... calculate 5th and 6th order approximations for next step
DO 90 I=1,N
YNEXT5(I)=YK(I)+(H/8448.0)*(682.0*K1(I)
1 +3375.0*K3(I)+2376.0*K4(I)+1375.0*K5(I)+640.0*K6(I))
YNEXT6(I)=YK(I)+(H/8448.0)*(42.0*K1(I)+3375.0*K3(I)
1 +2376.0*K4(I)+1375.0*K5(I)+640.0*K7(I)+640.0*K8(I))
C ... calculate absolute and relative errors
EABS(I)=ABS(YNEXT5(I)-YNEXT6(I))
IF (ABS(YNEXT6(I)) .LT. 1.0E-30) THEN
EREL(I)=EABS(I)
ELSE
EREL(I)=ABS(EABS(I)/YNEXT6(I))
ENDIF
90 CONTINUE

C ... IFLAG: value of 0 ---> keep taking steps, not close yet
C value of 1 ---> take last step, ready to RETURN,
C HOPTM is saved
C value of 2 ---> getting close to XEND, HOPTM saved
IF (IFLAG .EQ. 1) GOTO 100
C ... check errors
NERRLO=0
DO 95 I=1,N
C ... if error too big, don't take step; try again
IF (EREL(I) .GT. EMAX) THEN
H=H/2.0
GOTO 5
C ... if error very small
ELSEIF (EREL(I) .LT. EMIN) THEN
NERRLO=NERRLO+1
ENDIF
95 CONTINUE
IF (ABS(H) .GT. ABS(XEND-X)) THEN
HOPTM=H
H=XEND-X

```

```
        IFLAG=1
        GOTO 15
    ENDIF
100     CONTINUE
C ... take the step
    X=XK+H
    XK=X
    DO 120 I=1,N
        Y(I)=YNEXT6(I)
        YK(I)=Y(I)
120     CONTINUE
    NSTEP=NSTEP+1
    IF (IFLAG.EQ.1) RETURN
C ... error too small, take bigger step next time
    IF (NERRLO .EQ. N) H=2.0*H
    GOTO 5

END
```


FINAL.FOR: Extended Kinetic Model Calculations

```

C prediction of reburning effectiveness from primary NO
C REBURN ZONE: kinetic model, time < 0.18 s corrected for mixing
C empirical correlations to estimate H2, CH4 and temp quench
C BURNOUT ZONE: empirical correlation, Chen et al. (1986)
C NOTE: SUBROUTINE RATES in this program has one difference
C from that in MODEL.FOR
C for time < 0.18, HCN formation from hydrocarbon factored by 0.3
C IF (IPR .LE. 2) G(2) = RO + ROH + RCN1 + (RNIT+RHC)*0.3
PROGRAM FINAL
PARAMETER (NEQ=4)
C ... NEQ is the number of rate equations to be solved
IMPLICIT REAL (K)
REAL NH3DAT,N2DAT
CHARACTER*11 RUN
      DIMENSION TIMDAT(7),TMPDAT(7),H2DAT(7),NH3DAT(7),CH4DAT(7),
      2 H2ODAT(7),N2DAT(7),ACTNO(7),ACTHCN(7),Y(NEQ),RATE(NEQ)
C ... array Y holds YNO,YHCN,YNH3 and YOH values, RATE holds rates
      COMMON /RUNDAT/ NPTS,TIMDAT,TMPDAT,H2DAT,NH3DAT,CH4DAT,H2ODAT,
      2 N2DAT,ACTNO,ACTHCN
      COMMON /INTDAT/ TEMP,YH2,YNH3,YCH4,YH2O,YN2
      COMMON /NORXN/ RNO,RN1,RN2,RN3,RN4,FN,RC1,RC2,RC3,FC
      COMMON /HCNRXN/ RO,ROH,RCN1,RNIT1,RNIT2,RNIT3,RNIT,RHC
      COMMON /OHEXP/ A,B,IEQ,IN2,IPR,FACTOR
DATA H/0.02/,ITMAX/1000/,EMIN/1.0E-7/,EMAX/1.0E-5/
      OPEN (UNIT=7,FILE='FINAL.DAT',STATUS='OLD')
      OPEN (UNIT=8,FILE='FINAL.RES',STATUS='NEW')

      READ (7,*) NRUN
      DO 30 ISET=1,NRUN
      READ(7,101)RUN,SR1,SR2,COAL,SR3,RTIM,PRNO,WNO,TEM,TF,YE
101 FORMAT (A11,4(F6.3),F5.2,F6.3,F6.0,F5.0,F5.0,F5.0,F5.1)
      *****
C PRNO=1000.0
C WNO=750.0
C WRITE (6,*) 'ENTER TIME AND TEMPERATURE (K)'
C READ (5,*) RTIM,TEM
C DO 30 ISET=1,60
C SR2=0.72+0.0044*ISET
      *****
      ITM=1
      *****
C specify data (time, temp, yH2, yNH3, yCH4, yH2O, yN2)
      TIMDAT(1)=0.0
      IF (RTIM .LE. 0.18) THEN
      NPTS=2
      TIMDAT(2)=RTIM
      ELSE
      NPTS=3
      TIMDAT(2)=0.18
      TIMDAT(3)=RTIM
      ENDIF
C empirical correlation for temperature quench rate
      SLOP=178.0-0.00162*TEM*TEM

      DO 40 I=1,NPTS
      TMPDAT(I)=SLOP*TIMDAT(I)+TEM
C empirical correlation for H2 concentration
      H2DAT(I)=(8.0-7.9*SR2)/100.0
      IF (H2DAT(I) .LE. 0.001) H2DAT(I)=0.001

```

```

C empirical correlation for CH4 concentration
CH4DAT(I)=(3.5-0.0024*SR2*TEM)/100.0
IF (CH4DAT(I) .LE. 0.0) CH4DAT(I)=0.0
C average values for H2O and N2 concentrations
H2ODAT(I)=0.1
N2DAT(I)=0.735
40 CONTINUE
H2DAT(1)=0.0
CH4DAT(1)=0.0
Y(1)=WNO/1000000.0
Y(2)=0.0
Y(3)=0.0000001
Y(4)=35.0*EXP(-24100.0/TMPDAT(ITM))
C OKk BASED ON TRIAL AND ERROR
*****
TIME=TIMDAT(ITM)
DO 10 IPR=ITM,NPTS
C for each interval:
TIMFIN=TIMDAT(IPR)
IF(IPR.NE.ITM)CALL RKF56(NEQ,TIME,Y,H,EMIN,EMAX,ITMAX,TIMFIN)
CALL RATES (TIME,Y,RATE)
10 CONTINUE
a1=y(1)*1000000.0
a2=y(2)*1000000.0
a3=y(3)*1000000.0
write (21,102)sr2,a1,a2,a3
102 format (1x,f8.3,3(f8.1))
DO 20 I=1,3
20 IF (Y(I) .LE. 0.0) Y(I)=0.0
C a factor of 1.3 to convert wet values to dry, 0% excess O2
YOFNO=Y(1)*1000000.0*1.3
YTFN=(Y(2)+Y(3))*1000000.0*1.3
C empirical correlation estimates final NO from reburn zone values
EXNO=53.0+0.81*SR2*YOFNO+(0.36*YTFN/(1.0+0.0024*YTFN))
RE=100.0-100.0*(EXNO/PRNO)
IF (RE .LE. 0.0) RE=0.0
WRITE (8,100) SR2,RE
100 format (1X,F7.3,F7.1)
30 continue
CLOSE(7)
CLOSE(8)
STOP
END

```

**DATE
FILMED**

5/01/92

